TELECONNECTIONS BETWEEN SEASONAL RAINFALL IN COASTAL TANZANIA AND ENSO

Agnes Lawrence Kijazi

A thesis submitted in fulfillment of the
Degree of Master of Science

Department of Environmental and
Geographical Sciences
University of Cape Town

July 2003

To my beloved husband Mwara, son David,
Daughters Doreen and Elizabeth.

Jeremiah 33:3
``Call to me and I will answer you and tell you great and
Unsearchable things you do not know``

DECLARATION

This is to certify that the dissertation entitled 'Teleconnections between seasonal rainfall in coastal Tanzania and ENSO ' submitted in fulfilment of the requirements of the degree of Master of Science of the University of Cape Town is a record of bonafide research work. The subject matter embodied in this report has not been submitted at any other university.

Name; Agnes Lawrence Kijazi

Signature; Signed by candidate

Signed this 16th day of July 2003.

ABSTRACT.

The modulation of Tanzanian coastal rainfall variability with the El Nino/Southern oscillation (ENSO), the largest known mode of Southern Hemisphere climatic variation is examined. A rainfall index was formulated from variable Tanzanian coastal stations and used to identify the rainfall characteristics of each ENSO year. Monthly anomalies of selected meteorological fields were analyzed for El Niño/La Niña composites and each individual event to determine the mechanisms associated with seasonal rainfall over the Tanzanian coast during ENSO years.

Northern Coast rainfall tends to be above average during the warm phase of ENSO while Southern coast tends to be wet during the early season (OND). The reverse is true during La Niña years. The proposed link between ENSO and rainfall over the coast of Tanzania is influenced by SST anomalies in the western Indian Ocean. Strong wind convergence at low and middle levels are preferentially located over the coast during periods of above-normal rainfall and enhanced easterly flow, both of which coincide with the warm phase of ENSO. Dry conditions during La Niña events are usually associated with cooling over the equatorial western Indian Ocean and moisture flux divergence over the Tanzanian coast.

A contrasting warm (cool) SST anomaly pattern in the western (eastern) equatorial Indian Ocean was observed to be the dominant feature for each El Niño year. On the other hand, a contrasting cool (warm) SST anomaly pattern in the western (eastern) equatorial Indian Ocean is apparent during La Niña years. These patterns are sometimes related to the positive and negative phases of the Indian Ocean Zonal Mode.

The moisture flux and wind circulations during non-ENSO years showed significant departures from La Niña/El Niño composites. This suggests that the

involvement of regional surface forcing boundary conditions including vegetation cover, soil moisture and topography of the Tanzanian coastal region may influence rainfall. However, lack of high-resolution data, which can identify these regional forcing conditions, is the main cause of observed difficulties in the seasonal rainfall forecasting.

The intraseasonal analysis results show that increased rainfall during El Niño years was due to longer than normal rainfall season associated with early onset while reduced rainfall during La Niña years was associated with late onset and hence shorter than average rainfall season. The increased rainfall during El Niño years was associated with low-level easterly anomalies during the onset of the rainfall season implying enhanced advection of moisture from the Indian Ocean while the reverse is true for La Niña years. The Hovmöller plots for OLR and zonal wind at 850hPa and 200hPa show the eastward, westward propagating and stationary features over the Indian Ocean. It was observed that the propagating features were absent during strong El Niño years. Based on the Hovmöller results, it is shown that the convective oscillations over the Tanzanian coast have some of the characteristic features of intraseasonal oscillations observed elsewhere.

List of Figures

List-2

6.1(a-c)	Hovmöller plots of OLR and zonal wind at 850hPa and 200hPa for ENSO and post ENSO+1 years.
6.2(a-c)	Climatological pentad rainfall time series plots for the Tanzanian coast.
6.2d	Rainfall time series over the Tanzanian coast for ENSO and ENSO+1 composites.
6.2e	850hPa, 700hPa, and 200hPa zonal wind time series over the Tanzanian coast for ENSO and ENSO+1 composites.
6.3(a-d)	Climatological fields of OLR, moisture flux at 850hPa, wind at 700hPa and 200hPa for P-1, P0, P1 and P+1 of the OND and MAM seasons.
6.4(a-d)	El Niño and El Niño+1 composite anomaly fields of OLR, moisture flux at 850hPa, wind at 700hPa and 200hPa for P-1, P0, P1 and P+1 of the OND and MAM seasons.
6.5(a-d)	La Niña and La Niña+1 composite anomaly fields of OLR, moisture flux at 850hPa, wind at 700hPa and 200hPa for P-1, P0, P1 and P+1 of the OND and MAM seasons.
6.4(a-d)	Anomaly fields of OLR, moisture flux at 850hPa, wind at 700hPa and 200hPa for P-1, P0, P1 and P+1 of the 1997 OND and 1998 MAM seasons.

List of Tables

Acknowledgement.

The Third World Organization for Women in Science (TWOWS) funded this research. Prof. Chris Reason gave constructive criticism and advice as my supervisor and played a significant role in the interpretation of the results and correction of the final report. Special thanks are extended to Dr. D. Jagadeesh for tireless support and guidance on computing and plotting. Valuable and constructive comments and suggestions were available at different stages of my study from members of Climate System Analysis Group (CSAG). My thanks goes out to the National Center for Environmental Prediction (NCEP) and the National Center for Atmospheric Research (NCAR) for providing data on the internet through their website http://www.cdc.noaa.gov/. I am also grateful for ENSO documents received from WMO.

I wish to thank the government of Tanzania for giving me the permission to travel outside the country. I am also grateful to the Director General and staff of the Tanzania Meteorological Agency who not only provided the data but granted me the study leave. I would like to thank Dr. Henry Mulenga of the Oceanography department, university of Cape Town for valuable discussion.

Finally, and more important, profound thanks are extended to my husband Mwara, and our children, David, Doreen and Elizabeth for their patience and understanding. Their prayers together with church prayers gave me the required impetus to go on. Many thanks go to my lord and saviour Jesus Christ, who has been a source of strength, peace and joy during the period of this research.

CONTENTS

Chapter 1: Introduction.

The economy of Tanzania largely depends on rain fed agriculture, which is highly vulnerable to the amounts and distribution of rainfall. Both cash and food crops are vulnerable to extreme fluctuations in amounts and distribution of rainfall. Extreme occurrences results in droughts and floods, which are common in Tanzania but their frequency and severity, varies from one area to the other and also from year to year. Extreme weather events are often associated with food, energy and water shortages, loss of life and property, and many other socio-economic disruptions. The adverse effects of drought and floods can be minimized if skilful short and long-range forecasting methods are available.

In order to acquire the capability to predict extreme climate variability a thorough understanding of the meteorological mechanisms is needed. Nicholson (1996) has noted that East African rainfall is clearly linked to large- scale features of the general circulation including sea-surface temperatures. Camberlin (1995) and Mutai *et al.* (1998) have shown significant relationships between rainfall over East Africa and the atmospheric flow pattern over the region. Janowiak (1988) showed evidence of association between rainfall anomalies during the austral summer over eastern and southern Africa and both the warm (El Niño) and cold (La Niña) phases of ENSO events. The improving skill in predicting ENSO phases up to a year in advance suggests good prospects of successful applications of ENSO forecasts to seasonal rainfall prediction in Tanzania. Indeje et al (2000) found unique seasonal evolution patterns in rainfall over East Africa during the different phases of the ENSO cycles. They suggested that the observed patterns can be applied in conjunction with skilful long lead up to 12 months ENSO prediction. Goddard and Graham (1999) found high correlation between SST variability in the Indian and Pacific Oceans with Pacific leading by 3 months and speculated approach to climate prediction over central-east and southern Africa. ENSO explains about 50% of the East African rainfall variance (Ogallo, 1988), with other factors explaining the remaining variance.

This study is confined to the analysis of the teleconnection between seasonal rainfall in the Tanzanian coast with phases of ENSO. The following section gives a brief explanation of what is meant by the term teleconnection.

1.1 Teleconnection.

Earlier work by Walker and Bliss (1932, 1937) and Namias (1963), among others, provided evidence of relationships between meteorological variables at remote locations of the world. Many of these relationships have been based on fluctuations of Sea Surface Temperatures (SST) and the Southern Oscillation, the North Atlantic Oscillation and more recently the Quasi- Biennial Oscillation. The atmosphere is a compressible, rotating, 'spherical' fluid with both density and temperature gradients, and so it can support a great variety of wave motions. Waves in the atmosphere can be considered as perturbations on a slowly changing background. They propagate energy from one place to the other. Tropical and subtropical heat sources are able to force equatorial Kelvin, Rossby and Yanai waves (Gill, 1980) and off equatorial Rossby waves (Hoskins et al, 1999) which can propagate vast distances to interact with remote regions in the tropics and extra tropics. This wave propagation is likely to have global impacts on intra-seasonal to interannual time scales. On account of their relatively large wavelengths and periods, Rossby and Kelvin waves are considered important dynamical links in weather anomalies in the tropics and extra-tropics through interaction with extra-tropical waves and meridional circulation (Matsuno, 1966).

It is now believed that any large persistent mechanical (e.g.orographic) or heat (SST) source near the equator can excite Rossby and Kelvin waves. A clear example is the interaction between Africa and the maritime continent, which occurs during October-December when there is a tendency for an equatorial east-west heating anomaly pattern across the Indian Ocean whose origin is believed to be linked to tropical heating dynamics (Reverdin et al, 1986) and

which, in part, gives rise to East Africa-ENSO teleconnection at this time of the year. Hirota (1978) observed the dominant semi-annual oscillation of easterly and westerly winds in the stratosphere. These large-scale waves in the atmosphere propagate energy from forcing regions to the impact regions resulting into worldwide climate anomalies, which are referred to as teleconnections. Sir Gilbert Walker (1923, 1924, 1928) documented the teleconnections between El Niño and climate anomalies in the Indian subcontinent.

El Niño /Southern Oscillation can have profound effects on global weather and ocean conditions. Under non-El Niño conditions, trade winds in the equatorial Pacific normally blow from east to west and form the near surfaces branch of the Walker Circulation (Bjerknes, 1969). This causes warm surface water to pile up in the western equatorial Pacific and cool subsurface water to upwell off Peru. Generally, high pressure builds over the cool Pacific waters off Peru producing stable atmospheric conditions while low pressure and convective precipitation develops over the maritime continent. Since Bjerknes's introduction of the Walker Circulation, similar east-west circulation cells spanning different longitudinal sectors along the Equator have been identified. Today, the Walker Circulation generally refers to the totality of the circulation cells as shown in figure 1.1. This is the mean circulation, which controls climate all over the tropics. The shift in location of the ascending and descending branch of the Walker Circulation which occur in association with tropical SST and convection anomalies leads to wave generation and propagation both zonally and meridionaly. Then large scale waves results in near global climate anomalies in regions remote for the origin forcing and comprises the teleconnection process.

In short, teleconnections refer to atmospheric interactions between widely separated regions that may be identified through statistical correlations in space and time. For example, anomalously wet conditions in tropical East Africa have been found to be associated with El Niño (Indeje et al, 2000). Therefore teleconnection in this study refers to the process of associating a specific societal impact thousands of miles away from the core ENSO region of the tropical eastern Indian Ocean/western Pacific Ocean with the rainfall anomalies along the coast of Tanzania.

1.2 Ocean–atmosphere- coupling ENSO.

The ENSO phenomenon is now recognised as a remarkable example of coupled ocean-atmosphere interactions, centered in the tropical Indo-Pacific but with worldwide impacts. The ability of models to forecast certain ENSO parameters (e.g. Niño 3.4 SST) and the coherence of its impact in certain locations facilitates the long range forecasting of major anomalies of weather around the globe.

In tropical Eastern Africa, the conventional knowledge of the regional circulation suggests that there are two primary factors which may determine the climate anomalies during ENSO events. The first factor is associated with the longitudinal shifts in the rising branch of the Walker circulation. During the warm phase of ENSO, positive rainfall anomalies tend to occur during the October to December short rain season. This is also accompanied by enhanced moisture availability associated with the evolution of positive SST anomalies and hence increased evaporation over the western Indian Ocean, which would also favour positive rainfall anomalies during the short rains. The second factor tends to counteract the effect due to the shift in the Walker circulation. During the warm phase of ENSO, reduced surface pressure due to the higher temperatures over

the Indian Ocean adjacent to Eastern Africa could lead to weaker land-sea pressure gradient. This weakening could result in offshore wind anomalies and hence suppress the transport of moisture towards the interior of the region, contributing to reduced rainfall. (Semazzi and Indeje 1999)

Using various numerical model experiments Goddard and Graham (1999) demonstrated the importance of the Indian Ocean atmospheric response for simulating rainfall over East Africa. They indicated that the central-eastern/southern African dipole pattern arises primarily from circulation changes induced by changes in SSTs and convective heating in the tropical Indian Ocean, with considerable modification from changes directly forced from the Pacific. They summarised the dynamics involved as follows: firstly, warmer (cooler) SSTs in the western tropical Indian Ocean produce convergent (divergent) flow and enhanced (diminished) convective heating resulting into decelerating and convergent westerly (accelerating and divergent easterly) low-level flow and moisture flux over central East Africa. And secondly, increased (decreased) convective heating in the low-latitude western Indian Ocean, induces the formation of anomalous cyclonic (anticyclonic) circulations off southeast Africa contributing to moisture flux convergence (divergence) and increased (decreased) rainfall over central-East Africa. They concluded that during El Niño years, the Indian Ocean warms produce an anomalous convergent moisture flux over central-East Africa, which is a consequence of less vigorous flow into western equatorial Africa and anomalous cyclonic circulation over the Indian Ocean off southern Africa. They further noted that during La Niña episodes these changes are approximately reversed.

1.3 Tanzania Rainfall Variability.

In the tropics, rainfall occurs mainly via organized deep cumulus convection embedded in a large-scale disturbance, with most precipitation occurring in a confined area. The daily rainfall can vary greatly within a few hundred kilometers while long-term means may be similar throughout an area. Southern and western parts of Tanzania including the southern coast, experience one rainfall season (November to April fig 1.2a) whereas northern Tanzania including the northern coast experience two rainfall episodes (short rains in October to December and long rains in March to May fig 1.2b) in sympathy with the movement of the ITCZ. The lag period between the latitudinal cycle of the sun and the ITCZ is between one to two months (Riehl, 1979; EAMD 1963b)

Despite the fact that Tanzania lies within the tropics, considerable variations of climate occur throughout the country on account of complex topographical patterns, the existence of large lakes, variations in vegetation type and land-ocean contrasts. The country lies within 1-12°S and 29-41°E, covering an area of about 945,000 km² between the great East African lakes, namely: Lakes Victoria in the north, Tanganyika to the west and Nyasa to the south. To the east, lies the Indian Ocean. The country includes Africa's highest point (Mount Kilimanjaro, 5950m above sea level) and lowest point (the floor of Lake Tanganyika, 358m below sea level). However most of Tanzania, except the eastern coastline lies above 200m altitude.

Unlike the mid-latitudes where climatic seasons are classified in terms of temperature, rainfall is the climatic factor of maximum significance in the tropics, with extreme occurrence resulting in droughts and floods. Topography plays an important role in the rainfall distribution over Tanzania. Annual rainfall totals vary from 500mm in the drier central areas to just over 1000mm in the wet areas,

although the coastal regions including the Islands of Zanzibar and Pemba and parts of southwestern Tanzania may receive over 1500mm (Griffiths, 1972).

The area of study in this thesis covers the region enclosed by latitudes 4°S-12°S and longitudes 38.5°E-41°E (fig 2.1). The area north of 8°S experiences two main rain seasons, namely the long rains (March-May) and the short rains (October – December), which are associated with the northward and southward movement of the ITCZ respectively. The Southern coast (south of 8°S) experiences one rain season November to April. The onset and end of the rainfall seasons over Tanzania has received considerable attention, with work by Alusa and Gwange (1978), Mhita and Nassib (1987), Mhita and Venäläinen (1992) among others. In their study using time series of rainfall station observed data Mhita and Venäläinen looked at reliability and variability of rainfall in different regions of Tanzania. They discussed the start and end dates of the rains, looked at the occurrence of long dry spells and the probability of rainfall exceeding certain threshold in ten days. They found that in single peak rainfall areas, rainfall starts between mid-November and early December and ends between mid-April and mid-May. For double peak areas, the short rains (OND) begin by 25 October and end by mid January while long rains (MAM) start by mid-March and end by early week of June. On the basis of a few selected stations, they found that the probability of long dry spells exceeding15 days during OND season does not fall bellow 50%.

Besides the seasonal migration of the ITCZ, other factors known to influence rainfall over Tanzania include Monsoon wind systems, Tropical cyclones, Subtropical cyclones, Land and sea breeze, the African jet streams, Easterly/Westerly wave perturbations and thermally induced meso scale circulations (Ogallo, 1989, Hills, 1979 and Nyenzi, 1984). Teleconnections with global scale system like the El Niño/ Southern oscillation (ENSO) play an important role, which is the main focus of this research.

In this thesis, linkages between the observed rainfall anomalies in the Tanzanian coast with ENSO years are investigated, and monthly rainfall patterns associated with the various ENSO signal in both Indian and Atlantic Ocean identified. In an attempt to establish relationships between SST, wind, velocity potential, OLR, latent heat and moisture flux over the tropical Indian and Atlantic Ocean with rainfall anomalies in the coast of Tanzania during ENSO events, a composite approach (e.g. Rasmusson and Carpenter, 1982) and year to year analyses were carried out.

Intraseasonal variability was also given attention in this research. In Tanzania, agriculture is mainly rainfed. Therefore the intraseasonal research is important for the benefit of farmers. In some areas agriculture is limited by the length of the rain season while in others it is amount limited (Mhita, 1984). Long dry spells can lead to withering or complete failure of some crops while prolonged wet spells can lead to flooding of farms thus destroying crops. Therefore intraseasonal rainfall forecasts can assist farmers in decisions regarding planting, fertilising, pesticide application, irrigation demand etc.

This introduction has provided the scientific background of ENSO and Tanzanian rainfall variability. Following this introduction, a review of past research concerning the teleconnection between ENSO and East African rainfall is presented in chapter 2. Chapter 3 describes the data and the analysis methods while chapter 4 gives a brief outline of the monthly climatology. Chapters 5 and 6 present the interannual variability and intraseasonal variability results respectively and chapter 7 provides a summary and the conclusions.

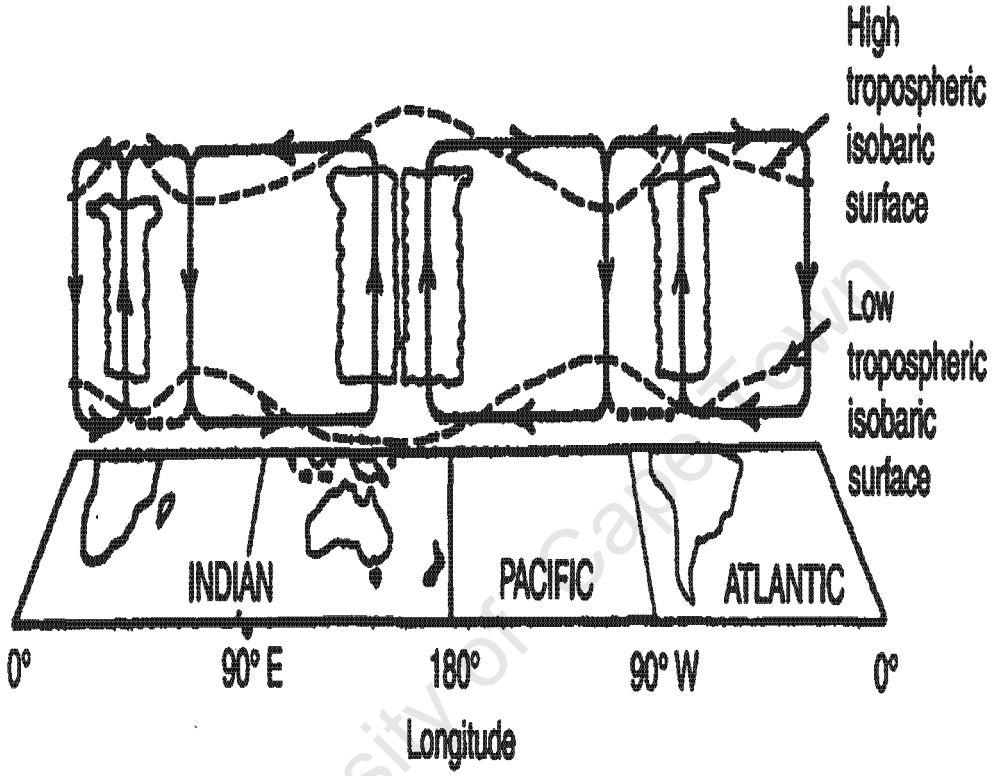

Figure 1.1: Walker Circulation. (Adapted from Webster (1983).)

a

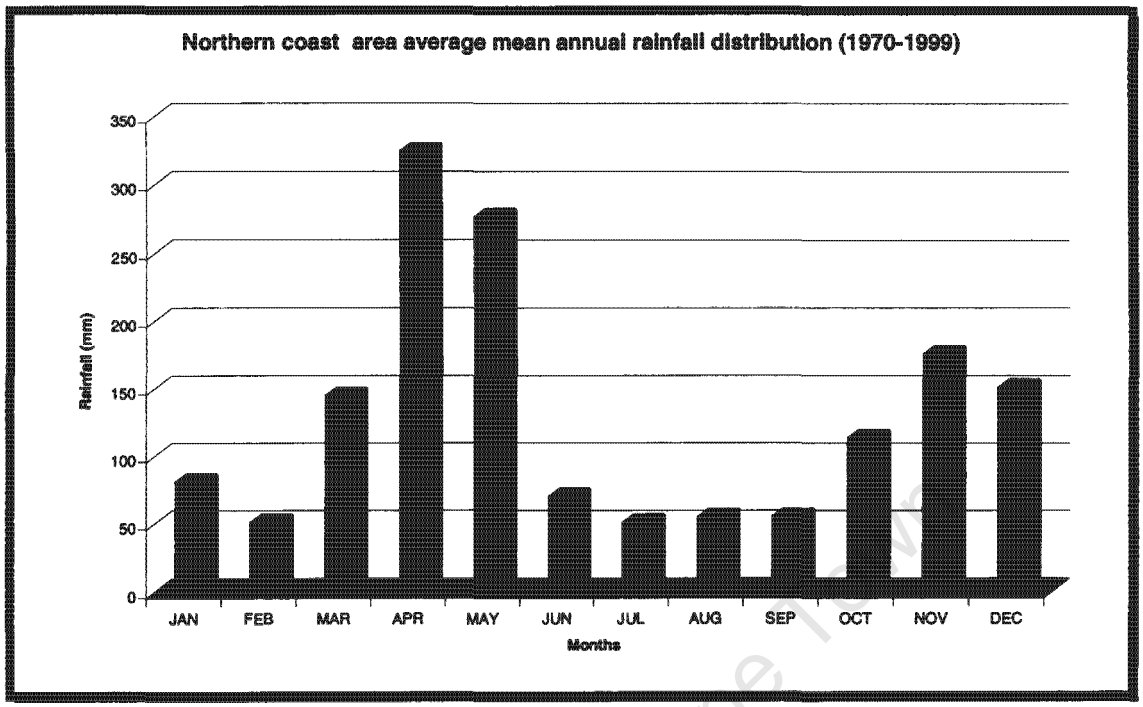

b

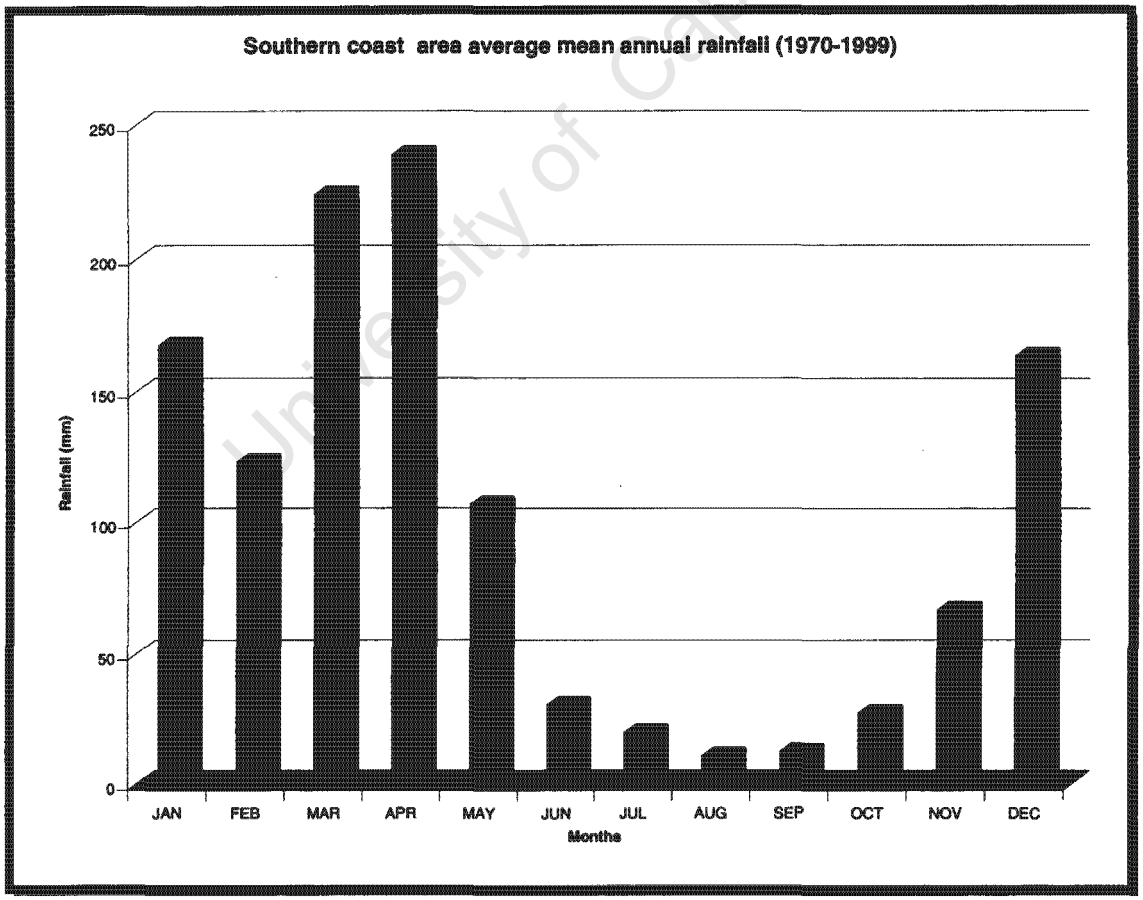

Figure 1.2: Northern coast (a) and southern coast (b) area averaged mean annual rainfall.

Chapter 2: Previous Research

2.1 East African rainfall variability.

Rainfall in East Africa (Uganda, Kenya and Tanzania), exhibits great spatial and temporal variability (Ogallo, 1989). The rainfall seasons are ambiguous and complex with no single month during the year when all East Africa is dry. The variations of rainfall over East Africa operate on a number of time scales, from diurnal (Johnson, 1962; Asnani and Kinuthia, 1979) to quasi-periodic fluctuations on interannual, interdecadal and longer scales (Ronde and Virji, 1976; Nicholson, 1996). The seasonal patterns of rainfall in East Africa follow the seasonal patterns of the Inter Tropical Convergence Zone (ITCZ), which lags the seasonal migration of the overhead sun by four to six weeks (EAMD, 1963b). Most parts of the equatorial East African region have two main rainfall seasons: March-May (long rains period) and October-December (short rains period). The former rains are more abundant but the latter tend to be more variable.

Much attention has been given to rainfall variability over Eastern Africa (Ogallo, 1983, 1988; Barring, 1988; Beltrando, 1990; Nicholson, 1996). Ogallo (1980) and Ogallo et al. (1994) have shown the existence of three major peaks, centered on the Quasi-Biennial Oscillation (QBO) of 2.5-3.7 years, El Nino-Southern Oscillation (ENSO) of 4.8-6 years and quasi-decadal of 10-12.5 years. Nicholson and Nyenzi (1990) and Nicholson (1996) observed a strong quasi-periodic fluctuation in the East African rainfall with a time scale of 5-6 years corresponding to the ENSO and sea surface temperature (SST) fluctuations in the equatorial Indian and Atlantic Oceans.

The interannual variability of the East African seasonal rains results from a complex interaction between SST forcing, large scale atmospheric patterns and synoptic scale weather disturbances, including monsoon and trade winds especially in the Indian Ocean, the African jet streams, sub-tropical anticyclones, tropical cyclones, easterly/westerly wave perturbations and extra tropical weather systems (Krishnamurti, 1961; Fremming, 1970; Krishnamurti et al., 1973; Cadet

and Diehl, 1984; Ogallo, 1988; Okeyo, 1986; Ogallo *et al.*, 1989; Mukabana and Pielke, 1991). In general considering its equatorial position, East Africa does not receive much rainfall (Griffith, 1972). In the past, East Africa has suffered from serious meteorological droughts (extended periods of anomalously low rainfall), particularly in Kenya and Tanzania, as shown by instrumental climate records for the past 100 years. On the other hand, some parts of East Africa are not spared from floods; a remarkable example is the catastrophic flooding of 1961/62, which resulted in a dramatic increase in level of Lake Victoria, and increased White Nile discharge (Flohn, 1987, Conway and Hulme, 1993, Mistry and Conway, 2003). A more recent example of unusually heavy rains occurred during the short rains of 1997.

2.2 Teleconnections of East African rainfall with El Niño–Southern Oscillation (ENSO).

The El Niño/Southern Oscillation, or ENSO, causes fluctuations in sea surface temperature over the equatorial Pacific Ocean with regional climate extremes in many parts of the globe. The recurring pattern of droughts and floods observed during 1972-73, 1982-83 and 1997-98 broadly describe the climate extremes associated with strong warm ENSO or (El Niño) events. The ENSO phenomenon has been studied largely in the context of the Pacific Ocean and adjacent regions, although research has long established that it is a global-scale phenomenon (Horel and Wallace, 1981, and Arkin, 1982). Worldwide teleconnections in rainfall including areas of eastern Africa, where El Niño events produce abnomally high rainfall have been established (Kiladis and Diaz, 1989, Nicholson and Entekhabi, 1986). In sub-Saharan Africa, the most dominant mode of interannual climate variability appears to be ENSO (Ropelewski and Halpert, 1987), characterized by a rainfall anomaly pattern over Eastern and Southern Africa. Tourre and White (1997) and Reason *et al* (2000) show strong evidence of ENSO signals in the Indian Ocean.

Tropical Eastern Africa is one of the areas where global ENSO impacts have been reflected in both precipitation and temperature anomalies. It has long been noted that interannual variability in rainfall over East Africa during the October to December season correlates strongly with the sea surface temperature (SST) changes in the tropical Pacific associated with the El Niño- Southern Oscillation (ENSO) phenomenon (Stoeckenius, 1981; Ogallo 1988). Numerous studies have illustrated that gradually varying surface boundary forcing conditions, including SST and vegetation cover, influence variability of tropical general circulation patterns on seasonal and longer time scales (Charney, 1975; Charney and Shukla, 1981). Empirical studies by Cadet and Beltrando (1987), Ininda (1994), and Latif *et al* (1999) have demonstrated the existence of an association between rainfall variability in East Africa and SST patterns.

Several studies have investigated the relationship between East African rainfalls with ENSO. Indeje et al (2000) for example, found a strong relationship between rainfall over East Africa and phases of ENSO. Their results showed that ENSO plays a significant role in determining the monthly and seasonal rainfall patterns in East African region. They observed shifts in the onset/cessation of rainfall patterns over some regions while in others a significant reduction in the seasonal rainfall peak was evident. Nicholson and Kim (1997) found a strong connection between ENSO and rainfall over much of the African continent and suggest a linkage through ENSO induced SST anomalies in the Indian Ocean, which in turn modulate interannual variability of rainfall over Africa. They further noted that ENSO has little influence on long rain season (MAM) but significantly modulates the short rains (OND). Hastenrath et al (1993) found that the East African short rain season is related to the Southern Oscillation through zonal pressure gradients produced by SST anomalies in the Indian Ocean. During La Niña events, SST anomalies are cool in the western Indian Ocean and surface westerly wind anomalies result in lower tropospheric divergence over equatorial

East Africa. A global La Niña thus acts to suppress convection from October to December.

Further support for those observational findings was provided by Goddard and Graham (1999). Using an atmospheric general circulation model forced with various combinations of Indian and Pacific SST anomalies, these authors noted that while the SST variability of the tropical Pacific exerts some influence over the African region, it is the atmospheric response to the Indian Ocean variability that is essential for the model simulating robust rainfall responses over eastern, central and southern Africa. They further noted that during La Niña years, large-scale moisture flux divergence was observed at low levels over the Indian Ocean centered at 5°S and 80°E.This divergence was accompanied by anticyclonic and cyclonic circulations at 850hPa east of southern Madagascar and western Australia respectively resulting in reduction of rainfall over East Africa. During El Niño years, the model results produced roughly the reverse situation. Anomalous moisture flux convergence over the western Indian Ocean with cyclonic circulation centered southeast of Madagascar and anomalous anticyclonic circulation centered west of northern Australia led to increased rainfall over East Africa. Precipitation patterns during ENSO extremes were studied by Kiladis and Diaz (1989), they observed that equatorial eastern African signal first appears during SON and appears to be the western extension of large region of heavy rainfall covering the western Indian Ocean at this stage of a warm event, as reflected in the strong signal in the Seychelles during both phases of ENSO.

Many studies have been carried out in the past to investigate the association of some extreme rainfall anomalies in East Africa with ENSO (Ropelewski and Halpert, 1987; Janowiak, 1988; Ogallo, 1988, among others). Ropelewski and Halpert (1987) found statistical associations between rainfall over East Africa and SOI to be weak but they concluded that there is a high probability of abnormally wet conditions in the region during El Niño years. The 1997-1998 ENSO event

associated with catastrophic disruption of socio-economic infrastructure and loss of life in East Africa appears to give further support to this notion. Ogallo (1988) observed significant teleconnection between the Southern Oscillation Index (SOI) and abnormally wet/dry conditions over parts of East Africa. Janowiak (1988) found the association between rainfall anomalies over Eastern and Southern Africa and both cold and warm phases of ENSO events. Amissah-Arthur *et al* (2002) observed that all El Niños are not equal in terms of their regional impact on East African rainfall. Nicholson (1997) indicated that the ENSO signal in African rainfall variability is a manifestation of ENSO's influence on SSTs in the Atlantic and Indian Oceans and, in turn, their influence on rainfall. She found the timing of warming and cooling to be constant in the Indian Ocean.

Some studies indicate significant decadal-multidecadal variability in ENSO and its expression over the Indian Ocean / African region (e.g. Richard et al 2001, Reason and Rouault 2002, Allan et al 2003). There is also evidence of decadal variability in African rainfall (Nicholson 2000). However, this thesis focuses only in interannual and intraseasonal variability, possible decadal signals in Tanzanian coastal rainfall are not considered herein.

The relationship between the pre-rainfall season SST anomaly patterns and the inter annual variability of short rains (OND season) over East Africa were demonstrated by Mutai et al (1998). They found moderately strong relationship between July-September Sea Surface Temperature (SST) patterns and October –December (OND) seasonal rainfall total averaged across East Africa. Similarly Ogallo (1988) found a strong relationship between ENSO and East African rainfall, he suggested that ENSO explains about 50% of East African rainfall variance. Ogallo and Suleiman (1987) observed that the chance of receiving below normal rainfall in East Africa associated with El Niño events, is low for most parts of the region during both OND and MAM season. Similar results observed by Njau (1987) from 300hPa temperatures and the Southern Oscillation

Index. Ogallo (1989) noted that some East African rainfall principal component patterns could be associated with warm and cold episodes over the eastern Pacific. Most previous work looked at the association of ENSO with regional East African rainfall while this thesis focuses particularly on the influence of ENSO on rainfall over the Tanzanian coast.

SSTs in the Indian and Atlantic oceans have important influence on rainfall variability over Africa (Nicholson et al 2000, Reason et al 2000). These SST anomalies in the Indian Ocean may arise in different ways. Reason et al 2000 focused on the seasonal evolution of the ENSO signal over the Indian Ocean while Saji et al (1999) and Webster et al (1999) proposed on east-west SST anomaly patterns, the so-called tropical Indian Ocean dipole or Indian Ocean zonal mode. This mode may sometimes strongly influence OND rainfall over East Africa, e.g. in 1997. Saji et al (1999) found that during a dipole mode event rainfall decreases over the Oceanic Tropical Convergence Zone (OTCZ) and increases over the western tropical Indian Ocean consistent with convergence/divergence shifts associated with the wind field thus suggesting strong empirical evidence for coupling between the SST and wind field through the precipitation field. They further noted that the shift of the convergence zone, manifest the weakening or reversal of the zonal (Walker) circulation across the Indian Ocean, which leads to floods in East Africa and drought in Indonesia. They concluded that during dipole mode events the zonal surface wind over the tropical Indian Ocean experiences large changes resulting in anomalous climatic conditions in eastern Africa and Indonesia. They associated the positive dipole mode with above normal rainfall over Eastern Africa and negative dipole mode with below normal rainfall. More recent work (Loschnigg et al, 2003) suggested that the dipole mode is infact an inherent component of the ENSO-monsoon interaction over the Indian Ocean and is not an independent mode as originally suggested by Saji et al (1999).

2.3 Intra seasonal variability

Over 30 years ago, Madden and Julian (1971) detected an intraseasonal (ISO) in the zonal wind in the tropics, which today is generally known as the Madden Julian 40-60 day Oscillation (MJO). According to Weickman *et al* (1985), certain properties of 40-60 ISO have been established and have been associated with eastward moving equatorial- trapped Kelvin waves. However Anyamba (1992) have reported meridional propagation in the Indian Ocean region. Vincent *et al* (1991) found that the MJO is absent during the austral winter and they further observed that velocity potential and OLR were the best indicators of the oscillatory convective activity. Rui and Wang (1990) have explained the temporal evolution of ISO's in the equatorial region. They documented the development and dynamic structure of tropical intra-seasonal convection anomalies using 5-day mean anomalous OLR and ECMWF analysed 200 and 850 hPa wind data. A study by Makarau (1994) observed intra-seasonal oscillations with two cycles: 10-25 and 40-50 days, when studying wet and dry spells in Zimbabwe summer rainfall. Similarly Levey (1993) found 20-35 day oscillations in precipitation and evaporation pentad time series for central South Africa during austral summer.

Other intra-seasonal oscillation studies, which link tropical Africa and the adjacent oceans, include the study by Zhu and Wang (1993) who observed two prominent action centres in the central Indian and western Pacific oceans for tropical 30-60 day convective variability. Anyamba (1992) has identified the 20-30 day oscillation in the tropical outgoing long wave (OLR) spectra in the western Indian Ocean and found that while the 40-50 day ISO is characterized by an eastward propagating wave in the Indian and West Pacific Oceans, the 20-30 day ISO has a much weaker zonal propagation. Some different studies have revealed the ISO in the tropics to have periods of oscillation between 16-76 days, with coherence between areas of upper air divergence and areas of convection. On Intraseasonal time scales, not much work has been done on Tanzania

signals and this study will help to fill the gap. Chapter 6 of this thesis considers the intraseasonal oscillations over the Tanzanian coast.

2.4 Objective and motivation of the study.

The previous sections of this chapter reviewed previous research on East African rainfall variability and its association with ENSO. Certain areas of ENSO-induced SST anomalies in the Indian and Atlantic Ocean have been considered as key areas linked to anomalous wet/dry conditions over some regions of East Africa. Most of this work has dealt with rainfall averaged over the region with relatively few investigators considering the association of ENSO and rainfall over specific sub regions of East Africa. Further more many investigators concentrated on the association of ENSO with averaged seasonal rainfall variability. This research will help to fill the gap by investigating the month-to-month variability rather than averaged seasonal variability. The thesis will also put emphasis on intraseasonal variability, from which relatively little research has been done for Tanzania (Kabanda 1995, Mpeta, 1997). These authors did not look at how ENSO influence the intraseasonal variability and there fore this thesis intends to address that gap.

Coastal Tanzania has a high population and is important for the natural economy through marine transportation, industry and tourism. The main aim of this research is to examine the time space evolution of the El Niño /Southern Oscillation (ENSO) signal in the equatorial Atlantic and Indian Ocean, and to investigate the observed teleconnections with rainfall over the coastal regions of Tanzania with a view of extracting the main seasonal rainfall precursors during ENSO years.

To accomplish the above-mentioned aim of the study the following research questions will be addressed.

- How does seasonal rainfall in the Northern and Southern coast of Tanzania respond to El Niño and La Niña induced SST anomalies over the equatorial Indian and Atlantic Oceans?
- What are the mechanisms associated with seasonal rainfall over northern and southern coast of Tanzania during El Niño and La Niña years?
- What are the main precursors of rainfall over northern and southern coast of Tanzania?
- What is the nature of the intraseasonal rainfall variability over coastal Tanzania and how is it related to ENSO?
- What other modes of interannual variability (e.g. the Indian Ocean zonal mode) influence coastal Tanzanian rainfall?

Chapter 3 will discuss the data used and methods of analysis.

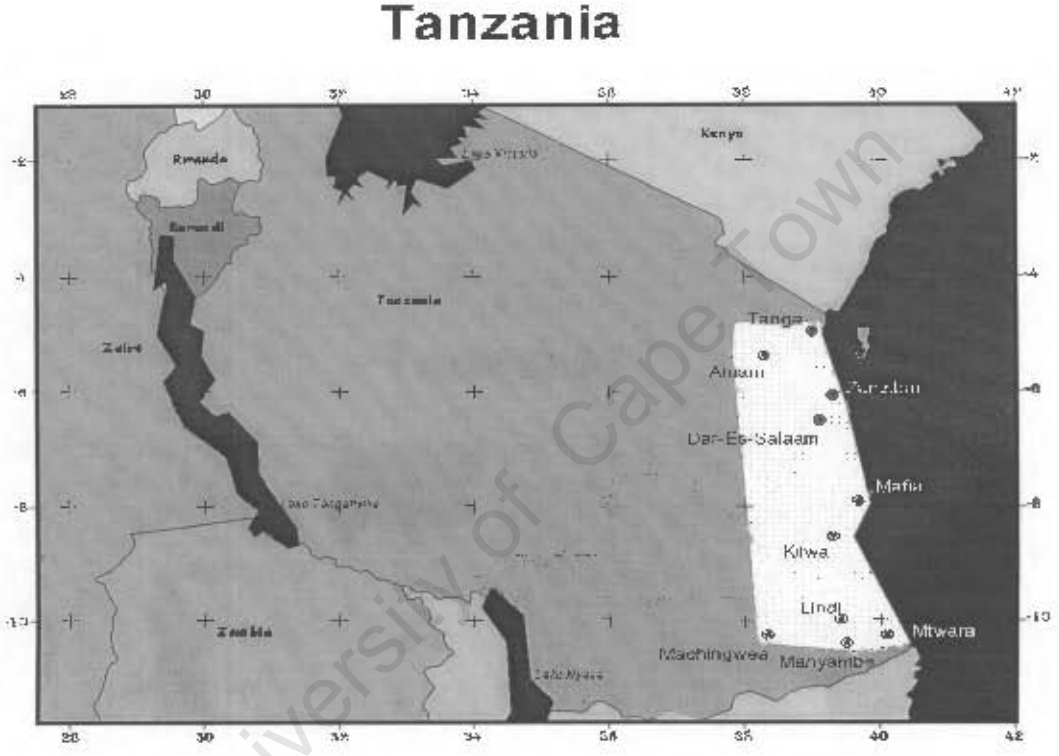

Figure 2.1: Map of Tanzania showing the study region (shaded) and rainfall stations used in the study

Chapter 3: Data and methodology.

3.1 Data.

3.1.1 Introduction.

This chapter discusses the data used and the methods of analysis. Many studies have been undertaken to assess the currently available model-based global data sets of atmospheric circulation. These data sets have been useful for studying dynamical and physical processes and for describing the nature of the general circulation of the atmosphere. Studies made by Bengtsson and Shukla (1988) have observed that not all the available model based global data sets are suitable for studying global climatic variability. They stated reasons such as limitations in the early data assimilation system and inconsistencies caused by numerous model changes. However, the NCEP/NCAR data sets (Kalnay et al. 1996) can be used in the current study to address the rainfall variability related to El Niño/ Southern Oscillation (ENSO) over the coast of Tanzania.

3.1.2 Rainfall station data.

The rainfall station data used in this study consists of monthly totals obtained from the Tanzania Meteorological Agency. The database includes data from 10 rainfall stations scattered throughout the coast of Tanzania as illustrated in figure 2.1.The period 1970-1999 was selected since all stations had continuous quality records. The rain gauge used in Tanzania since 1921 is the standard 12.9cm and rainfall is measured at a height of 25cm above the surface.

3.1.3 Rainfall CMAP data.

The CMAP precipitation data used in this study is the merged Satellite, Rain Gauge, and model precipitation estimates discussed in Xie *et al* (1997). These data are gridded with a resolution of 2.5x2.5 degrees. To assess intra-seasonal variability, the data were analysed in the form of pentads (non-overlapping 5-day means) starting at pentad 1 for each year (1-5 January) and ending at pentad 73 (27-31 December). Pentad 12 contains an additional day to include Feb 29 in the case of a leap year. Monthly mean values were used for interannual variability.

CMAP data is available from 1979 onwards. Since the period of this study runs from 1970-1999, the rainfall station data is important for comparison with CMAP data and filling the gap where CMAP data is absent.

3.1.4 NCEP reanalysis data

The NCEP/NCAR Project is a joint project between the National Center for Environmental Prediction (NCEP) and the National Center for Atmospheric Research (NCAR) Kalnay et al. (1996). This joint effort has produced atmospheric re-analyses using historical data from 1948 onwards. This effort involves the recovery of land surface, ship, rawinsonde, aircraft, satellite and other data sources. Quality control and assimilating these data is the responsibility of NCEP/NCAR. These data are gridded with a resolution of 2.5x2.5 degrees.

The NCEP/NCAR reanalysis data used in this study consists of zonal and meridional wind components, specific humidity, Sea Surface Temperature (SST), and latent heat flux. Both daily and monthly mean data sets were used. Some parameters such as divergence, velocity potential and moisture flux were derived from these data sets and the detail of derivation procedure is given in section 3.2.3. However, due to the fact that NCEP has probable errors in specific humidity (Kanay et al 1996) this thesis will focus more on the sign rather than the magnitude of the moisture flux. The OLR data used in this study is a product of NOAA.

3.2 Methodology

This section highlights the various methods, which were used in this study. Different analysis techniques have been utilised to understand the association of El Niño/ Southern Oscillation (ENSO) with rainfall variability in the coast of Tanzania. A detailed account of each is discussed:

3.2.1 Interannual variability analysis

3.2.1.1 Rainfall Index formulation

Various indices have been used to assess the intensity of the rainfall anomaly in East Africa. These include the standardized rainfall anomaly index (Ogallo and Nasib, 1984, Kabanda 1999), the decile index, weighted rainfall anomaly index (Ininda, 1987) and many others. The standardized rainfall anomaly index was used in the present study.

In order to investigate the teleconnection between seasonal rainfall in the coast of Tanzania and ENSO, rainfall indices for the Northern and Southern coast were created. To represent the northern coast, two indices for both long rain (MAM) and short rain (OND) seasons were developed (fig. 3.1a&b). The northern coast region includes the stations located to the north of 8°S. The stations to the south of 8°S represent the southern coast with indices for January to March (JFM) and October to December (OND) seasons (fig. 3.2a&b). Mafia that is located at about 8°S is included in the southern coast Index. Although the southern coast rainfall season starts in late October and ends in May, the OND and JFM were chosen to facilitate the investigation of the influence of ENSO phases and SST anomalies. The two indices were used to find the appropriate months where ENSO signal projects itself over the southern coast. The rainfall station data were used for the creation of indices and CMAP rainfall time series were also used for comparison (fig 3.3a-b).

Rainfall data from the 10 selected stations were all normalized appropriately with respect to the means and standard deviation as follows:

$Z = (A-\bar{A}) / \sigma$

where Z is the normalised standard departure of the rainfall, A is individual data point (total rainfall for a month), $\bar{A}$ is the historical mean rainfall and σ is the historical standard deviation. The values of Z provide immediate information about the significance of a particular deviation from the mean (Nyenzi, 1988). An area rainfall index was computed by averaging time series of standardized departures for each month and then combining into seasonal values. This type of normalization has been used by Nyenzi (1988), Levey (1993) and Makarau (1994) amongst others. The control limit used is the zero line where the years with values above zero are considered to be wet while those with values below zero are considered to be dry. However, a departure of at least 1 standard deviation is considered significant. El Niño years are associated with above normal rainfall and La Niña years are associated with below normal rainfall for northern coast. For the southern coast the OND season seems to portray similar features to the northern coast while the JFM season seems to have confused ENSO signals.

Comparison of the Tanzanian coastal station data indices (fig.3.1&3.2) with CMAP data indices (fig3.3a&b) indicates that the wet and dry years generally agree. A detailed comparison is given in chapter 5.

3.2.1.2 Composite analyses

Rasmusson and Carpenter (1982), Matarira and Jury (1992), Reason *et al* (2000) and many others have used the composite analyses techniques to investigate the regional climate variability. Composites are useful for indicating pronounced and common features and patterns in the variables and also reduce the total number of maps and figures associated with each case study. Various ways are used in selecting cases to composite. It is important however, to select cases with similar characteristics to composite. In this study, El Niño/La Niña years are the cases used for compositing. However the analysis of individual cases shows that not all El Niño /La Niña years have the same characteristics. With this in

mind, individual cases were also given attention. The compositing procedure consists of adding each parameter value at the same level at each grid point in the domain for all cases and dividing by the sample size to get the mean value. Monthly analyses were performed starting two months before the season for both composites and individual cases analysis.

3.2.1.3 Cross-Sectional Analyses

Height-Latitude/Longitude cross sections of moisture flux anomaly were used in this thesis to study the moisture flux circulations during ENSO years. The longitude height section was for an average over latitude 15°S and 4°S while the latitude height sections were for the fixed longitudes of 37°E and 40°E. These cross-sections were used to examine the vertical structure of moisture flux associated with the evolution of ENSO signal over the Tanzanian coast.

3.2.2 Intra-seasonal variability analysis.

3.2.2.1 Hovmöller Analysis.

Longitude-time diagrams or Hovmöller plots are useful in identifying zonal propagating features in the atmosphere. Anomalies of OLR and zonal wind at 850hPa, and 200hPa have been plotted in this study to identify propagation of intraseasonal convection oscillation anomalies. Mean values of meteorological parameters between 4°S and 8°S on the northern coast of Tanzania were calculated along each longitude from longitude 38° to 130°E. This was done for both short rain season (OND) and long rain season (MAM) starting from one month before the season and ending one month after the season. Hovmöller diagrams for each ENSO year were plotted. Chapter 6 represents and discusses the results.

3.2.2.2 Time series analysis

Both rainfall and wind pentad data were subjected to time series analysis to examine the intraseasonal variability. Mean values and anomalies of wind and rainfall between 4°and 8°S, 38.5° and 41° E were calculated. Pentad-area averaged rainfall time series were inspected and rainfall onset peak and end dates derived. For the start and end of rains, the method of Mhita and Nassib (1987) was used with a few adjustments. For the northern coast the OND (MAM) rainfall season is considered to be started if 5-day rainfall exceeds 7.5 (10) mm followed by three consecutive pentads having rainfall amount of not less than 5 (10) mm/pentad while in both cases the rainfall ends if three consecutive pentads have mean rainfall of at most 2mm/day. The Southern coast procedure is similar to the MAM season. The detailed criteria used to select the dates are given in chapter 6.

3.2.3 Derived parameters.

The reason for producing secondary derived parameters is that such values when used in combination with primary parameters such as winds and temperature yield results, which describe meteorological dynamics and thermodynamic structure (Parker, 1994).

3.2.3.1 Divergence

Divergence is defined as the acceleration and diffluence experienced by the air in the local horizontal plane. On an isobaric surface a region of divergence is one from which there is a net out flow of air mass. The horizontal divergence in the total two-dimensional velocity field is given by the following equation (Bluestein, 1992):

Divergence = $\partial u/\partial x + \partial v/\partial y$ .....Eq 2.1

where u = zonal wind component.

v = meriodional wind component.

x = longitudinal distance.

y = Latitudinal distance.

3.2.3.2 Velocity potential

Chen and Yen (1991) have shown that the velocity potential at 200hPa is a useful meteorological parameter in the study of climatology. Velocity potential and stream function may be more useful than divergence and vorticity since they are components of the horizontal circulation wind vector and give useful representations in the tropics where mean winds are light. The physical properties of the horizontal two-dimensional wind field (V) can be described by considering the rotational and irrotational terms, also known as non divergent and divergent respectively.

That is: $V = v_\psi + v_\chi$ .....Eq 2.2

where v_ψ is the stream function (rotational) part of the wind, while v_χ is the velocity potential (irrotational) part of the wind (Krishnamurti et al., 1973).The irrotational component of wind was used by various researchers (e.g. Kabanda, 1995, Mistry and Conway, 2003) and seems to give significant structure for Tanzania, therefore it will be used in this study.

3.2.3.3 Moisture flux

The horizontal moisture flux for a given level can be obtained from the product of specific humidity and horizontal wind vector. In the tropics, the bulk of the horizontal transfer of moisture takes place below 700hPa (Newell et al 1972). The low tropospheric wind field can therefore, determine most of the moisture transport. Earlier studies e.g. Goddard and Graham (1999) observed 850hPa level to be the most representative of the behavior of the vertically integrated moisture flux over East Africa. Based on this idea, 850hPa level will be used in this research for analyses of moisture flux.

Having looked at the data used and methods of analysis, chapter 4 will give a brief outline of the climatological fields.

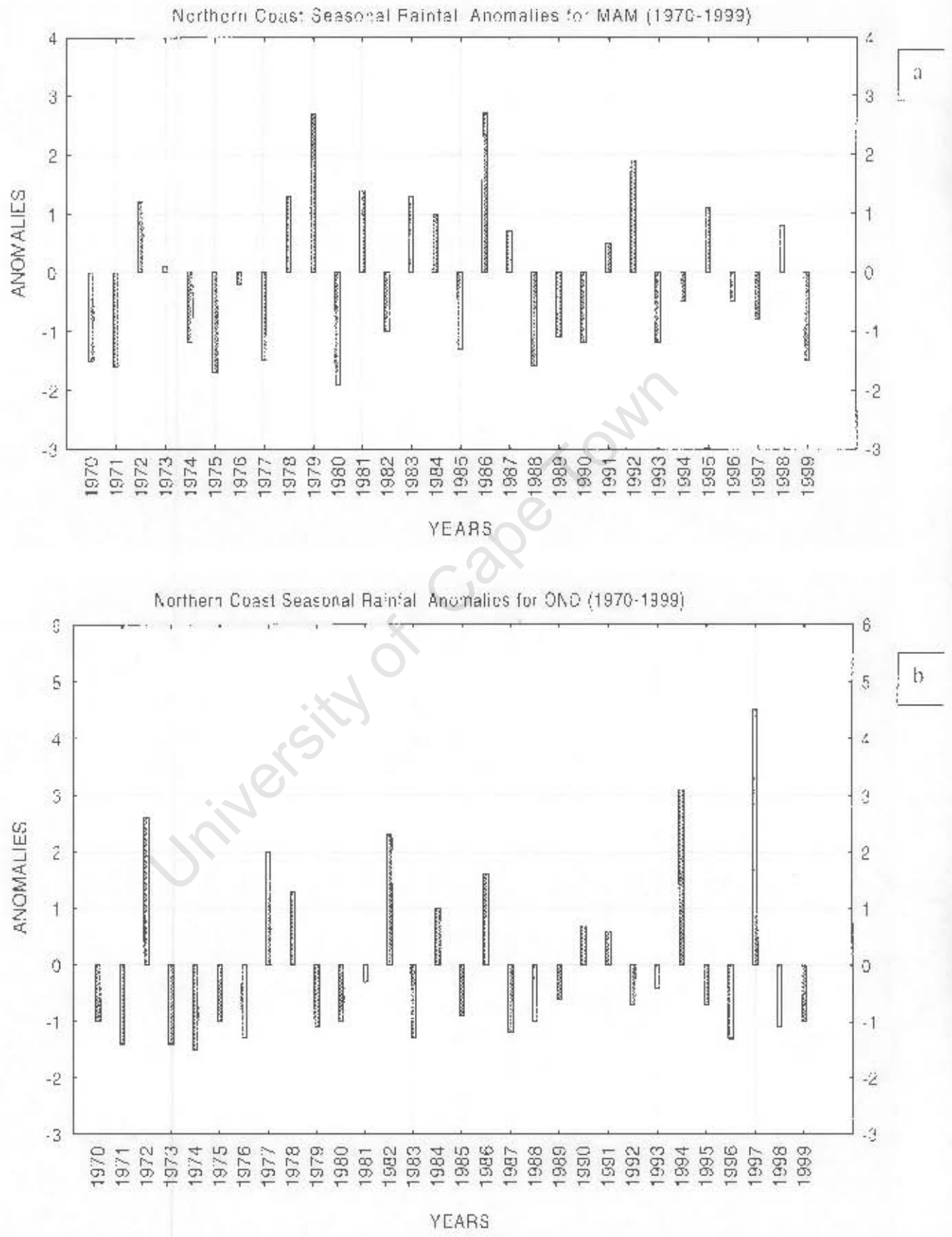

Figure 3.1: MAM (a) and OND (b) rainfall time series for the northern coast of Tanzania.

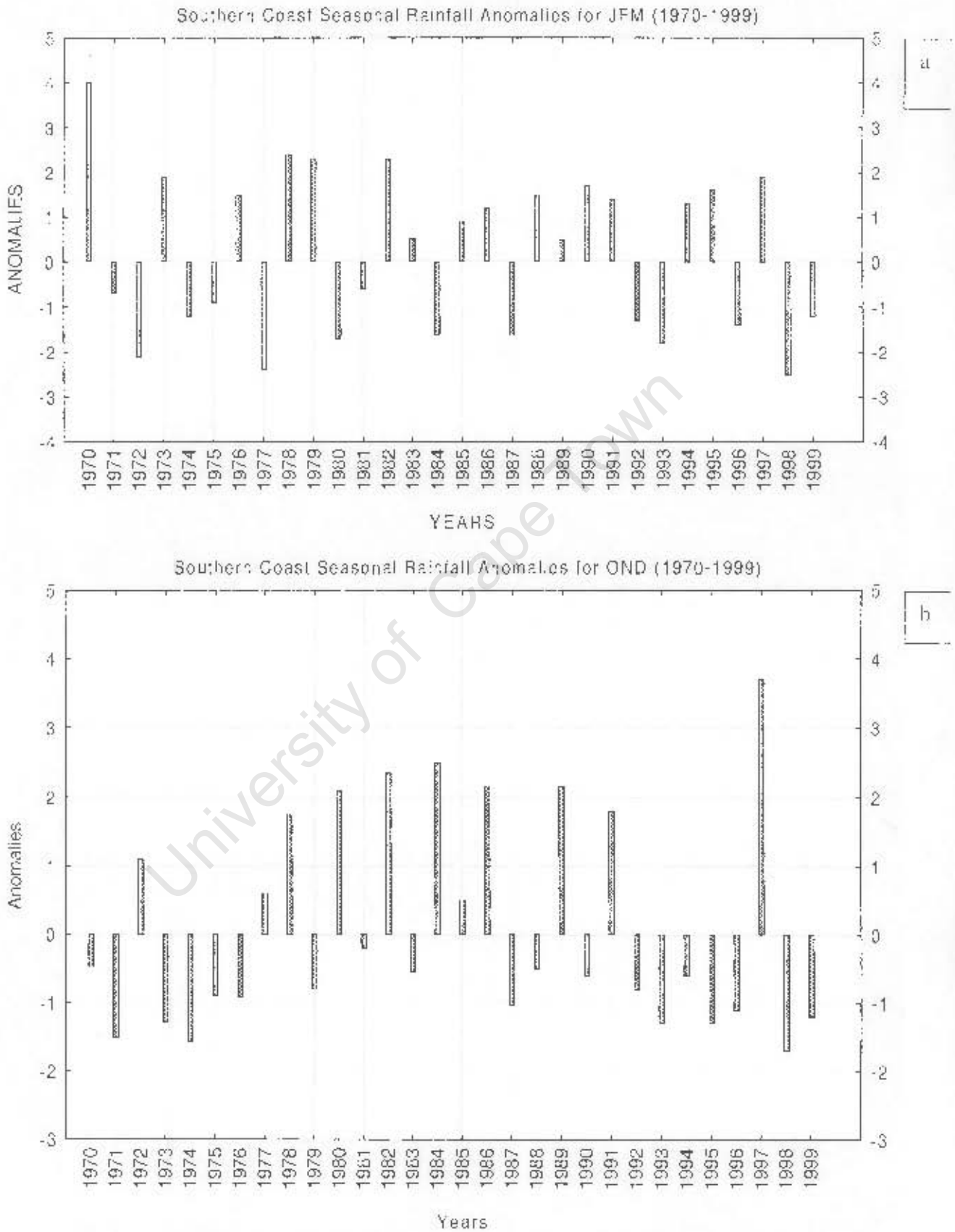

Figure 3.2: JFM (a) and OND (b) rainfall time series for the southern coast of Tanzania.

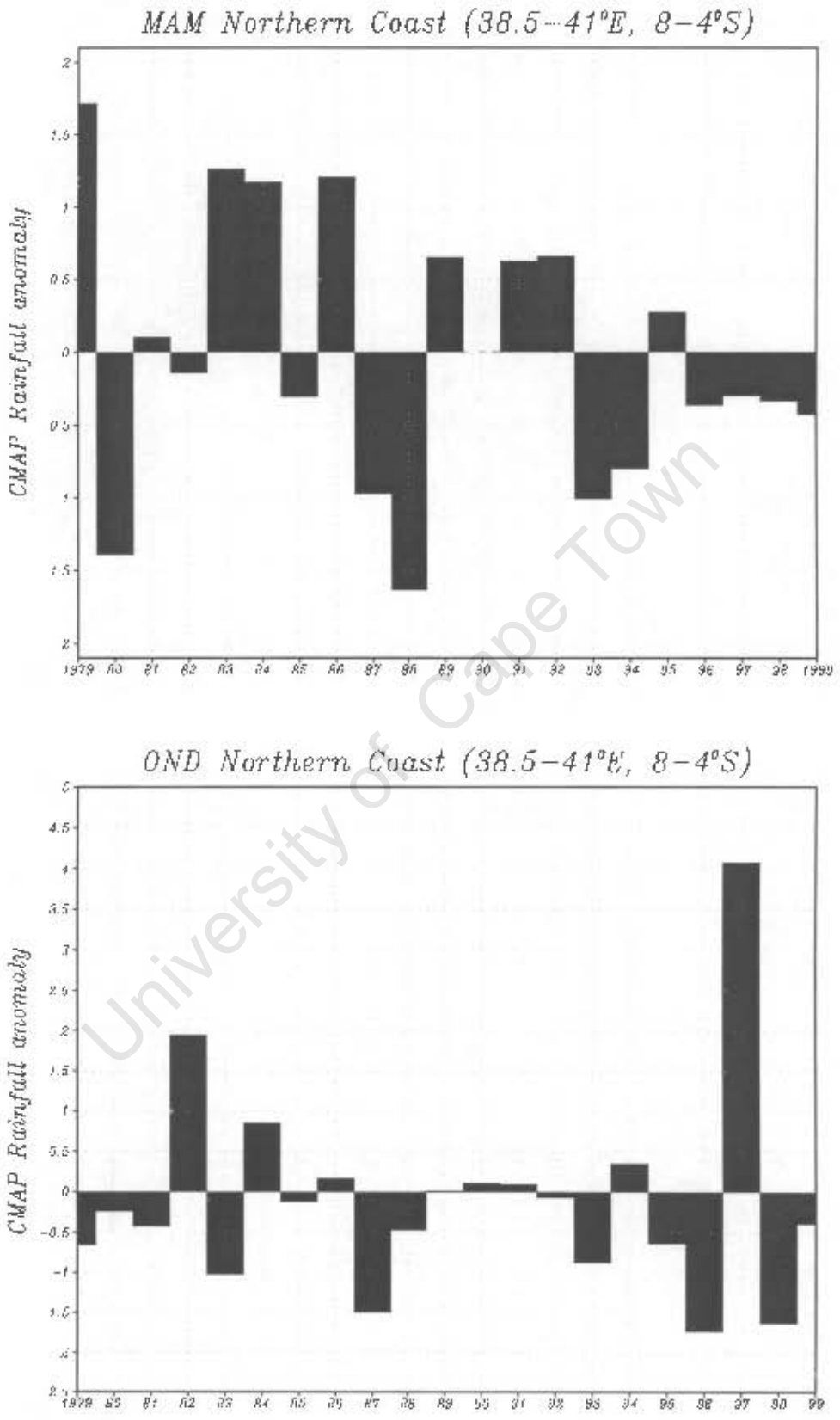

Figure 3.3a: Northern coast CMAP data rainfall time series for MAM and OND season.

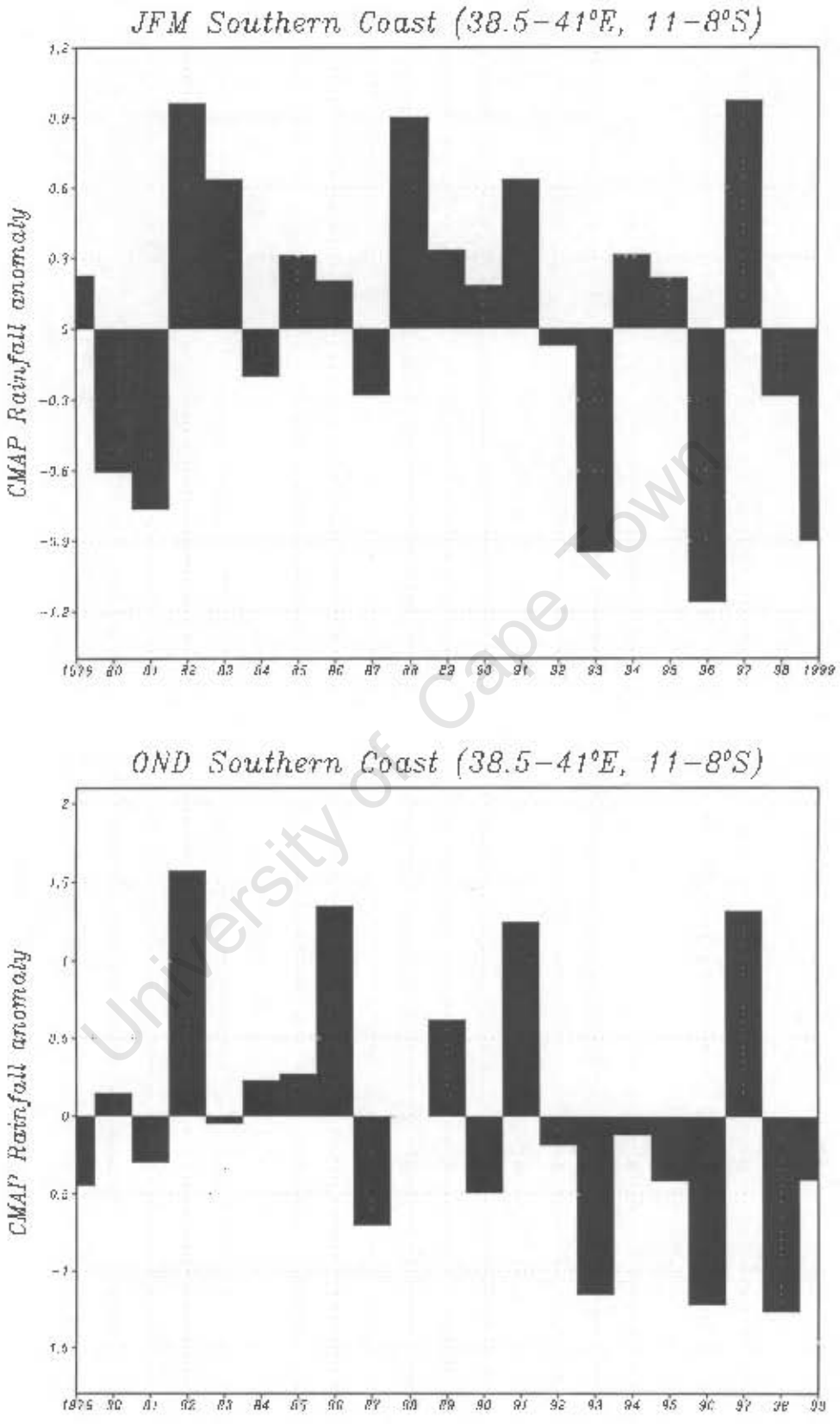

Figure 3.3b: As for figure 3.3a but for JFM and OND southern coast rainfall seasons.

Chapter 4: Climatology of selected Meteorological fields.

4.1 Introduction.

The tropical atmosphere is conditionally unstable. Major zones of convection in the tropics, hence regions of potential precipitation, have been associated with low OLR (Riehl, 1979). It is evident in the tropics that high values of outgoing long wave radiation are indicative of areas of clear sky while low values of outgoing long wave radiation are indicative of high cold clouds including the tops of deep convective clouds. It has also been observed that regions of high precipitation, hence low OLR, are associated with regions of high SST (Bjerknes, 1969; Liebmann and Hartman, 1982). For development of clouds and rainfall vertical motion and moist air are required. With sufficient moisture in the atmosphere, one mechanism that can initiate convection is wind convergence at low levels and wind divergence at upper levels. As suggested by Steiner (1989), and many others the combination of the dynamics and moisture fields results in a closer relationship to convection than either the wind convergence or moisture alone. Vertical motion and resulting convection can be induced by forced ascent of airstreams over topography, horizontal convergence, and unequal heating of land and water masses.

The purpose of this chapter is to analyse the mean characteristics of selected long-term meteorological fields responsible for seasonal rainfall in Tanzania with specific objective of understanding the primary factors, which determine the climate of Tanzania. The monthly mean structures calculated for the period 1970-1999 are analysed and used as a background in understanding the evolution of composite anomalies of El Niño and La Niña years. Two months prior to the onset of each season (OND and MAM) was included in the analysis for potential predictive purposes.

4.2 Monthly climatological fields for OND season

Figures 4.1(a-j) illustrates monthly climatological plots of SST, wind at 850, 700 and 200hPa, latent heat flux, CMAP data precipitation, moisture flux and moisture flux divergence at 850hPa, velocity potential and divergent wind at 850 and 200hPa, OLR, longitude height moisture flux between 15-4°S and zonal moisture flux along 37°E and 40°E for each month of the OND season starting two months before the onset of the season.

It should be mentioned that the low-level divergence field might be significantly influenced by the coastal topography, which varies greatly as one moves inland from the Indian Ocean. About a hundred kilometers inland from the coast, the ground rises rapidly westwards, attaining a height of 1.5km or more above Mean Sea Level (G.C Asnani, Tropical meteorology). The lower tropospheric winds near the coast were observed to have an easterly component. These rise over the slopes of the high grounds, which run roughly north- south parallel to the coast a few hundred kilometers inland. When the rising air has sufficient moisture, clouds develop. Therefore most of the rainfall observed over eastern Tanzania may result from the interaction between the moist easterly trades and orography. Similarly, Mulenga (1999) found the wet spells over the eastern coast of the RSA to be associated with low-level divergence and he concluded that the wet spells were due to the interaction between moist trades and orography. With 2.5x2.5 degrees resolution of NCEP data these regional topographic features are not evident and hence divergence persists over the coast throughout the rainfall season.

Two months prior to the onset of the OND rainfall season in August (fig 4.1a&b), the ITCZ is over the northern hemisphere lagging behind the position of the overhead sun. Its mean position is well defined over the equatorial North Indian

Ocean by high SST values of about 28°C, strong westerly wind flow at 850hPa and 700hPa coupled with easterly flow at 200hPa. These wind flow patterns feed the Indian Ocean convective Zone and their origin marks the position of the descending limb of the Indian Ocean Walker circulation cell (descending region of atmospheric overturning), which is roughly at about 40°E during this period. The upper level wind plot shows strong westerly wind flow south east of Madagascar in the latitude band 25-35°S coupled high surface evaporation and strong low-level easterly fluxes. This marks the position of Indian Ocean subtropical high-pressure cell and the descending branch of Hadley circulation.

Two regions of moisture source with high latent heat flux values of about 200W/m² were observed, one in the Southern Hemisphere east of Madagascar and the other in the Northern Hemisphere closer to the Somalia coast. These supply moisture to the southwest monsoon, which is near its peak in August. A well-organized East African low-level jet feeds the southwest monsoon shown near India and denies penetration of moisture further inland over the Tanzanian coast resulting in dry conditions. Much of Tanzania is characterized by low-level moisture flux divergence. Convergence is apparent over the western part of the country and Lake Victoria basin where the rainfall of about 30-60mm was recorded. There is a band of low-level westerly flow in the neighborhood of the equator over the Congo basin, which feeds the continental convection. The maritime and continental convective zones, which are identified by low OLR values of about 190W/m² over the Indian Ocean and 210 W/m² over the Congo basin mark the rising limbs of the Walker circulation cell over the Indian Ocean and African continent respectively as portrayed by velocity potential and divergent wind plots at 850 and 200hPa.

The East-west vertical section of moisture flux shows an easterly moisture flux extending from 1000hPa to 650hPa. Between 39°E and 42°E, the moisture flux increases with height reaching a maximum at about 900hPa and decreasing

thereafter. Further inland at about 34°E, the highest value of moisture flux was observed at 850hPa. Further evidence of the easterly moisture flux over the region is shown by the zonal moisture flux plot along 40°E and 37°E. Easterly moisture flux over the coast is transported further inland with high concentration of moisture in the lower levels. This indicates that the main source of moisture over the coast of Tanzania is the Indian Ocean consistent with the latent heat and moisture flux plots. North of the equator a tongue of westerly moisture flux was observed above 850hPa along 40°E.

One month before the onset of rain season in September (fig 4.1c&d), almost all the meteorological fields portray similar characteristics as August except that latent heat values over the Indian Ocean north of the equator show a dramatic decrease. Strong low-level divergence is present near the Tanzanian coastal region, which is relatively dry for the month. For the zonal moisture flux along 40°E, the westerlies in the northern hemisphere at 850hPa were replaced by easterlies. The plots show an increase in the moisture content of the atmosphere as indicated by high values of easterly moisture flux with greater vertical extent compared to August.

At the onset of rainfall season in October (fig 4.1e&f), the ITCZ has migrated south to about 2°S. Its mean position can be identified by high SST values of about 28°C and marked southward shift of westerly flow at 850 and 700hPa over the equatorial west Indian Ocean. These westerly flows over the equatorial western Indian Ocean show a significant eastward shift indicating a change in the position of the descending limb of the Indian Ocean Walker circulation from 40°E to 55°E. As a result, low-level easterlies occur over the Tanzanian coast. The upper level westerly flow over the Indian Ocean subtropical high-pressure cell has intensified indicating strengthening of the high-pressure cell consistent with strong easterly flow in low latitudes. The East African low-level jet was now reversed to a weak northeasterly over Somalia allowing the southeast monsoon

to penetrate further inland and converge with westerlies from Congo basin over the western part of the country and Lake Victoria basin.

Strong easterly moisture flux was observed over the region of high latent heat flux between 15°S to the vicinity of the equator indicating the ascending branch of Hadley circulation. The rainfall plot shows 60mm contour covering the entire Tanzanian northern coast, which is consistent with decelerating moisture flux at 850hPa near the coast as indicated by moisture flux convergence over equatorial West Indian Ocean.

The convective zone over the Congo basin shows a marked eastward extent consistent with an eastward shift of the rising limb of the Walker circulation cell over the African continent, as indicated by the 850 and 200hPa velocity potential and divergent wind plots. This eastward shift of the convective zone leads to an eastward shift of the rainfall belt. The convective zone over the equatorial Indian Ocean deepens and shows a slight shift southwards indicating the southward movement of the ITCZ and intensification of the rising limb of Walker circulation over the Indian Ocean. The east-west vertical section of moisture flux shows increased moisture flux in both strength and vertical extent. The zonal moisture flux along 40°E shows replacement of westerlies in the Northern Hemisphere by easterlies, which implies an intensification of the Arabian high pressure cell consistent with 850hPa wind flow and moisture flux plots. Further inland along 37°E, more moisture penetrates high up in the atmosphere, which suggests the potential development of convective clouds.

During the peak of the short rain season in November (fig 4.1g&h), the position of the ITCZ is apparent at about 5°S where SST indicates temperature of about 28°C with strong westerly wind over central Indian Ocean at 850hPa level. The northeast monsoonal flow from Asia converges with the southeast monsoon at about 5°S near the Tanzanian coast giving further identification of the position of

the ITCZ. The position of descending limb of the Walker circulation is maintained at about 55°E as identified by negative velocity potential with strong divergent wind in lower levels and positive velocity potential with wind convergence in the upper levels.

Both the northeast and southeast monsoon are moist as indicated by high latent heat flux on their path. The rainfall over the northern coast of Tanzania increases to over 100mm consistent with the larger amount of moisture advected from the northwest and southwest Indian Ocean that converges over the northern coast as indicated by moisture flux plots.

The two convective zones over the Indian Ocean and Congo basin maintain their position with low OLR values of 190W/m² and 200W/m² respectively. These convective zones mark the position of the rising limbs of the Walker circulation cell as indicated by the velocity potential and divergent wind plots. The rising limb of the Walker cell over the African Continent oscillates east west in sympathy with the position of the meridional arm of the ITCZ, which is over western Tanzania during this period.

The longitude height moisture flux plot shows a westward tilt with height of larger easterly moisture flux reaching a maximum at about 850hPa near 35°E. The zonal moisture flux along 40° and 37°E maintains the October configuration except there is a strong easterly moisture flux over the Northern Hemisphere with highest concentration at 850hPa. This indicates advection of moisture from the Indian Ocean, which is consistent with 850hPa moisture flux and wind plots.

Towards the withdrawal of rain season in December (fig 4.1i&j), the 28°C SST contour extends further south and penetrates into the Mozambique Channel. The 850hPa westerly flow in the equatorial west and central Indian Ocean shows a southward shift to about 8°S where the northeast monsoon converges with

southeasterlies, thereby indicating the position of the ITCZ. The northeast monsoon crosses the equator and spreads over much of Tanzania on its way to the ITCZ. This reflects the intensification of the Arabian winter high-pressure cell, which lies beneath the descending branch of the Northern Hemisphere Hadley circulation while the subtropical high pressure over the southwest Indian Ocean relaxes and shifts south.

The two moisture sources in the Indian Ocean persist except that the Northern Hemisphere one is intensified with latent heat fluxes of about 200W/m² (due to the colder, drier air existing from Asia) while the moisture source east of Madagascar shows a slight eastward shift and weakens. The descending limb of the Walker circulation shows a slight westward shift to about 50°E as shown by the velocity potential plots, which is consistent with dominant easterly low-level flow over the Tanzanian coast.

The rainfall patterns shows a north south gradient over the coast with higher rainfall amounts to the south (consistent with December marking the peak of the wet season over northern Mozambique and Zambia) and also over the western part of the country to Lake Victoria basin. This marks the withdrawal of rainfall over the northern coast consistent with strengthening low-level moisture divergence over the region.

The strong moisture convergence over the western part of the country is associated with the position of the meridional arm of the ITCZ and low OLR values over the region. The velocity potential and divergent wind at 850 and 200hPa plots indicate the rising limb of the Walker circulation over this convective zone. Over the region, a marked decrease of low-level moisture compared to November is evident as shown by low easterly moisture flux value in the longitude height moisture flux plot. The patterns for zonal moisture flux along 40°E and 37°E are more or less similar to the November patterns.

4.3 Monthly climatological fields for MAM season

Figures 4.2(a-l) illustrates monthly climatological plots of SST, wind at 850, 700 and 200hPa, latent heat flux, precipitation, moisture flux and moisture flux divergence at 850hPa, velocity potential and divergent wind at 850 and 200hPa, OLR, longitude height moisture flux between 15-4°S and zonal moisture flux along 37°E and 40°E for each month of the MAM season starting two months before the onset of the season.

Two months prior to the onset of the long rain season in January (fig 4.2a&b), the ITCZ is located far to the south of Tanzania with southern most position over the Mozambique Channel at about 20°S, where easterly trade winds converges with northerly flow at 850hPa level. Over the Tanzanian coast, the westerly flow at 850 and 700hPa over the western Indian Ocean feeds the maritime convection. The descending branch of the Walker circulation is at about 45°E as indicated by 850 and 200hPa velocity potential and divergent wind plots. This strong descending motion over the Tanzanian coast marks the end of the short rains over the northern coast.

A southward shift of the rainfall belt is evident with higher rainfall values over the southern coast and western part of the country consistent with the moisture flux patterns, which show moisture flux divergence over the coast with convergence over the western part of the country and over northern Mozambique. The Indian Ocean subtropical high-pressure beneath the descending branch of Hadley circulation relaxes, while the Arabian winter high-pressure cell intensifies. Strong northeasterly and cool winds originate from southern Asia leading to larger evaporation values over the Arabian Sea. The South Indian Ocean convective zone merges with the continental convective zone creating a coherent ITCZ over the tropical South Indian Ocean and southern Africa. These convective zones are associated with low-level wind convergence and upper level wind divergence as shown by the velocity potential and divergent wind plots.

The longitude height moisture flux shows a tongue of westerly moisture flux emanating from the Indian Ocean at about 850hPa overlaying the easterly moisture flux. This westerly moisture flux extends to about 35°E at 700hPa level. The zonal moisture flux along 40°E and 37°E confirms this presence of westerly moisture flux with highest intensity at about 850hPa.

One month prior to the onset of rainfall season in February (fig 4.2c&d), the ITCZ is at its southernmost position. Its mean position over the Indian Ocean is indicated by high SST values exceeding 28°C, low OLR values and westerly flow in the lower levels over southwest Indian Ocean at about 15°S. High values of latent heat flux over the Arabian winter high pressure and tropical south Indian Ocean lead to increased evaporation and convergence of moisture over the coast where about 100-150mm of rainfall was observed over the southern coast. Other meteorological fields maintain the January configuration except for the penetration further inland of westerly moisture flux between 15-4°S.

During the onset of rain season in March (fig.4.2e&f), the ITCZ starts its northward movement as it follows the seasonal movement of maximum solar heating. Its mean position is at about 12°S as indicated by high SST values of about 29°C and the boundary between the westerly and easterly flow over the tropical South Indian Ocean with low OLR values. Unlike January and February, there is now a return of easterly moisture flux from the tropical south Indian Ocean to Tanzania.

The descending limb of the Walker circulation shows a slight eastward shift to about 50°E as indicated by westerlies over the western Indian Ocean and easterlies over the Tanzanian coast. All of Tanzania is covered by a moist air mass as indicated by high values of latent heat flux from their source regions over the Indian Ocean east of Madagascar and closer to the Somalia coast. The northward shift of rainfall zone is evident with all of Tanzania covered by higher

rainfall values exceeding 100mm consistent with easterly moisture flux convergence over the western parts of the country.

There are two zones of low OLR values, one centered over the Congo basin extending to western Tanzania and the other over the equatorial central Indian Ocean. These convective zones marks the position of continental and maritime rising limbs of Walker circulation cells as indicated by the velocity potential and divergent wind plots. The westerlies in the longitude height moisture flux plots are replaced by easterlies and indicate an enhanced moisture fetch from the Indian Ocean. Similarly for zonal moisture flux along 40°E and 37°E, easterly moisture flux dominates the region giving further confirmation of the Indian Ocean being the main source of moisture for the Tanzanian coast rainfall.

In April, when the rainfall is at its peak over the northern coast (fig 4.2g&h), the westerly flow at 850 and 700hPa over the equatorial western Indian Ocean is at about 8°S marking the position of the ITCZ which is also indicated by high SST values exceeding 29°C and converging northeast and southeast monsoon well defined in 700hPa.

The descending limb of the Indian Ocean Walker circulation cell shows a slight eastward shift from March to about 52°E with enhanced low-level easterly flow over the Tanzanian coast. The moisture source over the northwest Indian Ocean is very small in April while that east of Madagascar and just off Tanzania has strengthened (i.e. larger latent heat fluxes) and is now the major contribution. Significant low level moisture convergence occurs just offshore of Tanzania and also over the western part of the country. Maximum rainfall of about 240mm occurs at the northern coast.

The regions of tropical convection show a slight northward shift in sympathy with movement of maximum solar heating as indicated by low OLR values.

Continental and maritime ascending limbs of the Walker circulation are well defined over the positions of strong convective zones as shown by velocity potential and divergent wind plots. Within the region, easterly moisture flux dominates with a slight increase in moisture over the previous month as indicated by high values of moisture flux in the longitude height plot. This easterly moisture flux is further indicated by zonal moisture flux along 37 and 40°E. The presence of easterly moisture flux over the northern coast is consistent with high rainfall values recorded, which marks the peak of long rain season.

Towards the withdrawal of rain season in May (fig 4.2i&j), the ITCZ is at about 2°S characterized by high SST values exceeding 28°C, the boundary between easterly and westerly flow at 850hPa over equatorial west Indian Ocean and converging northeasterly and southeasterly flow at 700hPa. Strong low-level southeasterlies originating from remote areas of high latent heat flux over the tropical South Indian Ocean are incident over the northern coast before veering southwest towards the developing Indian monsoon. A northward shift of rainfall belt is evident consistent with the northward shift of the ITCZ and the offshore low-level moisture convergence extending up to the Somali border. A zone of low OLR values spans the equatorial regions extending from the Atlantic Ocean across African continent to the Indian Ocean with strong convective zone over the Congo basin and equatorial East Indian Ocean. The low-level easterlies (westerlies) over the south (equatorial) Indian Ocean feed these convective zones. The velocity potential and divergent wind plots indicate the rising limb of Walker circulation over these convective regions identified by strong wind convergence at 850hPa and divergence at 200hPa. The longitude height moisture flux plot shows dominance of easterly moisture flux over the region. This was further confirmed by the zonal moisture flux along 37 and 40°E that maintains the April configuration.

In June (fig 4.2k&l), the ITCZ is well established over the northern tropics as revealed by high SST values over the North Indian Ocean and low OLR values of the strongly convective zone over the Indian subcontinent. The East African low-level jet starts to build up its transport of moisture towards the Indian monsoonal region and creates a diffluent flow over the Tanzanian coast. Southeast moisture flux is incident over the southern Kenyan coast where high rainfall occurs. Velocity potential and divergent wind plots show convergence over the Northern Hemisphere in sympathy with the position of the ITCZ and convective zones. A northward shift of the rainfall belt occurs consistent with the decrease of moisture concentration over the Tanzanian region at the end of the long rain season. The latter is indicated in the longitude height moisture flux and zonal moisture flux at 37 and 40°E that shows a significant decrease on the amount of moisture from previous month.

Figures relating to the climatological field results follow. Thereafter chapter 5 will further explore the interannual variability. Month to month anomaly fields for El Niño/La Niña composites will be discussed.

Chapter 5: Inter annual variability.

5.1 Introduction

This chapter deals with interannual variability or year-to-year variability in the climate of the region. Monthly anomalies discussed in this chapter were calculated by simply subtracting individual monthly means for a given year or composite from long-term monthly averages. This chapter examines anomalies in sea surface temperature (SST), outgoing long wave radiation (OLR), latent heat flux, winds at 850, 700 and 200hPa, moisture flux and moisture divergence at 850hPa, rainfall, velocity potential and divergent wind at 850 and 200hPa, zonal moisture flux along 40°E and 37°E and longitude height moisture flux between 15-4°S. Both rainy seasons October to December (OND) and March to May (MAM) were considered for the northern coast. Only the early rainy season (OND) was considered for the southern coast since the ENSO impacts are most pronounced during early season for the southern coast (fig 3.2b). A brief discussion of the results of rainfall time series will also be presented in this chapter.

The NOAA-CIRES climate diagnostic center (CDC) gives yearly updates of the strongest ENSO years. Also some researchers have used SST anomalies over the equatorial Pacific and the Southern Oscillation Index (SOI) to derive strong ENSO years (e.g. Allan et al, 1996; Indeje et al, 2000; Reason et al, 2000). In this chapter, the El Niño/La Niña onset years were considered for the OND season and the post mature phase El Niño+1/La Niña+1 years were considered for the MAM season. This is because the impacts of El Niño/La Niña over the northern coast of Tanzania were found to extend to the MAM season following the mature phase of the ENSO year (fig3.1a). Only strong ENSO years having rainfall anomaly values of at least one standard deviation (fig 3.1b) and occurring within the study period (1970-1999) are considered in this chapter. The El Niño years to be considered are 1972, 1982, 1986, 1994, and 1997 with the corresponding following year for the MAM season. La Niña years considered are

1970, 1973, 1975, 1988 and 1998 with the corresponding following year for the MAM season.

Note that the selection of years is based on the rainfall anomaly over the northern Tanzanian coast during the ENSO onset year (OND) season. For the MAM season, the years following the selected ENSO onset years are considered regardless of the rainfall anomaly value. Therefore the selection of years for MAM season were not based on the specific rainfall amount, however all post mature phase El Niño (La Niña) years were wet (dry).

5.2 Results of rainfall time series analysis.

Rainfall information has a great value especially to the social-economic benefit of farmers, water managers, energy suppliers and public policy makers in Tanzania. In this section, inter-annual rainfall time series, seasonality and in-seasonal distribution will be illustrated.

5.2.1 Inter annual rainfall variability.

Figures 3.1(a&b) and 3.2 (a&b), shows inter annual time series analysis for northern and southern coast of Tanzania. For the northern coast long rain season MAM (fig 3.1a), years 1979 and 1986 were anomalously wet years while 1980 was the driest year. Further investigation of this time series shows that virtually all El Niño+1 years (1973,1983, 1987 and 1998) were associated with above average rainfall while La Niña+1 years (1971,1974,1976, 1989 and 1996) shows below average rainfall. Most of the protracted El Niño years in the early 90's also show above average rainfall (e.g. 1991,1992 and1995) During the northern coast short rain season OND (fig 3.1b), 1997 was the anomalously wet year and 1974 was the driest year. All El Niño years and Indian Ocean positive zonal mode years were observed to have above average rainfall

(1972,1982,1986,1994and 1997). Again only some of the protracted El Niño years were wet (1990, 1991 and 1994). La Niña years and negative Indian Ocean zonal mode (IOZM) years reported dry anomalies (1970,1973,1975, 1988,1995,1998 and 1999).

The unimodal rainfall season of the southern coast was separated into early season (OND) and late season (JFM). JFM for the southern coast (fig 3.2a) shows that 1970 was the wettest year while 1977 and 1998 were the driest years. In general, ENSO impacts during the mature phase (JFM) were mixed for the southern coast. Some El Niño+1 years were found to be dry while others observed to be wet. Similarly wet and dry La Niña+1 years were observed. This may be partly due to the location, since the Tanzanian southern coast is in the transition zone between southern and East Africa, which tend to show opposite significant rainfall anomalies during ENSO events. For this reason, the southern coast JFM season was not considered for further analysis in this thesis. Figure 3.2b show that with the exception of the protracted El Niño event during the early 90's, El Niño (La Niña) tends to be associated with wet (dry) conditions over the southern coast for the OND season. There is also a hint that the OND southern coast rainfall time series shows a near decadal signal in rainfall with mainly dry years (1970's and 1990's) separated by the mainly wet 1980's.

Figure 3.3(a&b) illustrates the rainfall time series for the CMAP data. The CMAP data is available from 1979 onwards; therefore the series extends from 1979 to 1999. Comparison of the station data series and CMAP data series reveal the consistency of the two series for most years.

For the northern coast (fig 3.1 and 3.3a), both series are consistent for the OND season except for 1989 where CMAP data series indicates near normal rainfall while the station data series shows below average rainfall anomalies. For MAM season, 1987 and 1998 illustrates wet anomalies for station data series while

CMAP data series shows dry anomalies. 1989 was a dry year for the station data series while for the CMAP data series was a wet year. 1990 indicates near normal rainfall for CMAP data series while for the station data series it was a dry year. In general the station data series illustrate larger anomalies than the CMAP data series. This may be partly due to the difference in the climatology used, 1970-1999 for the station data series and 1979-1999 for the CMAP data series and partly due to differences in the way the data were derived. CMAP is a merge of gauge and satellite rainfall gridded with 2.5x2.5 resolution grid whereas the station data is the gauge data.

For the southern coast (fig 3.2 and 3.3b), both JFM and OND season series are consistent except for OND 1988 where CMAP data series indicate near normal rainfall while the station data series shows negative anomalies. Similarly, the station data anomalies are larger than the CMAP data anomalies.

It is evident from the above discussion that the CMAP data can be used to represent Tanzanian coast station data rainfall with reasonable accuracy for the northern coast OND season and the southern coast JFM and OND seasons. The degree of accuracy seems to be lower for the northern coast MAM season. However, the CMAP data will be used in section 5.3 of this thesis for the analysis of monthly anomaly fields.

5.2.2. Seasonality and distribution.

In the tropics, where day length and solar heating are more or less uniform throughout the year, humidity and rainfall are better markers of seasonality. Figures 1.2 (a&b) illustrated monthly area averaged rainfall time series for the northern and southern coast stations respectively. The south coast is a unimodal rainfall region with rains covering the months of November to May with a peak at March/April. The north coast is a bimodal with two rainfall peaks centered at April and November, namely the long rain (March –May) and short rain (October

– December) seasons. It is evident from the figures that there is no month without rain, however two major seasons are well defined for the northern coast and one major season for the southern coast.

5.3: Monthly evolution of the ENSO signal over the western Indian Ocean and East Africa.

5.3.1: El Niño and El Niño+1 composites

5.3.1.1: El Niño composites during OND season.

Figures 5.1(a-j) illustrate monthly anomaly fields prior and during the OND El Niño composite. Two months before the onset of the short rainfall season in August (fig 5.1a&b), warm SST anomalies of up to 0.4°C are evident over western Indian Ocean. Cool anomalies are confined to the eastern Indian Ocean and reach –0.3°C south of Java. Strong easterly low-level wind dominate the central and eastern Indian Ocean with northeasterlies backing to northwesterlies over the Tanzanian coast. At 700hPa, a cyclonic circulation centered south of Madagascar denies inland penetration of northeasterlies creating a centre of diffluent flow over the coast. Reduced evaporation occurs over western Indian Ocean closer to the East African coast, which is consistent with moisture flux divergence and rainfall deficit over the region.

The descending branch of the local Indian Ocean Walker cell is located over the equatorial central Indian Ocean as identified by strong westerly wind anomalies at the 200hPa level, which opposes the background flow implying convergence. This descending branch was further identified by the negative velocity potential anomalies associated with wind divergence in the lower levels and the positive velocity potential anomalies associated with wind convergence in the upper levels. The easterly moisture flux emanating from this moisture source feeds the convective zone over the equatorial western Indian Ocean.

The longitude height sections of moisture flux anomaly indicate the existence of westerly moisture flux anomalies over the region except for low level easterly moisture flux anomalies observed between 41-36°E. Further evidence of these westerly moisture flux anomalies over the region is illustrated by the zonal moisture flux anomalies along 40°E and 37°E. At about 850hPa, within the region of interest (i.e.4-11°S), easterly moisture flux anomalies occur along 40°E weakening further inland along 37°E with westerlies further south. This is consistent with the 850hPa moisture flux anomaly plot, which indicates backing of northeasterly moisture flux over the coast. In summary, a coherent ENSO signal is evident over the Indian Ocean two months before the onset of short rain season; however rainfall deficit occurs over the coast due to the presence of a cyclonic anomaly centered south of Madagascar, which causes enhanced divergent flow over the coast.

One month prior to the onset of short rainfall season in September (fig 5.1c&d), the maximum positive SST anomaly is no longer located near the coast, but shows a slight eastward shift. This may be due to increased upwelling near the coast caused by strong northeasterly wind anomalies observed in the previous month. The lower and middle level wind anomalies show a significant eastward shift of the cyclonic circulation over Madagascar from the previous month, which is consistent with an eastward shift of warm water over the tropical South Indian Ocean. The moisture flux plots indicate strong easterly moisture fluxes along the equator, which originate from the central Indian Ocean moisture source of high evaporation. The presence of this easterly moisture flux along the equator is important for Tanzanian rainfall since it indicates moisture availability one month before the onset of the rainfall season. However the convergence of this moisture is mainly over the ocean.

The OLR plot shows an area of subsidence over the equatorial central Indian Ocean with positive OLR anomalies of about 30W/m^2. This region of diffluence is

further identified by strong westerly wind in the upper levels over much of the equatorial western Indian Ocean, negative velocity potential anomaly with strong divergent wind in the lower levels and the reverse at upper levels. These velocity potential anomalies reflect the location of the descending limb of the Indian Ocean Walker circulation. Within the region, westerly moisture flux anomalies occur over the coast with easterly moisture flux anomalies further inland. Zonal moisture flux plots further reflect this. Along 40°E, westerly moisture flux occur between 3°S and 8°S while along 37°E the region is occupied by easterly moisture flux, implying moisture flux divergence over the region which is consistent with dry conditions observed during this month.

At the onset of short rainfall season in October (fig 5.1e&f), the contrasting warm (cool) SST anomaly pattern in the western (eastern) Indian Ocean intensifies. The largest SST anomalies (about 0.7°C) occur near the Somali coast. This westward shift of the positive SST anomalies may be due to suppressed upwelling resulting from weakening of the seasonal upwelling favourable winds and the arrival of the ITCZ over the region. The low level cyclonic anomaly east of Madagascar is no longer apparent and strong easterly anomalies cover all of the equatorial Indian Ocean in the lower and middle levels opposing the background flow. As a result the low level flow decelerates and hence converges near the coast. At 700hPa, westerly wind anomalies from the Atlantic Ocean converge with easterly anomalies from the Indian Ocean over western Tanzania and Lake Victoria basin.

Increased evaporation occurs over the maritime source region of the NE monsoon in the Arabian Sea. Almost all of Tanzania is covered by positive latent heat anomalies suggesting enhanced evapotranspiration over the landmass. Strong easterly moisture flux anomalies are evident over the equatorial western Indian Ocean. These converge at the coast consistent with above average rainfall recorded over Tanzania. The OLR plot suggest a convective zone

developing over the western Indian Ocean/eastern African region. Negative OLR anomalies of about $-10W/m^2$ were observed over the Tanzanian coast while positive OLR anomalies are confined to the area of cool SST anomalies in the central Indian Ocean and suppressed convection there.

The upper level wind implies westerly overturning over the equatorial western Indian Ocean with easterly overturning over the continent, which suggests a reversed Indian Ocean local Walker cell with its rising limb over East Africa. This is further identified by positive velocity potential and convergent wind in the lower levels over East Africa coupled with negative velocity potential and divergent wind in the upper levels. The longitude height moisture flux plot shows easterly moisture flux over the entire region from the Indian Ocean moisture source. This is further reflected by the zonal moisture fluxes along 40°E and 37°E that indicate further inland penetration of easterly moisture flux anomalies within the region of interest (i.e. 11-4°S). The combination of anomalous easterly moisture flux from the equatorial central Indian Ocean with moisture flux convergence and increased convective heating over much of East Africa leads to above average rainfall received during El Niño years.

During the peak of short rainfall season in November (fig 5.1g&h), the SST anomaly plot shows continued warming over the central and western Indian Ocean and weakening of the cool anomalies in the east. The maximum SST anomalies show a decrease of about 0.2°C from 0.7°C in October to 0.5°C in November, this arises due to evaporation and increased cloud cover. The low and middle level wind anomaly plots show a weak cyclonic anomaly southeast of Madagascar with a strong easterly wind anomaly over the equatorial western Indian Ocean between 5°S and 5°N that suggests anomalous convergence across East Africa (Goddard and Graham, 1999). The convergence over East Africa is further reflected in the moisture flux anomaly plots, which reveal strong easterly moisture flux anomaly over the equatorial western Indian Ocean and

westerly moisture flux anomaly from the Atlantic Ocean through the Congo basin. The resulting broad zone of moisture flux convergence across East Africa leads to anomalous rainfall over the region. The latent heat flux anomaly plot maintains the October configuration with increased evapotranspiration over much of Tanzania.

The 200hPa wind anomaly plot shows an anticyclonic circulation centered over the Mozambique Channel with strong accelerating easterly anomalies over East Africa implying upper level divergence, which is further reflected in the velocity potential and divergent wind plots. At the 850hPa level, positive velocity potential and wind convergence occurs across East African region coupled with negative velocity potential and wind divergence at the 200hPa level, thereby reflecting the position of ascending limb of local Indian Ocean Walker type circulation. A convective zone further reveals this ascent with negative OLR anomalies over the region. The corresponding zone of subsidence is seen over the equatorial central Indian Ocean. The longitude height moisture flux plot shows the occurrence of easterly moisture flux anomaly over the Indian Ocean at about 42°E at 850hPa with westerly moisture flux anomaly further inland. Zonal moisture fluxes along 40°E (37°E) indicate the occurrence of easterly (westerly) anomalies inferring moisture flux convergence consistent with the 850hPa moisture flux anomaly plots.

Towards the withdrawal of the short rainfall season in December (fig 5.1i&j), almost all the meteorological fields maintain the November patterns except for a southward shift in sympathy with the movement of the ITCZ. Maximum rainfall anomalies lie over Tanzania while in the previous month it was over Kenya. Westerly moisture flux anomalies appear over the far western Indian Ocean between 5°S and 8°S reflecting the withdrawal of rainfall season.

5.3.1.2:Post El Niño (+1) composites during MAM season.

Figures 5.2(a-l) illustrate monthly anomaly fields prior and during the MAM post El Niño (+1) composite. Two months prior to the onset of the long rainfall season in January (fig 5.2a&b), warm SST anomalies are evident over much of the tropical Indian Ocean with cool anomalies southeast of Madagascar. At 850hPa and 700hPa, strong easterly wind anomalies over the equatorial Indian Ocean advect moisture towards the Tanzanian coast. Westerly moisture flux anomalies occur over the southern Congo basin and these converge with easterly moisture flux anomalies from the Indian Ocean over eastern Tanzania. Enhanced evaporation occurs over the tropical western Indian Ocean and extends over much of Kenya and eastern Tanzania consistent with the significant rainfall observed.

Upper level wind divergence exists over the equatorial western Indian Ocean, which is further indicated by negative OLR anomalies, positive (negative) velocity potential anomalies with convergent (divergent) wind in the lower (upper) levels. These velocity potential anomalies reflect the location of the ascending limb of the Indian Ocean Walker circulation.

The moisture flux transects show low-level easterly moisture flux anomalies along the Tanzanian coast with westerly moisture flux anomalies further inland. This implies low-level moisture flux convergence over the region. Easterly moisture flux anomalies exist over the entire region in the middle levels indicating high vertical extent of moisture over the region consistent with above average rainfall observed. The zonal moisture fluxes along 40°E and 37°E indicate this easterly moisture flux anomaly along the Tanzanian coast sandwiched between westerly moisture flux anomalies to the north and south. The significantly increased rainfall observed in this month implies an extension of the OND season of the El Niño composite.

One month prior to the onset of the long rainfall season in February (fig 5.2c&d), the warm SST anomalies have strengthened over most of the Indian Ocean and the cool feature southeast of Madagascar has weakened. A low level cyclonic anomaly is evident east of Madagascar together with strong southerly wind anomalies through the Mozambique Channel. Westerly wind anomalies occur over much of Tanzania, and converge with the Indian Ocean equatorial easterlies near the Tanzanian coast.

Positive latent heat flux anomalies occur over the equatorial western Indian Ocean where strong easterly moisture flux anomalies advect moisture towards the Tanzanian coast. Enhanced moisture flux convergence over the Tanzanian coast is consistent with the significant rainfall observed over the northern coast of Tanzania. Weak easterly wind anomalies occur over much of East Africa in the upper levels implying weak Walker circulation. The rising limb of the Indian Ocean Walker circulation is located over the equatorial western Indian Ocean as identified by positive (negative) velocity potential with convergent (divergent) wind in the lower (upper) levels there.

The OLR plot suggests a convective zone developing over the tropical western Indian Ocean east of Madagascar with a northwestward extent of negative OLR anomalies over East Africa. The moisture flux transects indicate westerly moisture flux anomalies in the lower levels between 38°E and 42°E with easterly moisture flux elsewhere. This implies low level moisture flux divergence consistent with the decrease of the rainfall over the region compared to the previous month. The zonal moisture fluxes along 40°E and 37°E show alternating westerly and easterly moisture flux anomalies with easterly moisture flux anomalies over much of the Tanzanian coast at 37°E. The above discussion indicates extension of the wet conditions of the El Niño composite OND season to January and February of the El Niño+1 composite. This implies longer than

normal OND rainfall season during El Niño years with significantly increased rainfall over East Africa.

During the onset of the long rainfall season in March (fig 5.2e&f), warm SST anomalies of up to 0.4°C are evident over the equatorial Indian Ocean with larger anomalies near the East African coast. The low level wind and moisture flux anomaly plots indicate an eastward shift from the previous month of the cyclonic anomaly east of Madagascar to about 70°E. Associated with this shift is a westerly moisture flux anomaly over the Tanzanian coast. The latter converges with the easterly moisture flux anomaly over the Indian Ocean at about 60°E consistent with below average rainfall observed over the northern Tanzanian coast. The significant rainfall observed during this month over central and southeastern Tanzania results from the westerly moisture flux anomaly originating from the Atlantic Ocean moisture source, which converges locally over the region.

The 200hPa wind shows strong easterly anomalies over the equatorial western Indian Ocean implying a stronger Indian Ocean Walker type circulation. The descending limb of the Indian Ocean Walker circulation is located over the equatorial western Indian Ocean as indicated by negative (positive) velocity potential with divergent (convergent) wind in lower (upper) levels.

Positive OLR anomalies extend over the Tanzanian coast consistent with the below average rainfall observed. The moisture flux transects indicate the existence of westerly moisture flux anomalies over the Tanzanian coast, which is further confirmed by the zonal moisture flux along 40°E and 37°E implying reduction of moisture and dry conditions. It is observed from this analysis that the position of the cyclonic anomaly over the Indian Ocean east of Madagascar is important for modulating rainfall over Tanzania. When located between 45° and 60°E, this cyclonic anomaly results in moisture flux convergence and increased

rainfall over the Tanzanian northern coast while the eastward shift from this location seen in this month results in suppressed convection and reduction of rainfall over the Tanzanian northern coast.

During the peak of the long rainfall season in April (fig 5.2g&h), the positive SST anomalies over the western Indian Ocean intensify with low-level easterly (westerly) wind anomalies north (south) of 5°S. Positive latent heat flux anomalies dominate much of the western Indian Ocean and extend to the Kenyan and Somali coasts with strong easterly moisture transport. The moisture flux anomaly plot indicates moisture flux convergence over southwestern Tanzania where above average rainfall occurs. The source of this moisture is the tropical South West Indian Ocean and the Mozambique Channel where there are large areas of positive latent heat flux anomalies and southerly moisture flux anomalies over northern Mozambique and the Channel.

The upper level wind indicates strong easterly anomalies converging with westerly anomalies over the Tanzanian coast, which reflect the location of the descending limb of Walker cell. This is further identified by negative velocity potential with divergent wind in the lower levels coupled with the reverse at the upper levels. Weaker positive OLR anomalies are apparent over most of the country and there is reduced rainfall over the coast. Westerly moisture flux anomalies dominate over the coast as revealed by the longitude transect plot and the zonal moisture transects along 40°E and 37°E, which further confirm the rainfall deficit over the Tanzanian coast.

Towards the withdrawal of the long rainfall season in May (fig 5.2i&j), the positive SST anomalies shift more over the equatorial Indian Ocean between 15°N and 15°S with negative SST anomalies poleward of this region. Low-level westerly wind anomalies occur over the Indian Ocean between the equator and 10°S with

easterly wind anomalies to the north. Much of Tanzania is characterized by easterly wind anomalies at middle levels.

Positive latent heat flux anomalies exist over large areas of the equatorial and tropical South Indian Ocean particularly over the cyclonic moisture flux anomaly northeast of Madagascar. Associated with this cyclonic feature is low-level convergence over northern Mozambique and the Channel. However there is reduced rainfall here, which extends to the southern Tanzanian coast with a large positive rainfall anomaly over the north coast. This rainfall over the northern coast could be accounted for local factors such as strengthened sea breezes rather than large-scale anomalies as suggested by Indeje et al (2000).

The longitude transect plot indicates westerly moisture flux anomalies at lower levels with easterly moisture flux anomalies at middle levels. The latter indicates moisture availability from the Indian Ocean at this level, which may partly account for above average rainfall observed. The zonal moisture flux transects along 40°E and 37°E indicate the occurrence of westerly moisture flux anomaly over the coast. It is evident that this month contributes a large amount of rainfall to the seasonal total. Similarly the intraseasonal analysis (chapter 6) in this thesis shows that the peak of rainfall during El Niño+1 years is centered on the first week of May. As a result, the signal may be partially observed in a monthly analysis.

In June (fig 5.2k&l), the warm SST anomaly intensifies to the northeast of Madagascar and near the Somali coast but weaken near the Tanzanian coast. Westerly wind anomalies dominate larger areas of the western Indian Ocean from lower to upper levels. Positive latent heat flux anomalies occur over most of the tropical Indian Ocean with westerly moisture flux anomalies feeding the convective zone over the central and eastern Indian Ocean. The latter is indicated by significant negative OLR anomalies. Only the Lake Victoria basin

shows an obvious rainfall increase and this is associated with westerly moisture flux anomalies from the Atlantic Ocean through the Congo basin, which converge over the Lake. Positive latent heat flux anomalies exist over the Lake Victoria basin suggesting increased evaporation.

The main convective zone shows a significant eastward shift from the previous month with positive OLR anomalies extending over all of equatorial and East Africa. This marks the end of the long rainfall season over Tanzania where westerly wind anomalies dominate. The anomalies are seen in the longitude and latitude transects plots. These westerly moisture flux anomalies over the region indicate a decrease of moisture over the coast due to a long continental track, which is consistent with dry conditions observed.

5.3.2: La Niña and La Niña+1 composites.

5.3.2.1: La Niña composites during OND season.

Figures 5.3(a-j) illustrate monthly anomaly fields for the La Niña composite prior and during the OND season. Two months prior to the onset of the short rainfall season in August (fig 5.3a&b), the La Niña composite is roughly the reverse of the El Niño composite. Cool anomalies exist over much of the western Indian Ocean with warm anomalies in the east. At 850hPa, strong southerly wind anomalies occur over the Tanzanian coast veering to westerly over the equatorial northwestern Indian Ocean. An extensive region of positive latent heat flux anomaly is observed over the South West Indian Ocean with reduced evaporation over the cool anomalies in the equatorial West Indian Ocean.

The 200hPa winds show an anticyclonic anomaly centered south of Madagascar with strong easterly anomalies covering much of the western Indian Ocean. This suggests that the position of the ascending limb of the Walker circulation is over the equatorial central Indian Ocean. This ascending branch of the Indian Ocean Walker circulation is further identified by positive velocity potential and

convergence in the lower levels coupled with negative velocity potential and divergence in the upper levels. The OLR plot indicates a convective zone centered over this region of upper level overturning. Easterly moisture flux dominates the region, which is further identified by the zonal moisture flux anomaly along 40°E and 37°E that indicates easterly anomalies south of the equator.

One month prior to the onset of short rainfall season in September (fig 5.3c&d), the cool anomalies have intensified over much of the western Indian Ocean while those in the eastern region have weakened. Wind anomalies show roughly the reverse pattern to the El Niño composite. At 850hPa, strong westerly wind anomalies occur over the equatorial Indian Ocean with southeasterly anomalies near the East African coast. Aloft, there is a strong easterly return flow, which forms the upper branch of the Walker type circulation.

Two convective zones exist; one over the equatorial eastern Indian Ocean and the other over the Congo basin. These zones are reflected by negative OLR anomalies, which suggest the position of maritime and continental rising limbs of Walker circulation. Positive velocity potential anomalies with convergent wind in the lower levels exist together with negative velocity potential anomalies and divergent wind in the upper levels over these convective zones, further identifying the location of rising limbs of the Walker circulation. The increased rainfall that occurred over the Congo basin during this period is consistent with the enhanced convection over the region. Near Tanzania, easterly moisture fluxes dominate at low levels with negative latent heat flux anomalies and no obvious anomalies in precipitation. Along the 40°E and 37°E transects, westerly moisture flux dominates the region north of 3°S and between 6°S and 12°S. The occurrence of westerly moisture flux anomaly over the equatorial western Indian Ocean one month before the onset of rainfall season implies moisture deficit over the coast and relatively dry conditions.

During the onset of the short rainfall season in October (fig 5.3e&f), the La Niña composite is again roughly the reverse of the El Niño composite. Cool anomalies develop further over the western Indian Ocean with warm anomalies present in the eastern Indian Ocean. Westerly wind anomalies dominate the lower and middle levels with easterlies in the upper levels over much of the equatorial Indian Ocean.

Much of East Africa and the central Indian Ocean are characterized by negative latent heat flux anomalies. The moisture flux anomaly plots show strong westerly flux over the equatorial western Indian Ocean with moisture flux divergence over central and western Tanzania and Kenya. The weak moisture flux convergence over eastern Tanzania and Kenya is insignificant mainly due to suppressed convection (positive OLR anomalies) leading to below average rainfall.

The position of the descending limb of the local Indian Ocean Walker cell and strong subsidence is located over East Africa as indicated by westerly wind anomalies in the lower levels with strong easterly overturning at 200hPa. Negative velocity potential and divergent wind in the lower levels coupled with positive velocity potential and convergent wind in the upper levels confirm this position of the Walker circulation. Within the region, the westerly moisture flux anomaly extends between up to 900hPa over the coast with easterly moisture flux anomaly in the middle and upper levels and westerly moisture flux anomaly further inland. The zonal moisture flux anomaly along 40°E confirm this coastal configuration while along 37°E the westerly moisture flux dominates the region with easterly moisture flux south of 12°S. These westerly moisture flux anomalies over the region tend to suppress convection resulting to reduced rainfall over the region.

At the peak of the short rainfall season in November (fig 5.3g&h), the La Niña composite indicates roughly the reverse patterns of the El Niño composite. Cool

anomalies are apparent over most of the tropical Indian Ocean except near the Tanzanian coast and south of Java. An anticyclonic anomaly exists at low levels southeast of Madagascar with a westerly anomaly over much of the equatorial Indian Ocean, implying anomalous divergence over East Africa as suggested by Goddard and Graham (1999). The moisture and latent heat flux anomaly plots further identify this broad zone of moisture flux divergence and reduced evaporation over East Africa, consistent with dry conditions over the region.

At the upper level, the anticyclonic circulation is still present southeast of Madagascar and a cyclonic feature is evident over southern Africa. Strong westerly wind anomalies over much of Tanzania converge with easterly anomalies over the equatorial western Indian Ocean and reflect the descending limb of the Indian Ocean Walker type circulation. This is further indicated by the positive OLR anomalies over East Africa and the western Indian Ocean and negative (positive) velocity potential with divergent (convergent) wind in the lower (upper) levels. Over the region, westerly moisture flux dominates, which is further identified by the zonal moisture transects along 40°E and 37°E showing westerly moisture flux anomaly between 4°S and 12°S sandwiched between easterly moisture flux to the south and north. The existence of westerly moisture flux anomaly over the region implies a long continental track and suppressed convection leading to reduced rainfall over the Tanzanian coast.

Towards the withdrawal of the short rainfall season in December (fig 5.3i&j), almost all the meteorological fields maintain the November patterns. Cool SST anomalies, particularly in the southern tropics now exist over almost all the Indian Ocean except the midlatitudes and also south of Java. The area of positive OLR anomalies over the Indian Ocean has reduced substantially compared to the previous month. Negative latent heat flux anomalies occur over much of the Indian Ocean and East African region with easterly moisture flux anomalies between 5°S and 10°S reflecting the withdrawal of the rainfall season.

5.3.2.2:Post La Niña (+1) composites during MAM season.

Figures 5.4(a-l) illustrate monthly anomaly fields prior and during the MAM post La Niña (+1) composite. Two months prior to the onset of the long rainfall season in January (fig 5.4a&b), the La Niña+1 composite indicates roughly the reverse patterns to the El Niño+1 composite. Cool SST anomalies extend over much of the Indian Ocean except southeast of Madagascar.

Much of the equatorial Indian Ocean between 5°N and 5°S is characterized by strong westerly wind anomalies in the lower and middle levels. Negative latent heat flux anomalies extend over much of the equatorial Indian Ocean and East African region except over the southern coast of Tanzania where moisture flux convergence and rainfall occurred. This implies that during this month the southern coast tends to acquire a southern Africa La Niña impact i.e., wet anomalies during La Niña years. However, most of the increased rainfall occurs over the ocean. The 200hPa level indicates deceleration of the easterly anomalies over the northern coast of Tanzania with positive OLR anomalies, which implies subsidence over the region consistent with the below average rainfall observed there. The longitude height moisture flux anomaly plot shows the dominance of westerly moisture flux anomalies over the region, which is further indicated by the zonal wind transects along 40°E and 37°E. The westerly moisture flux anomaly over the region leads to suppressed convection and reduced rainfall.

One month before the onset of the long rainfall season in February (fig 5.4c&d), the cool SST anomalies have intensified over the tropical Indian Ocean with some warm anomalies in the southwestern Indian Ocean. The wind anomaly patterns in the lower and middle levels indicate the reverse patterns to the El Niño+1 composite with anticyclonic circulation east of Madagascar associated with strong easterly (northerly) wind anomaly over much of Tanzania (the Mozambique Channel) which is also reflected in the moisture flux anomaly plot.

This type of circulation leads to strong divergence over the Tanzanian coast with rainfall deficit as reflected in moisture flux divergence and rainfall plots consistent with the observations of Goddard and Graham, (1999). Negative latent heat flux anomalies occur over much of the western Indian Ocean water reducing the moisture supply.

The upper level wind suggests convergence over much of Tanzania, which is also reflected by the velocity potential and divergent wind plots together with positive OLR anomalies over the region indicating the location of the descending limb of Walker cell. A convective zone develops over South East Africa, which is consistent with above average rainfall over this region during La Niña years. Similarly, the longitude height plot shows the reverse of the El Niño+1 composite with easterly moisture flux anomalies in the lower levels over the coast and westerly moisture flux anomalies elsewhere. The zonal moisture flux transect along 40°E indicates easterly moisture flux anomaly over the region except for the weak westerly moisture flux anomalies between 6°S and the equator. These easterly moisture flux anomalies extend further inland as reflected in the zonal moisture flux anomaly along 37°E. However, these easterly moisture flux anomalies are mainly divergent in nature resulting in reduction of rainfall over Tanzania.

At the onset of the long rainfall season in March (fig 5.4e&f), most of the meteorological fields again indicate the reverse patterns to the El Niño+1 composite. The negative SST anomalies over much of the Indian Ocean have intensified compared to the previous month. Low-level westerly wind anomalies are apparent over the Indian Ocean between equator and 10°S. The middle levels show westerly wind anomaly over Tanzania backing to southwesterly anomaly over the coast. The moisture flux anomaly plots indicate a cyclonic anomaly over southern Tanzania/northern Mozambique with westerly moisture flux anomaly from the equatorial Atlantic Ocean converging over western and

southern Tanzania consistent with the increased rainfall observed over that region.

Consistent with the observed rainfall, much of East Africa and the adjacent oceans show negative OLR anomalies. The negative latent heat flux anomalies exist over most of Tanzania implying that the rainfall observed over western and southern Tanzania may result from local air mass convergence and orographic lifting rather than evaporation. However, a small area of increased latent heat flux over the nearby ocean may also contribute.

The continental rising limb of the Walker cell is over western Tanzania as indicated by the positive (negative) velocity potential with convergent (divergent) wind in the lower (upper) levels. Easterly moisture flux anomalies occur over the coast at lower levels with westerly moisture flux anomalies elsewhere as reflected in the longitude height plot. The zonal moisture fluxes along 40°E and 37°E show westerly moisture flux anomalies over the Tanzanian coast sandwiched between easterly moisture flux anomalies to the north and south consistent with below average rainfall over the northern coast of Tanzania.

During the peak of the long rainfall season in April (fig 5.4g&h), the negative SST anomalies over the tropical Indian Ocean weaken. Strong low and middle level westerly wind anomalies exist over the equatorial north Indian Ocean between. Southwestern Tanzania experiences above average rainfall consistent with moisture flux convergence over the region. Over the Tanzanian coast, negative latent heat flux anomalies are apparent consistent with reduced rainfall.

A zonal contrast in OLR anomaly is evident over the equatorial Indian Ocean with enhanced convection over the equatorial eastern Indian Ocean and suppressed convection over the west. The velocity potential and divergent wind plots indicate the position of the continental ascending limb of the Walker cell at about 20°E

along the equator with the corresponding descending limb over the equatorial western Indian Ocean. These are identified by negative (positive) velocity potential with divergent (convergent) wind over the western Indian Ocean (Congo basin) over the lower levels with the reverse at the upper levels. Westerly moisture flux extends over much of the region as indicated by longitude height and zonal moisture flux anomaly plots along 40°E and 37°E. These imply a long land track with suppressed convection and dry conditions over the Tanzanian coast.

Towards the withdrawal of the long rainfall season in May (fig 5.4i&j), the La Niña+1 composite still indicate the reverse patterns to El Niño+1 composite. Surprisingly, the negative SST anomalies seem to strengthen over much of the tropical Indian Ocean. Low-level southeasterly wind anomalies veer to a westerly anomaly after crossing the equator over the western Indian Ocean. Negative latent heat flux anomalies occur over much of the western Indian Ocean and adjacent land. One exception occurs over southern Tanzania where positive latent heat flux anomalies are co-located with increased rainfall.

An anticyclonic anomaly occurs northeast of Madagascar with a strong westerly moisture flux anomaly further north. Positive OLR anomalies occur over the equatorial western Indian Ocean and extend over northern Tanzania (which shows reduced rainfall) with enhanced convection over southern Tanzania and increased rainfall. Much of the Tanzanian coast is covered by easterly moisture flux anomaly in the lower levels as reflected in the longitude height and zonal moisture flux anomaly plots. However these easterly anomalies are in the same sense as the background flow implying divergence and reduction of rainfall over the northern coast. While for the southern coast, the zonal moisture transects indicate large values consistent with increased evaporation over the region and enhanced convection with significant rainfall.

In June (fig 5.4k&l), the negative SST anomalies over the South Indian Ocean strengthen while those in the North Indian Ocean weaken. Positive SST anomalies are evident near the Somali coast. The low and middle level anticyclonic anomaly shifts north and lies over the equatorial western Indian Ocean. The north-south contrast in latent heat and precipitation anomalies over Tanzania continues in June.

Positive OLR anomalies extend over much of the equatorial western Indian Ocean near the Tanzanian coast. Westerly moisture flux anomalies exist over much of the region except for easterly anomalies at midlatitudes occurring east of 39°E. The zonal moisture flux transects along 40°E and 37°E indicate westerly moisture flux anomaly over the Tanzanian coast sandwiched between easterly moisture flux anomalies to the south and north which implies reduction of moisture fetch from the Indian Ocean and further indicate the withdrawal of the long rainfall season.

It is evident from the above discussion that below average rainfall occurred over the northern coast of Tanzania throughout the rainfall season consistent with below average rainfall observed in the seasonal total for the La Niña+1 years (fig 3.2a). The southern coast of Tanzania observes significant rainfall in March, May and June while during the peak of rainfall season in April dry conditions occurred, which resulted in below average rainfall in the seasonal total. However it is evident from these monthly plots that some months indicate significant rainfall over the southern coast during MAM season of the La Niña+1 composites while the northern coast remains dry throughout the season. It is worth noting here that combining the three months into seasonal totals may therefore be misleading.

Note: The case-by-case examination of ENSO years composited for the OND season is given in Appendix B. Generally; the El Niño and La Niña composites were considered to be representative of each ENSO year under this study and will be used to derive the main rainfall precursors for predictive purposes over the Tanzanian coast. Similarly, the post ENSO (+1) composites are considered robust and will be used to derive the main rainfall precursors during MAM season. However, the plots for each ENSO (+1) years are not discussed and only November is shown during the OND season of each ENSO year for brevity.

Scrutiny of the El Niño/La Niña composites together with each ENSO year suggests that the La Niña signal is more robust than the El Niño signal for the Tanzanian northern coast. Some of the El Niño years were associated with cooling over the equatorial western Indian Ocean with below average rainfall e.g. 1992 and 1993. It should be noted that these years were part of the protracted El Niño of the early 90's. The El Niño signal is robust when it occurs together with a positive Indian Ocean Zonal Mode. For La Niña years, cooling occurs consistently over the equatorial western Indian Ocean with below average rainfall over the Tanzanian northern coast.

The detailed discussion of the circulations associated with non ENSO years is given in the Appendix C. Monthly anomalies for selected meteorological fields during the OND season of the selected strongest wet/dry non-ENSO years are discussed in there.

5.4:Significant rainfall predictors for the Tanzanian coast.

The previous sections investigated the characteristics of wet El Niño and dry La Niña years during the OND season with the corresponding following El Niño+1 and La Niña+1 years during the MAM season. Using composite anomaly fields starting two months prior to the onset of the rainfall season, the structure and magnitude of SST, OLR, upper and middle winds, lower winds and moisture flux was outlined under this section for understanding and potential predictive purposes.

5.4.1: Potential precursors during the OND season.

5.4.1.1: Wet El Niño years.

The wet El Niño years are preceded by the following significant predictors.

- A contrasting warm (cool) SST anomaly pattern in the western (eastern) equatorial Indian Ocean is evident two months before the onset of the rainfall season.
- A contrasting negative (positive) OLR anomaly pattern in the western (eastern) equatorial Indian Ocean is evident two months before the onset of the rainfall season in August. The negative OLR anomalies over the equatorial western Indian Ocean weaken in September and intensify during the onset of the rainfall season in October.
- Easterly wind anomalies over the equatorial eastern Indian Ocean between 5°N and 5°S exist two months prior to the onset of the rainfall season in August.
- Easterly moisture flux anomalies over the equatorial eastern Indian Ocean exist two months before the onset of the rainfall season in August with moisture flux convergence over the Tanzanian coast during the onset of the rainfall season in October.

- Strong upper level westerly wind anomalies over East Africa, starting in August and reversing to easterly anomalies during the onset of the rainfall season, create a centre of strong upper level overturning in the rising limb of the Indian Ocean Walker circulation.

5.4.1.2: Dry La Niña years.

The predictors for the dry La Niña years are roughly the reverse of the wet El Niño years.

- A contrasting cool (warm) SST anomaly pattern in the western (eastern) equatorial Indian Ocean is evident two months before the onset of the rainfall season.

- A contrasting positive (negative) OLR anomaly pattern in the western (eastern) equatorial Indian Ocean is evident two months before the onset of the rainfall season in August. The positive anomalies over the equatorial western Indian Ocean weaken in September and intensify during the onset of the rainfall season in October.
- Low and middle level westerly wind anomalies over the equatorial western Indian Ocean were apparent in August with the cyclonic wind anomaly in September and intensified westerly anomalies evident during the onset of the rainfall season in October.
- A cyclonic moisture flux anomaly over the equatorial western Indian Ocean with strong westerly moisture flux anomaly north of the equator occurs two months prior to the onset of the rainfall season in August. Southward extension of the westerly moisture flux anomaly occurs in September and October with weak moisture flux convergence mainly over the Kenyan coast in October.

- Strong upper level easterly wind anomalies over East Africa exist in August and weaken during the onset of the rainfall season in October, implying strong upper level convergence and subsidence over the region.

5.4.2: Potential precursors during the MAM season.

5.4.2.1: Wet El Niño+1 years.

- Positive SST anomalies exist over the equatorial Indian Ocean two months before the onset of the rainfall season in January.
- Positive OLR anomalies exist over the equatorial eastern Indian Ocean with negative OLR anomalies over the equatorial western Indian Ocean two months before the onset of the rainfall season. However, during the onset of the rainfall season in March, positive OLR anomalies extend over much of Tanzania and dry conditions occur over the Tanzanian coast.
- Strong low and middle level easterly wind anomalies are evident over the equatorial Indian Ocean two months before the onset of the rainfall season.
- Easterly moisture flux anomalies are evident over the equatorial Indian Ocean two months before the onset of the rainfall season with anticyclonic moisture flux anomaly over northeast of Madagascar during the onset of the rainfall season.
- Weak upper level easterly wind anomalies exist over East Africa in August and September, and intensify during the onset of the rainfall season in March consistent with dry conditions during the onset of the rainfall season.

5.4.2.2: Dry La Niña+1 years.

Similarly, the predictors for the dry La Niña+1 years are roughly the reverse of the wet El Niño+1.

- Negative SST anomalies are apparent over the equatorial Indian Ocean two months before the onset of the rainfall season in January.

- Negative OLR anomalies exist over much of the equatorial Indian Ocean with largest anomaly value over the equatorial eastern Indian Ocean in January. Positive OLR anomalies occur over the Tanzanian northern coast in January and extend to cover the entire country in February. Dry conditions persist during January and February while in March, a strong convective zone develops over Tanzania and above average rainfall occurs over western and southern Tanzania.
- Strong low and middle level westerly wind anomalies are apparent over the equatorial Indian Ocean two months before the onset of the rainfall season, weaken in February and intensify with southward shift during the onset of the rainfall season in March.
- A cyclonic moisture flux anomaly centered over Mozambique with variable moisture flux anomaly over equatorial Indian Ocean exist two months

before the onset of the rainfall season in January. During the onset of the rainfall season in March, strong easterly moisture flux anomalies cover much of the equatorial Indian Ocean with moisture flux divergence over the Tanzanian coast.

Figures relating to the monthly anomalies follow and thereafter chapter 6 will discuss the results of the intraseasonal analysis.

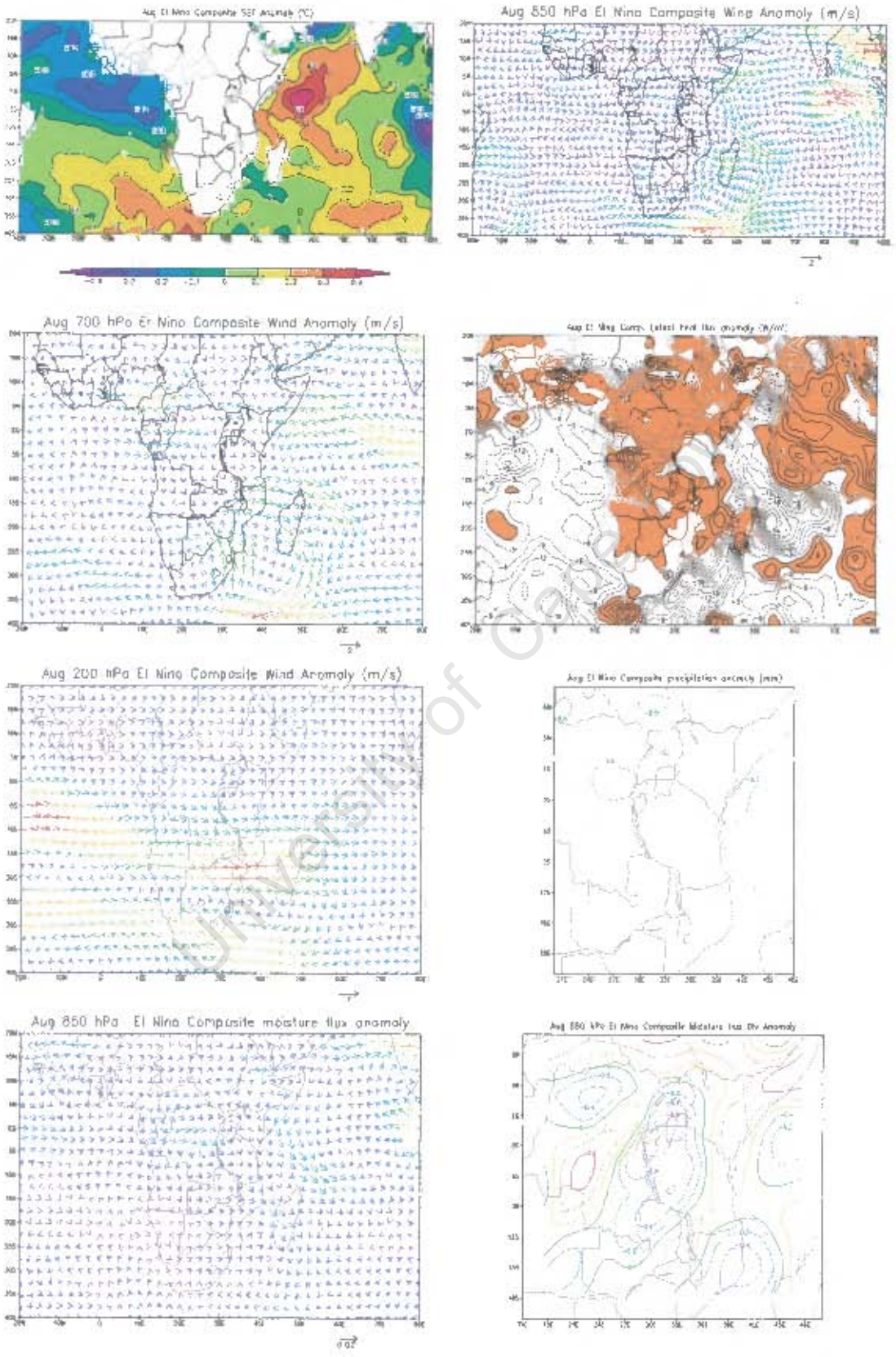

Figure 5.1a: August El Niño composite Anomaly fields Moisture flux g/kg.m/s

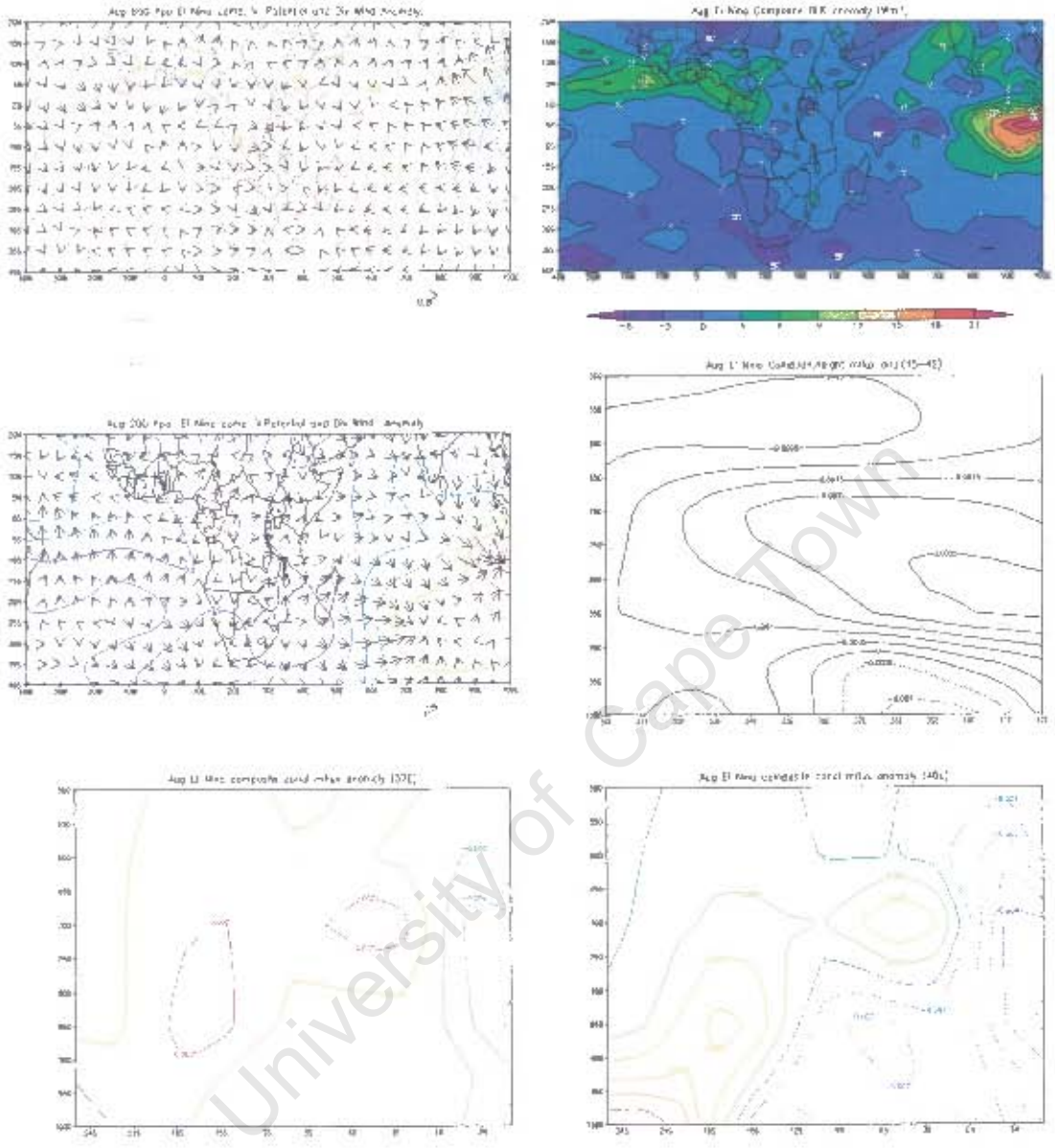

Figure 5.1b August El Niño composite anomaly fields
Velocity potential ($m^2 s^{-1}$)
Divergent wind (s^{-1})

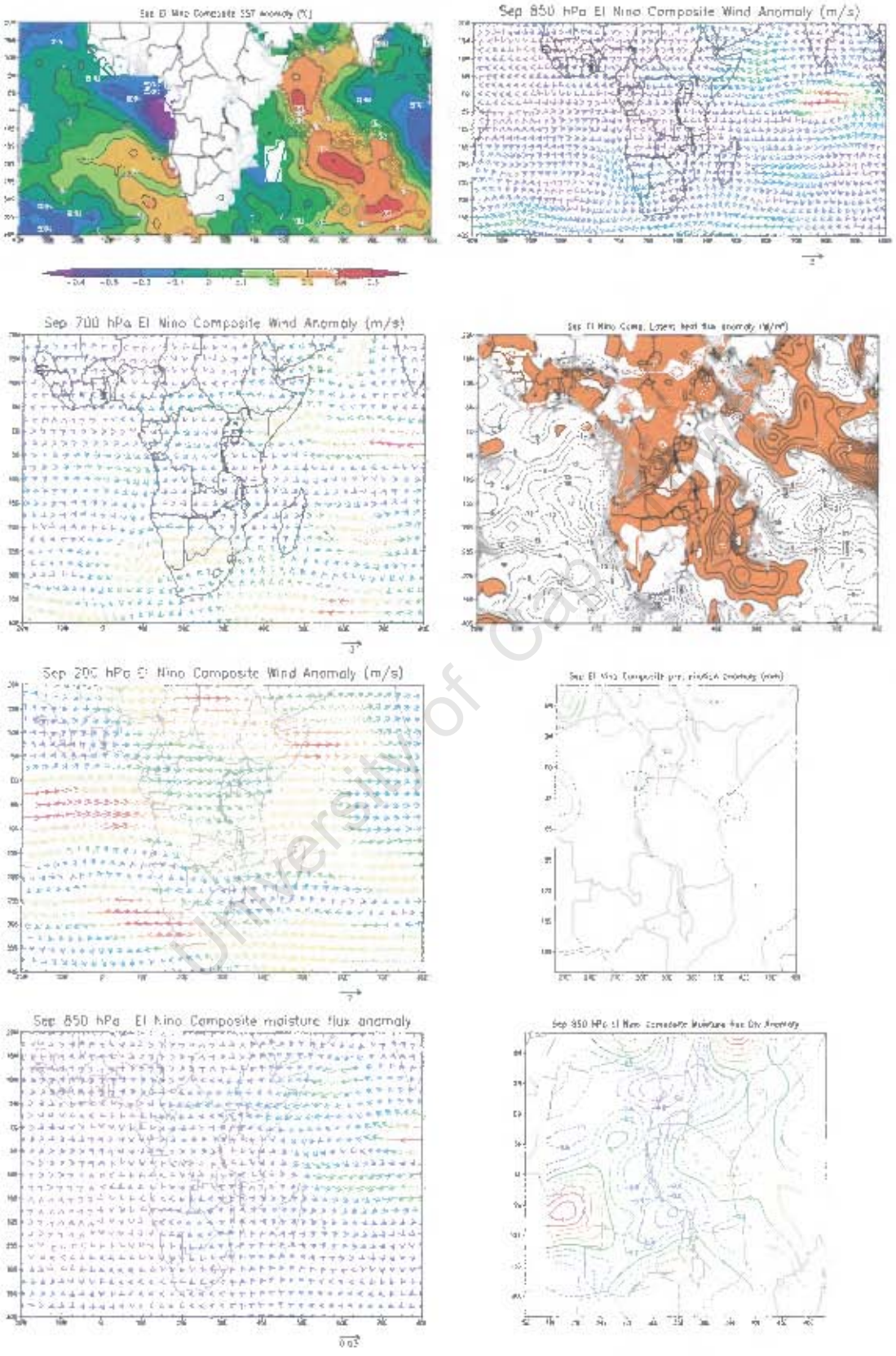

Figure 5.1c: As for figure 5.1a but for September

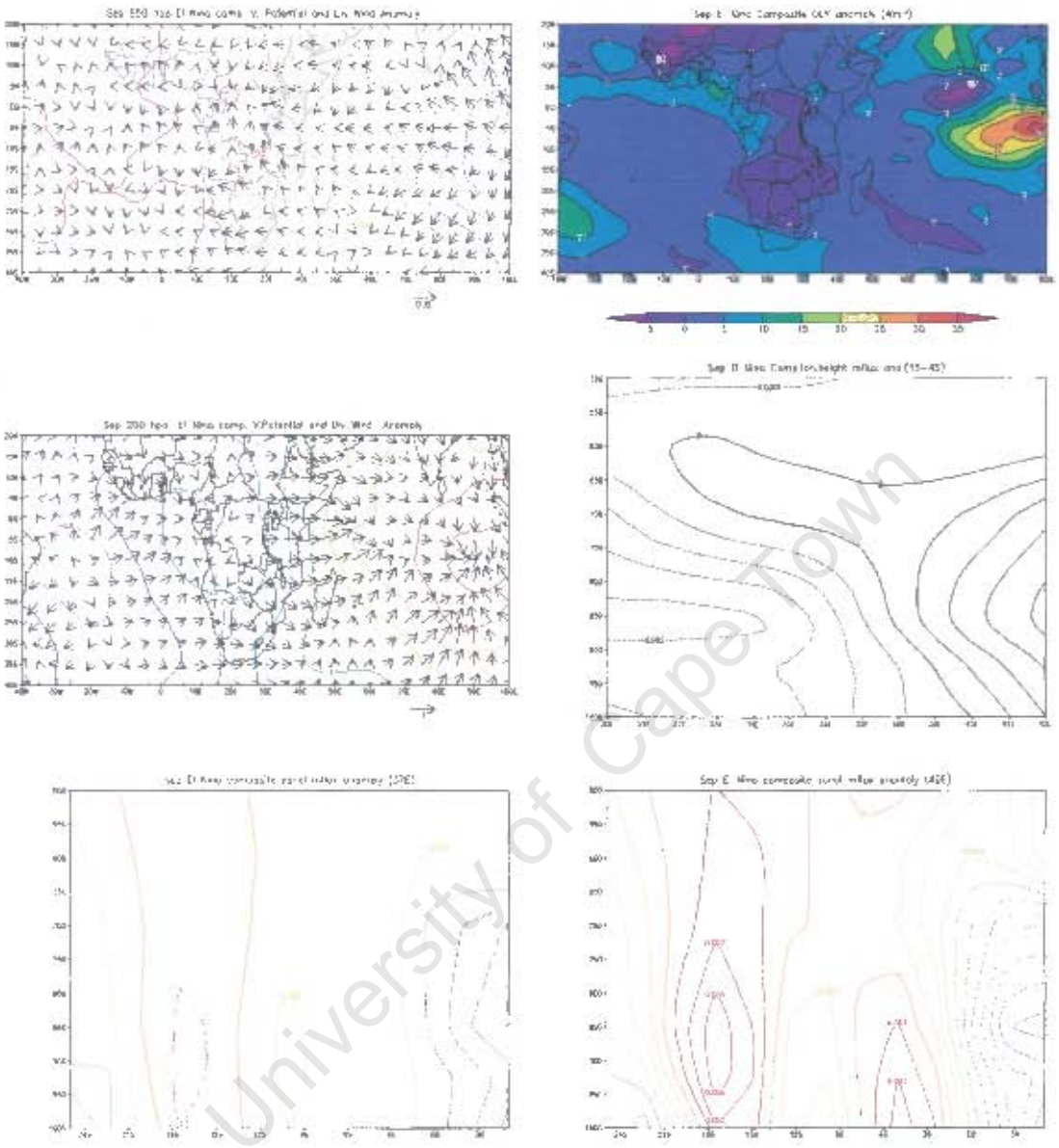

Figure 5.1d: As for figure 5.1b but for September

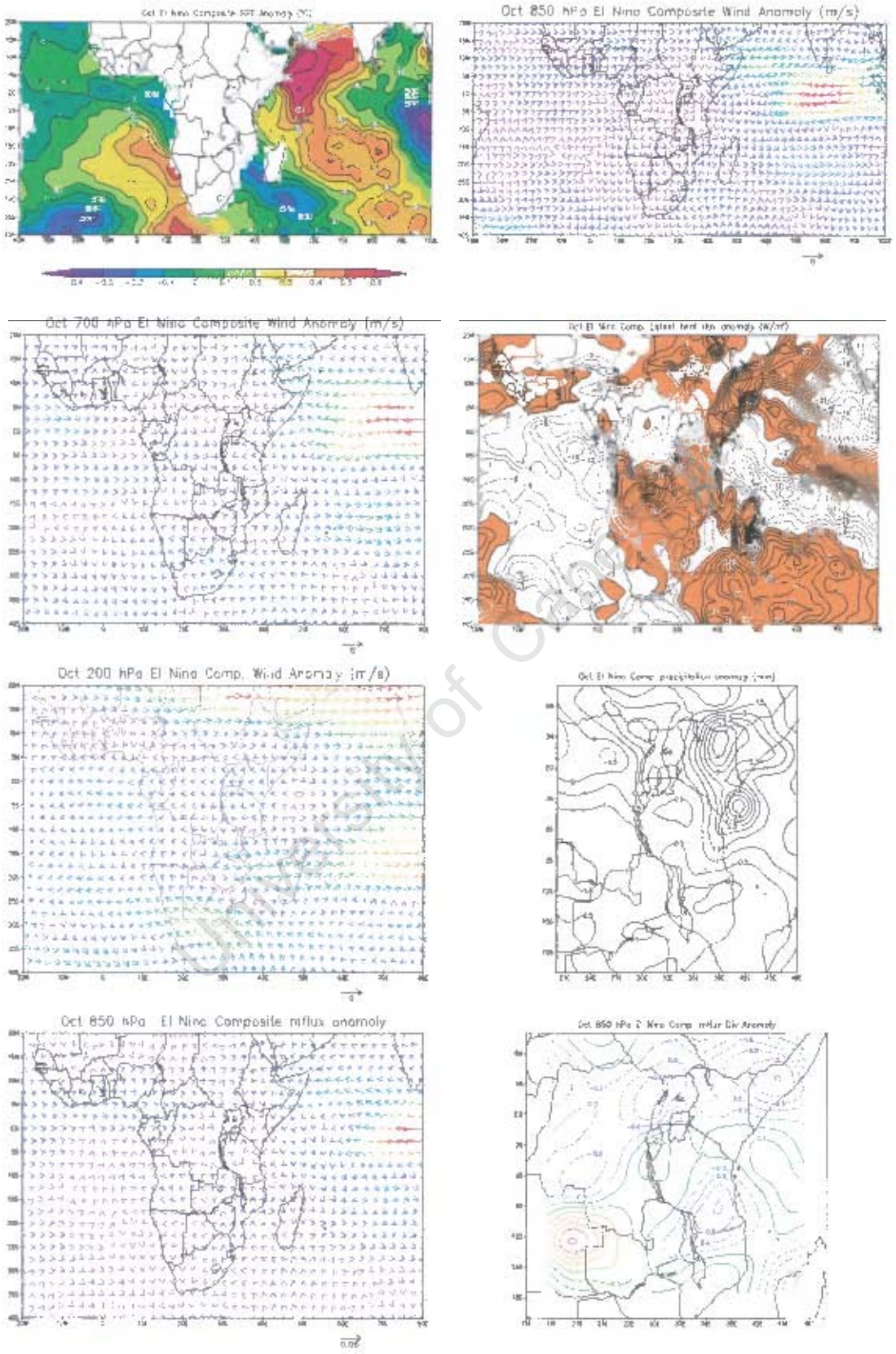

Figure 5.1e: As for figure 5.1a but for October

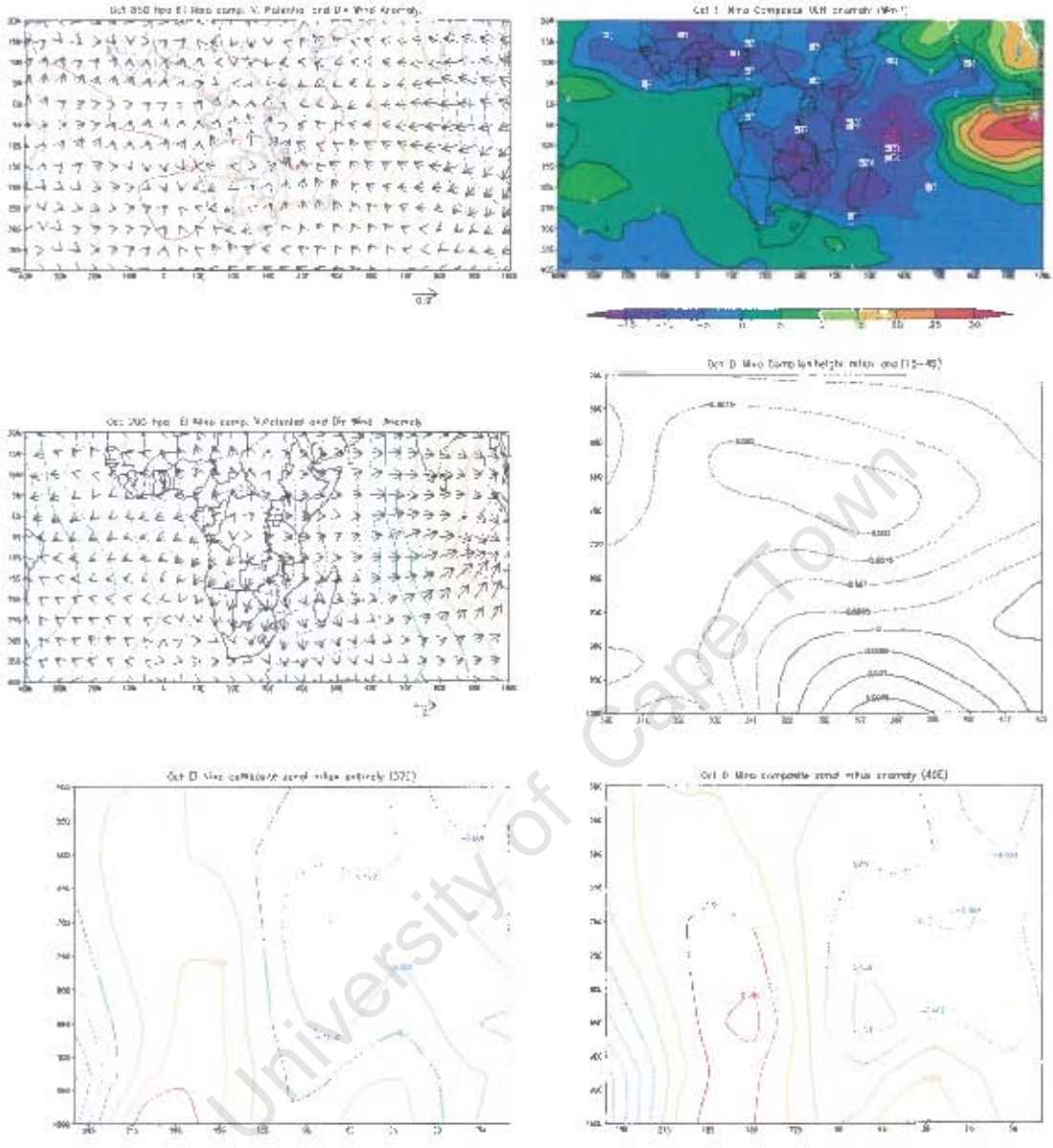

Figure 5.1f: As for figure 5.1b but for October

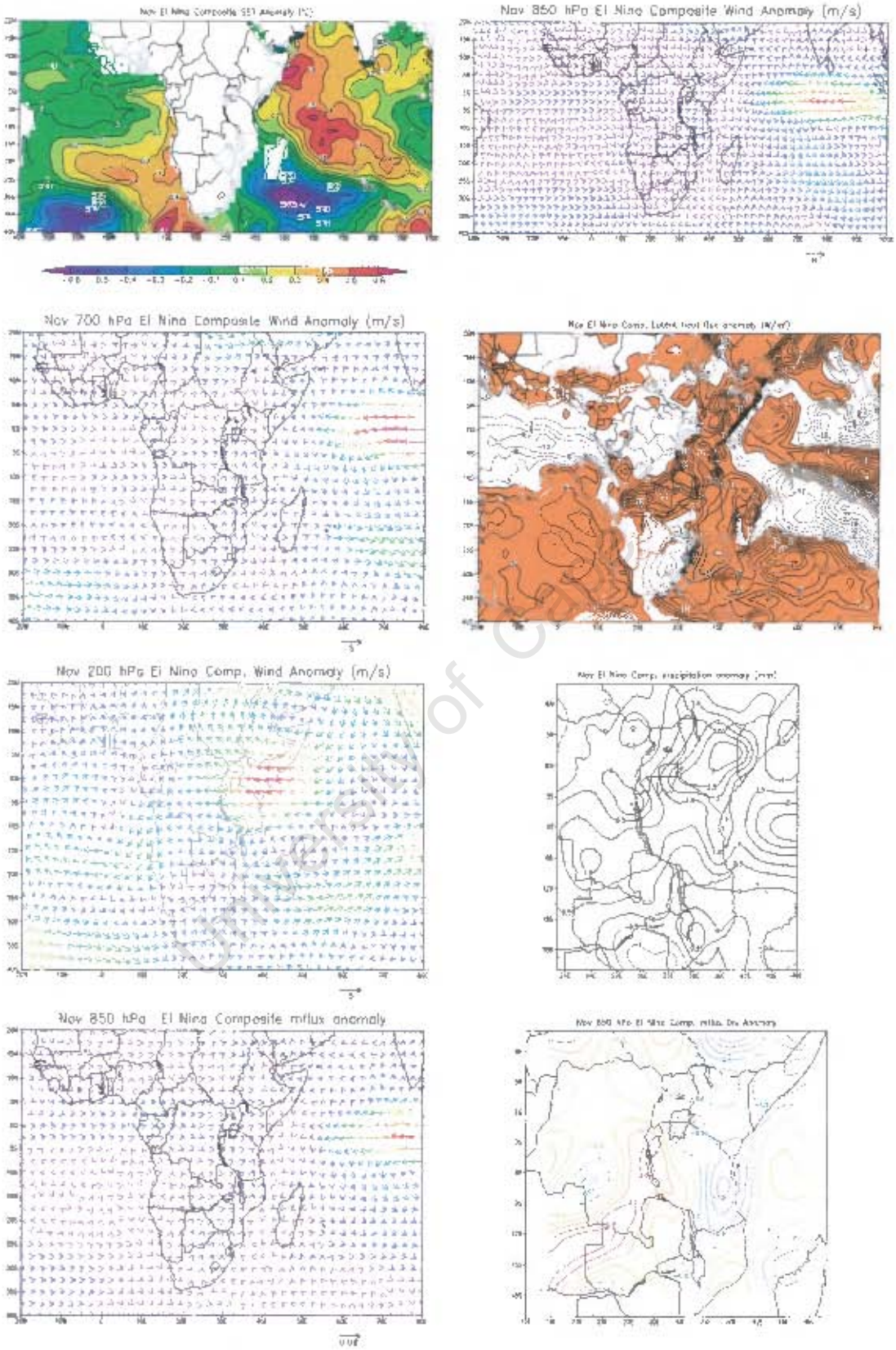

Figure 5.1g: As for figure 5.1a but for November

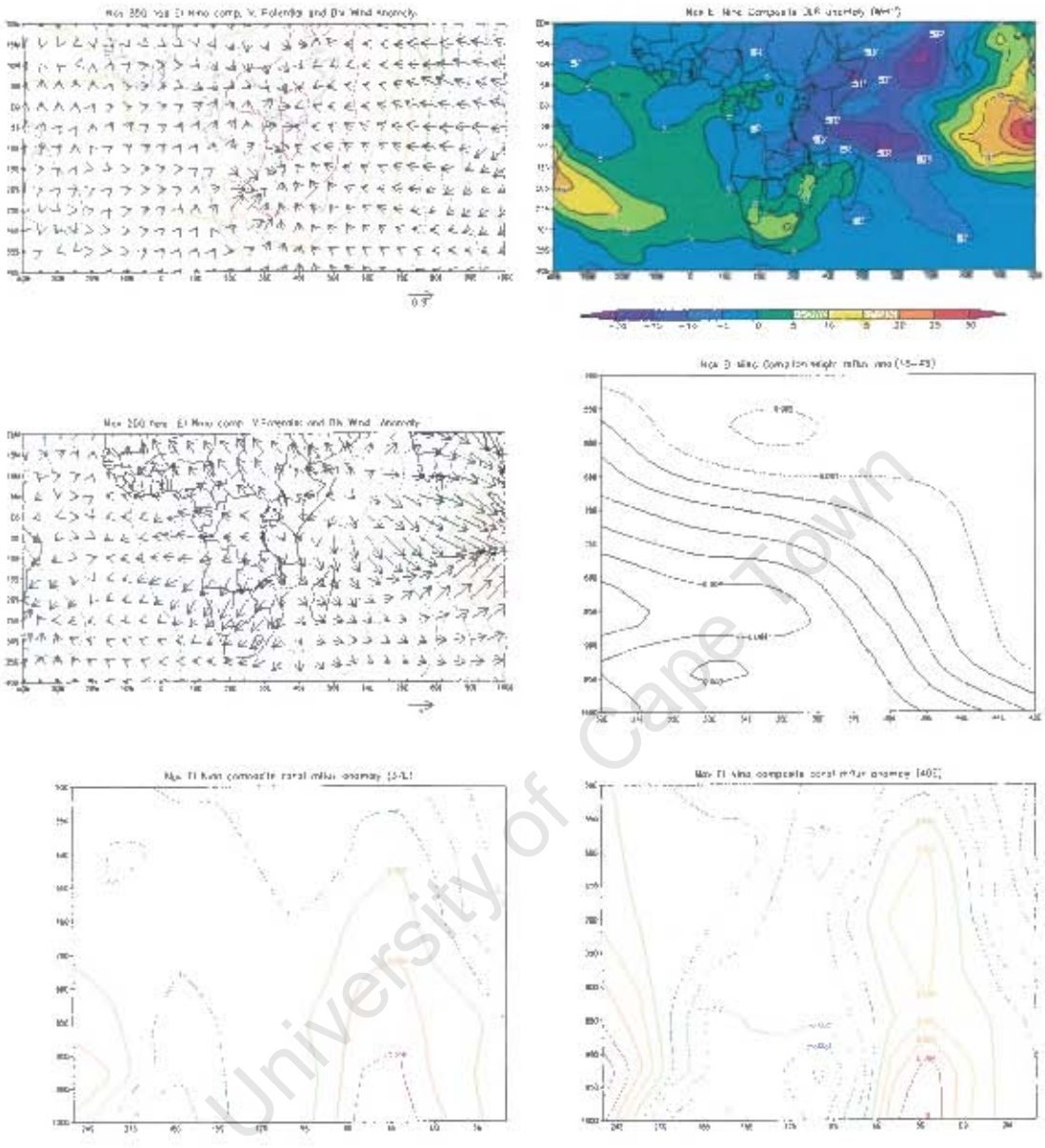

Figure 5.1h: As for figure 5.1b but for November

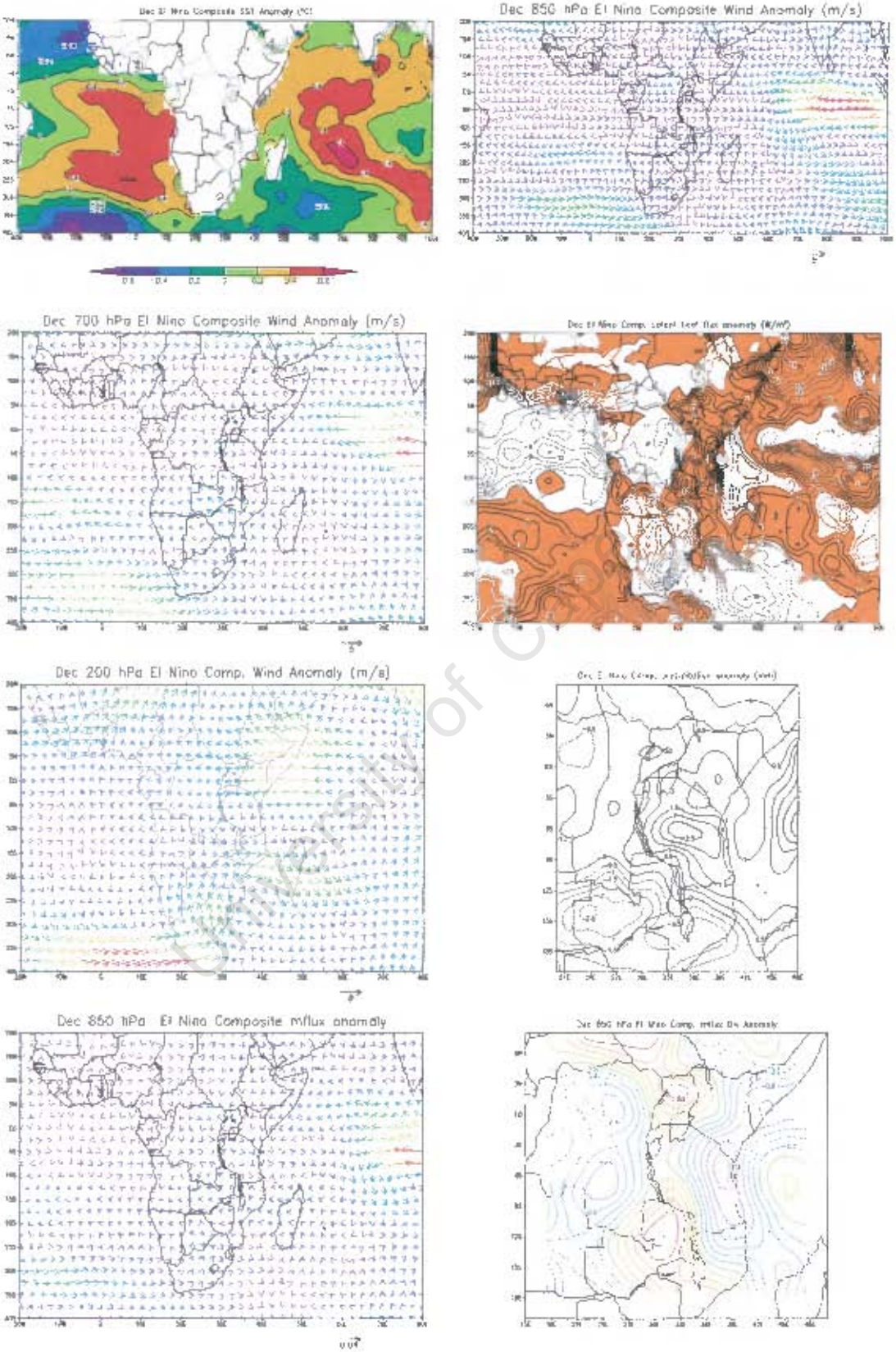

Figure 5.1i: As for figure 5.1a but for Dec

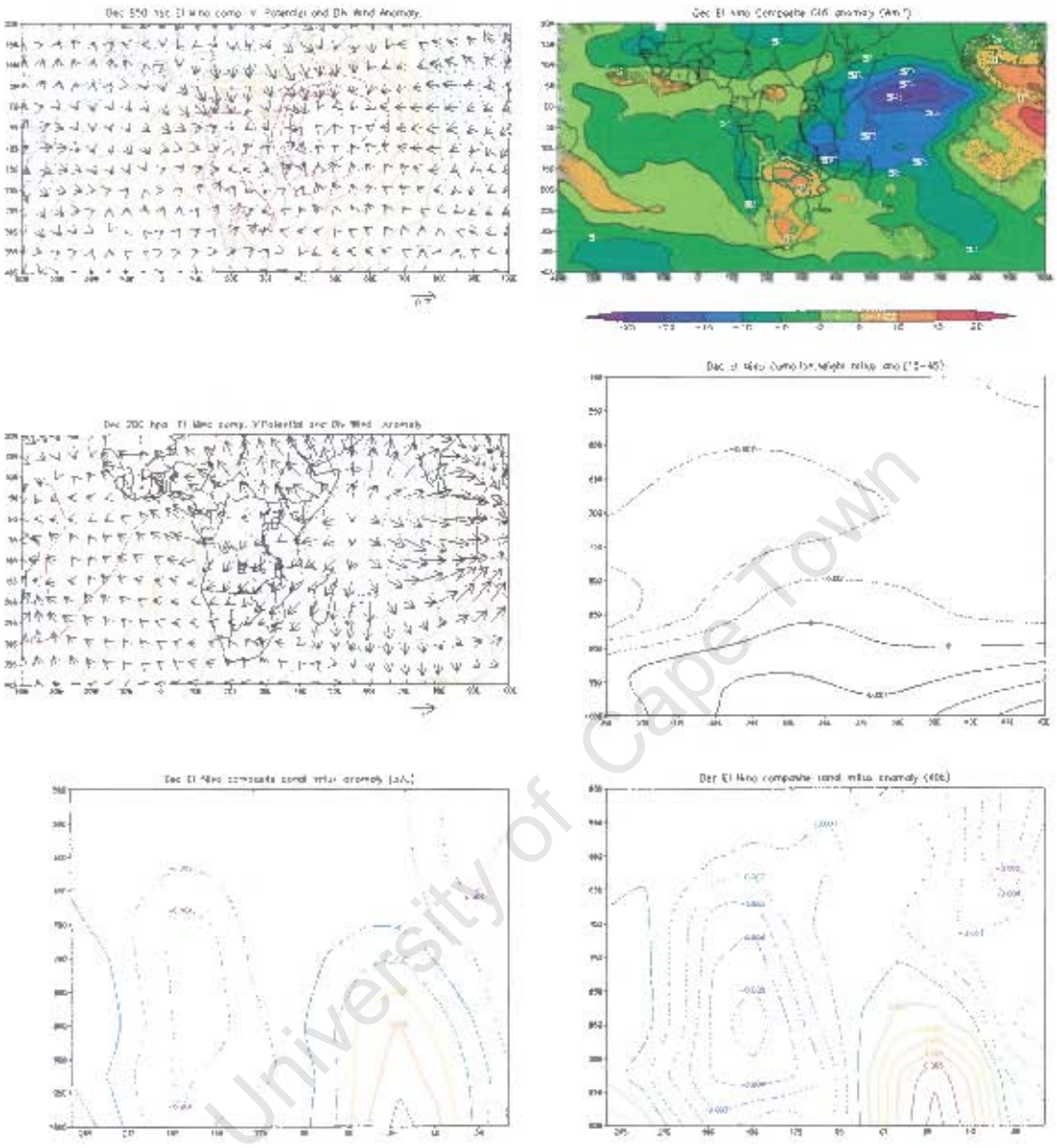

Figure 5.1j: As for figure 5.1b but for Dec

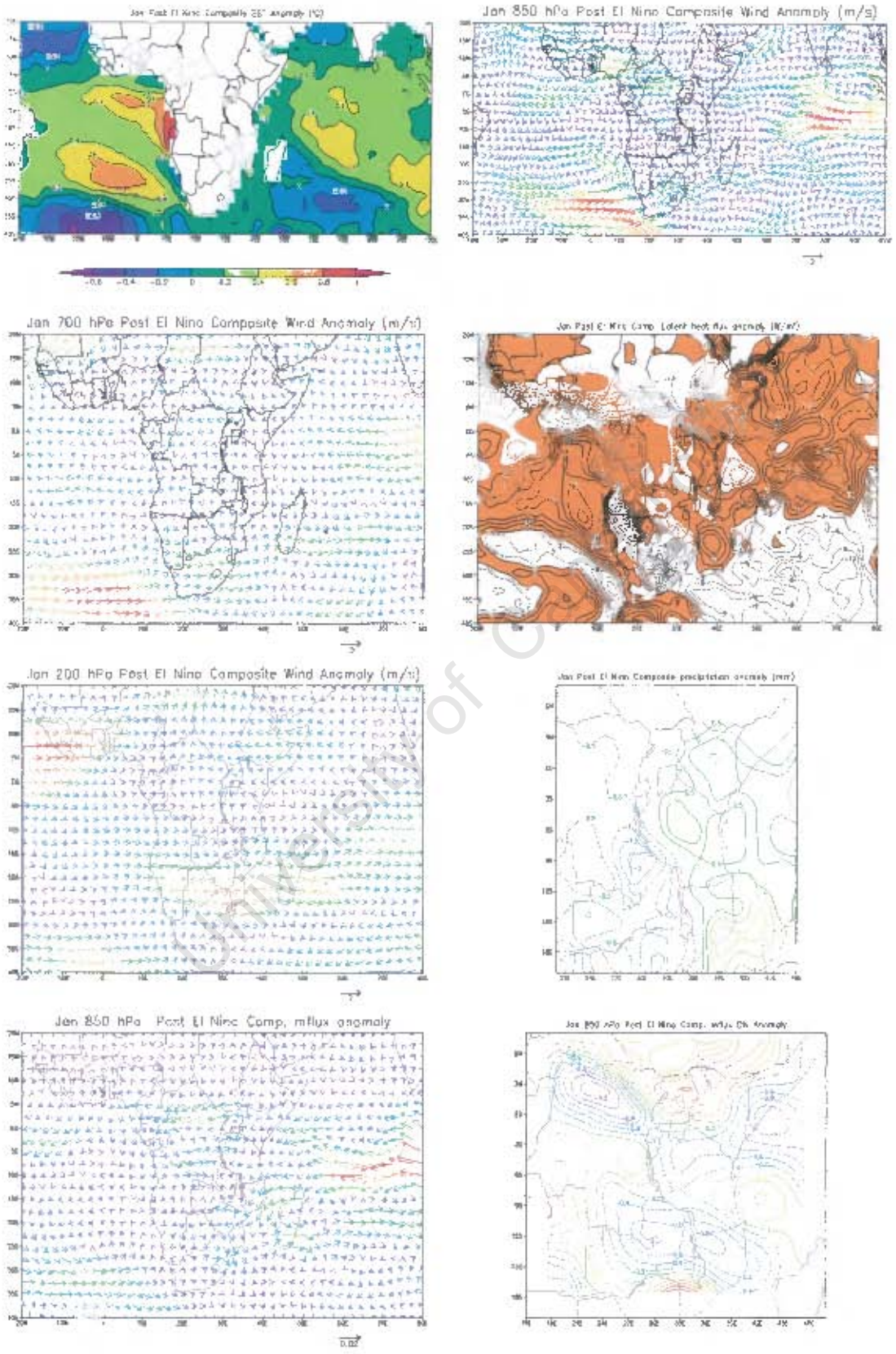

Figure 5.2a: January El Niño+1 composite anomaly fields
Moisture flux g/kg.m/s

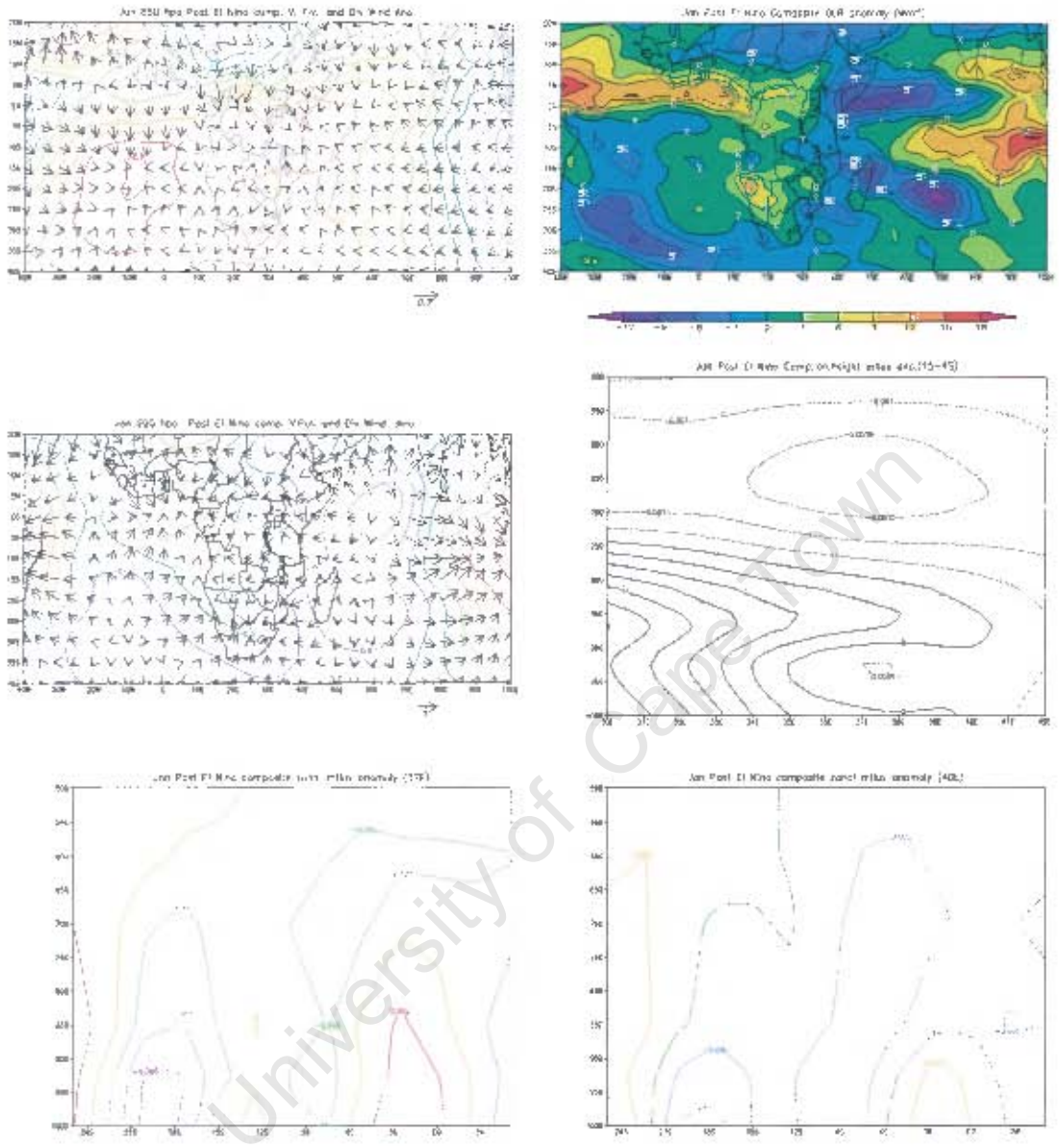

Figure 5.2b January El Niño+1 composite anomaly fields
Velocity potential ($m^2 s^{-1}$)
Divergent wind (s^{-1})

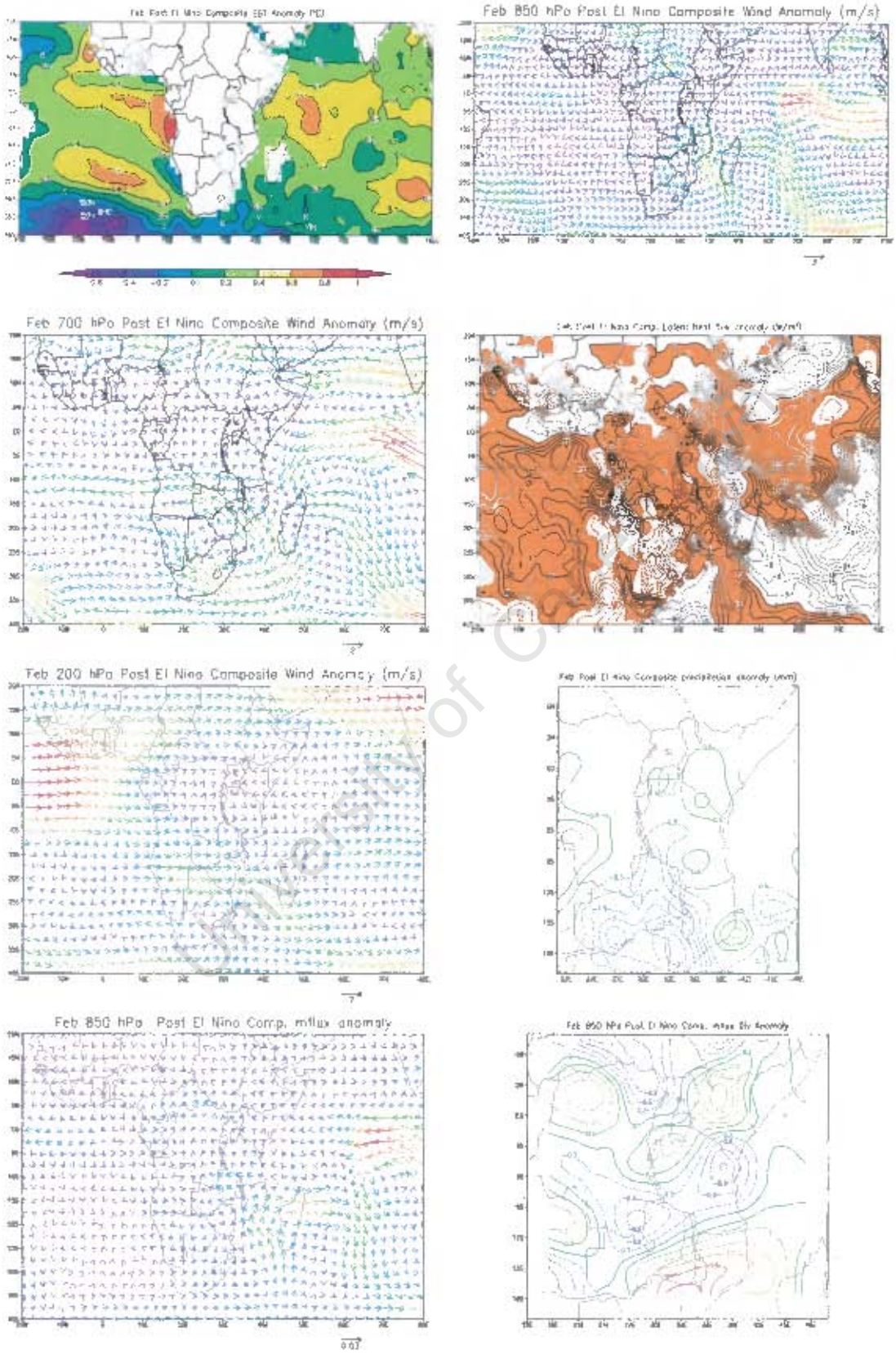

Figure 5.2c: As for figure 5.2a but for February

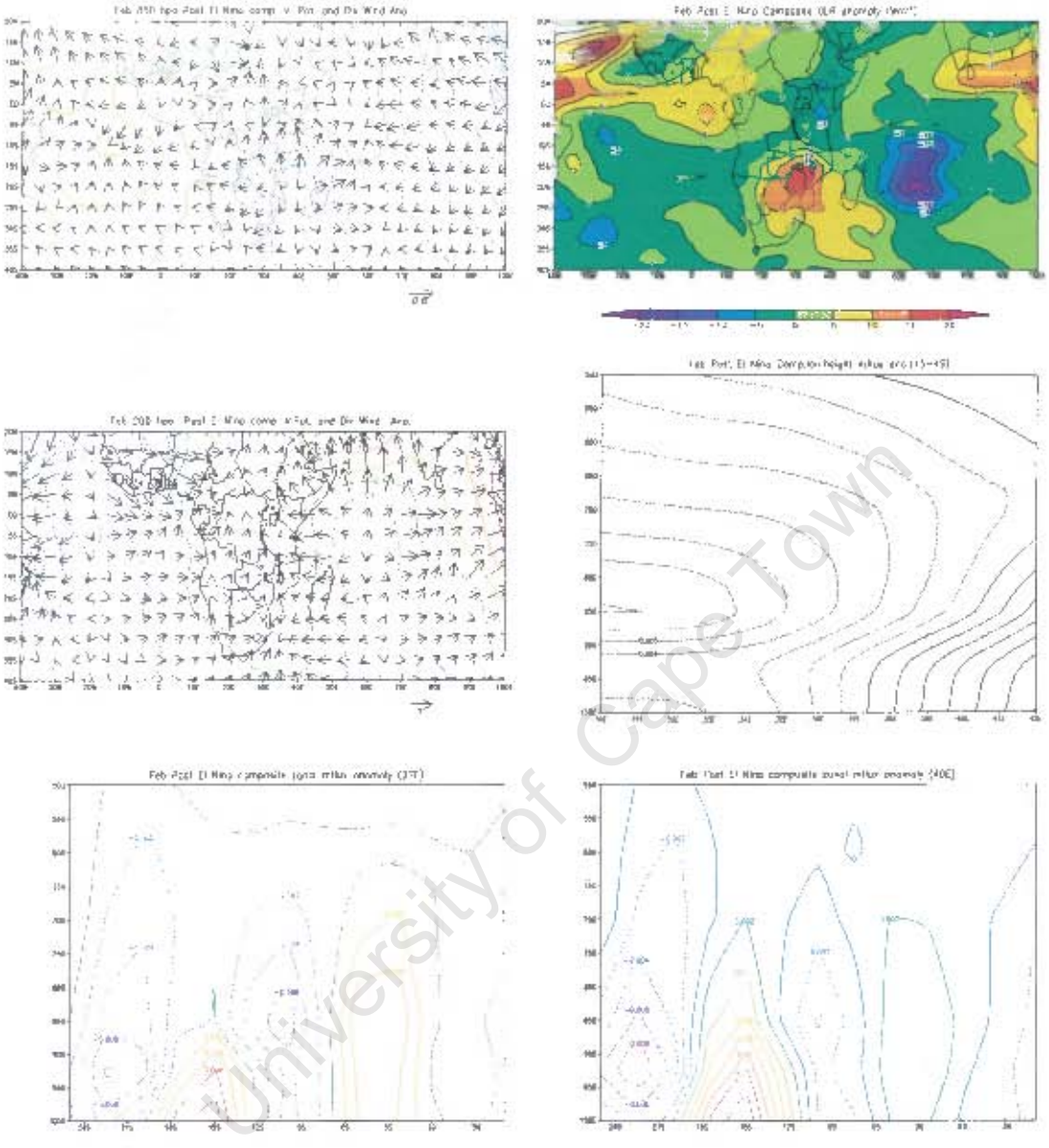

Figure 5.2d: As for figure 5.2b but for February

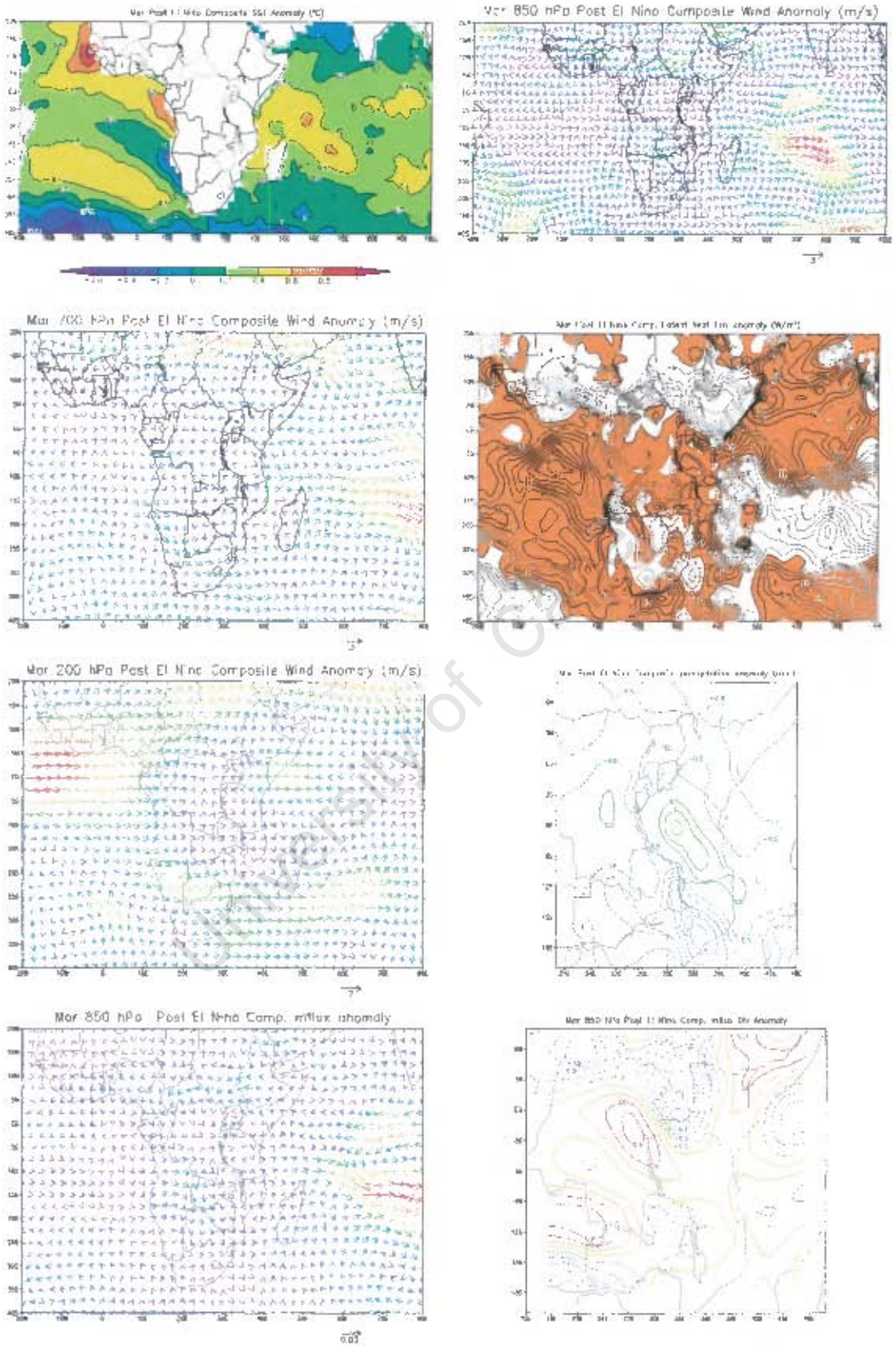

Figure 5.2e:As for figure 5.2a but for March

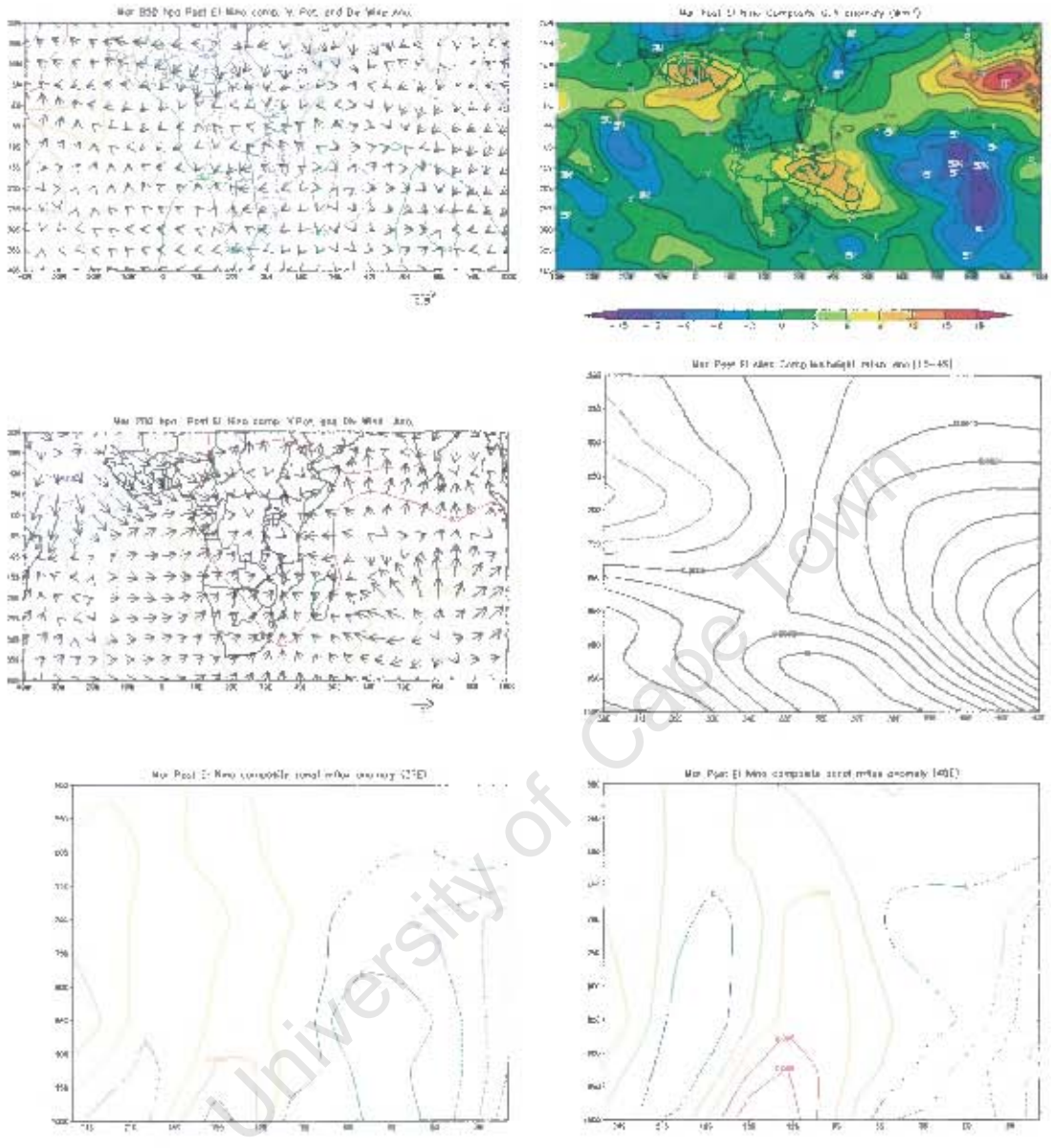

Figure 5.2f:As for figure 5.2b but for March

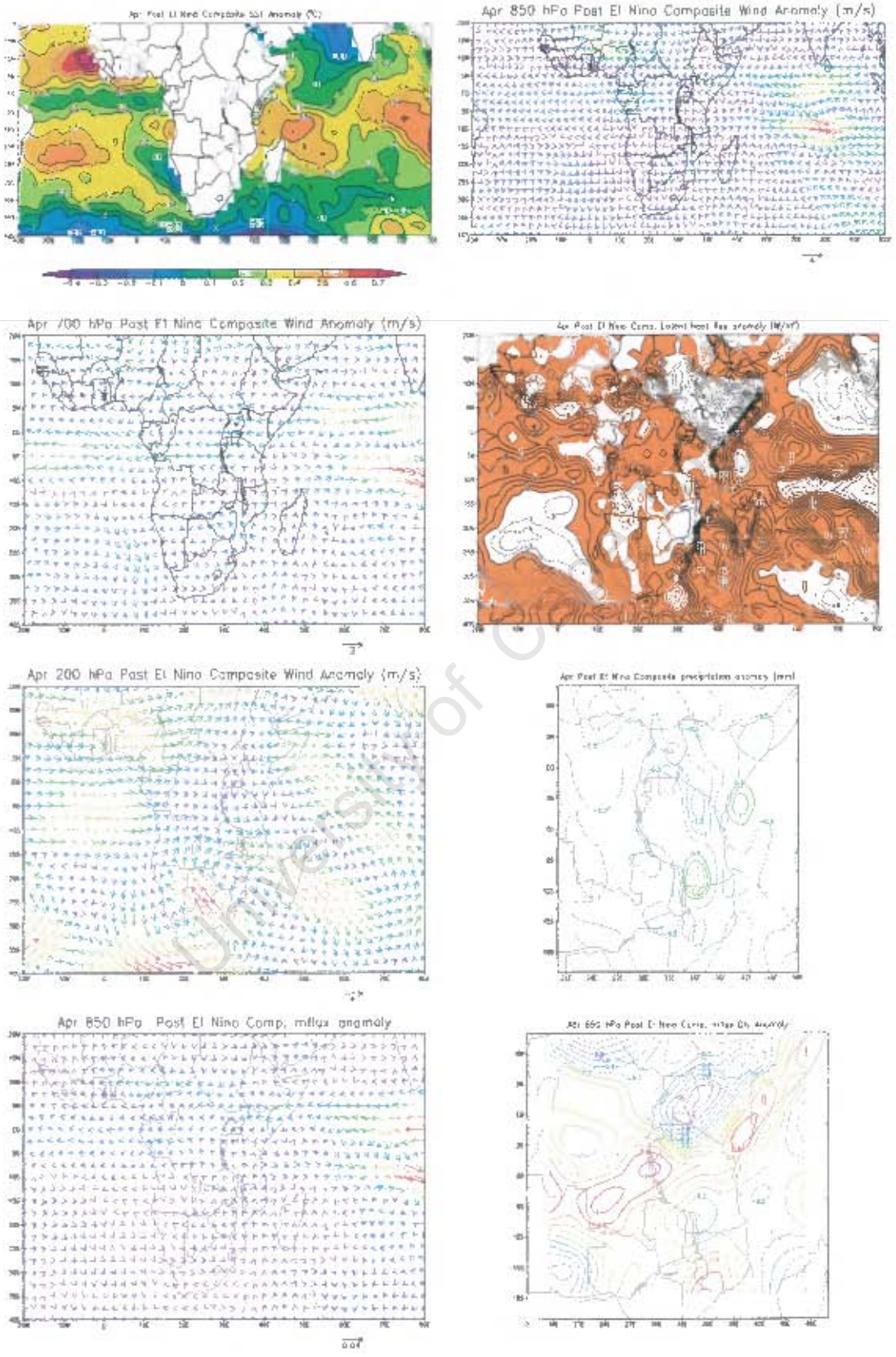

Figure 5.2g: As for figure 5.2a but for April

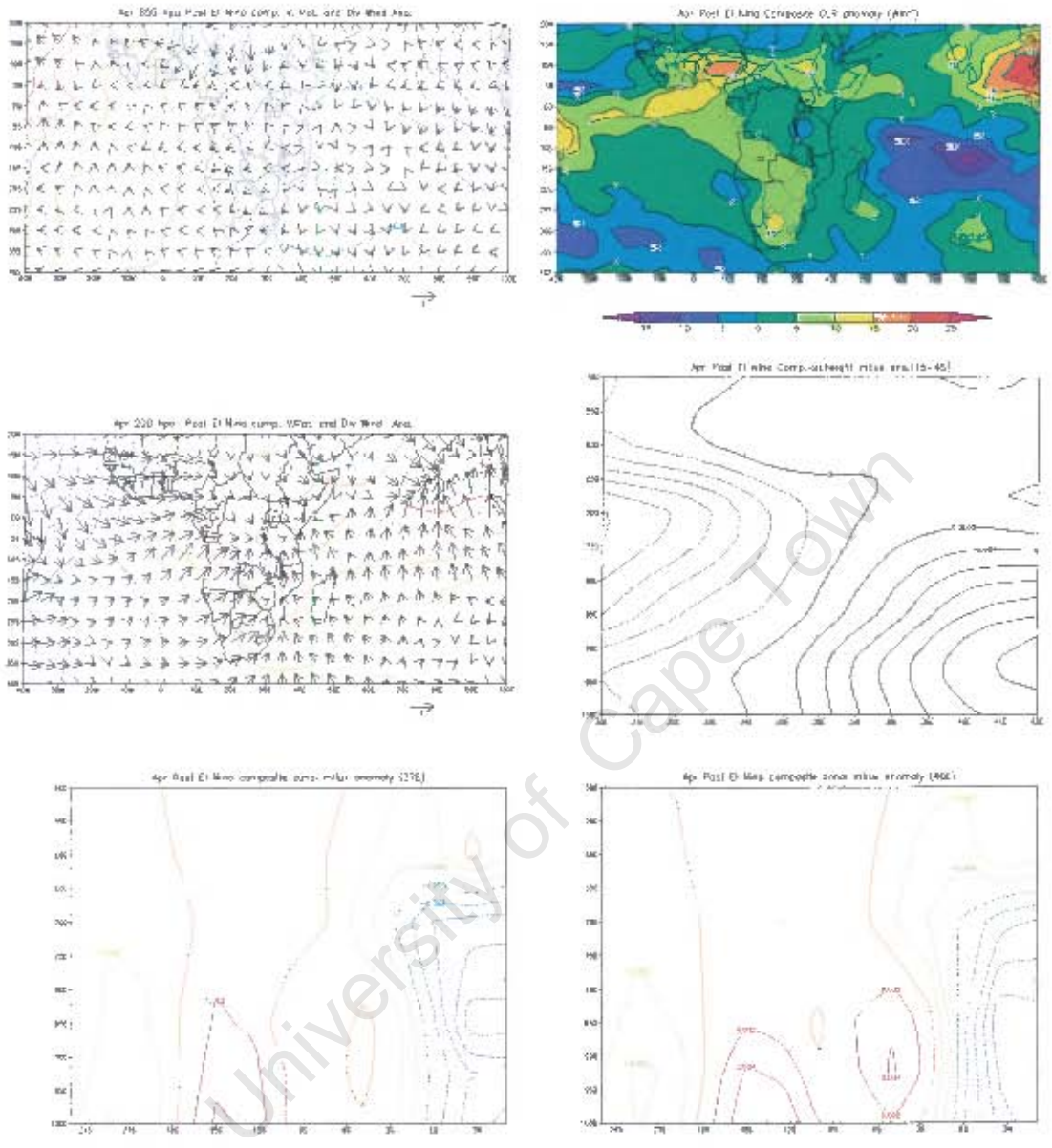

Figure 5.2h: As for figure 5.2b but for April

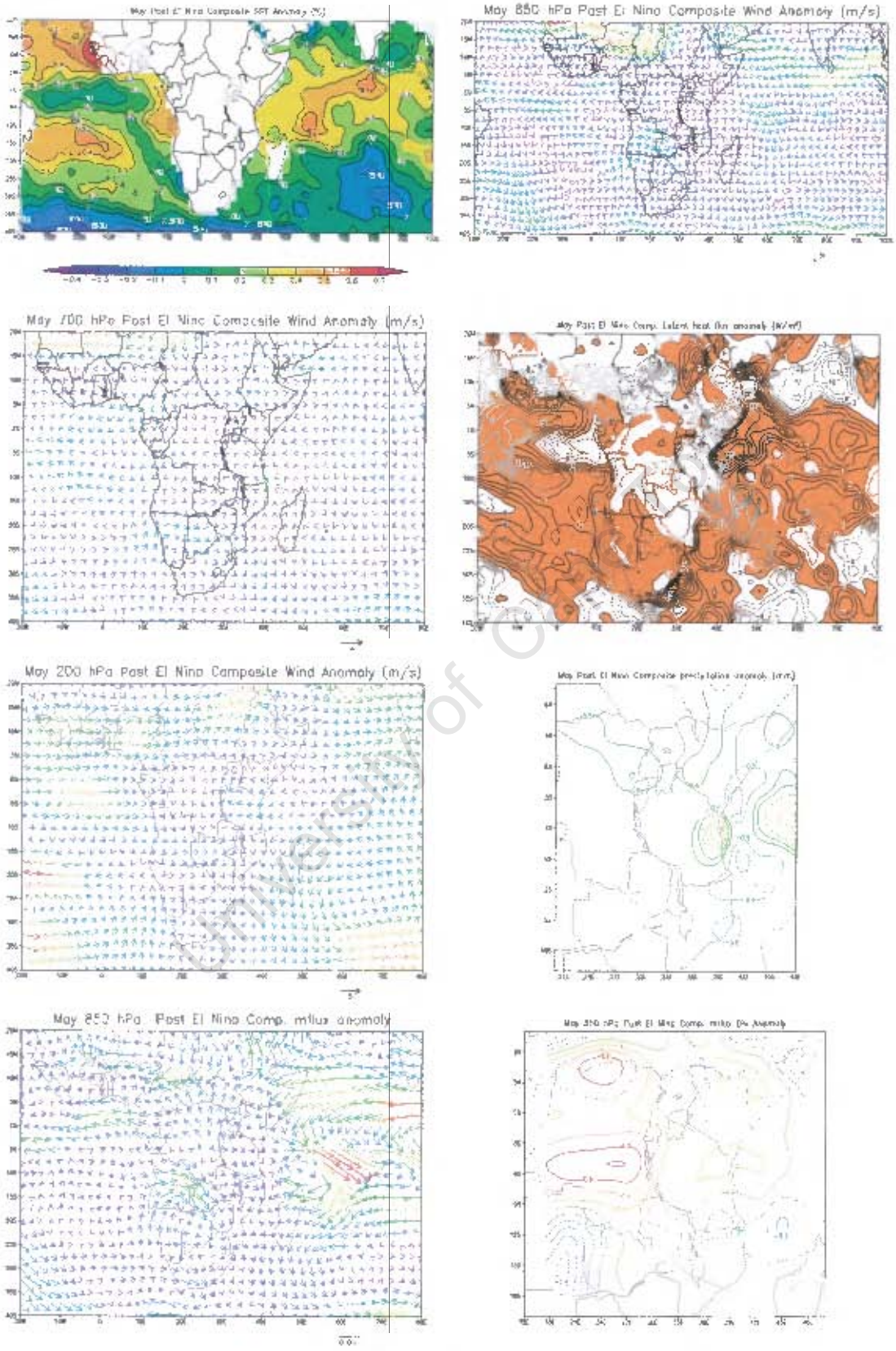

Figure 5.2i: As for figure 5.2a but for May

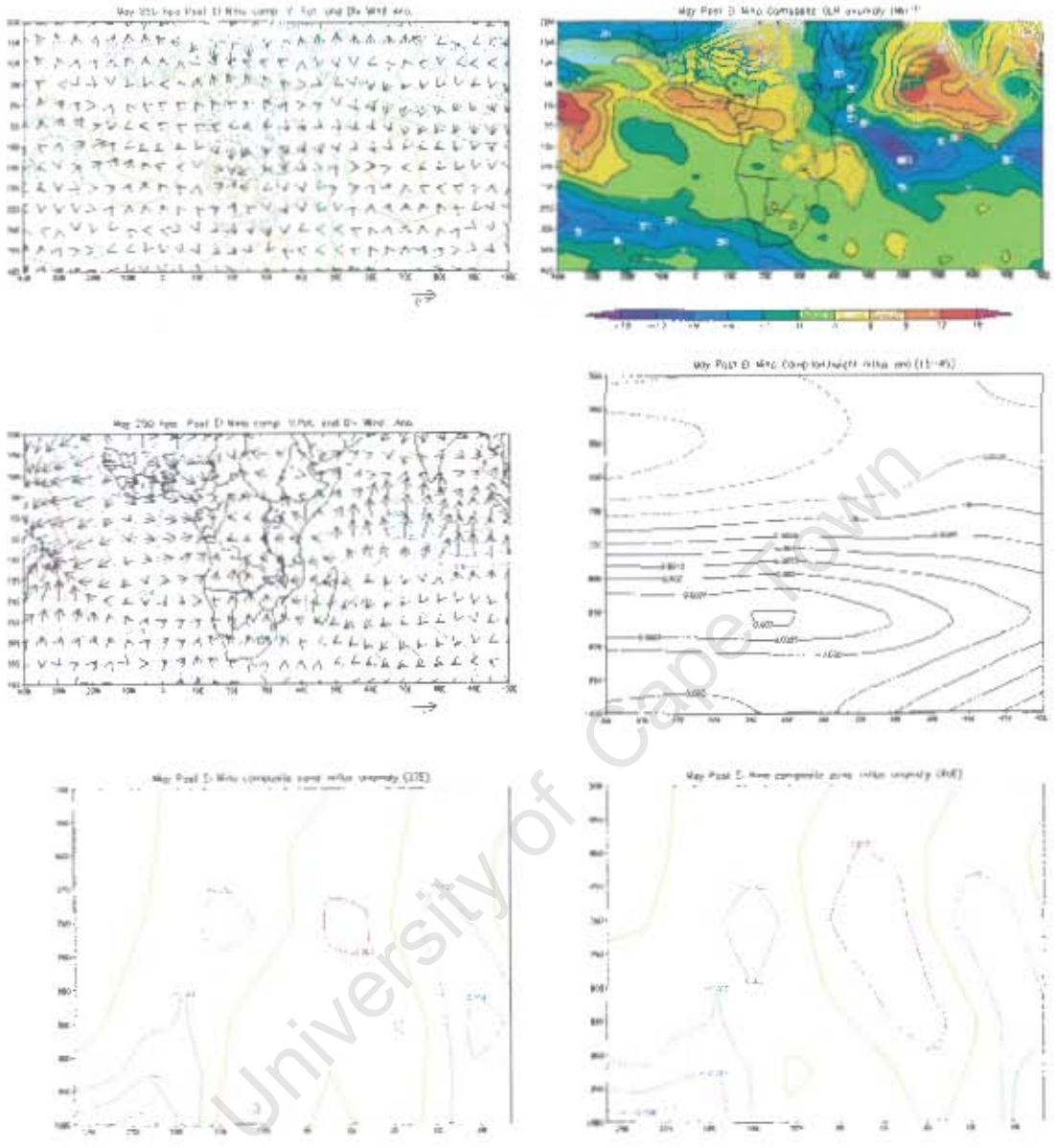

Figure 5.2j: As for figure 5.2b but for May

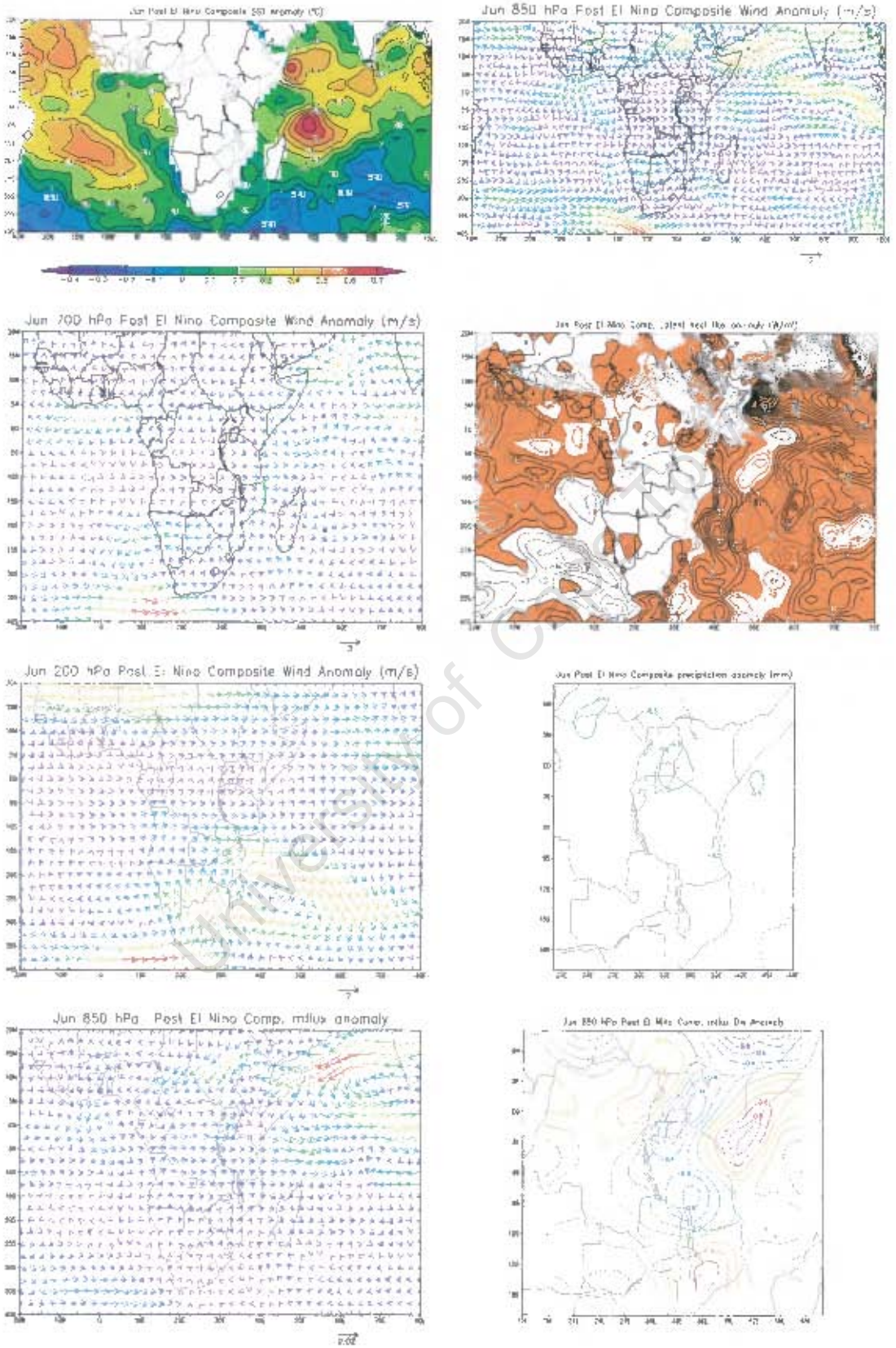

Figure 5.2k: As for figure 5.2a but for June

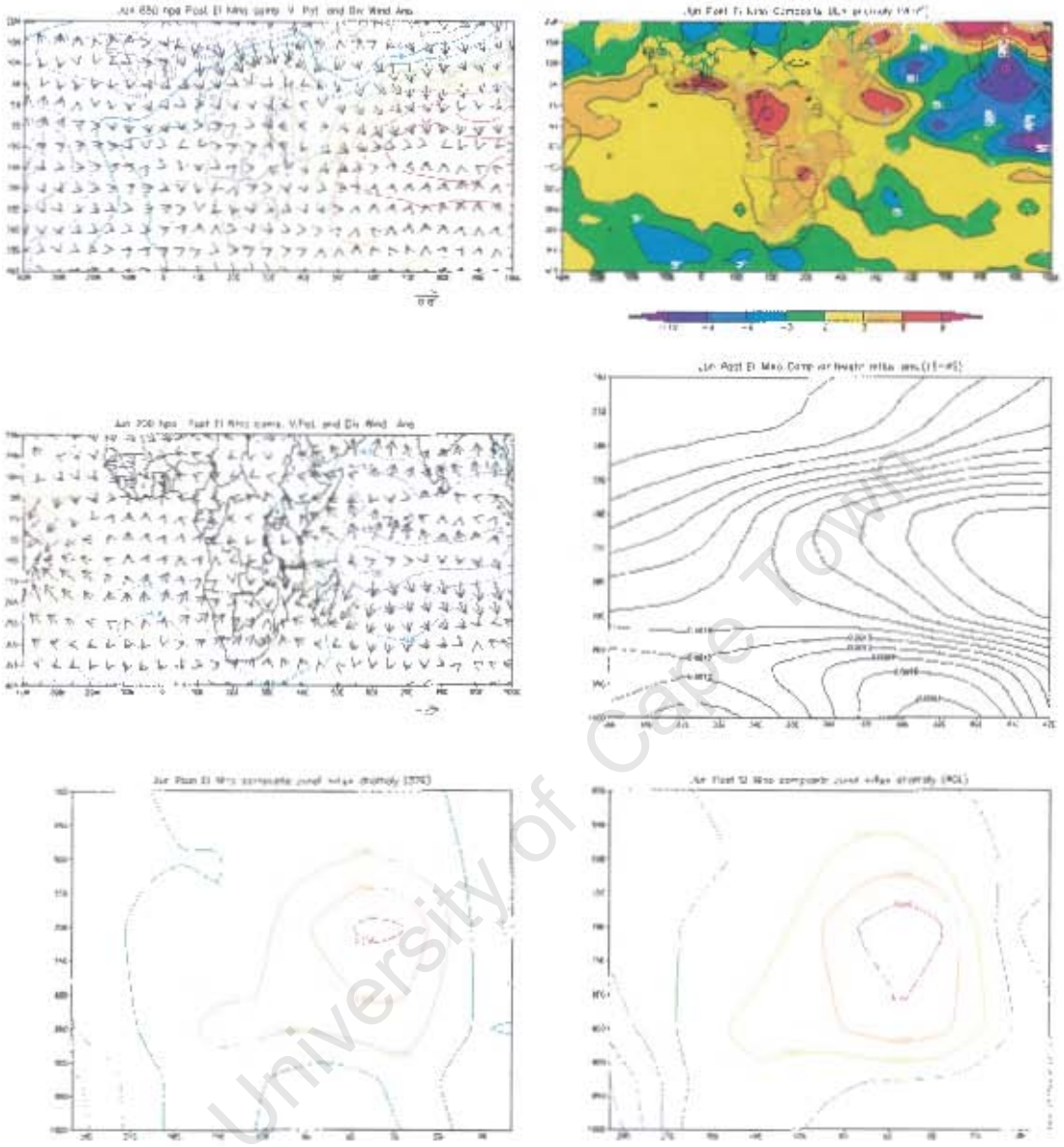

Figure 5.2l: As for figure 5.2b but for June

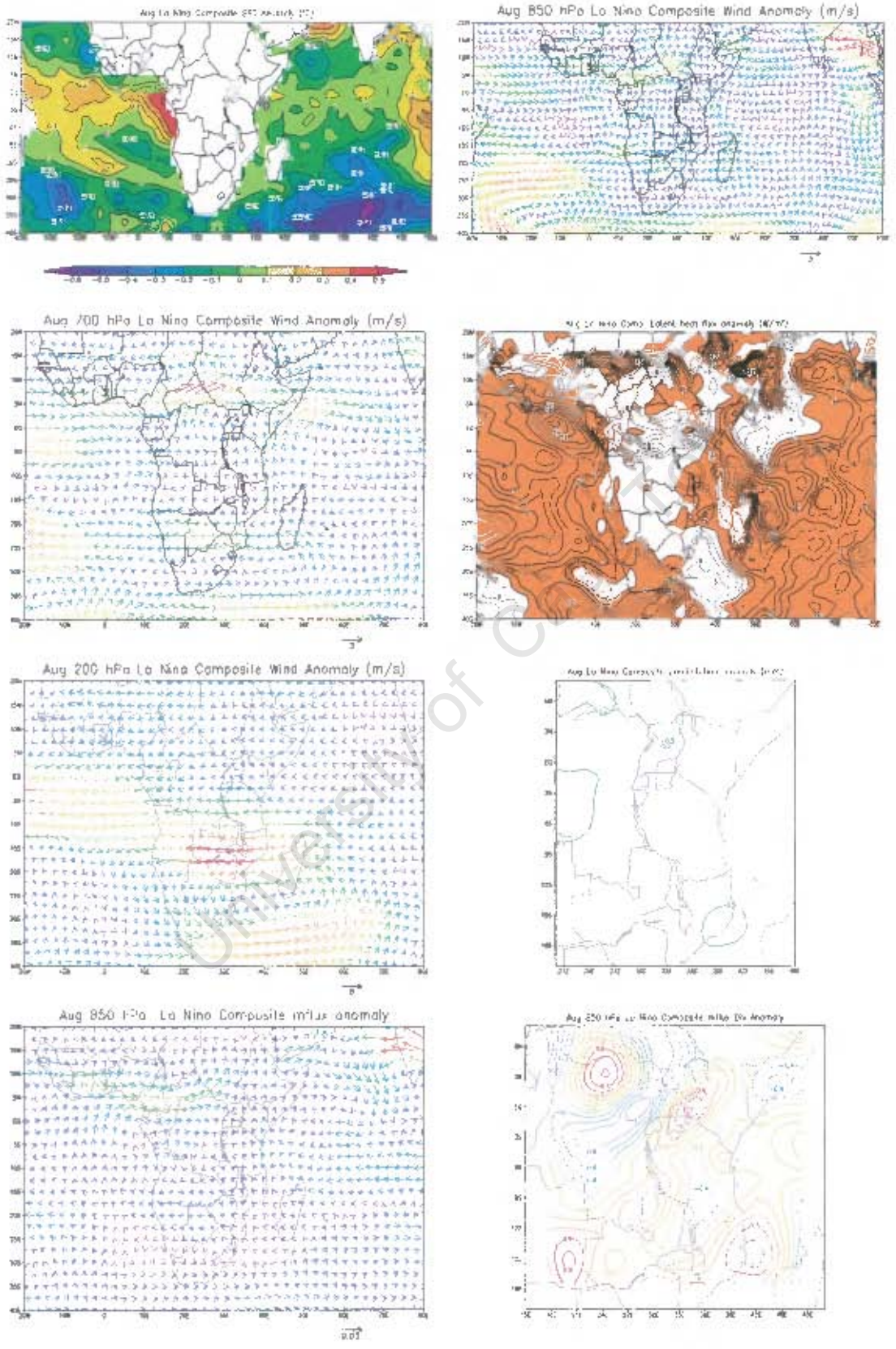

Figure 5.3a: August La Niña composite Anomaly fields Moisture flux g/kg.m/s

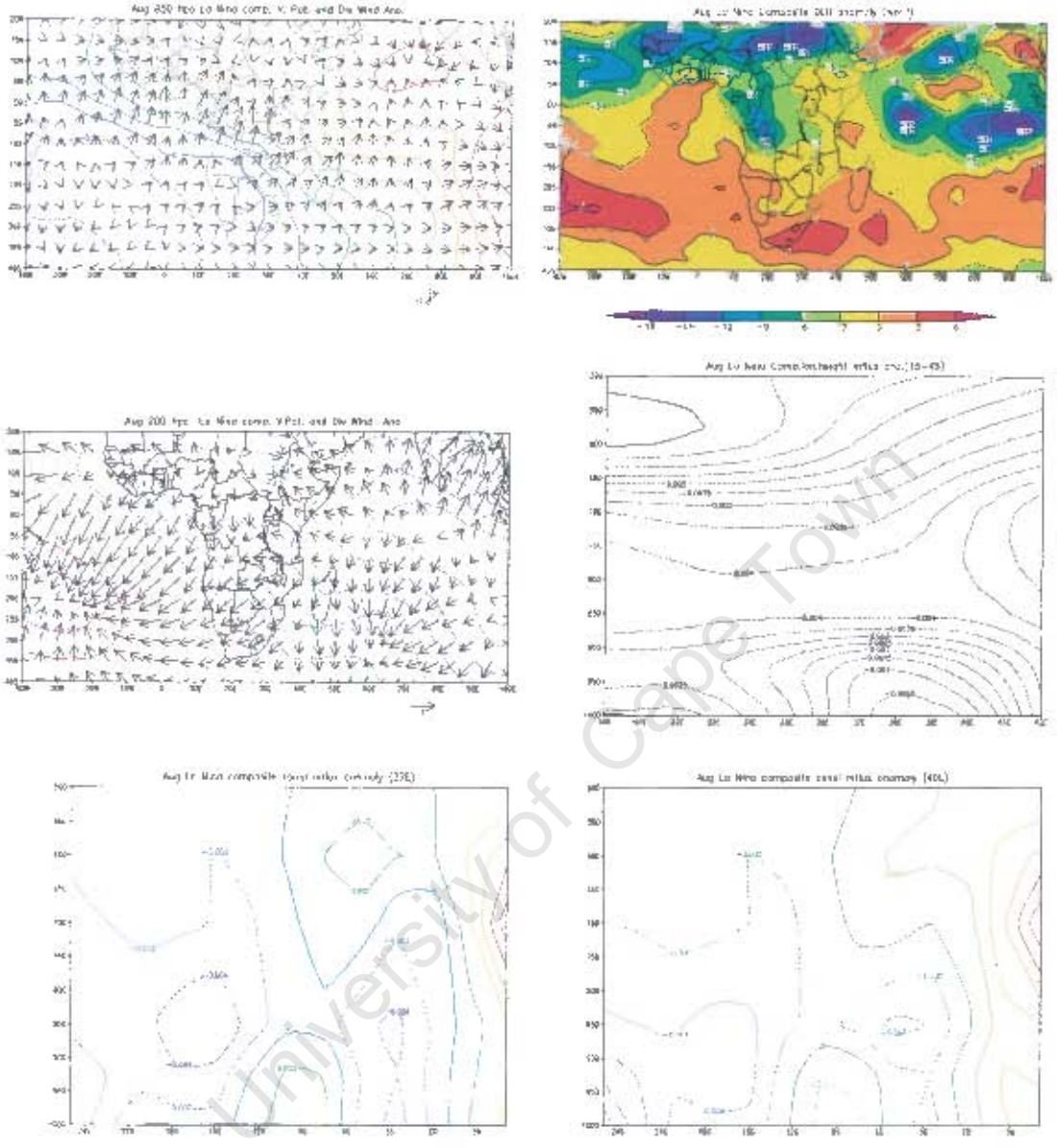

Figure 5.3b August La Niña composite anomaly fields
Velocity potential (m^2 s^{-1})
Divergent wind (s^{-1})

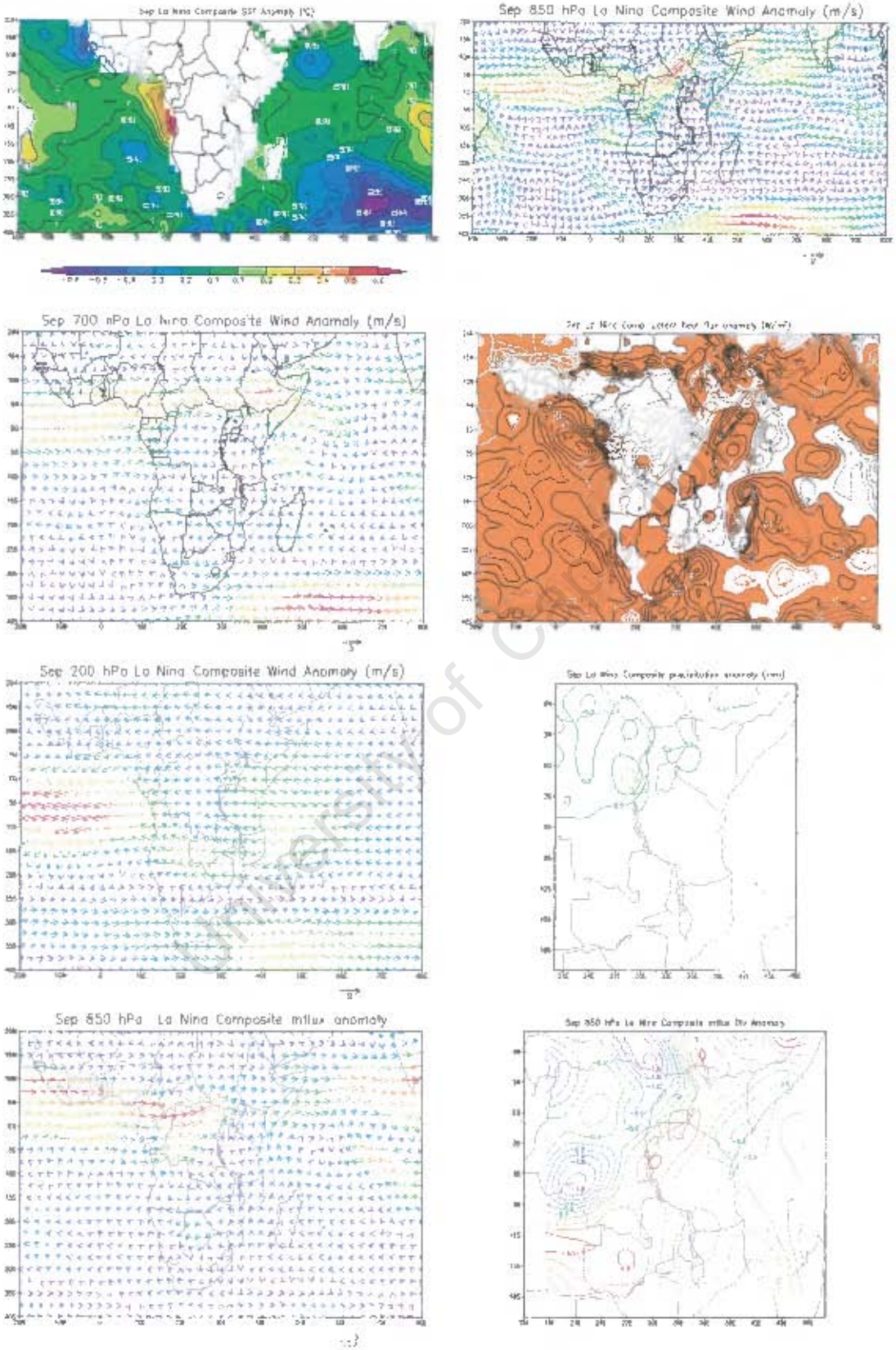

Figure 5.3c: As for figure 5.3a but for September

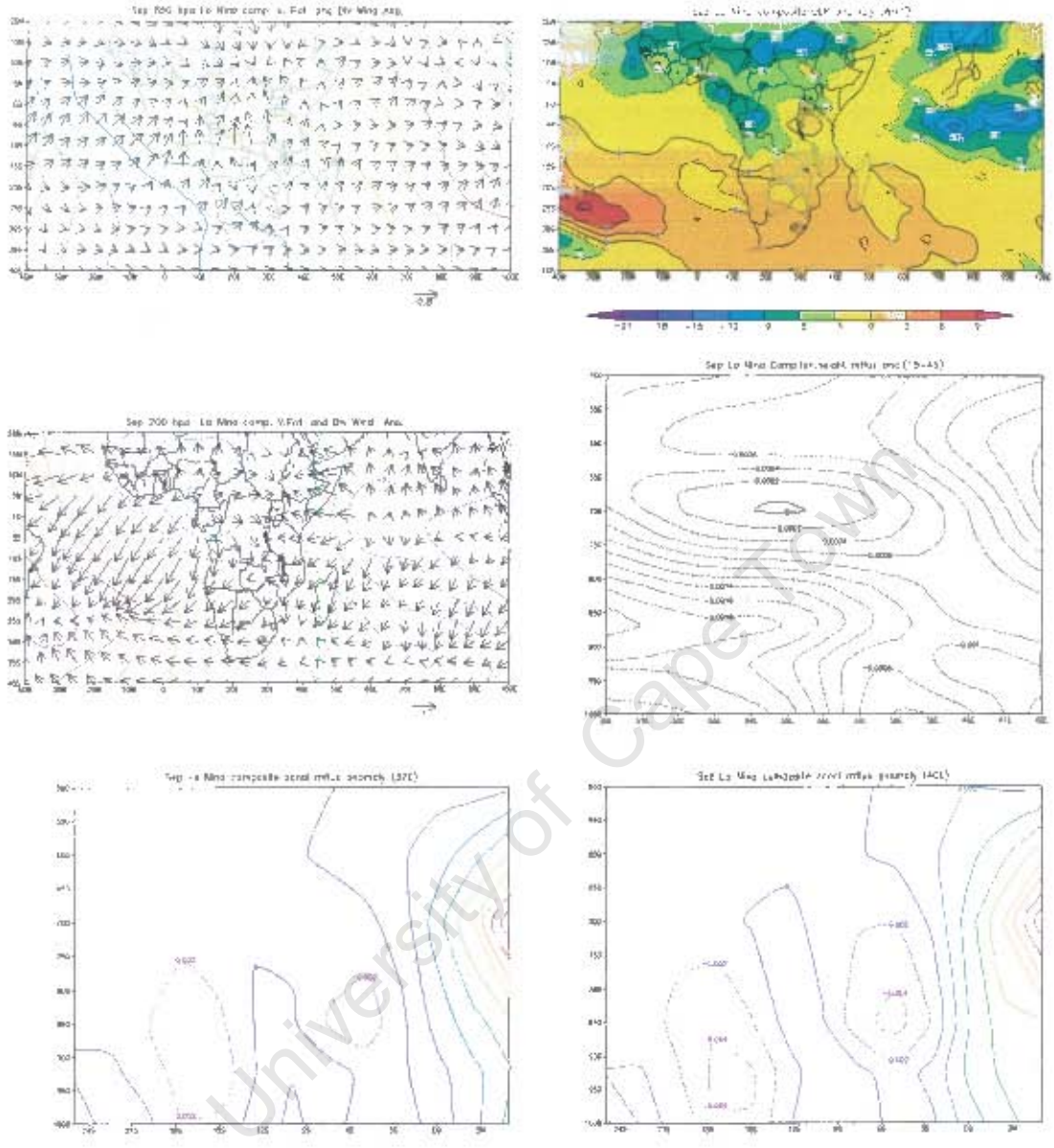

Figure 5.3d: As for figure 5.3b but for September

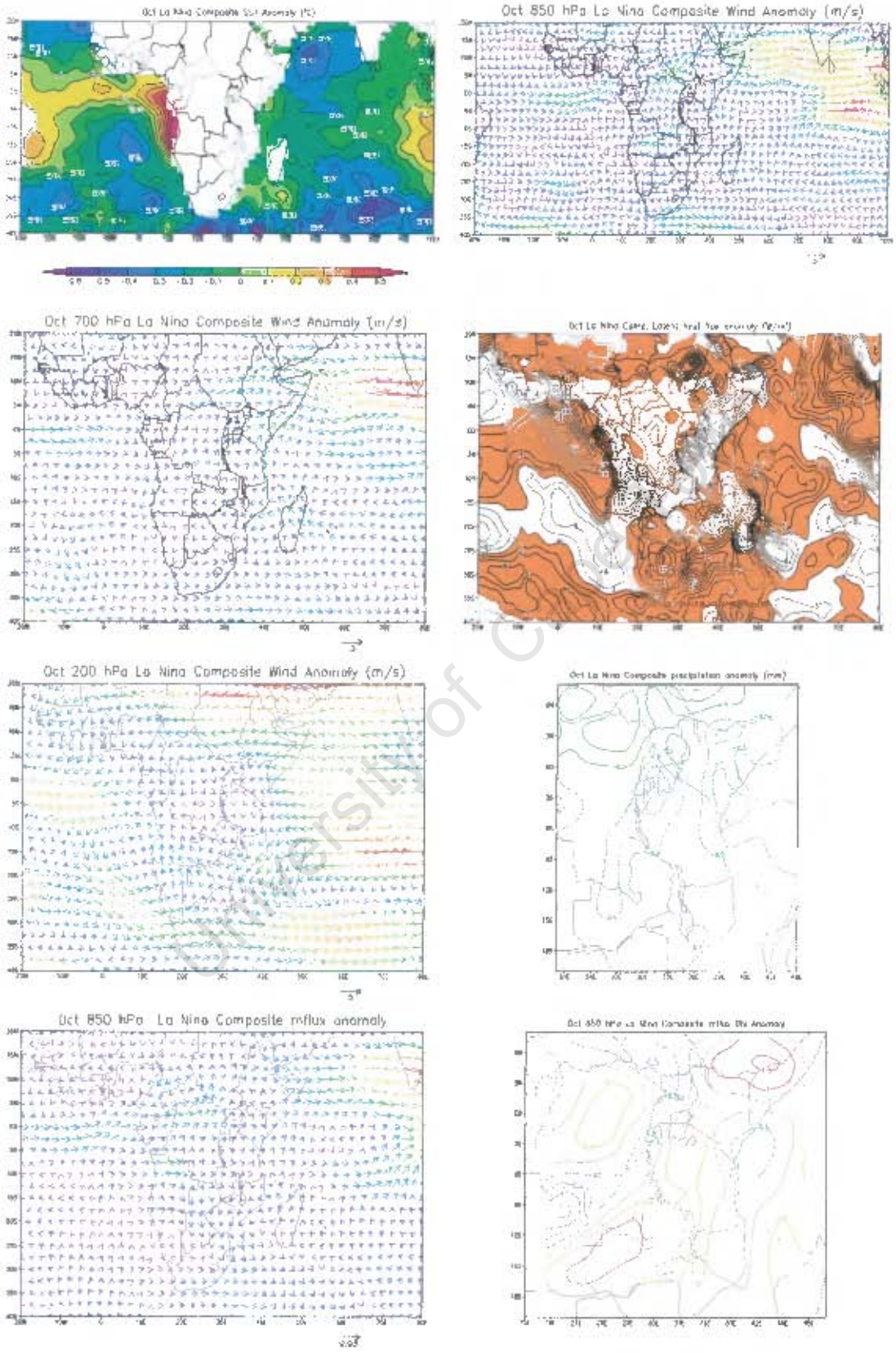

Figure 5.3e: As for figure 5.3a but for October

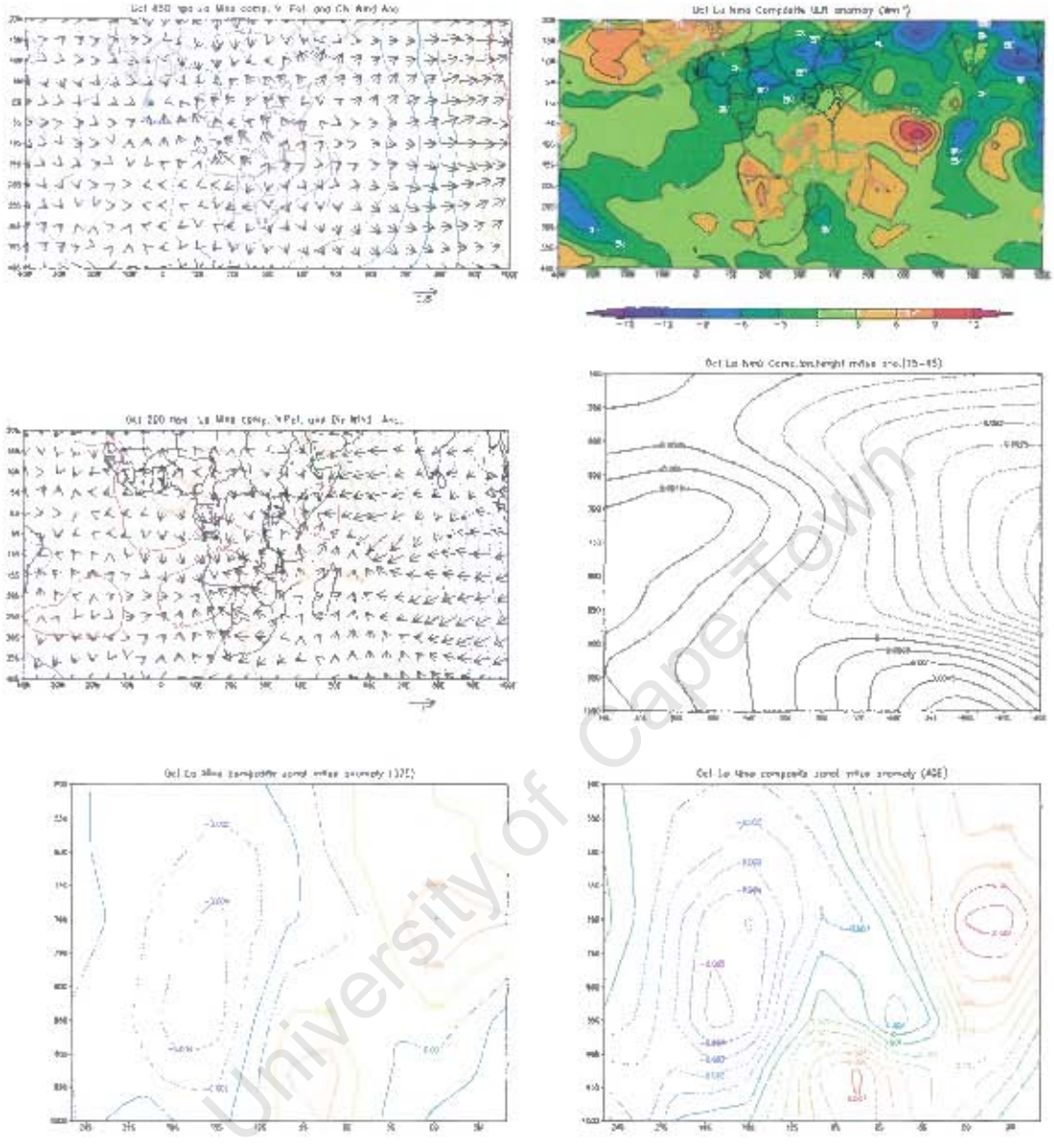

Figure 5.3f: As for figure 5.3b but for October

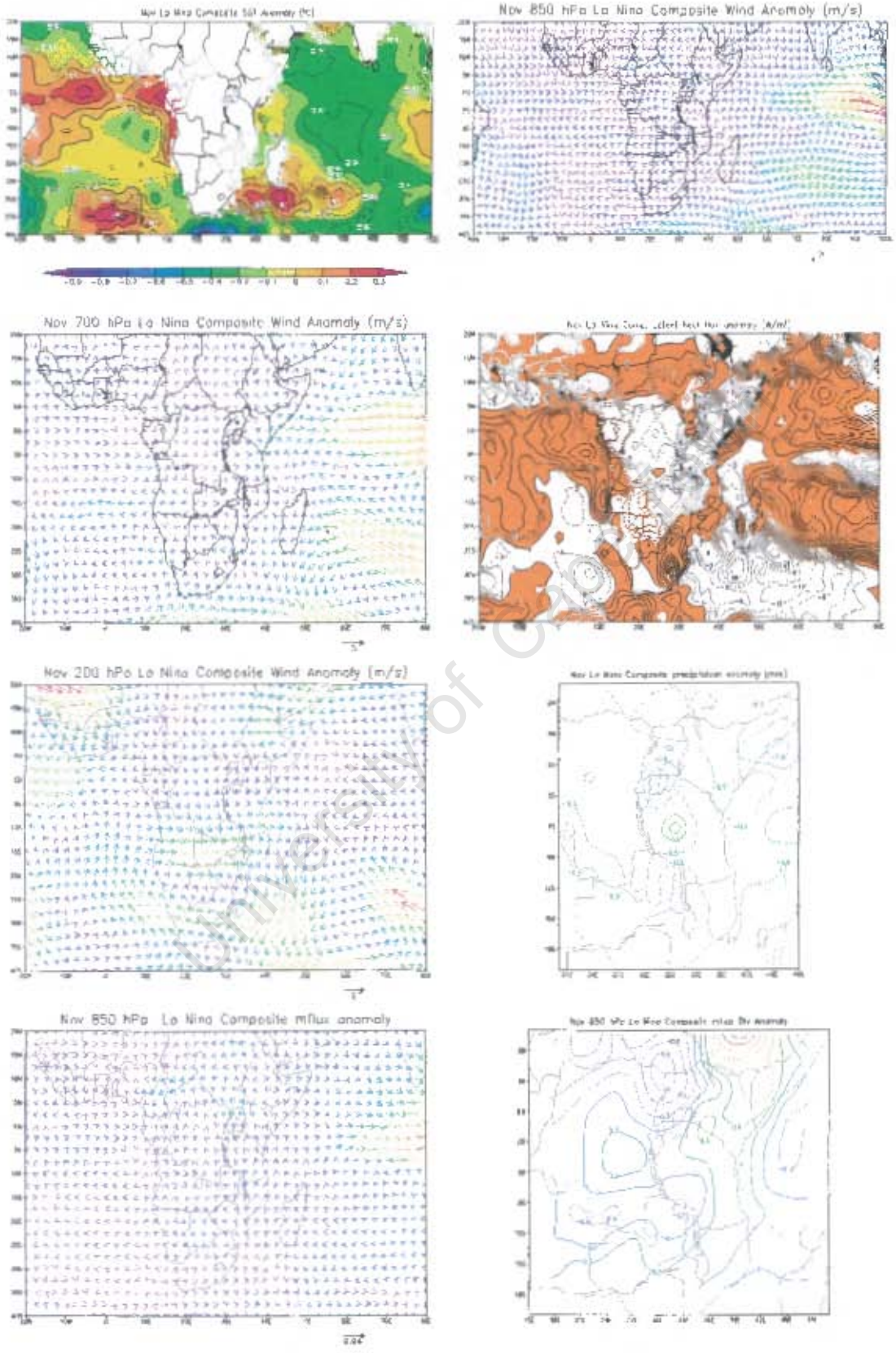

Figure 5.3g: As for figure 5.3a but for November

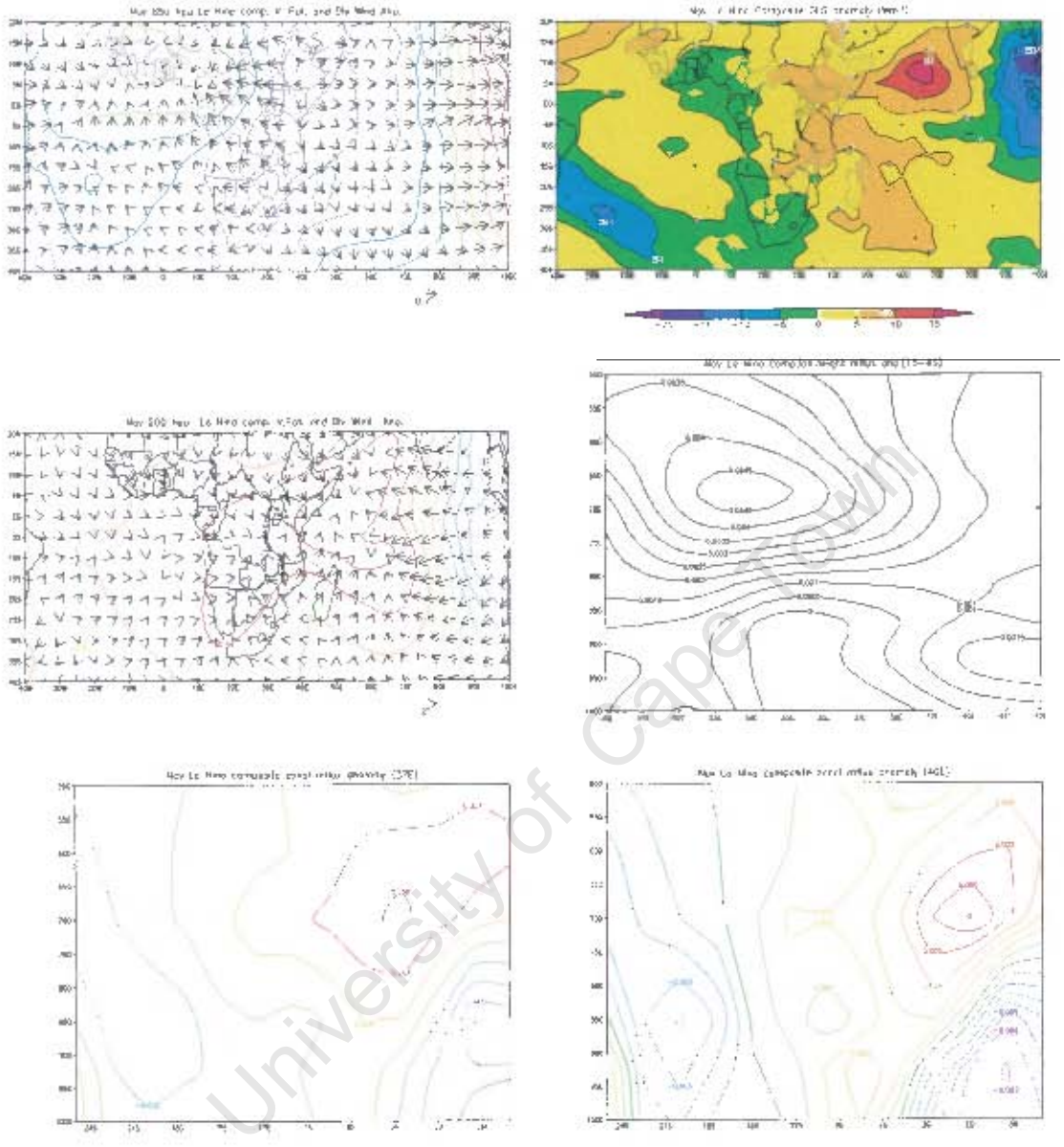

Figure 5.3h: As for figure 5.3b but for November

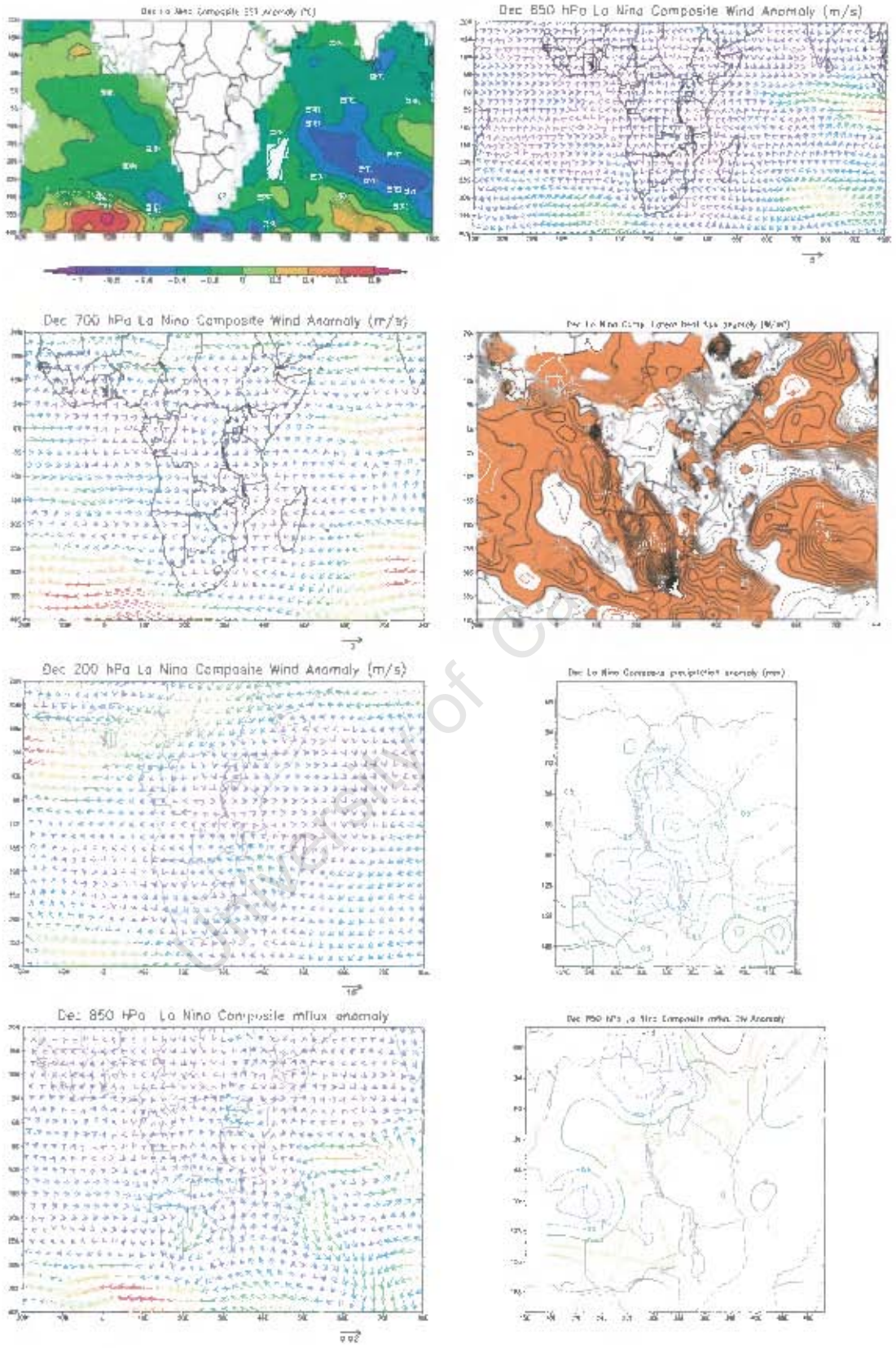

Figure 5.3i: As for figure 5.3a but for December

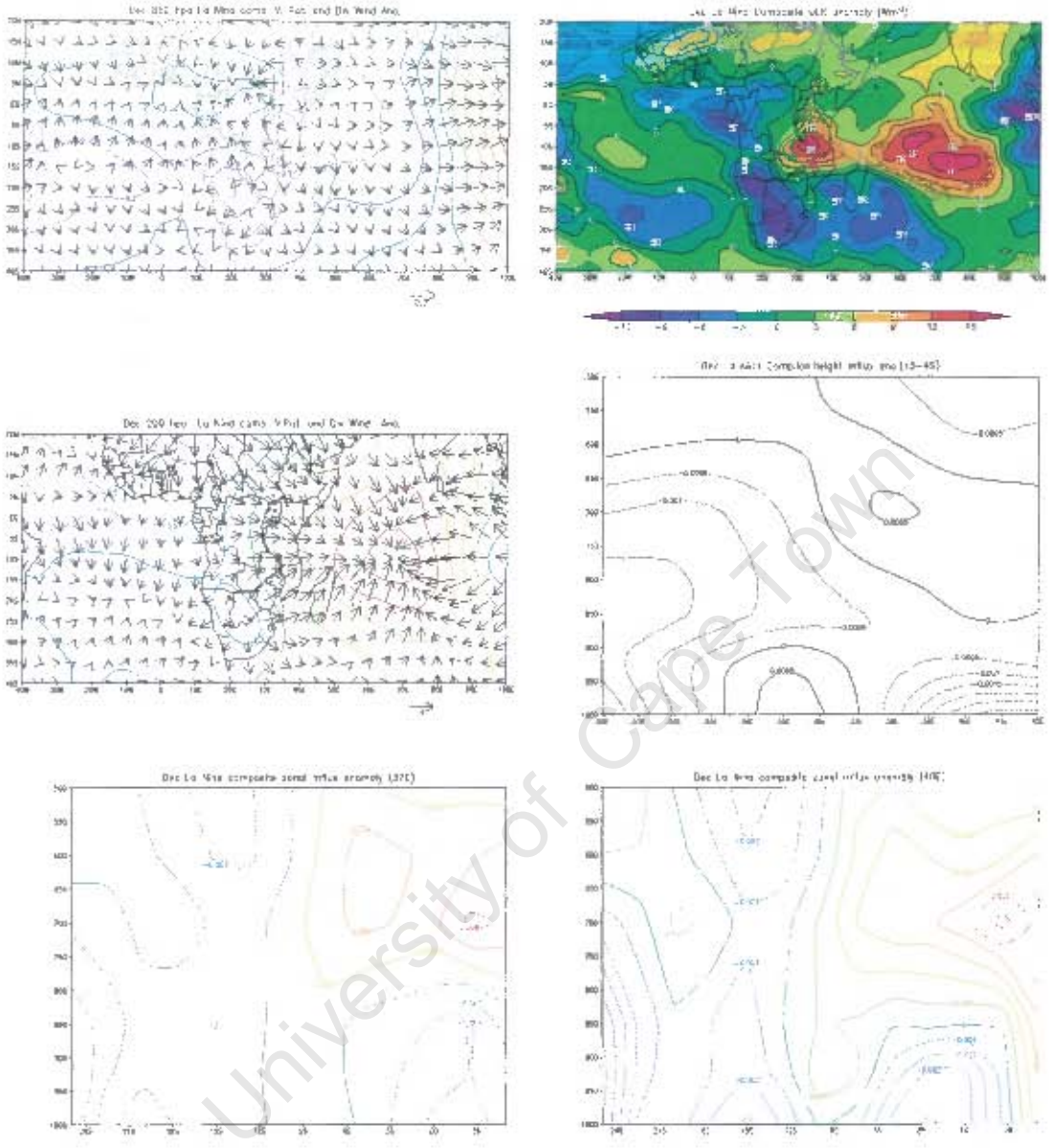

Figure 5.3j: As for figure 5.3b but for December

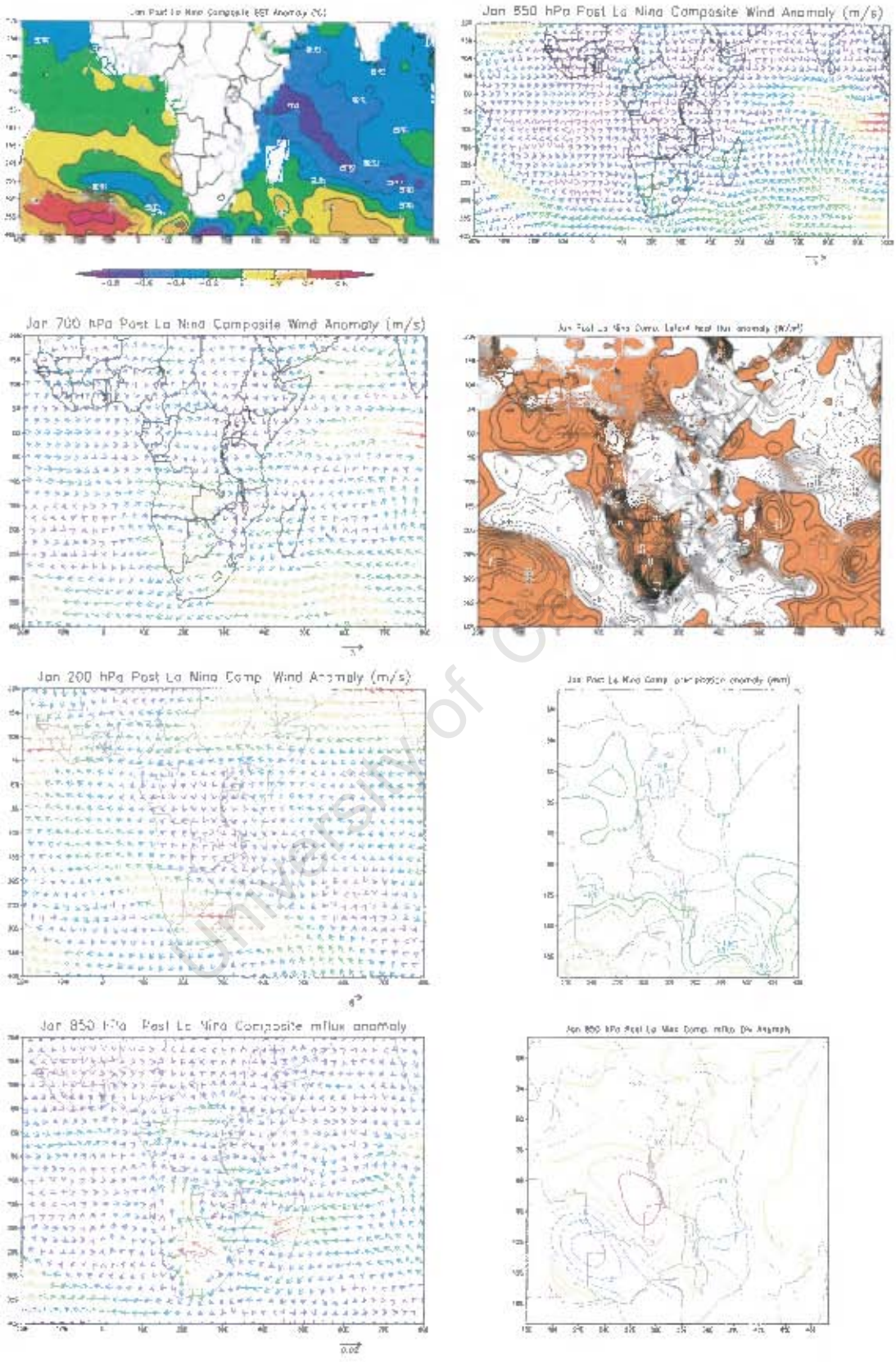

Figure 5.4a: January La Niña+1 composite anomaly fields Moisture flux g/kg.m/s

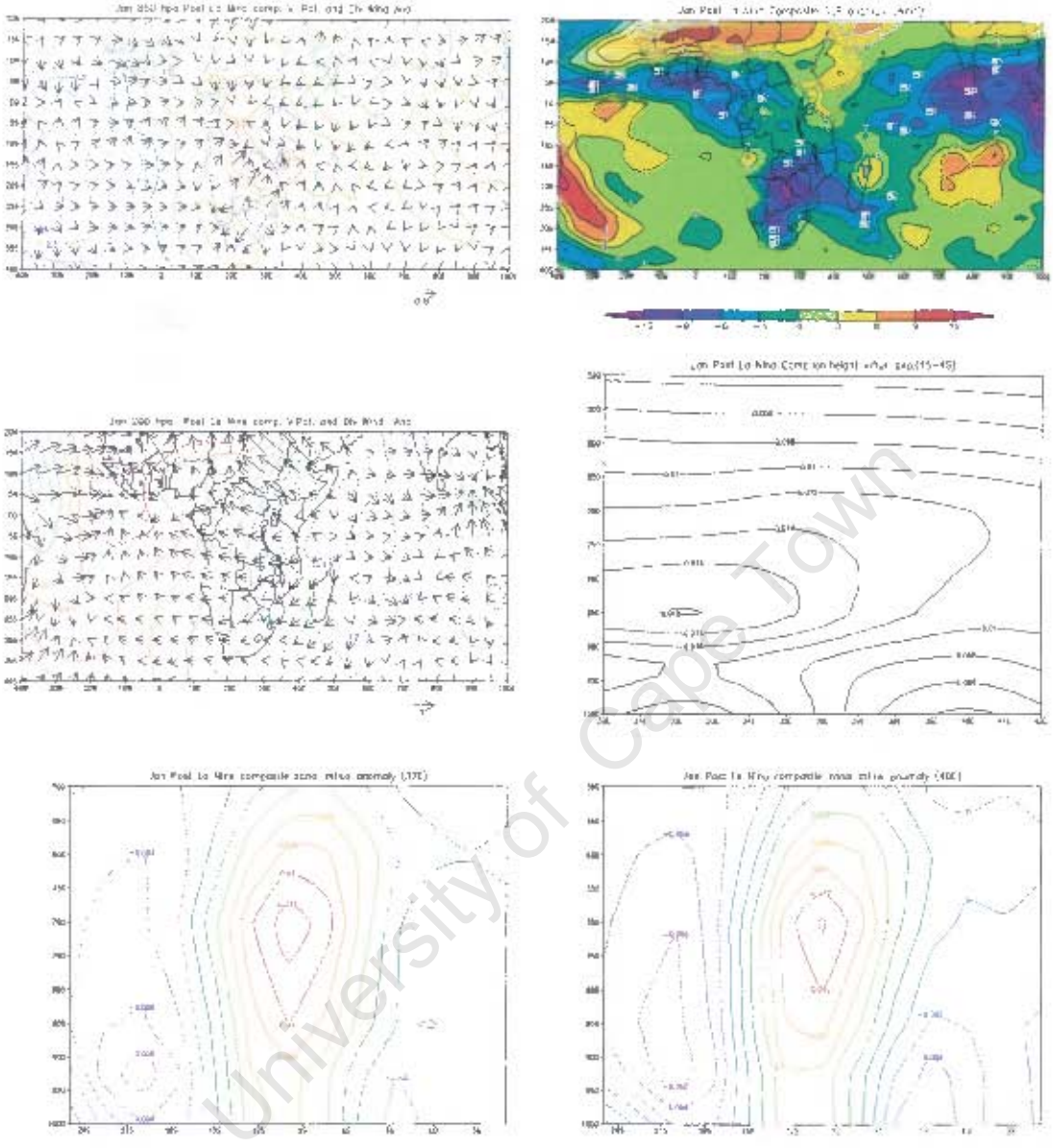

Figure 5.4b:January La Niña+1 composite anomaly fields
Velocity potential ($m^2 s^{-1}$)
Divergent wind (s^{-1})

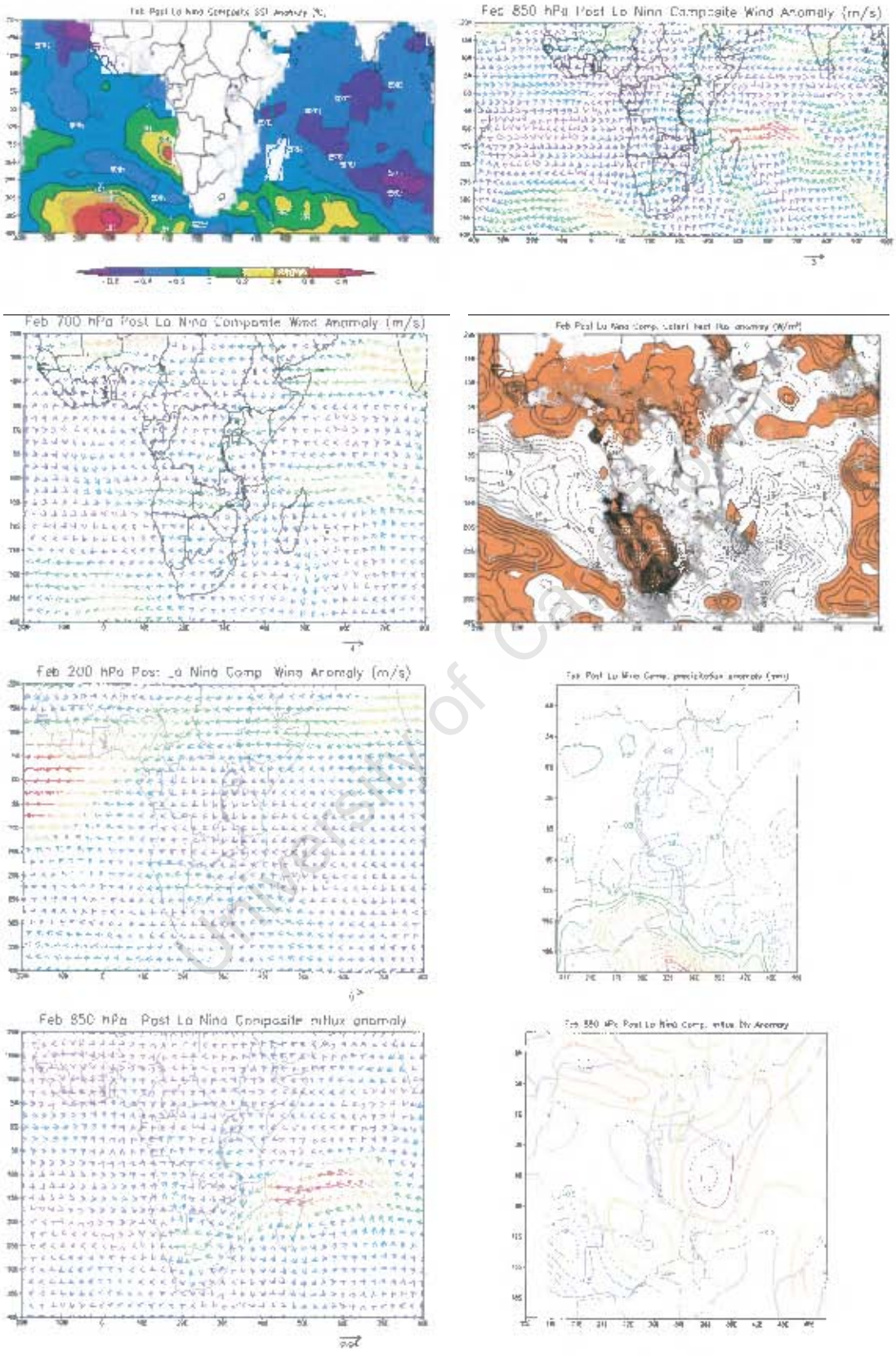

Figure 5.4c: AS for figure 5.4a but for February

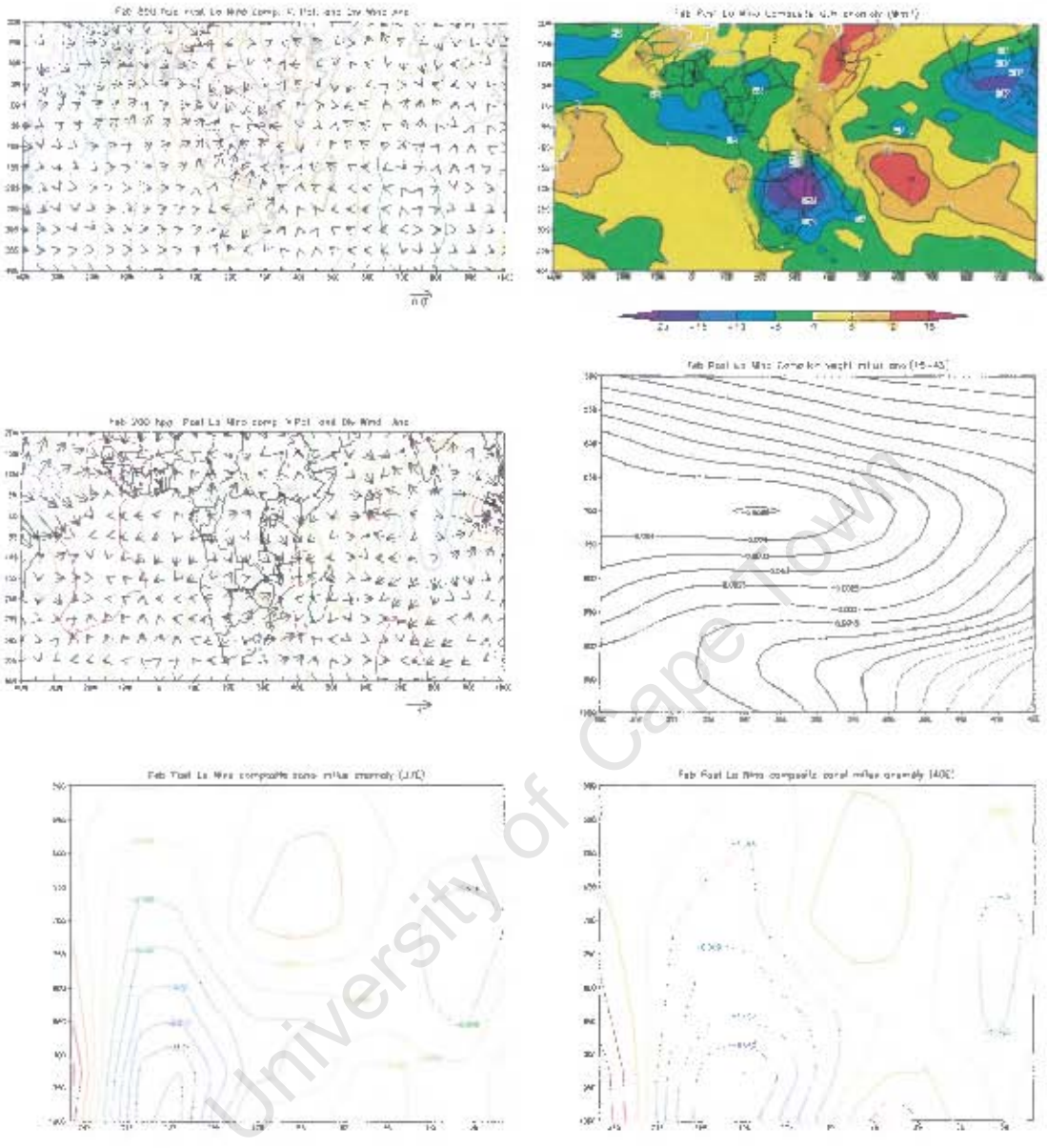

Figure 5.4d: AS for figure 5.4b but for February

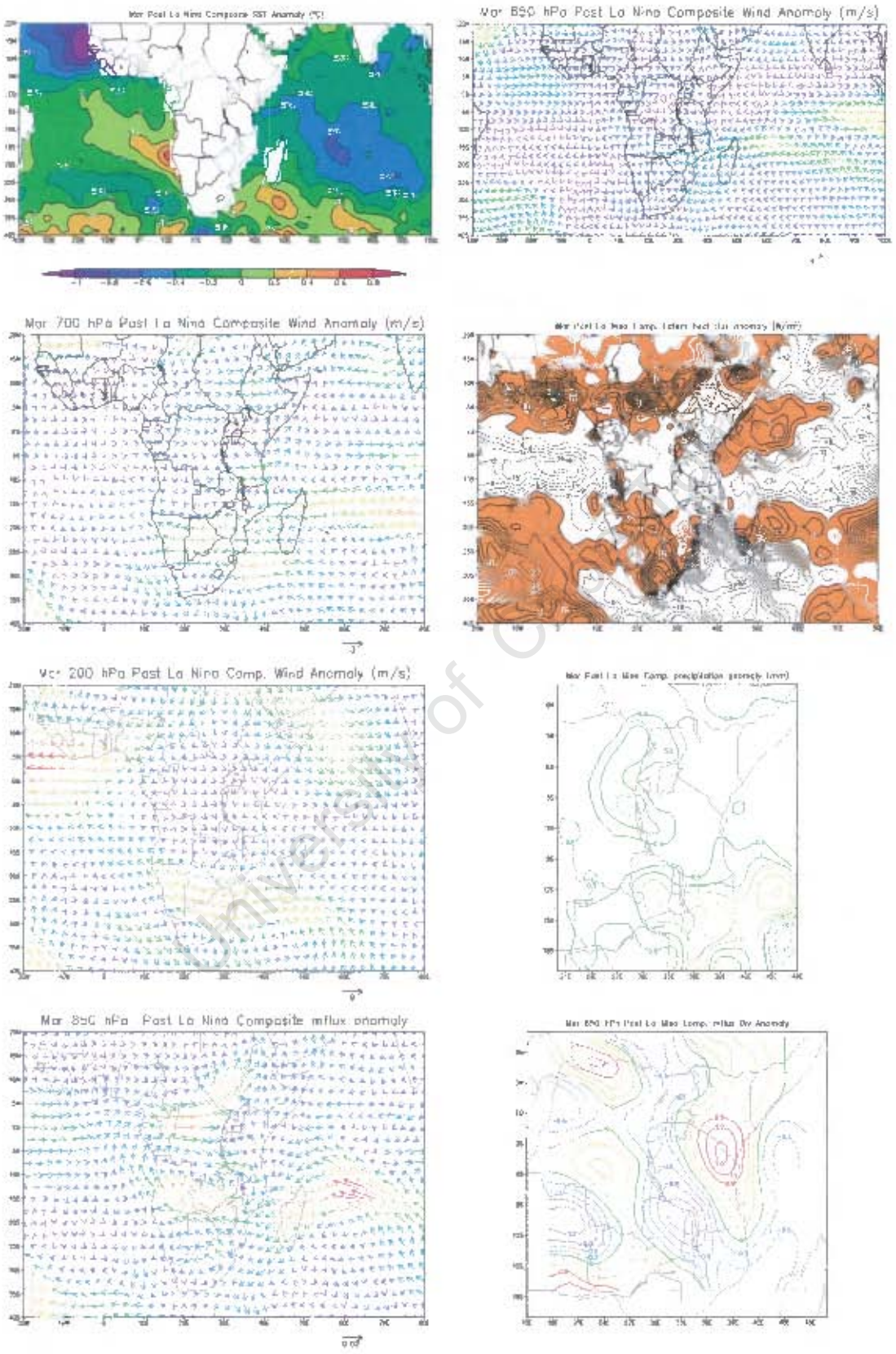

Figure 5.4e: As for figure 5.4a but for March

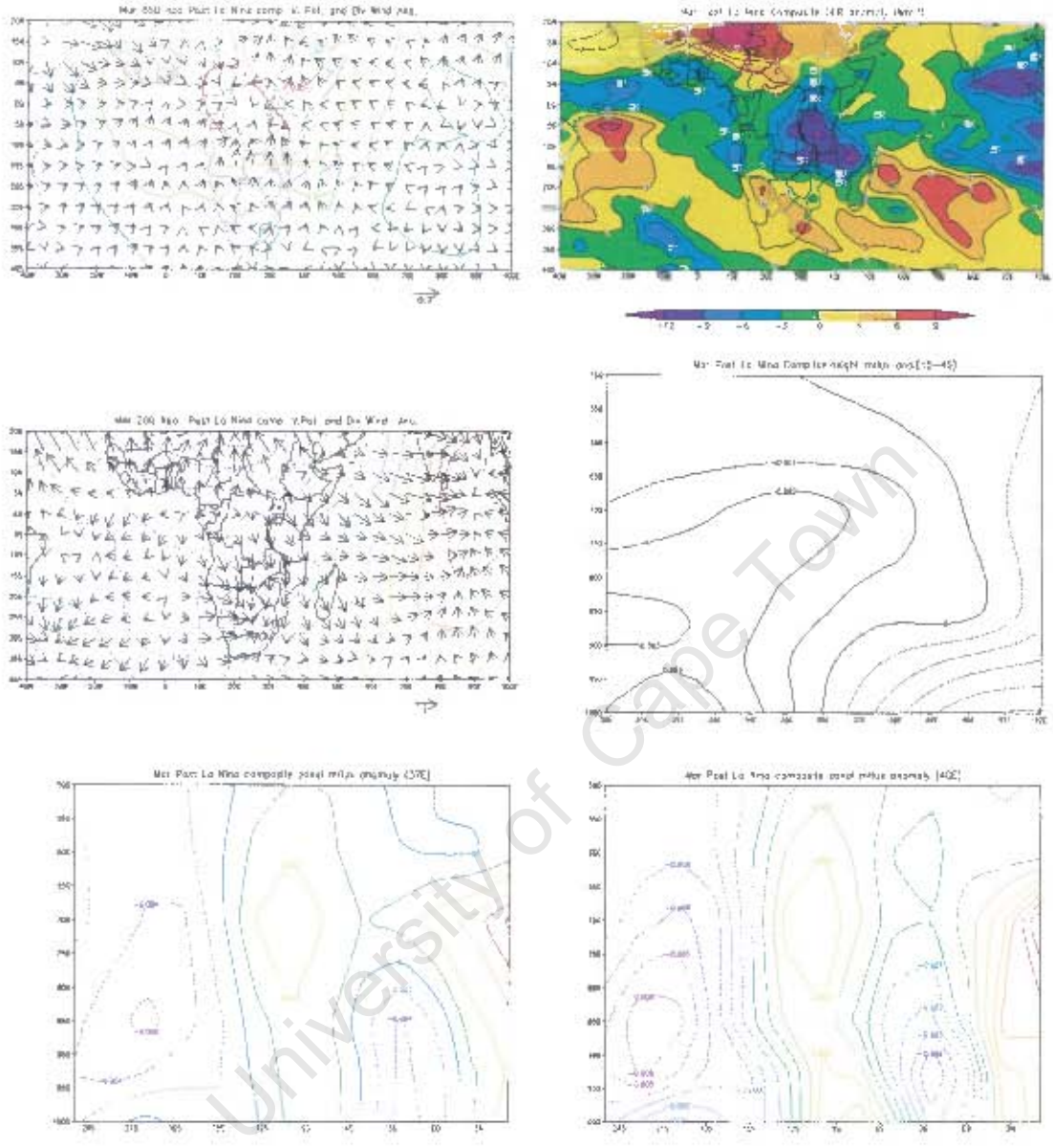

Figure 5.4f: As for figure 5.4b but for March

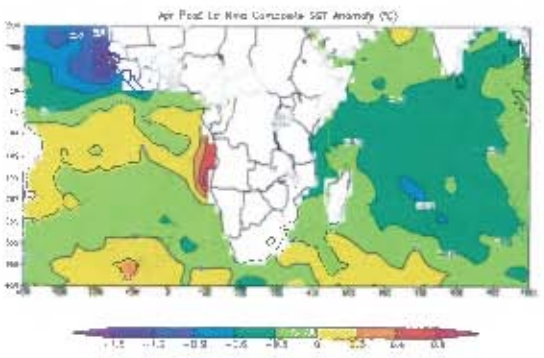

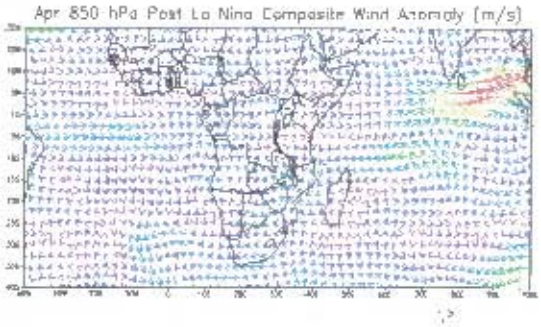

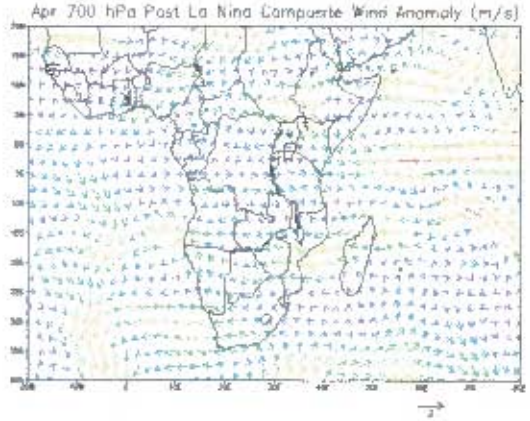

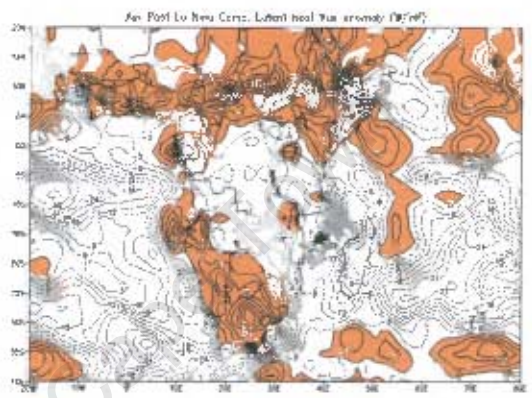

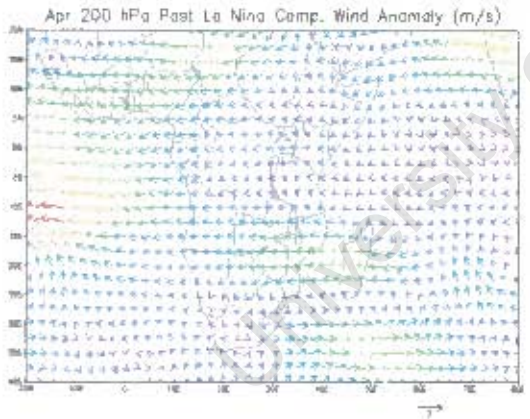

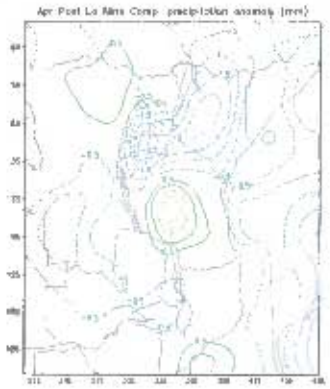

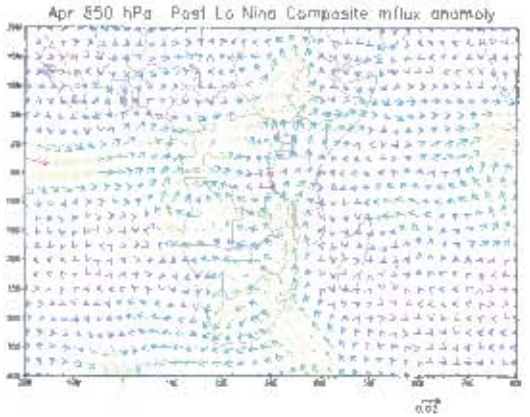

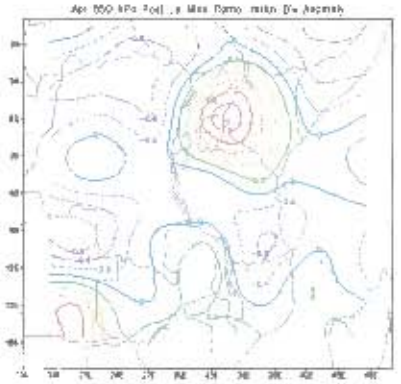

Figure 5.4g: as for figure 5.4a but for April

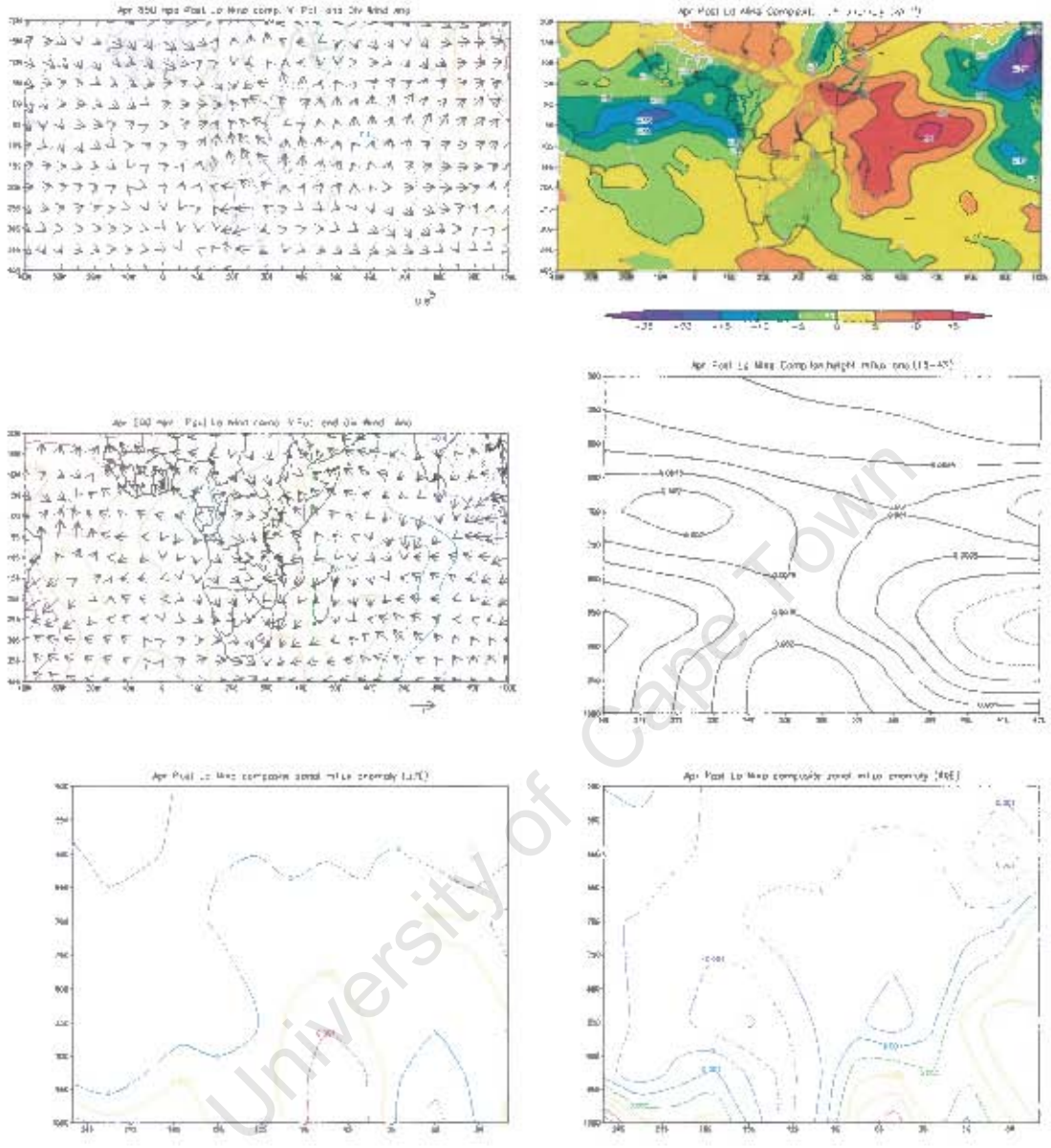

Figure 5.4h: as for figure 5.4b but for April

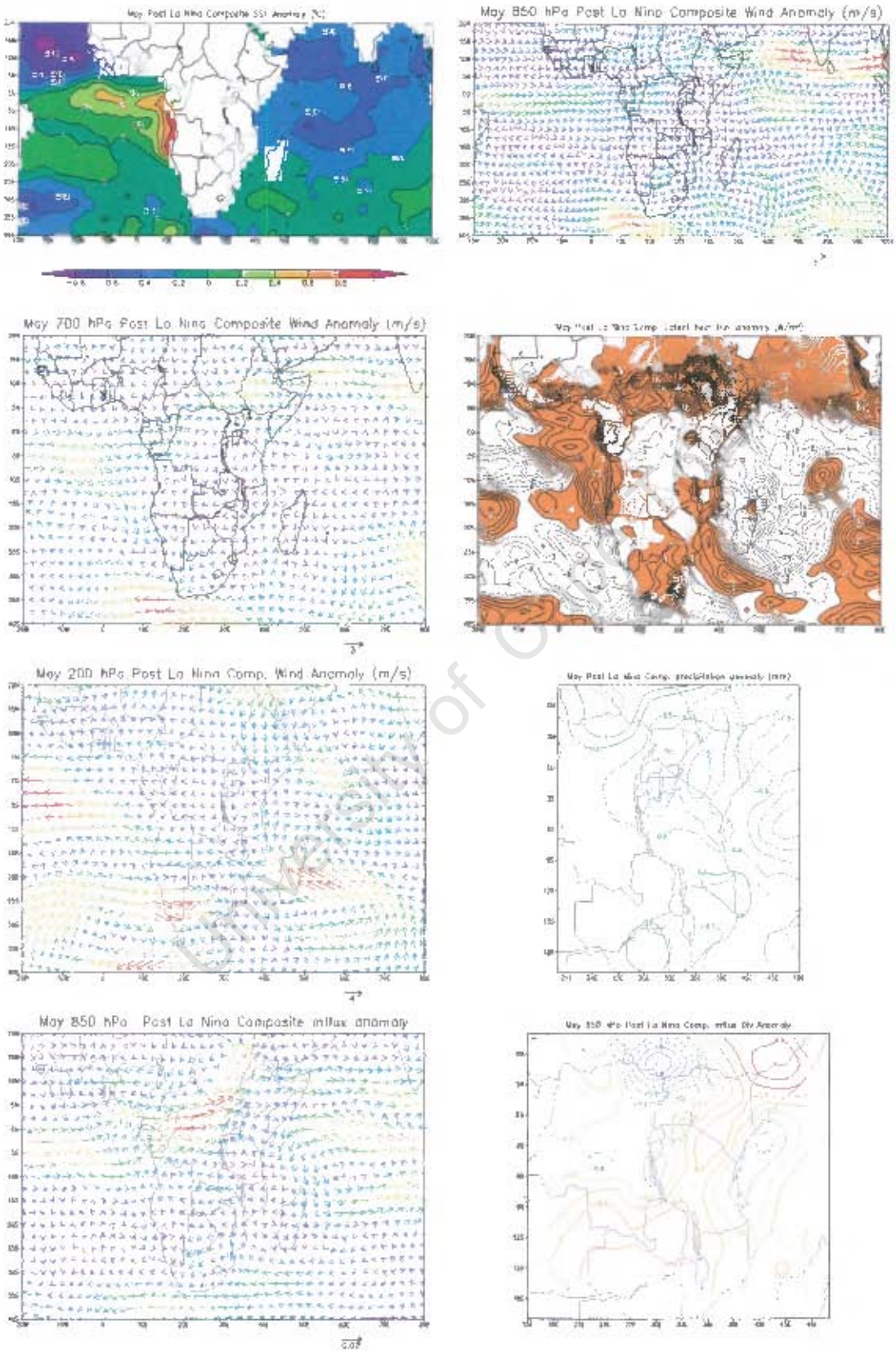

Figure 5.4i: As for figure 5.4a but for May

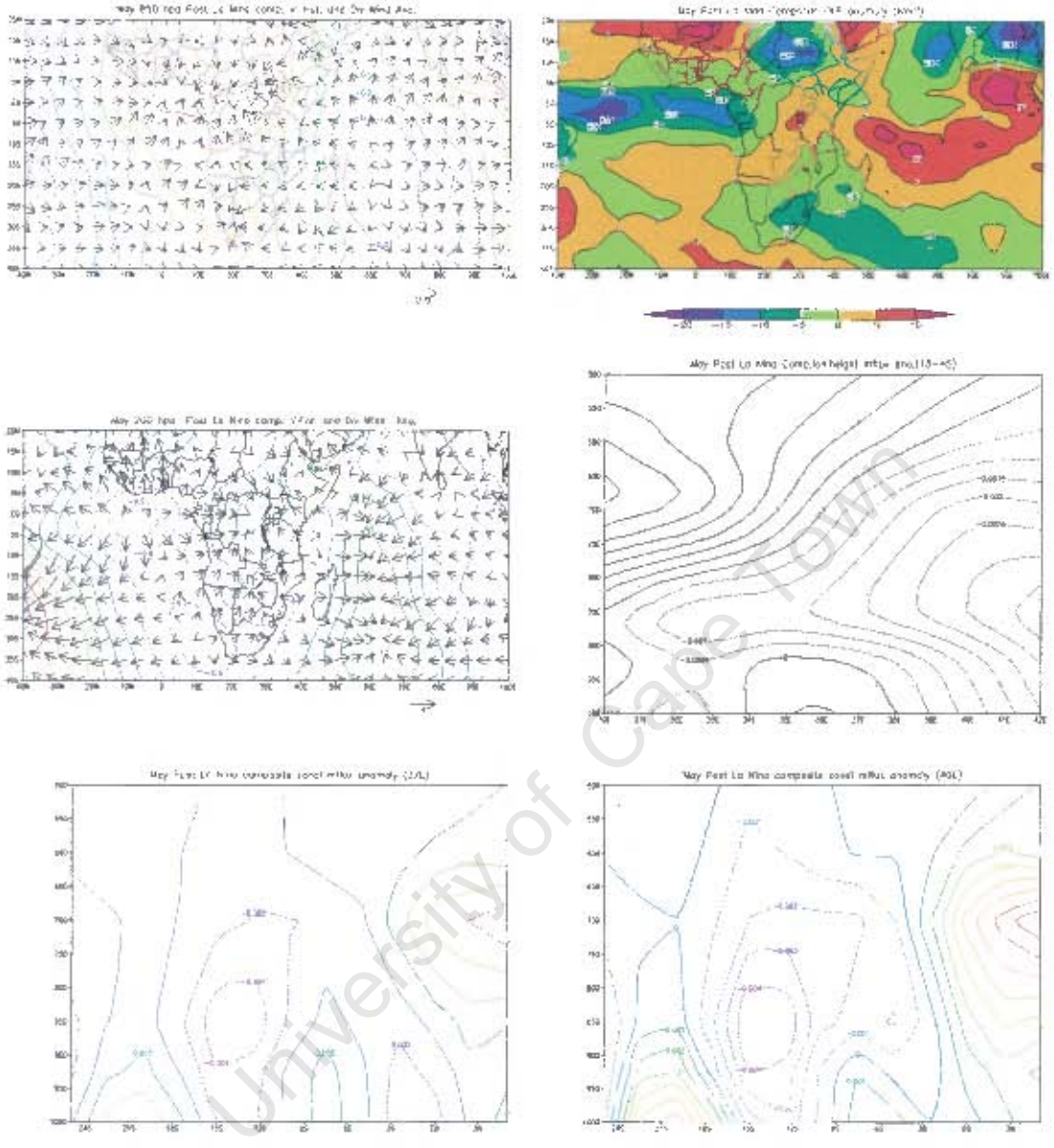

Figure 5.4j: As for figure 5.4b but for May

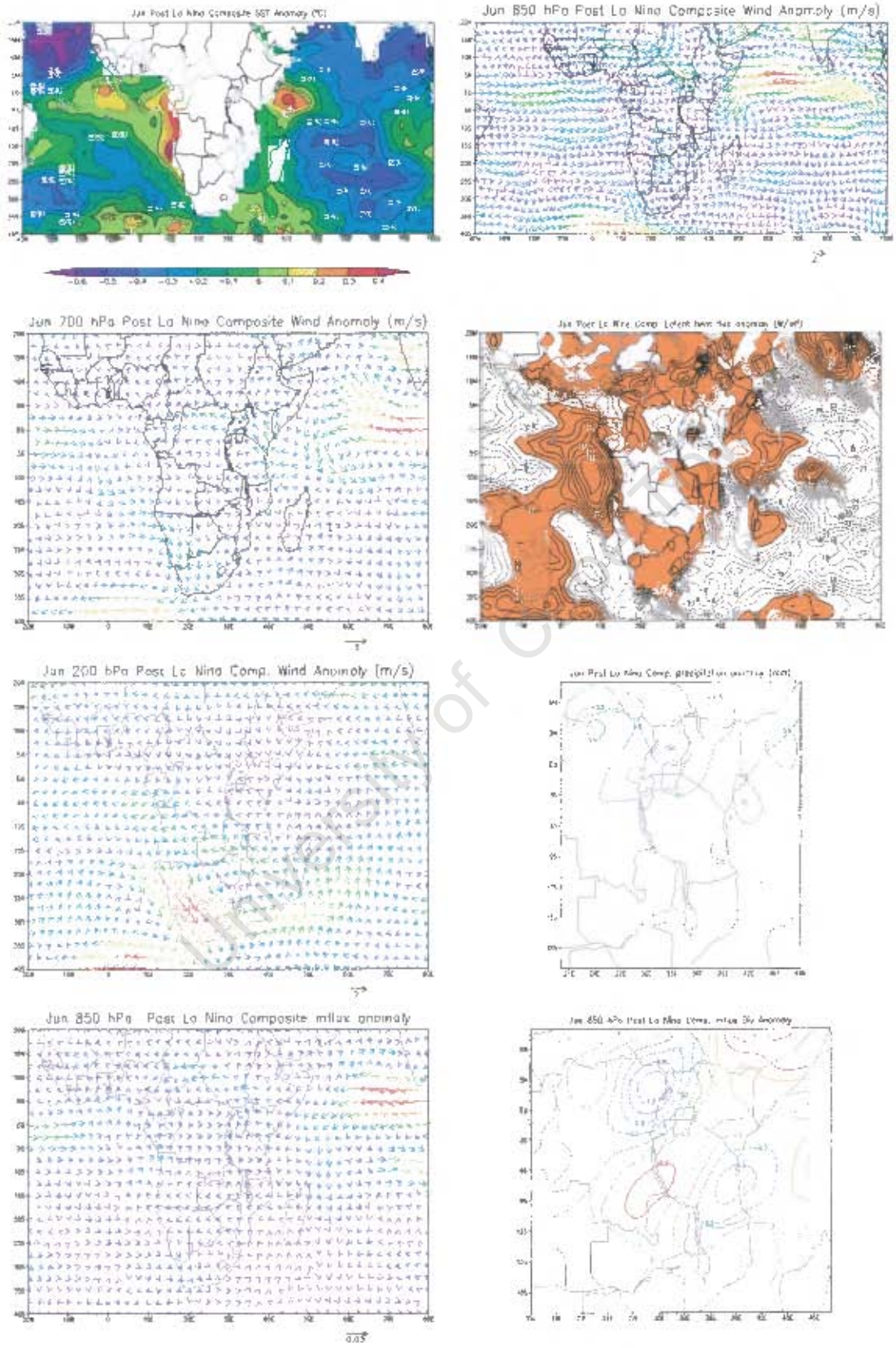

Figure 5.4k: As for figure 5.4a but for June

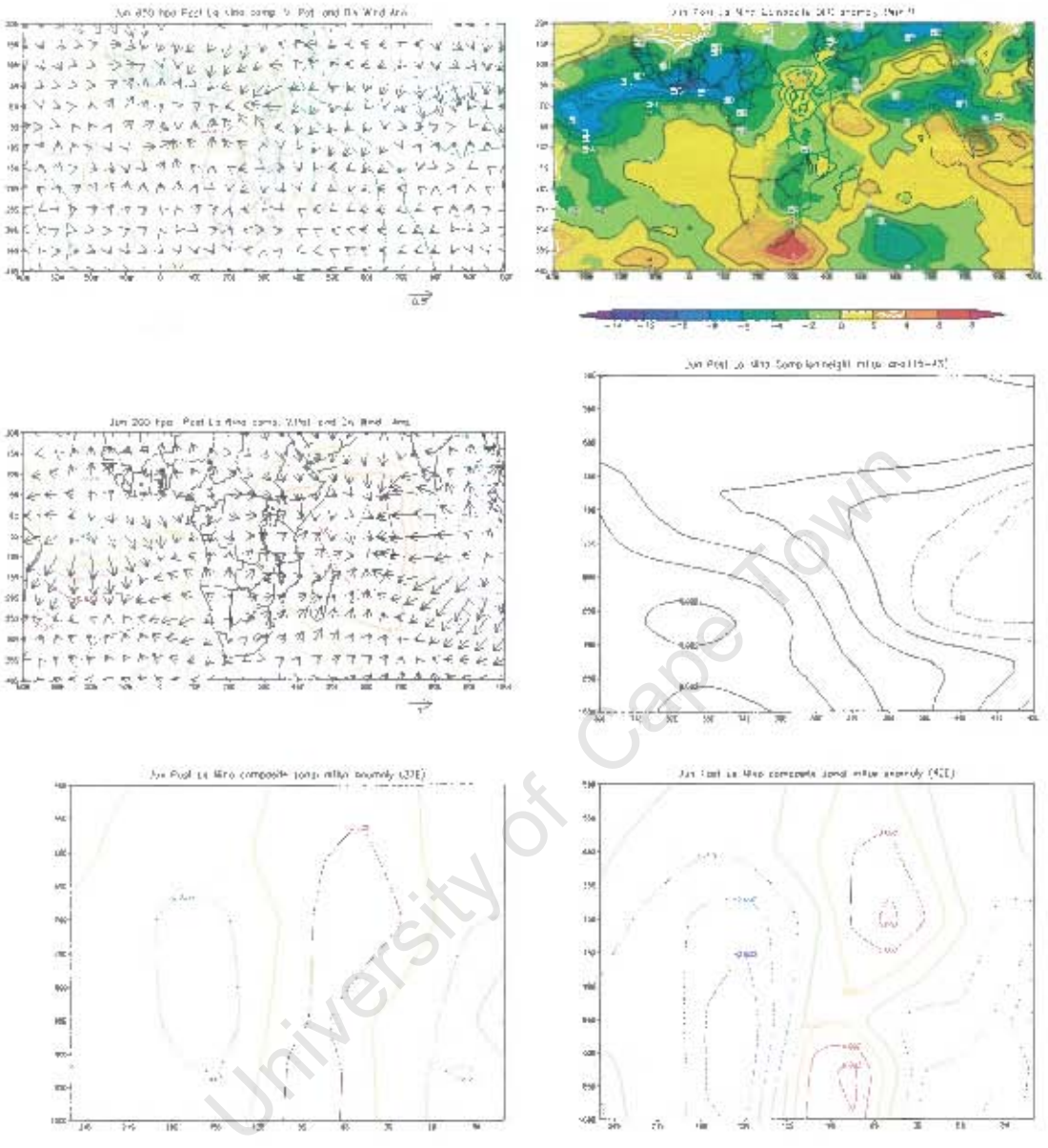

Figure 5.4l: As for figure 5.4b but for June

Chapter 6: Intraseasonal Oscillations

6.1 Introduction

Intraseasonal Oscillations (ISO) in the atmosphere are generally defined as fluctuations with periods longer than synoptic scale but shorter than the seasonal time scale. They are mostly of the order of 20-60 days (Madden and Julian 1971), the best known being the 40-50 day oscillation in the equatorial region. In their pioneering work, Madden and Julian (1971) described the oscillations as large scale eastward propagating zonal circulation cells along the Equator. The so-called Madden and Julian Oscillation (MJO), was discovered when studying a time series of zonal winds at Canton Island in the tropical Pacific and other individual tropical rawinsonde stations. Since then, low frequency oscillations have been studied by many researchers including Wang et al., (1990); Wang et al., (1997) and Vincent et al., (1991) among others.

Most studies of rainfall variability over East Africa have concentrated on seasonal to interannual scales. This study attempts to investigate the Intraseasonal Oscillations responsible for short-term rainfall variability in the Tanzanian coast during ENSO years. In particular, there is interest in the relationship between ISO and ENSO, e.g. are El Niño and La Niña years characterized by coherent difference in intraseasonal wet and dry spells over Tanzania? The selected ENSO years under this section are those occurring within the period of study (1970-1999) and having rainfall anomaly value of at least one standard deviation (fig 3.1b).

6.2 Analysis of system propagation, rainfall and wind time series Analysis.

6.2.1 Hovmöller analysis

The analysis in this section aims at identifying the characteristics of propagating convective systems. Hovmöller or longitude-time plots are used in identifying or detecting zonally propagating systems. Parameters used in longitude-time plots

are anomalies in OLR, zonal wind component at 850 and 200hPa. The anomalies used are simply departures from the long-term mean. Only the northern coast is considered for this analysis since ENSO impacts here appear to be more robust than for the southern coast. Values have been averaged over the latitude belt 4°- 8° S. The plots are for both OND and MAM season of the ENSO and post-ENSO (+1) years. For MAM season, plots are from 1st February to 30th June while for OND season the plots are from 1st August to 31st January. The data used in this analysis were first subjected to 30-50 day band pass filter using the Dolph – Chebyshev convergence window (Doblas-Reyes and Déqué, 1998). The advantage of the band pass filter is that both lower frequency and higher frequency components outside the band of interest are removed. Longitude-time plots reveal some westward and eastward propagating convection and non-propagating or quasi-stationary features.

Results of OLR and wind anomalies for ENSO and post-ENSO (+1) years.

The left panel of figure 6.1a are longitude time plots of 30-50 days filtered OLR anomalies for El Niño years 1982, 1986, 1994 and 1997 while the middle and right panels represent 30-50 days filtered lower and upper level wind anomalies respectively. The plots reveal alternating positive and negative OLR anomalies for all El Niño years. Eastwards propagating negative and positive OLR anomalies were observed between August and December over the central Indian Ocean (70°-100°E) while westward propagating negative and positive OLR anomalies were observed over the western Indian Ocean (west of 70°E) except in 1986 where westward propagating OLR anomalies were observed between August and November over the central Indian Ocean. Stationary features dominated 1997, which was the wettest year during the period of study. Similarly these non-propagating features were observed in 1982 over the central Indian Ocean, which suggests that propagating features are absent during strong El Niño years.

It is seen that the largest OLR negative anomaly values (less than - 30 W/m²) occur between 70 and 100°E. This result indicates that more active convection occurs over the central Indian Ocean as found by other researchers (e.g. Rui and Wang, 1990). Westward propagating negative OLR anomalies over the western Indian Ocean propagate with a mean speed of about 2m/s and are associated with strong convection over the Tanzanian coast and increased rainfall during El Niño years. Eastward propagating features were found to have different phase speeds in different years and over different areas. They generally propagate between 2-6m/s with mean speed of about 3m/s.

Considering the zonal wind anomalies at lower and upper levels, clear alternating negative and positive zonal wind anomalies and propagating features are readily identified. Eastward propagating features are revealed in most years with westward propagating systems over the western Indian Ocean at lower levels. It is found that the areas of large negative OLR anomalies (strong convection) couple well with areas of strong westerly anomalies in lower levels with strong easterly anomalies in upper levels. Such association has been revealed by Rui and Wang, (1990): Knutson and Weickmann, (1987) among others. The combination of strong convection over the Indian Ocean with westerly wind anomalies at lower levels coupled with easterly wind anomalies in the upper levels implies a well-established Indian Ocean Walker cell. This is associated with enhanced easterly flow over western Indian Ocean and creates conducive environment for increased rainfall over the Tanzanian northern coast.

The left panel of figure 6.1b are longitude time plots of 30-50 days filtered OLR anomalies for post mature phase El Niño years 1983, 1987, 1995 and 1998 while the middle and right panels represent 30-50 days filtered lower and upper level wind anomalies respectively. Alternating positive and negative OLR anomalies are a common feature of most years except in 1983 between May and June

where disorganised patterns were observed. Eastward propagating negative and positive OLR anomalies were observed in most years with a mean phase speed of 2m/s. Westward propagating features, which seem to originate from 80°E were observed in 1983 and 1987.

For 850hPa zonal wind, stationary features dominate the central Indian Ocean during the rainy season between March and May with westward propagating features over the western Indian Ocean. The dominant feature at the upper level was eastward propagating positive and negative wind anomalies except in 1987 where well-defined westward propagating features were observed between February and April. As for the OND season, the areas of large negative OLR anomalies (strong convection) couple well with areas of strong westerly anomalies in lower levels with strong easterly anomalies in upper levels, which leads to increased rainfall over the Tanzanian coast.

30-50 days filtered OLR anomalies and wind anomalies for La Niña and post mature phase La Niña years were shown in figure 6.1c. As in the previous discussion for El Niño, alternating positive and negative OLR anomalies were observed. A good example is in 1999 where OLR plot indicate eastward propagating negative and positive anomalies between April and May originating from central Indian Ocean. The features move in both eastward and westward direction. Stationary features were also observed. Between April and June1999, the eastward moving features seem to be well organised with mean phase speed of about 7m/s. Eastward propagating features were observed to be the dominant pattern of both lower and upper level winds except for 1999 where westward propagating zonal wind anomalies were observed between March and June. Comparing El Niño and La Niña years (fig 6.1a&c) two distinct features were highlighted. First, the eastward propagating OLR anomalies seem to have high phase speed during La Niña years, a good example is in 1999 (7m/s). Secondly, eastward propagating OLR anomalies dominated the western Indian Ocean

during La Niña years, a good example is 1988/89 while for El Niño years the anomalies maintain westward propagation (1986/87). The presence of eastward propagating OLR anomalies over the western Indian Ocean during La Niña years leads to suppressed convection and dry conditions over the Tanzanian coast.

6.2.2 Time series analysis

6.2.2.1 Intraseasonal rainfall variability and criteria for rainfall onset, peak and end dates' selection

Figure 6.2(a-c) show the climatological pentad rainfall time series plots for the coast of Tanzania. CMAP pentad rainfall data is averaged between 38.5°-41°E, 8°-4°S for the northern coast and between 38.5°-41°E, 11°-8°S for the southern coast. Figure 6.2a represents the time series of long-term mean rainfall over the area while figure 6.2(b-c) shows rainfall time series for each El Niño and La Niña year during the OND and MAM seasons and preceding months. The El Niño and La Niña composites with their corresponding El Niño+1 and La Niña+1 composites are shown in upper figure 6.2d. The rainfall onset, peak and end (withdrawal) dates were extracted from each time series and presented in tables 6.1-6.3. After a close inspection of time series, the following criteria were used for the selection of onset, peak, end and major dry spells for each season.

Short rain Season (OND).

Onset: 5-day rainfall ≥ 7.5mm followed by three consecutive pentads having rainfall amount of not less than 5mm/pentad.

Peak: The pentad with highest amount of rainfall in the season.

End: If three consecutive pentads have mean rainfall ≤ 2mm/day, the preceding pentad is considered to be the end of rain season.

Dry spell: 5-day rainfall less than 7.5mm.

Long rain season (MAM).

Onset: 5-day rainfall exceeds 10mm followed by three consecutive pentads having rainfall amount of not less than 10mm/pentad.

Peak: The pentad with highest amount of rainfall in the season.

End: If three consecutive pentads have mean rainfall ≤ 2mm/day the preceding pentad is considered to be the end of rain season.

Dry spell: 5-day rainfall less than 10mm.

November to May season (N-M) for southern coast.

Onset: 5-day rainfall exceeds 10 mm followed by three consecutive pentads having rainfall amount of not less than 10 mm/pentad.

Peak: The pentad with highest amount of rainfall in the season.

End: If three consecutive pentads have mean rainfall ≤ 2mm/day, the preceding pentad is considered to be the end of rain season.

Note: A pentad preceding the onset pentad is considered as the pre-onset.

The selected dates for each season are given in tables 6.1-6.3 below and are consistent with the dates observed by Mhita and Venäläinen (1992) in their study of the variability of rainfall in Tanzania using station observed data.

Table 6.1: Rainfall onset, peak, end and major dry spells dates as derived from CMAP data pentad rainfall time series for northern coast (OND season).

Events	Climatology	El Niño composite	La Niña composite
Pre-onset (P-1)	58th Pentad (13-17 October)	54th Pentad (23-27 September)	60th Pentad (23-27 October)
Onset (P0)	59th Pentad (18-22 October)	55th Pentad (28Sept.-02 October)	61st Pentad (28 October- 01Nov.)
Peak (P1)	65th Pentad (17-21 November)	65th Pentad (17-21 November)	72nd Pentad (22-26 December)
End (P+1)	4th Pentad (16-20 January)	4th Pentad (16-20 January)	4th Pentad (16-20 January)
Major dry Pentads	60th Pentad (23-27 October)	63rd Pentad (07-11 November)	63rd, 68th-69th Pentad (07-11 Nov., 02-11 Dec.)

Table 6.2: As for table 6.1 but for northern coast (MAM season).

Events	Climatology	El Niño composite	La Niña composite
Pre-onset (P-1)	13th Pentad (02-06 March)	16th Pentad (17-21 March)	13th Pentad (02-06 March)
Onset (P0)	14th Pentad (07-11 March)	17th Pentad (22-26 March)	14th Pentad (07-11 March)
Peak (P1)	24th Pentad (26-30 April)	25th Pentad (01-05 May)	27th Pentad (11-15 May)
End (P+1)	31st Pentad (31 May - 4 June)	30th Pentad (26-30 May)	30th Pentad (26-30 May)
Major dry Pentads	0	0	0

Table 6.3: As for table 6.1 but for each ENSO (northern coast OND season) and ENSO+1 (northern coast MAM season) year. E and L represent El Niño and La Niña year respectively with corresponding following year E+1 and L+1.

Year	Pre-onset Pentad (P-1)	Onset Pentad (P0)	Peak Pentad (P1)	End Pentad (P+10	Major dry Pentads
1982 (E)	54th	55th	57th	3rd (1983)	61st – 63rd, 70th, 2nd (1983)
1986 (E)	58th	59th	67th, 69th and 71st	4th (1987)	61st, 63rd, 68th, and 73rd
1994 (E)	57th	58th	69th	2nd (1995)	65th and 66th
1997 (E)	54th 23-27 Sept	55th 28 Sep – 02 Oct	59th 18-22 Oct	10th (1998) 15-19 Feb	60th, 63rd, and 5th (1998)
1983 (E+1)	16th	17th	24th	33rd	22nd and 26th
1987 (E+1)	19th	20th	26th	32nd	30th and 31st
1995 (E+1)	19th	20th	30th	30th	26th
1998 (E+1)	16th 17-21 March	17th 22-26 March	23rd 21-25 April	26th 06-10 May	0
1988 (L)	61st	62nd	73rd, 5th (1989)	5th (1989)	66th and 67th
1995 (L)	59th	60th	61st	2nd (1996)	63rd, 64th, 68-70th and 73rd
1998 (L)	SEE NOTE BELOW				
1999 (L)	62nd	63rd	64th	71st	68th and 69th

Table 6.3 continue

Year	Pre-onset Pentad (P-1)	Onset Pentad (P0)	Peak Pentad (P1)	End Pentad (P+10	Major dry Pentads
1989 (L+1)	18th	19th	22nd	30th	0
1996 (L+1)	13th	14th	28th	29th	26th
1999 (L)	12th	13th	24th	31st	28th
2000 (L)	15th	16th	24th	27th	22nd

NOTE: In 1998, the onset and end of rainfall were undefined as the whole season was dry except 65th, 66th and 67th pentads, which recorded rainfall.

The climatological onset, peak and end dates for the southern coast are given below. This region will not be considered for further analysis in this chapter since the ENSO impact seems less clear for the long season (November to May). Only the early season (OND) seem to be consistent with the northern coast OND season (fig 3.3b).

Onset: 65th pentad (Third week of November).

Peak: 16th pentad (Third week of March).

End: 29th pentad (Fourth week of May).

It is evident from table 6.1, that for OND season the rainfall starts earlier than climatology during the El Niño years and the peak of rainfall was observed to have large amount of rainfall of about 7mm/day (fig 6.2d). La Niña years show a late start of the rainy season leading to a short duration of the rainy season and below average rainfall.

During MAM season (table 6.2), the onset for El Niño+1 composite was three pentads late but the amount received was much higher than average with a peak of about 9mm/day. For La Niña+1 years, the rainfall starts about the same time

as the climatological mean but the amount received was more variable. Thus, the total amount of rainfall received during La Niña+1 seasons is below average.

Figures 6.2(b-c) illustrate the pentad rainfall time series for each ENSO year. The plots show that each year has its own characteristics in terms of onset, peak and end of the rainy season. The details for each year in terms of rainfall onset, peak, end and frequency of dry spells are illustrated in table 6.3. Most El Niño years are found to have a longer rainfall season due to an early onset. For example in 1997, which was the wettest year during the period of study, the rainfall started about three weeks before and the withdrawal was one month later than climatology. Most La Niña years have a shorter rainfall season than average and this results from late onset. For example in 1998, the length of the rainfall season was only about two weeks. The common feature for all El Nino years is above average rainfall during the season while La Nina Years show below average rainfall during the season.

The onset, peak and end dates of rainfall derived from pentad time series were used in section 6.3 for analyses of the circulations associated with the onset and peak of rainfall.

6.2.2.2 Intraseasonal Wind variability.

The lower panel of figure 6.2d and figure 6.2e show the climatological and composite ENSO years time series for zonal wind at 850, 700 and 200hPa averaged between 39-41°E, 8-4°S. The plots show zonal wind time series for both OND and MAM season with preceding months. The OND season was characterized by easterly wind anomalies for both El Niño and La Niña years at the 850hPa level.

Comparing the climatological time series with ENSO for 850hPa, the El Niño composite shows strong easterly anomalies during the onset of rain season weakening toward the peak of rain season. This leads to enhanced moisture convergence resulting in increased rainfall over the coast. The La Niña composite time series shows weaker easterlies during the onset of rain season and the rest of the season was dominated by easterly wind of variable strength leading to below average rainfall. At 700hPa, the El Niño composite shows stronger easterlies during the onset of rain season and the strength becomes variable as the season progress. The La Niña composite was dominated by weaker easterlies throughout the rain season.

At 200hPa, the climatological time series shows westerlies from the onset to the peak of the rain season while easterly wind flow was observed towards the end of rain season in December. During El Niño years, strong easterly anomalies were observed throughout the rain season while La Niña years shows westerly anomalies between October and November with weak easterly anomalies towards the end of the season. The occurrence of weak low-level easterly anomalies and upper level westerly anomalies during La Niña years indicate a weak Walker cell over the region. This is consistent with suppressed convection and below average rainfall.

For the long rain season, the climatological flow at low levels are easterlies from the Indian Ocean. During El Nino+1 years, the easterlies were observed to be stronger during the onset of rain season in March and the peak of the rain season in May while the rest of the season was characterized by weaker easterlies. This results in enhanced moisture convergence and increased rainfall over the coast during El Niño+1 years.

The dominant feature for La Niña+1 years (right panel of fig 6.2e) was weaker easterlies throughout the season with the exception of second week of March

and first week of May where strong easterly anomalies were observed. Weaker easterlies during the onset of rain season reduce the amount of moisture reaching the region from the Indian Ocean and result in below average rainfall. The features at 700hPa are more or less the same as the features at 850hPa for both El Niño+1 and La Niña+1 years.

At 200hPa, (upper fig. 6.2e) the MAM season was dominated by easterlies over the region in climatological time series. Generally, the easterlies are strong during El Niño+1 years implying upper level divergence, which leads to enhanced convection and moisture convergence in lower levels. For the La Niña+1 composite, stronger easterlies were observed in the middle of the season (April) while the rest of the season was characterized by weaker easterlies and hence suppressed convection in lower levels.

6.3 Circulations associated with onset, peak and withdrawal of rainfall.

6.3.1 Climatological patterns.

This section looks at mean characteristics of selected meteorological fields comprising each part of OND and MAM rainfall season. The objective is to investigate characteristics associated with onset, peak and withdrawal dates (table 6.1) of rain season over the northern Tanzanian coast. The pentads used are stratified into four stages: namely, pre-onset (one pentad prior to the onset of rainfall, or P-1), onset (P0), peak (P1) and the end or withdrawal of rainfall pentad (P+1). Further details concerning the procedure of selection of these pentads is given in section 6.2.2.1. The climatological circulation patterns are computed from data sets ranging from 1979-1999 for OLR and 1970-1999 for wind. These reference means will be used to compute intraseasonal oscillation anomalies in the next section.

6.3.1.1 Climatology for OND season.

Figures 6.3(a&b) illustrate mean patterns of OLR, moisture flux at 850hPa, wind at 700hPa and 200hPa for P-1, P0, P1 and P+1 phases during the OND season. One pentad before the onset of the rain season (P-1) (figure 6.3a), a strong zonal OLR gradient was observed over the equatorial Africa/Indian Ocean region. Strong convection is occurring over the Congo basin and central Indian Ocean with less over East Africa.

Westerly moisture flux over the equatorial Indian Ocean feeds the convection there whereas slightly further south, easterly moisture flux is incident on the Tanzanian coast. The convective zone centered over the Congo basin extends eastwards to cover much of western Tanzania and the Lake Victoria basin indicating the position of the meridional arm of the ITCZ. The belt of easterly moisture flux between 5°S and 15°S incident on the Tanzanian coast originates over the Indian Ocean. This indicates advection of moisture from across much of tropical south Indian Ocean five days before the onset of rain season.

The continental ascending limb of the Walker cell was located over eastern Congo/western Tanzania where westerly moisture flux from Congo Basin converges with southeasterly moisture flux from the Indian Ocean. It is further indicated by low OLR values over the region with wind divergence at 700hPa. The maritime ascending limb of the Walker cell is over the eastern Indian Ocean while the descending limb is over the western Indian Ocean.

During the pentad of rainfall onset (P0) (figure 6.3a) lower panel, the OLR value over the central Indian Ocean decreases by about 10W/m² with a slight shift southwards indicating a southward movement of the ITCZ. The moisture flux at 850hPa, wind at 700hPa and 200hPa maintains similar patterns as in P-1 except that the southerly wind near the Tanzanian coast at 700hPa level was replaced by westerly flow.

During the peak of the rain season (P1) (figure 6.3b), a marked eastward extent of the low OLR values from western Tanzania is evident. The OLR value over the Tanzanian coast decreases by about 10W/m² from 270W/m² to 260W/m² indicating a zone of convection over the coast. At 850hPa, much of Tanzania is covered by southeasterly moisture flux. At P1, the entire country is covered by easterly moisture flux. The ascending limb of Walker circulation maintains its position over western Indian Ocean with strong low-level easterly moisture flux incident over the Tanzanian coast and westerly moisture flux feeding the rising limb of Walker cell over eastern Indian Ocean.

At the withdrawal of the rain season (P+1) (figure 6.3b lower panel), a meridional gradient of OLR value exists over the coast with OLR values decreasing southwards towards Mozambique. A minimum value of 200W/m² is reached at about 15°S indicating the southernmost displacement of the ITCZ. This is well defined by the 850hPa moisture flux, which is northerly over the coast and converges with easterly moisture flux over northwest Madagascar. Maximum rainfall now occurs over northern Mozambique and Madagascar. A marked southward shift of the westerly moisture flux into the tropical South Indian Ocean that moves in sympathy with the convective zone over the central Indian Ocean is evident during this period. Both the continental and maritime ascending limbs of Walker cell persist from onset, peak to the withdrawal of rain season with the corresponding descending limb over the western Indian Ocean.

6.3.1.2 Climatology for MAM season.

The long rain season is associated with the northward movement of the ITCZ. Figures 6.3(c&d) represent long term mean patterns of OLR, moisture flux at 850hPa, wind at 700hPa and 200hPa for P-1, P0, P1 and P+1 phases during the MAM season. At one pentad before the onset of rain season (P-1) figure 6.3c, a band of low OLR values extends from the central Indian Ocean through southern Tanzania covering the entire western part of the country. At this time, the ITCZ

still lies across northern Mozambique. Between 5°S and 10°S over the Indian Ocean there was a zonal band of westerly moisture flux with northeasterly moisture flux closer to the Tanzanian coast. At 850hPa, much of Tanzania is covered by easterly moisture flux. The descending limb of the Walker cell is over the western Indian Ocean where westerly moisture flux, which feeds the convection over the maritime rising limb of Walker cell and easterly moisture flux originate.

The low OLR values show a slight northward shift in P0 indicating the northward advance of the ITCZ. The position of ITCZ is clearly indicated by converging southeasterly and northerly 850hPa moisture flux near northern Madagascar with strong westerly moisture flux in the Indian Ocean, near 10°S. This northward shift of the convective region in sympathy with the movement of ITCZ results in enhanced moisture convergence over the Tanzanian coast and increased rainfall marking the onset of rainfall season.

During the peak of rain season (P1) (figure 6.3d), the merged convective zone over Africa and the central Indian Ocean basins break up over the equatorial western Indian Ocean. Thus, a separate zone of low OLR values is established over the equatorial central Indian Ocean. Together these convective zones indicate the position of the ITCZ, which is over the northern part of country during this period. Elsewhere over the Indian Ocean, the OLR values are high suggesting less convection. At 850hPa, strong southeasterly moisture flux exists over Tanzania during this period. Westerly moisture flux exists over the central equatorial Indian Ocean and feeds the maritime convective zone. The slight eastward shift of the descending limb of the Walker circulation over the western Indian Ocean as indicated by the origin of easterly and westerly moisture flux results in enhanced easterly moisture flux convergence over the Tanzanian coast and increased rainfall marking the peak of rainfall season.

Towards the withdrawal of the rain season (P+1) (figure 6.3d lower panel), the ITCZ shifts northward to lie over northern Congo, Kenya and the tropical north Indian Ocean. The southeasterly moisture flux towards Tanzania curves northeastwards, i.e., is directed towards the monsoon convection developing over southern India and adjacent northwestern Indian Ocean. This curvature indicates the transit towards the East African Low Level Jet. The descending limb of the Walker cell persists over western Indian Ocean and conditions evolve to being unfavourable for significant rains over Tanzania.

6.3.2 Anomalies.

6.3.2.1 Results of OLR, moisture flux at 850hPa, wind at 700hPa and 200hPa anomalies for El Niño and El Niño+1, OND and MAM seasons.

The anomalies of OLR, moisture flux, middle and upper level wind for both El Niño (OND season) and corresponding El Niño+1 (MAM season) composite are given in figures 6.4(a-d). The El Niño years occurring in the period of study (1970-1999) with rainfall anomaly value of at least 1 standard deviation during the OND season (fig 3.2b) with their corresponding following year for MAM season were considered for compositing under this section. The El Niño years for the OND composite are 1972,1982,1986,1994 and 1997 with their corresponding El Niño+1 years 1973,1983,1987,1995 and 1998 for MAM season. Note that for OLR, daily data was available only from 1974. The pentads used are the same as those used in section 6.3.1 with dates for El Niño and El Niño+1 composites shown in table 6.1 and 6.2 respectively.

Figures 6.4 (a&b) show the OND El Niño composite anomalies. One pentad before the onset of OND rain season (P-1) figure 6.4a, much of the Indian Ocean was covered by positive OLR anomalies with highest anomaly value of the order of 40W/m^2 observed over the equatorial central Indian Ocean. At this time, most of the Indian Ocean north of the equator was characterized by a northeasterly moisture flux anomaly backing into northerly anomaly on approaching the

Tanzanian coast. As a result there is little penetration of moisture inland, which is consistent with positive OLR anomalies over the region. The presence of anticyclonic moisture circulation over the equatorial western Indian Ocean and wind convergence at 700hPa (converging in respect to the background flow) indicates the position of the descending limb of Walker circulation. This is further indicated by the presence of easterly wind anomalies over much of Tanzania at 200hPa level, which opposes the background flow implying convergence.

By the onset of the OND rain season (P0) (figure 6.4a lower panel), a deep convective zone had developed over the equatorial western Indian Ocean as indicated by low OLR values over the region. Enhanced moisture flux convergence over the Tanzanian coast as indicated by decelerating northeasterly moisture flux results in increased rainfall over the coast marking the onset of the rainfall season. At about 5°S, westerly moisture flux anomalies from the Atlantic Ocean converge with easterly moisture flux anomaly at about 25°E, suggesting that the influence of the Atlantic Ocean over the Tanzanian coast rainfall may be minimal.

The band of descending air over the equatorial western Indian Ocean is broken by the period of convection as the active convergence zone dominates the region indicating the weakening of the maritime Walker cell. At 700hPa, easterly wind anomalies occur over the equatorial western Indian Ocean closer to the Tanzanian coast while at 200hPa strong westerly wind anomalies dominate the region implying strong upper level divergence in respect with the background flow. This is consistent with the convective zone over the region, which suggests enhanced convection. The presence of an active convective zone over the equatorial western Indian Ocean with enhanced moisture convergence results in above average rainfall over the Tanzanian coast during El Niño years.

At the peak of OND rain season (P1) (figure 6.4b), the convective zone over western Indian Ocean shows significant westward extent with negative OLR anomalies of $-15W/m^2$ over the coast of Tanzania. The area between 10°N and 5°S over the Indian Ocean shows low-level easterly moisture flux anomalies opposing the background flow consistent with negative OLR anomalies over the region. Much of the Tanzanian coast indicates a westerly moisture flux anomaly, which converges with easterly moisture flux anomaly at about 55°E. Since the background moisture flux over the region during this time was easterly moisture flux (fig 6.3b), the westerly moisture flux anomaly tends to oppose the flow causing deceleration and enhanced moisture convergence over the coast. This convergence leads to the peak of rain during this pentad of above average rainfall. Moisture convergence over the Indian Ocean at about 55°E with stronger negative OLR anomalies over the region coupled with upper level divergence indicates the position of rising limb of Indian Ocean Walker cell, which shows a significant westward shift towards East Africa.

At the end of OND rain season (P+1) (figure 6.4b lower panel), the convective zone over the western Indian Ocean is replaced by periods of clear weather as is evident from the positive OLR anomalies covering the entire western Indian Ocean and the Tanzanian coast. The moisture flux over much of the Indian Ocean indicates a relative divergent pattern as it flows in the same sense as the background flow. The descending limb of the Walker circulation is over the Tanzanian coast with divergence in the lower levels as suggested by the moisture flux plot and convergence in the upper levels. The latter implied by the wind flow pattern at 200hPa that opposes the background flow. The existence of descending limb of the Walker cell over the coast suggests subsidence and reduced clouds, marking the end of the rain season.

Figures 6.4(c&d) represents MAM season. One pentad before the onset of MAM rain season (P-1) (figure 6.4c), a convective zone is apparent over the equatorial

western Indian Ocean (negative OLR anomalies). The other are of significant negative OLR anomaly east of Madagascar is too far south to be associated with the ITCZ. Strong westerly moisture flux feeds the equatorial convective zone, particularly at 700hPa. The upper level wind patterns shows convergence over much of the Tanzanian coast suggesting subsidence and hence reduced cloud one pentad before the onset of the rain season.

During the onset of the rain season (P0) (fig 6.4c lower panel), the negative OLR anomalies over the equatorial Indian Ocean extend westwards towards the Tanzanian coast consistent with easterly and southeasterly moisture flux anomaly opposing the background flow. The ascending limb of the Walker cell is over the equatorial western Indian Ocean as indicated by negative OLR anomalies and moisture convergence over the region coupled with upper level wind divergence. The enhanced moisture convergence over the equatorial western Indian Ocean results in increased rainfall over the coast during MAM season of the post mature phase El Niño years.

At the peak of MAM rain season (P1) (fig 6.4d), negative OLR anomalies over western Indian Ocean deepen reaching a minimum anomaly value of $-25W/m^2$ centered at 50-55°E and show the westward extent of convection, which covers the entire northern coast of Tanzania. A cyclonic moisture flux anomaly exists over the equatorial western Indian Ocean with westerly moisture flux anomaly across southern Tanzania. This leads to enhance moisture convergence over much of Tanzania and increased rainfall marking the peak of rainfall season over the Tanzanian coast. The 700hPa wind shows anticyclonic circulation centered over Madagascar with strong easterly anomalies over western Indian Ocean and Tanzania opposing the background flow. This anticyclonic circulation shows equatorward shift with height centered over the equatorial western Indian Ocean at 200hPa indicating the position of the ascending limb of the Indian Ocean Walker cell.

Towards the withdrawal of MAM rain season (P+1) (fig 6.4 lower panel), the convective zone over the equatorial western Indian Ocean shows an eastward shift leaving weak negative anomalies over the Tanzanian northern coast. The cyclonic moisture flux anomaly over the equatorial western Indian Ocean is no longer apparent and an equatorial westerly moisture flux, which feeds the maritime convective zone, is evident. The descending limb of the Walker cell is over the equatorial western Indian Ocean as indicated by high OLR values over the region with wind convergence at 200hPa implying reduced cloud cover. This marks the end of the rainfall season over the Tanzanian coast.

6.3.2.2 Results of OLR, moisture flux at 850hPa, wind at 700hPa and 200hPa anomalies for La Niña and La Niña+1 years.

The anomalies of OLR, moisture flux, middle and upper level wind for both La Niña (OND season) and corresponding La Niña+1 (MAM season) composite are given in figures 6.5(a-d). The La Niña years occurring in the period of study (1970-1999) with rainfall anomaly value of ≤ -1 during the OND season (fig 3.2b) with their corresponding following year for MAM season were considered for compositing under this section. These La Niña years composited for the OND season were 1970,1973,1975,1988, 1998 and 1999 with their corresponding La Niña+1 years being 1971,1974,1976,1989 and 1999 for the MAM season. The pentads used are the same as those used in section 6.3.1 with dates for La Niña and La Niña+1 composites shown in table 6.1 and 6.2 respectively.

Figures 6.5(a&b) shows the OND La Niña composite anomalies. One pentad before the onset of OND season (P-1) (figure 6.5a), the La Niña composite is more or less the reverse of the El Niño composite with negative OLR anomalies over the equatorial central Indian Ocean coupled with westerly moisture flux which feeds the convection there. The presence of off shore (westerly) moisture flux over the Tanzanian coast suggests suppressed moisture advection one pentad prior to the onset of rainfall season. The upper level divergent wind flow

suggests that the position of the rising limb of Walker cell is located over the equatorial central Indian Ocean consistent with negative OLR anomalies apparent over this part of the Ocean.

During the onset of the OND rain season (P0) (figure 6.5a), the negative OLR anomalies over the central Indian Ocean are strengthened reaching about -30W/m² at 80°E. Tanzania shows positive OLR anomalies suggesting reduced cloud and convection. Westerly moisture flux anomalies exist over much of the Indian Ocean, which feeds the convective zone centered at about 80°E. This offshore moisture flux results in reduction of rainfall over the Tanzanian coast during La Niña years. The ascending limb of the Walker cell over the central Indian Ocean maintains its position as identified by enhanced westerly moisture flux with wind divergence in the upper levels.

At the peak of the OND rain season (P1) (figure 6.5b), positive OLR anomalies were observed over the Tanzanian coast with highest values of 15W/m² indicating suppressed convection over the coast. The moisture flux anomaly plot is roughly a reverse of the El Niño composite with westerly moisture flux anomaly near the equator in the Indian Ocean and easterly moisture flux anomaly closer to the Tanzanian coast. The easterly moisture flux over the coast causes acceleration of background moisture flux resulting in moisture flux divergence and reduction of rainfall, which is consistent with positive OLR anomalies over the region. At 700hPa, there are strong westerly anomalies over the coast accelerating the background flow (fig 6.3b) and hence divergence. Divergence at middle levels weakens the vertical extent of convective clouds resulting in reduced rainfall.

At the end of the OND rain season (P+1) (figure 6.5b lower panel), the La Nina composite again shows roughly the reverse pattern to the El Niño composite. Negative OLR anomalies are apparent over most of the Indian Ocean indicating

a strengthened Walker cell over the Indian Ocean and reduced uplift over East Africa. Northeasterly to northerly moisture flux anomalies exist near the coast with relative divergence, marking the end of the rainfall season.

Figure 6.5(c&d) shows MAM La Niña+1 composite anomalies. One pentad before the onset of MAM rain season (P-1) (figure 6.5c), negative OLR anomalies cover the Tanzanian coast and positive OLR anomalies are located east of Madagascar. An anticyclonic moisture flux anomaly is evident over the Indian Ocean east of Madagascar. The northerly moisture flux anomalies over the Tanzanian coast are in the same direction as the background flow implying moisture flux divergence. The convective zone over the Tanzanian coast is short-lived since there is upper level wind convergence, which implies descending motion over the region.

During the onset of MAM rainfall season (P0) (figure 6.5c) lower plot, a dipole pattern in OLR anomalies exists over the Indian Ocean with positive anomalies south of 10°S and negative anomalies to the north. All of Tanzania shows weak negative OLR anomalies. The anticyclonic moisture flux anomaly east of Madagascar shows a slight westward shift, which allows easterly to southeasterly moisture flux to dominate much of the Indian Ocean south of the equator. The presence of this anomaly causes the moisture flux anomaly over the Tanzanian coast to be of the same sense as the background flow and therefore divergent, leading to and reduction of rainfall. At 700hPa, there is convergence implying subsidence and below average rainfall.

During the peak of MAM rainfall season (P1) (figure 6.5d), negative OLR anomalies were observed over the Tanzanian coast consistent with moisture flux convergence over the region. However, the development of deep convective clouds is unlikely due to persistence of upper level wind convergence at 200hPa. Below average rainfall over the Tanzanian coast is evident during this period.

Towards the withdrawal of MAM rain season (P+1), the convective zone develop over the northwest Indian Ocean with strong westerly moisture flux feeding the convection. This northward displacement of the convective zone is in sympathy with the movement of the ITCZ. The descending limb of the Walker cell is over the Tanzanian coast, with reduced cloud over the coast as indicated by positive OLR anomalies. This marks the end of rainfall season over the northern coast of Tanzania.

6.3.2.3 Results of OLR, moisture flux at 850hPa, wind at 700hPa and 200hPa anomalies for extreme El Niño event of 1997/98.

The 1997/98 El Niño was an extreme event during the period of study. This El Niño was extreme in the sense that widespread rainfall with flooding led to significant socio-economic disruption over East Africa. During OND 1997, which also occur a positive Indian Ocean Zonal Mode event, the northern coast of Tanzania recorded the highest rainfall anomaly value of the 1970-1999 period with a standardized departure of about 4.5 (fig 3.1b). A significantly longer than normal rainfall season extending from September 1997 to February 1998 (fig 6.2b), occurred with a relatively dry spell of only about one month before the onset of MAM rainfall season. The interannual analysis (chapter 5) of this thesis noted that 1997 was a positive Indian Ocean zonal mode year. The contrast in SST anomalies over the equatorial western and eastern Indian Ocean tends to amplify the El Niño signal, which was the case for 1997. This section aims at analyzing the anomalous intraseasonal circulations associated with this extreme El Niño event.

The anomalies of OLR, moisture flux, middle and upper level wind for both 1997 OND season and corresponding 1998 MAM season are given in figures 6.6(a-d). The pentads used are the same as those used in section 6.3.1 with dates for OND 1997 and MAM 1998 shown in table 6.3. For the 1997 OND season (fig 6.6a), one pentad before the onset of the rainfall season (P-1), positive OLR

anomalies of the order of 60W/m² were observed over the equatorial central Indian Ocean. These high positive OLR values seem to be the westward extent of high positive OLR values spreading out from the centre of suppressed convection over equatorial eastern Indian Ocean and Indonesia. Strong easterly moisture fluxes originating from this broad zone of subsidence advect moisture towards the Tanzanian coast one pentad before the onset of rainfall season.

During the onset of the OND rainfall season (P0) figure 6.6a lower panel, the positive OLR anomalies over the equatorial central Indian Ocean move eastward while a strong convective zone develops over the equatorial western Indian Ocean with larger negative OLR anomalies of about -50W/m². This convective zone extends westward to cover much of the East African coast and southward east of Madagascar over the tropical South Indian Ocean. Strong easterly moisture flux emanating from the zone of subsidence over the equatorial East Indian Ocean provides energy and moisture to sustain the convection. The convective zone over the equatorial western Indian Ocean is about –30W/m² below the El Niño composite OLR anomaly value indicating deep convective clouds over the region which resulted into extreme high rainfall over East Africa.

The establishment of a reverse circulation to the background flow over the Indian Ocean with strengthened easterly moisture flux along the equator caused by subsidence over the eastern Indian Ocean and convection over the western Indian Ocean is related to the eastward shift of the Walker circulation over the Pacific Ocean. With this reverse circulation, the ascending limb of the Indian Ocean Walker cell is located over the East African coast as indicated by strong westerly flow in the upper levels with a ridge over East Africa. The easterly anomalies and convective zone over the equatorial western Indian Ocean are stronger than El Niño composite.

During the peak of the OND rainfall season (P1) (figure 6.6b), the convective zone over the western Indian Ocean shows a significant westward extent covering all of East Africa with strongest negative OLR anomalies of about –60W/m² centered over the northern coast of Tanzania and southern Kenya. The subsidence zone over equatorial East Indian Ocean moves westward as indicated by high positive OLR anomaly values over the equatorial central Indian Ocean. Enhanced moisture flux convergence over the Tanzanian coast results in the highest peak of rainfall of about 21mm/day (fig 6.2b). The upper level flow shows equatorward displacement of the Indian Ocean high-pressure cell, with enhanced westerly anomalies over much of the East African regions, which sustain the convective zone there.

Towards the withdrawal of rainfall season (P+1) (figure 6.6b lower panel), positive OLR anomalies cover much of East Africa while a convective zone has developed over the central Indian Ocean. Strong westerly moisture flux exists over the western Indian Ocean feeding this convective zone. The descending limb of Walker cell is located over the western Indian Ocean near the Tanzanian coast as indicated by high OLR values over the region coupled with upper level wind convergence. This implies reduced rainfall over the region, marking the end of the wet season.

For the 1998 MAM season (fig 6.6c&d), one pentad before the onset of rainfall season (P-1) (figure 6.6c), a tongue of positive OLR anomalies, emanating from the tropical South Indian Ocean, extends westward through Madagascar over Tanzania. Over the equatorial western Indian Ocean, a convective zone centered at about 65°E was observed. Strong moisture flux convergence occurs over the convective zone with weak convergence closer to the Tanzanian coast. At 700hPa, strong winds feed the convective zone over the equatorial western Indian Ocean while at 200hPa; outflow motion is evident, indicating the rising limb of the Walker cell.

During the onset of rainfall season (P0) (figure 6.6c lower panel), the convective zone over the equatorial western Indian Ocean shows westward displacement to extend over the East African coast. Strong easterly moisture flux converging with southeasterly moisture flux along the Tanzanian coast feeds this convection. The presence of enhanced moisture convergence over the Tanzanian coast leads to above average rainfall.

During the peak of rainfall season (P1) (fig 6.6d), a zone of negative OLR anomalies is oriented in a NW-SE direction from the East African coast to the subtropical South Indian Ocean southeast of Madagascar with positive OLR anomalies elsewhere over the tropical western Indian Ocean. Easterly moisture flux over the equatorial western Indian Ocean feeds this convection. Enhanced moisture convergence of this flux with southeasterly flux near the Tanzanian coast leads to above average rainfall. The upper level flow shows a westerly wave pattern with a ridge over East Africa indicating the position of the rising limb of Walker cell.

Towards the withdrawal of rainfall season (P+1) (figure 6.6d lower panel), a dipole pattern in OLR exists with positive anomalies over southern Africa and the South West Indian Ocean and negative anomalies over the tropical Indian Ocean. A strong convective zone exists over the equatorial central Indian Ocean where strong westerly anomalies at lower levels supply moisture and energy to sustain it. At 200hPa, westerly wind anomalies exist over the equatorial Indian Ocean. These anomalies are in the same sense as the background flow implying divergence and indicate the position of the rising limb of the Walker cell over the equatorial central Indian Ocean.

It is evident from the above discussion that wet conditions during El Niño years are associated with enhanced convection and easterly flow over the equatorial western Indian Ocean and a reverse for dry La Niña.

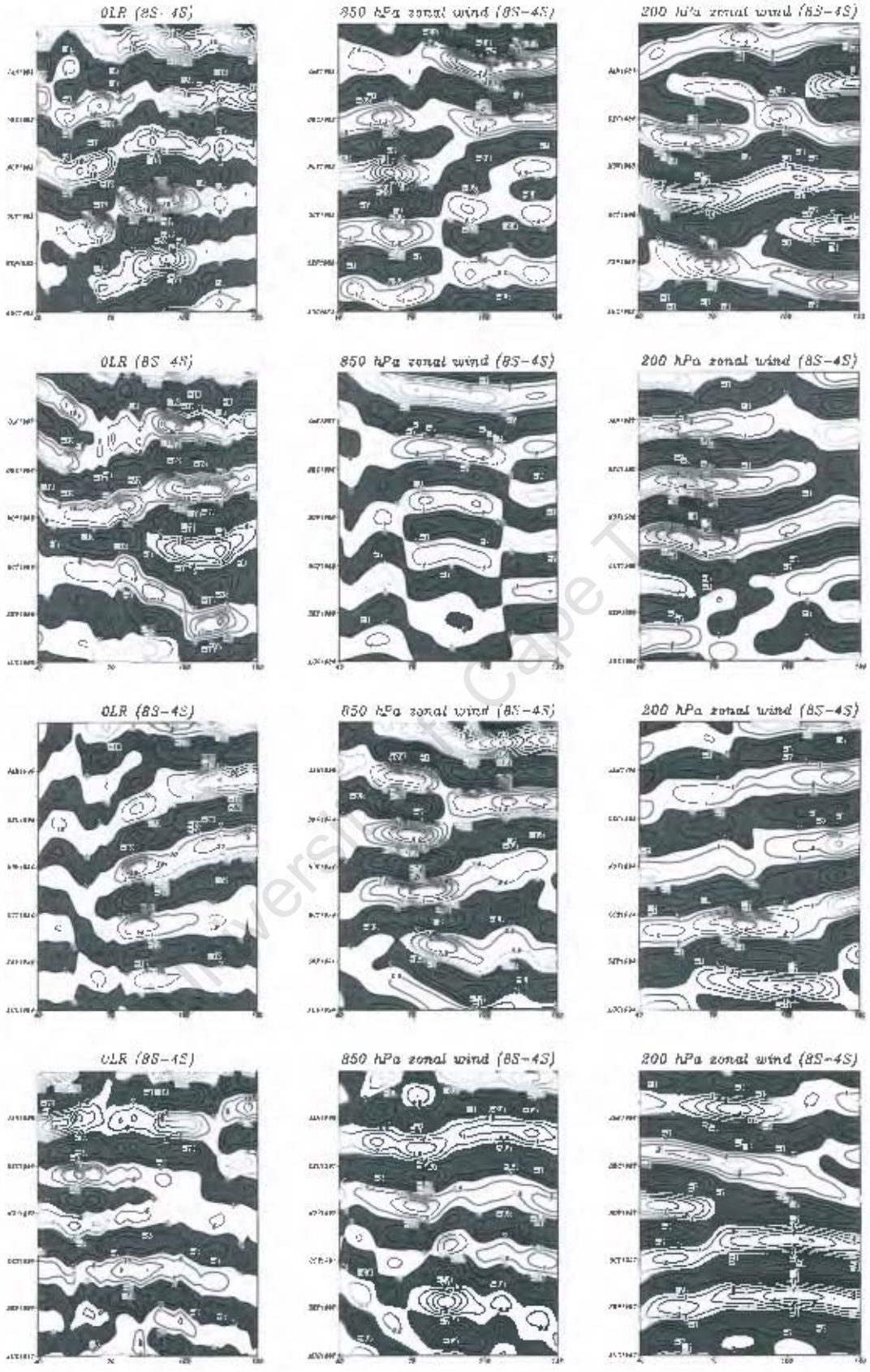

Figure 6.1a: Hovmöller plots of bandpass filtered OLR, zonal wind at 850hPa and 200hPa for El Niño years during OND season.

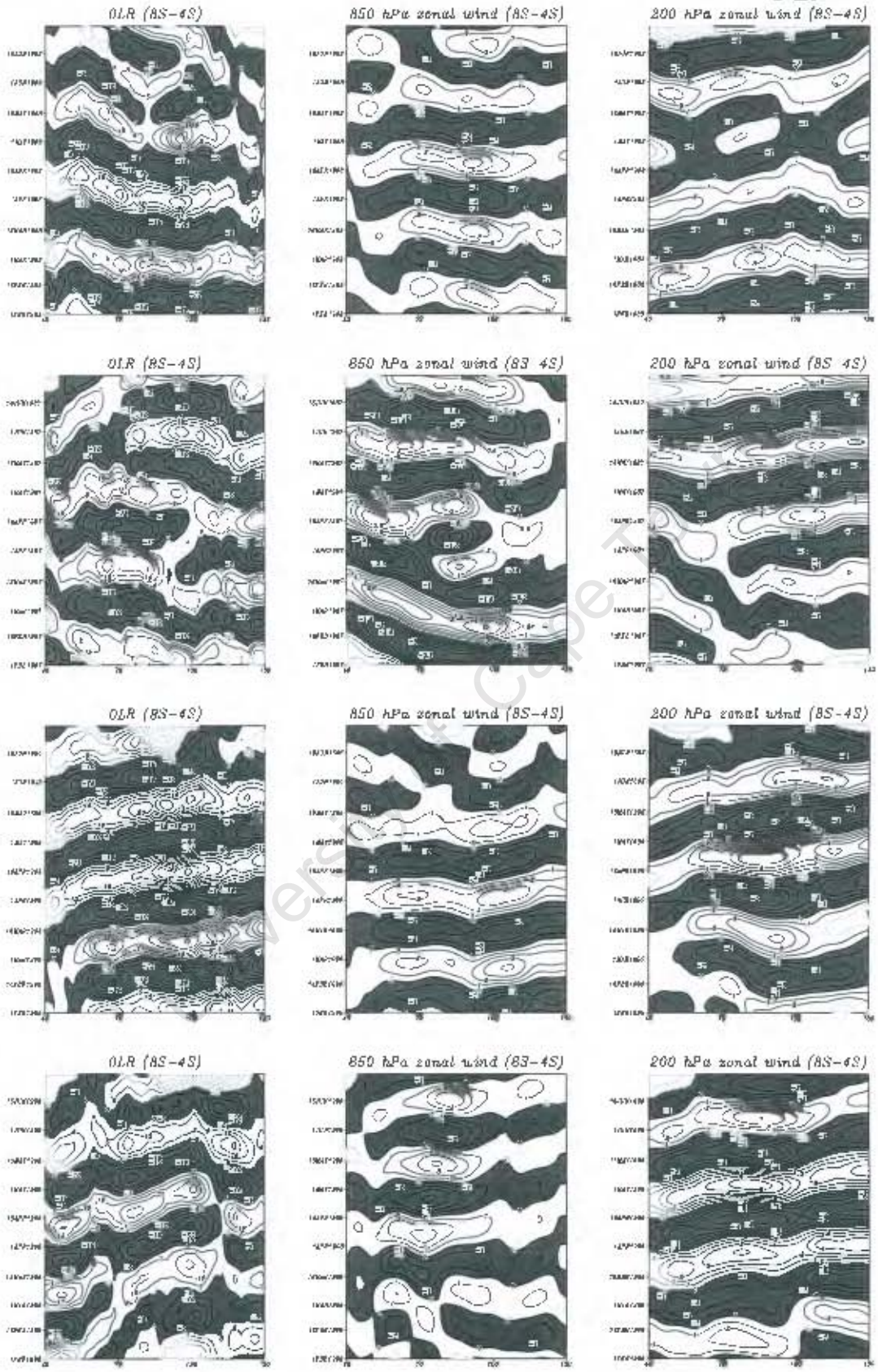

Figure 6.1b: As for figure 6.1a but for El Niño+1 years during MAM season

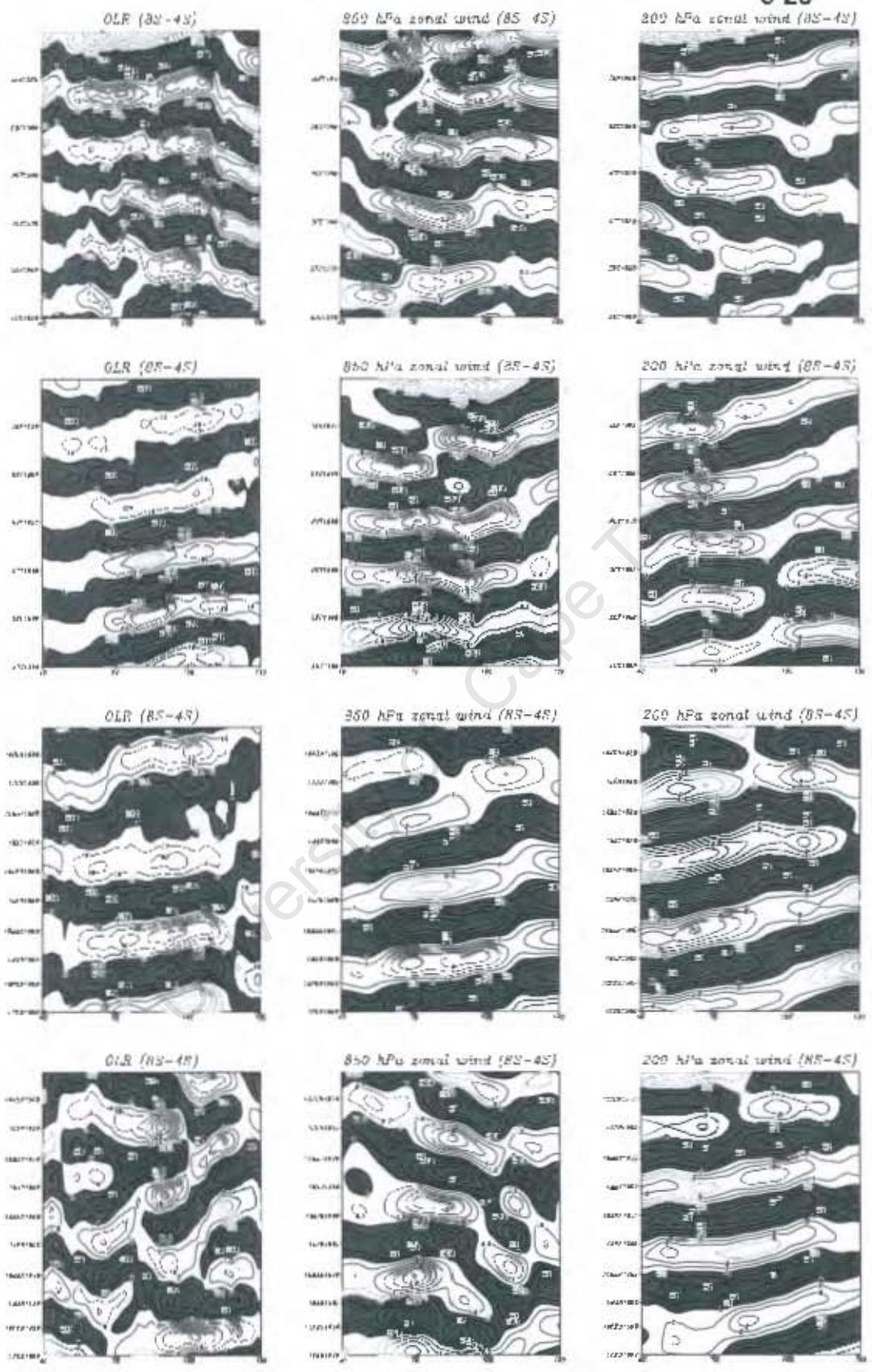

Figure 6.1c: As for figure 6.1a but for La Niña and La Niña+1 years.

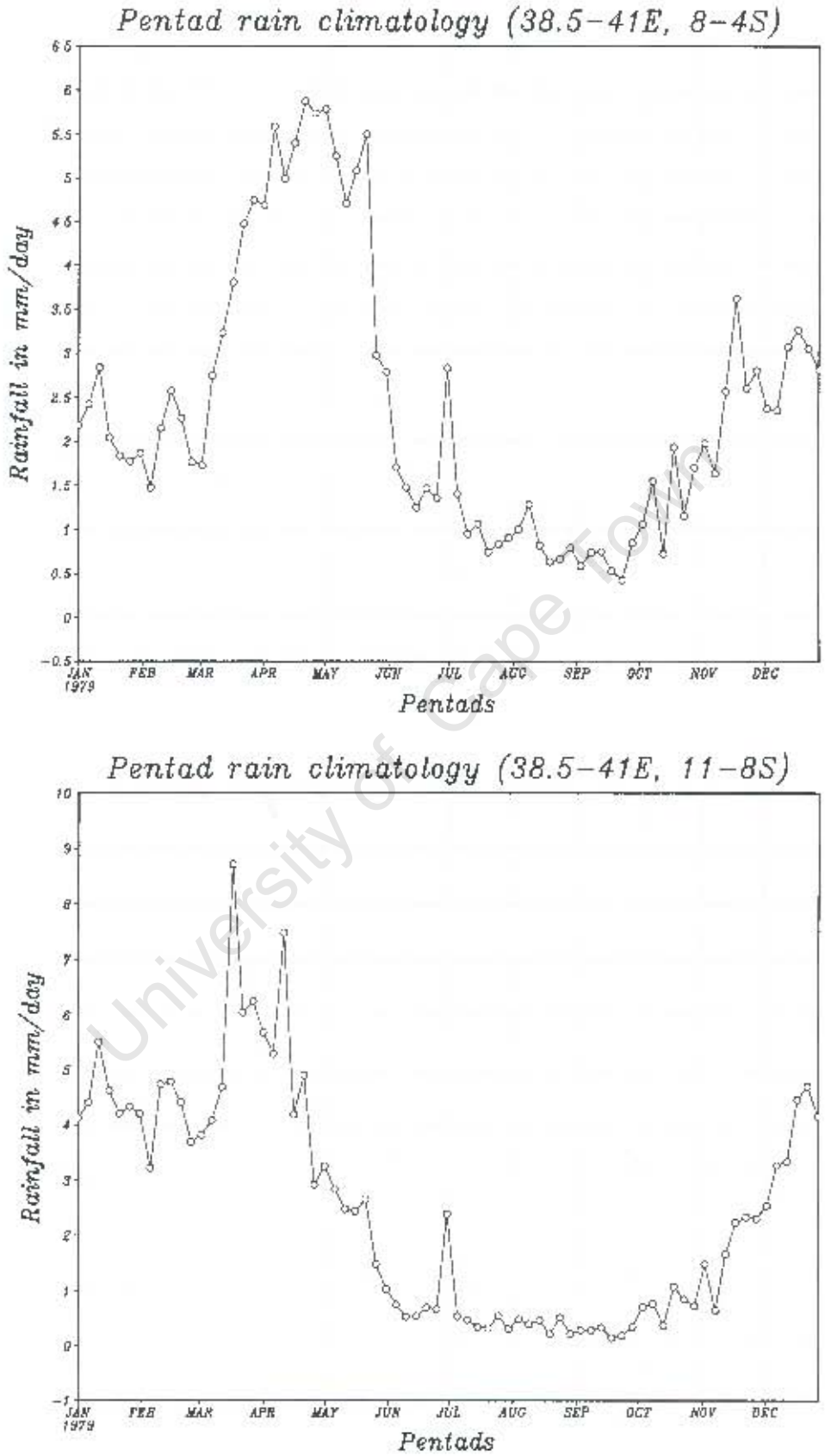

Figure 6.2a: Climatological Pentad rainfall time series for northern and southern coast of Tanzania

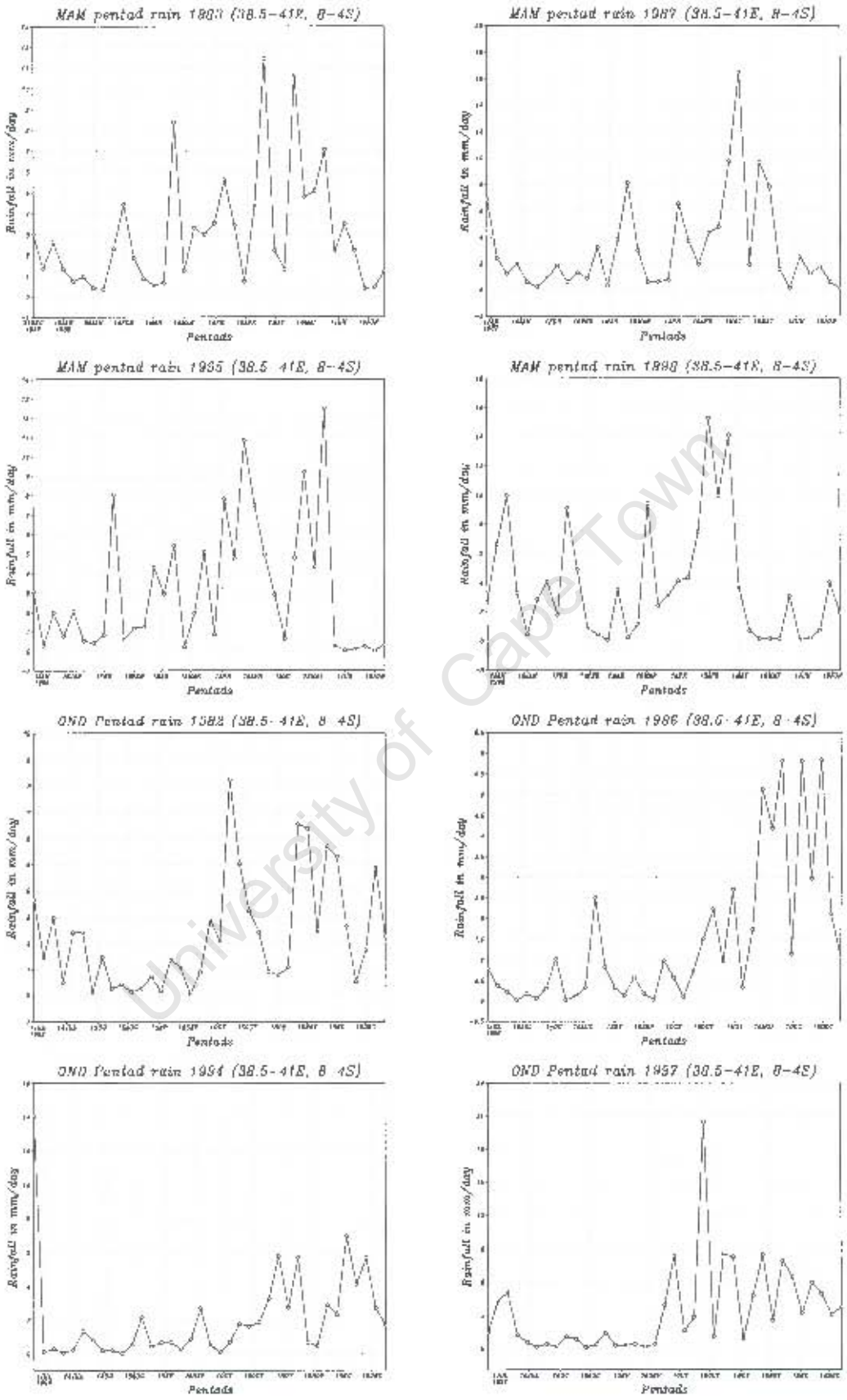

Figure 6.2b: Pentad rainfall time series for northern coast during MAM and OND season for each El Niño+1 and El Niño year

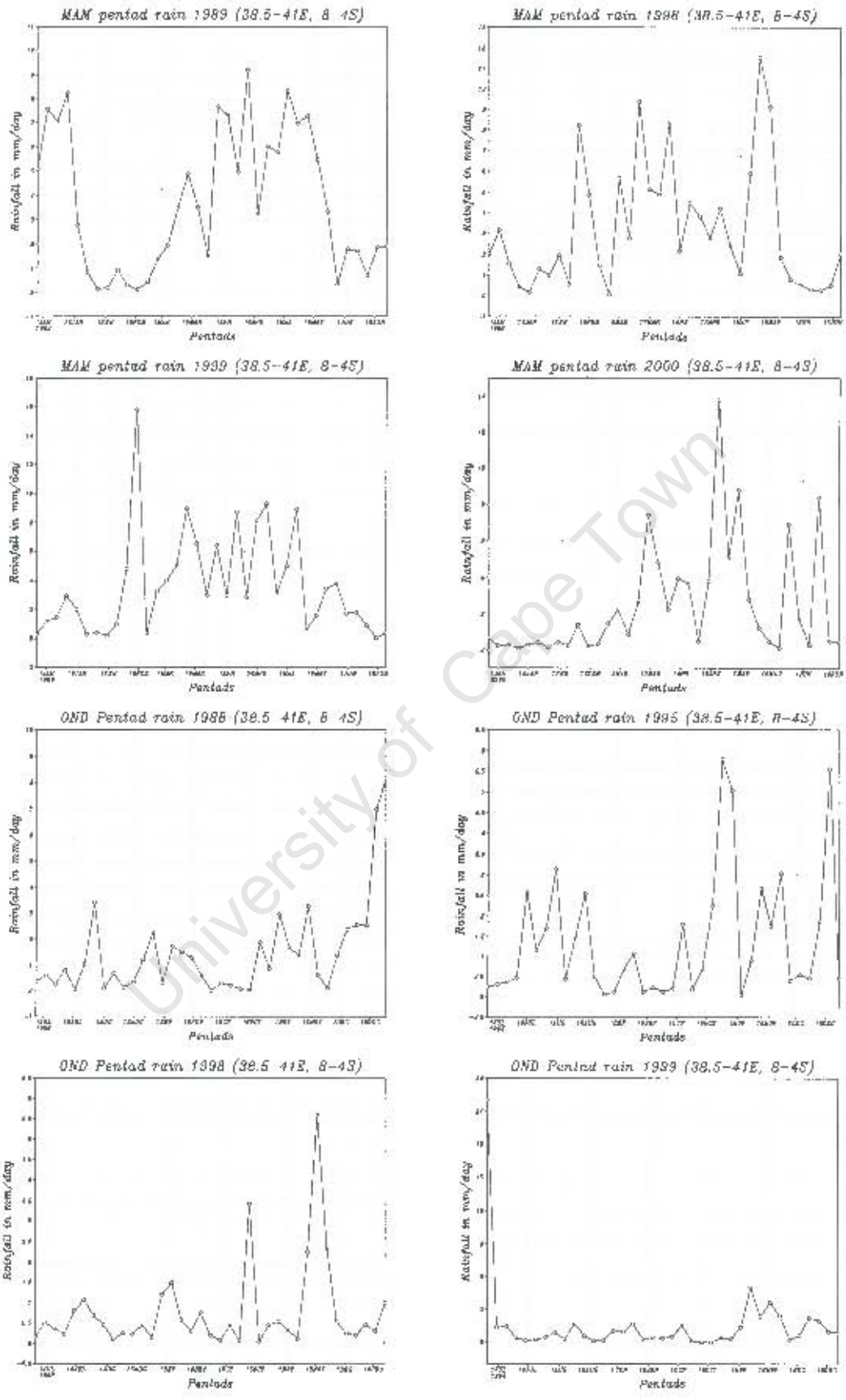

Figure 6.2c: As for figure 6.2b but for each La Niña+1 and La Niña year

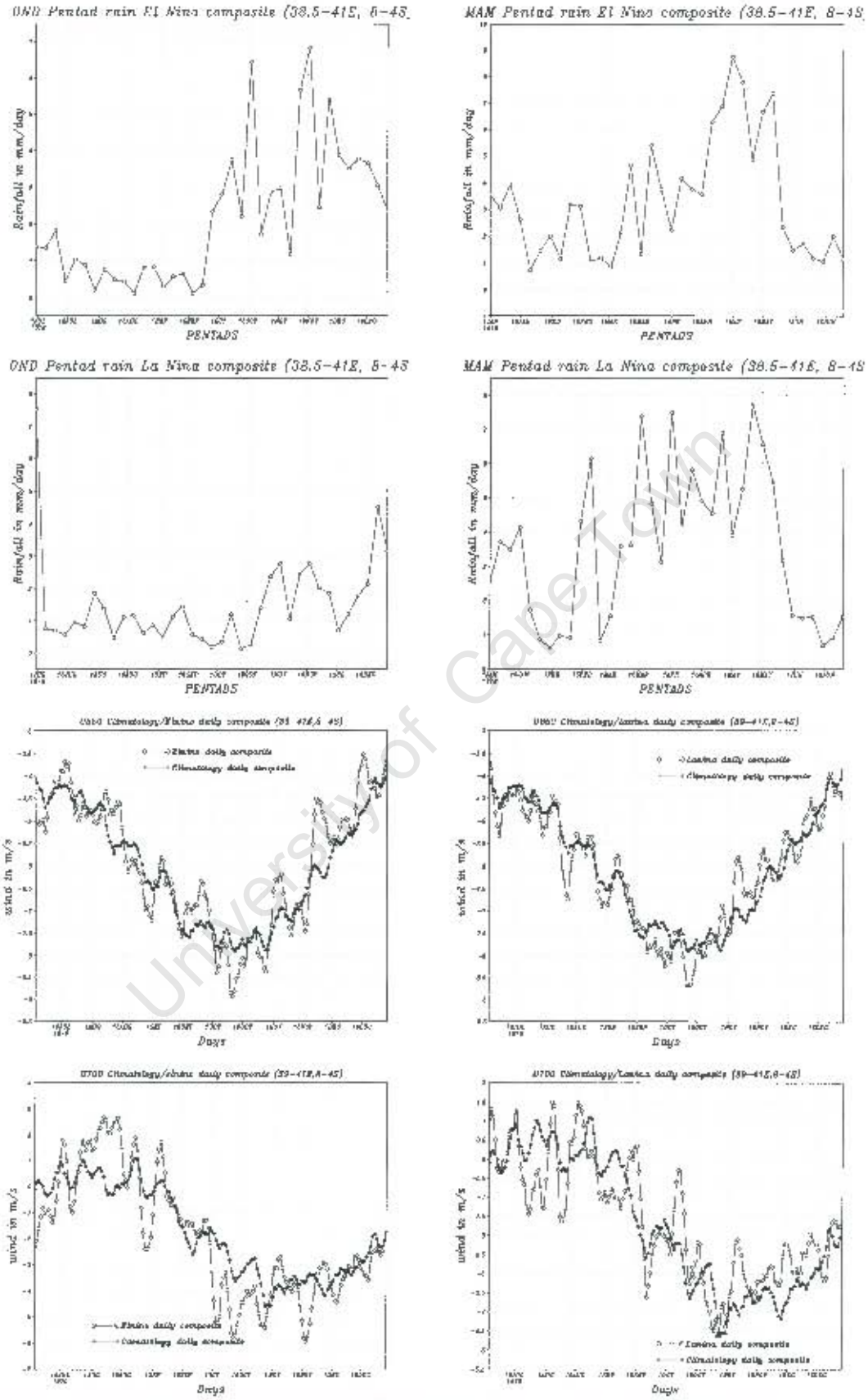

Figure 6.2d:Northern coast pentad rainfall time series for El Niño/La Niña and El Niño+1/La Niña+1 composites (upper), 850hPa and 700hPa climatology/El Niño and La Niña composite zonal wind for OND (lower).

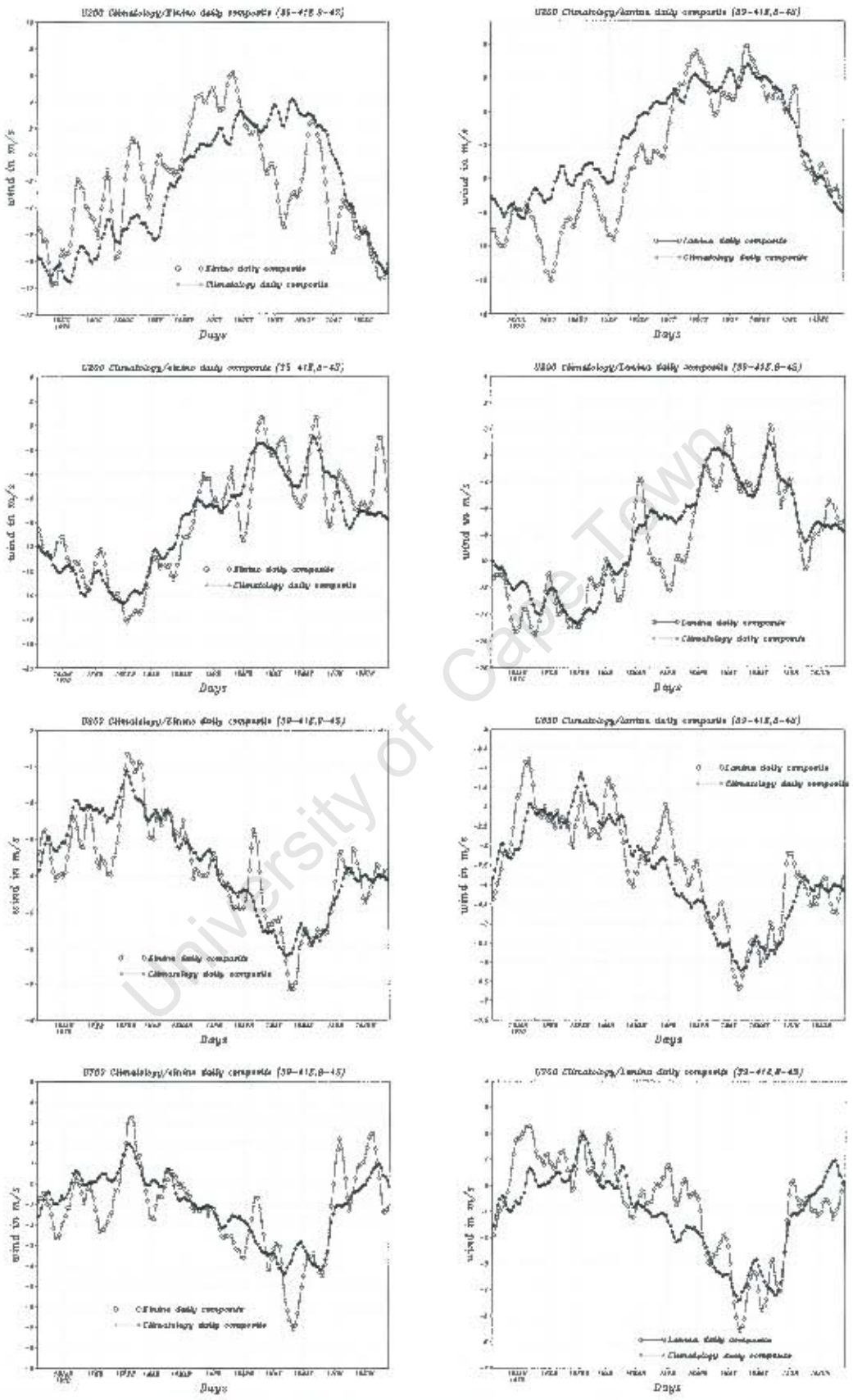

Figure 6.2e:Northern coast, 200hPa zonal wind time series for OND (upper), 200hPa, 850hPa and 700hPa for MAM (lower)

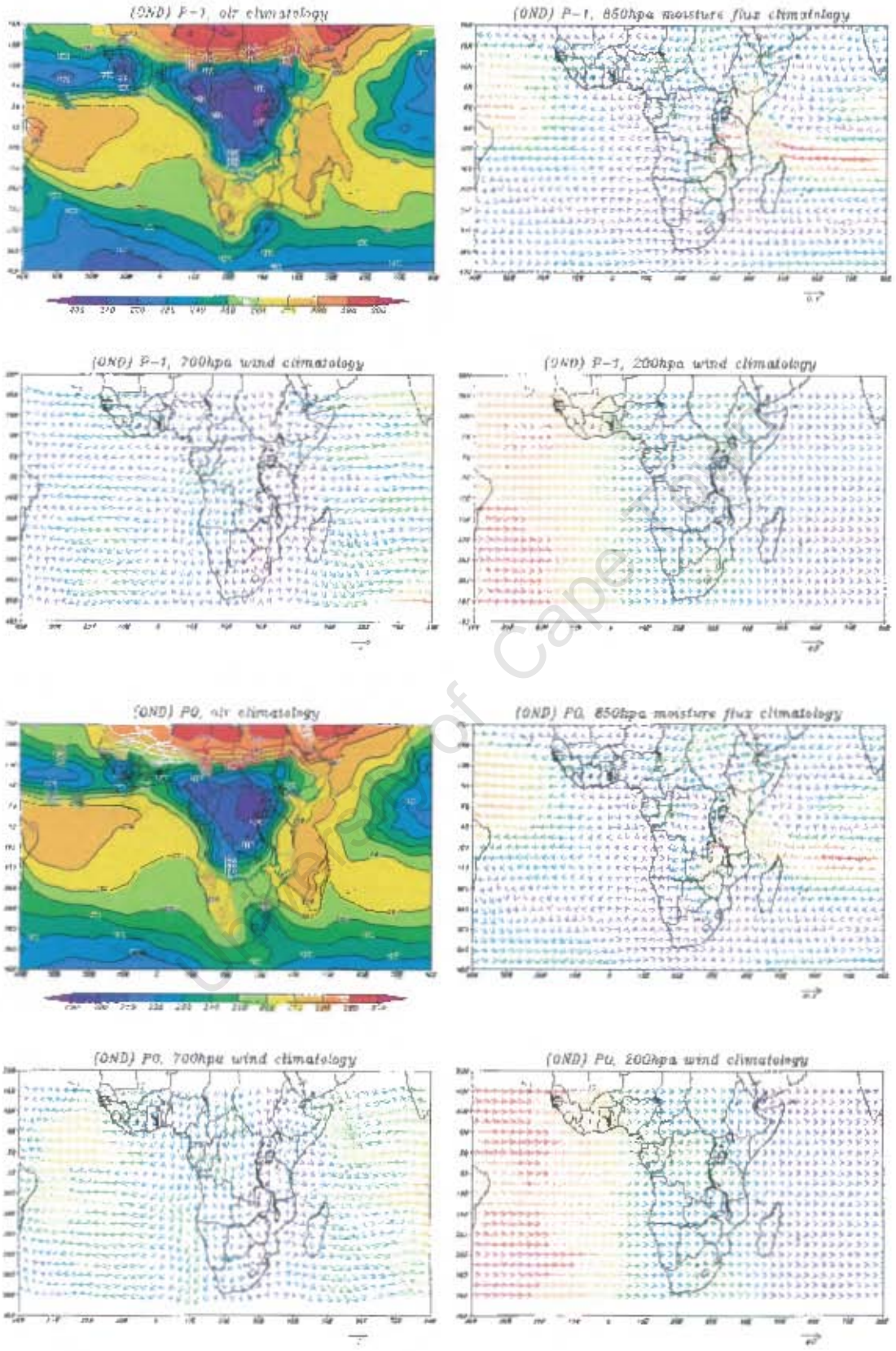

Figure 6.3a: OND climatological fields at P-1 and P0
OLR in (W/m²), Moisture flux in g/kg.m/s and wind in m/s.

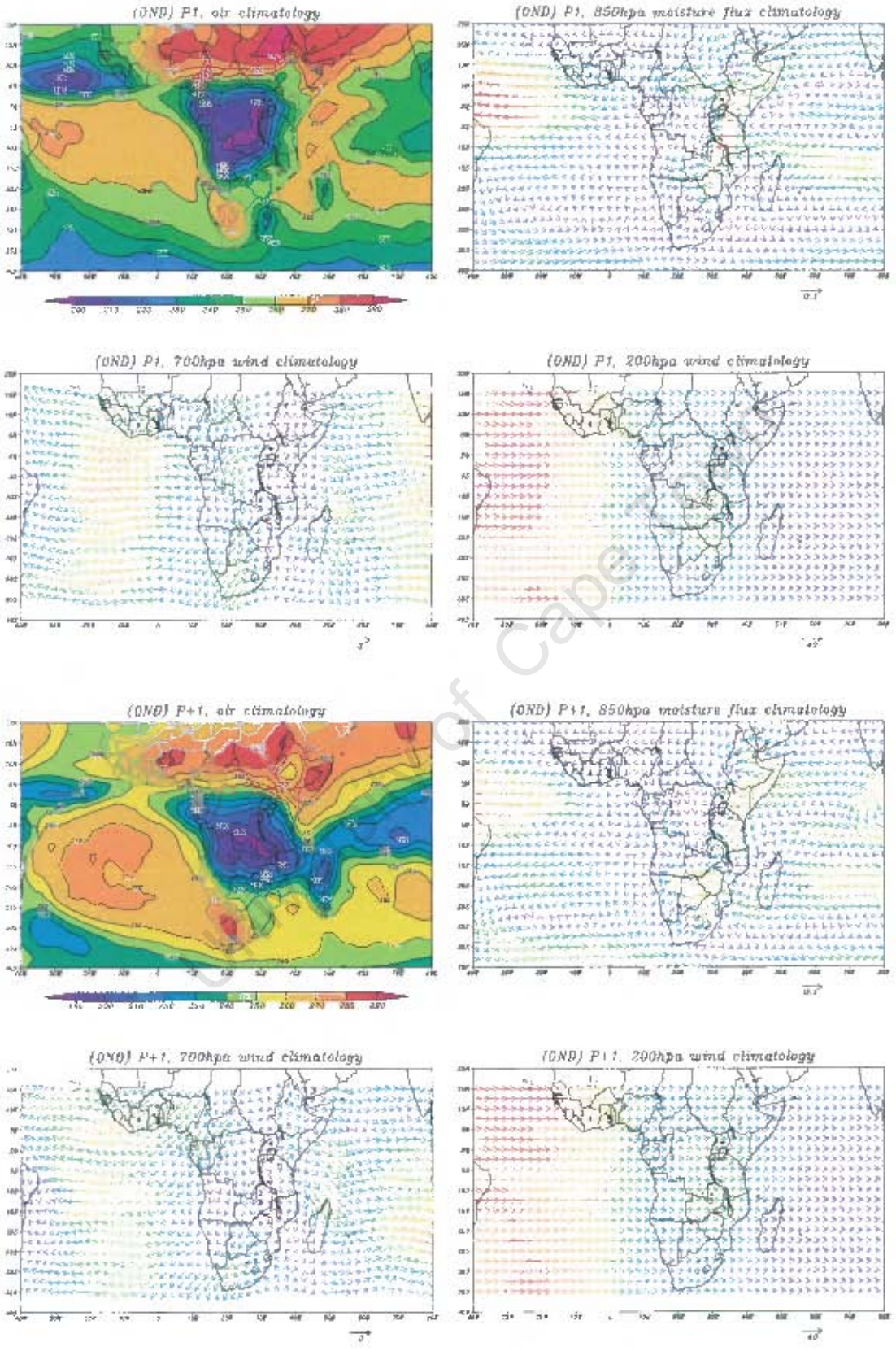

Figure 6.3b: As for figure 6.3a but for P1 and P+1

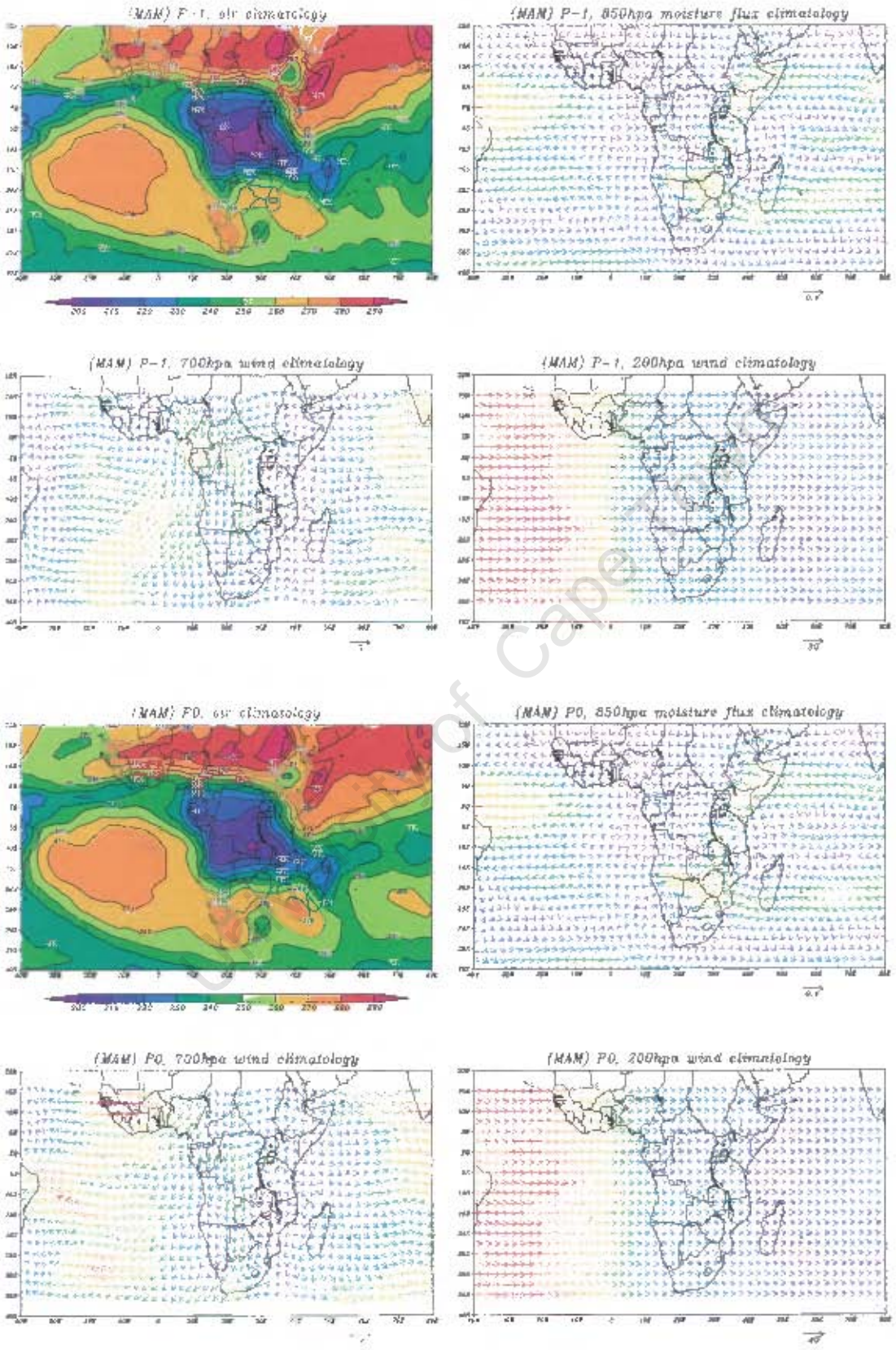

Figure 6.3c: MAM climatological fields at P-1 and P0
OLR in (W/m²), Moisture flux in g/kg.m/s and wind in m/s.

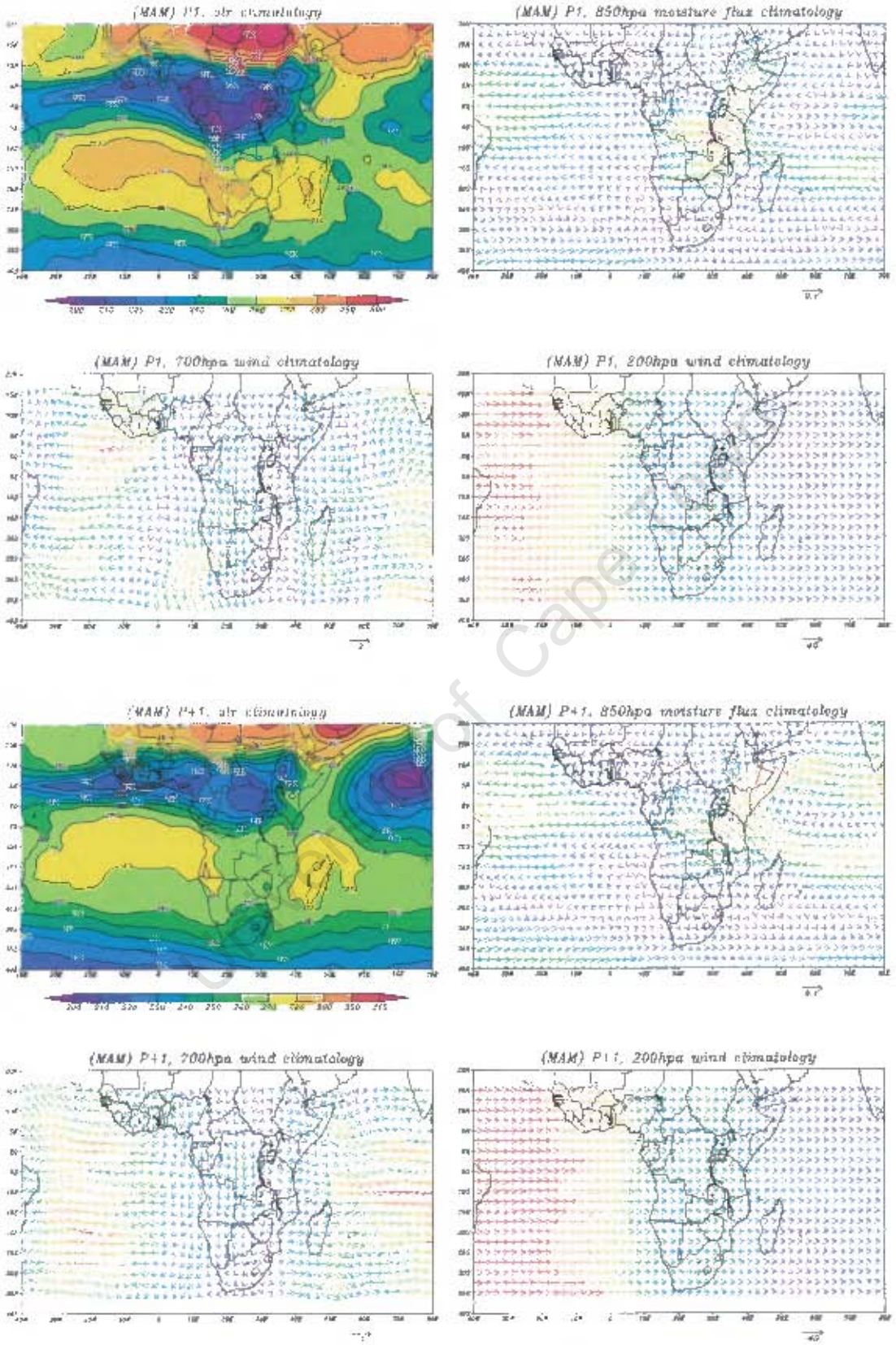

Figure 6.3d: As for figure 6.3c but for P1 and P+1

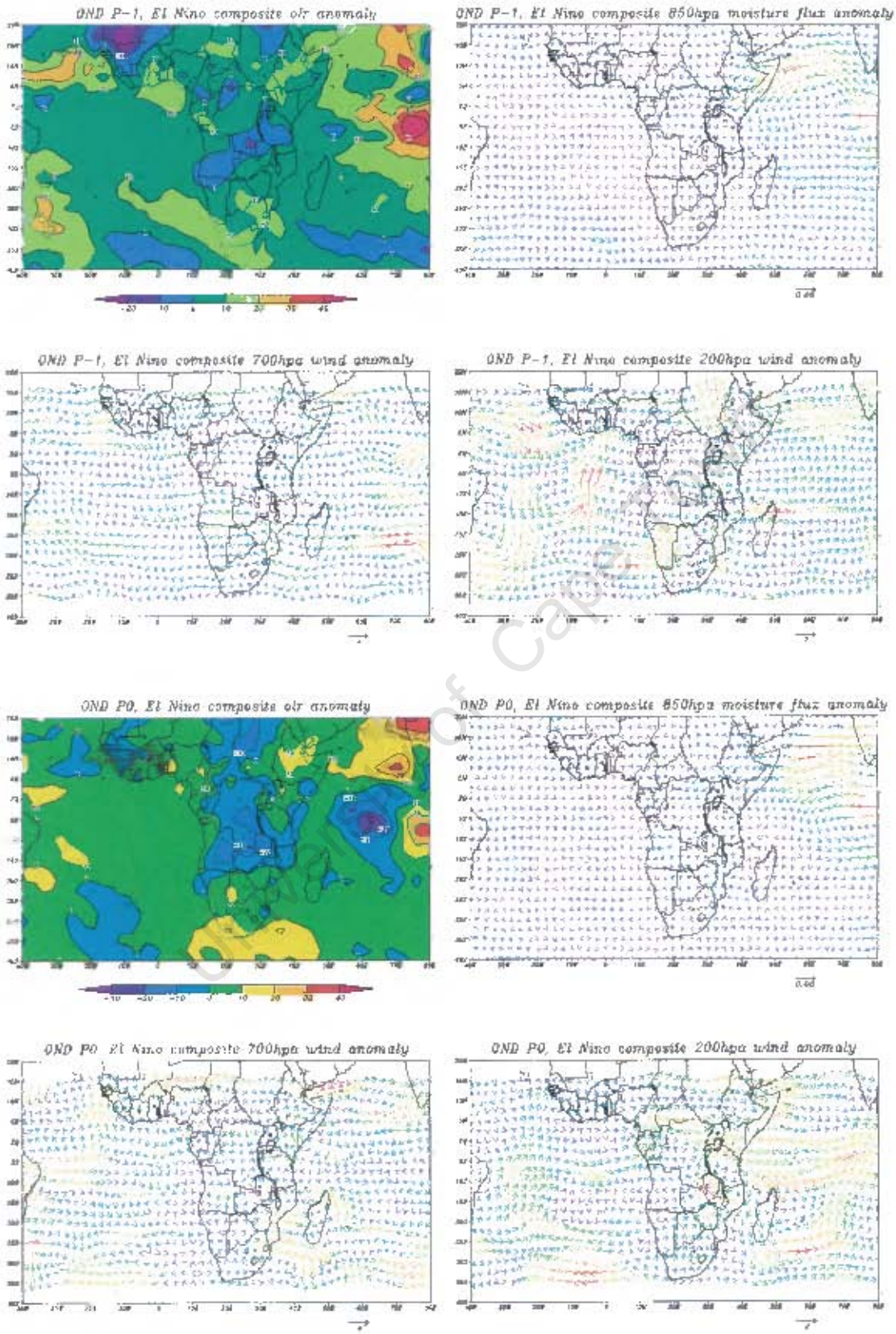

Figure 6.4a:El Niño composite OND anomaly fields at P-1 and P0 OLR in (W/m²), Moisture flux in g/kg.m/s and wind in m/s.

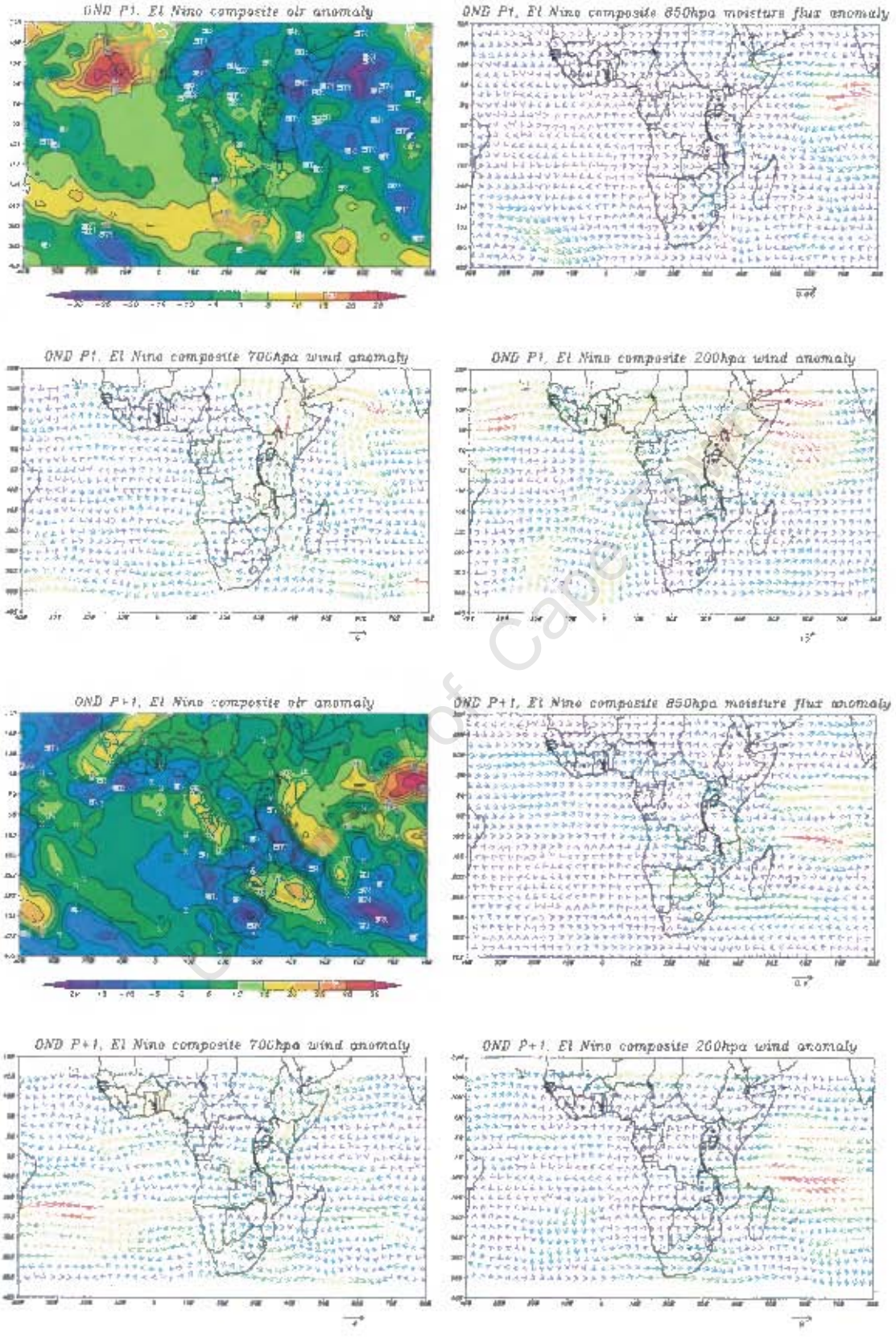

Figure 6.4b: As for figure 6.4a but for P1 and P+1

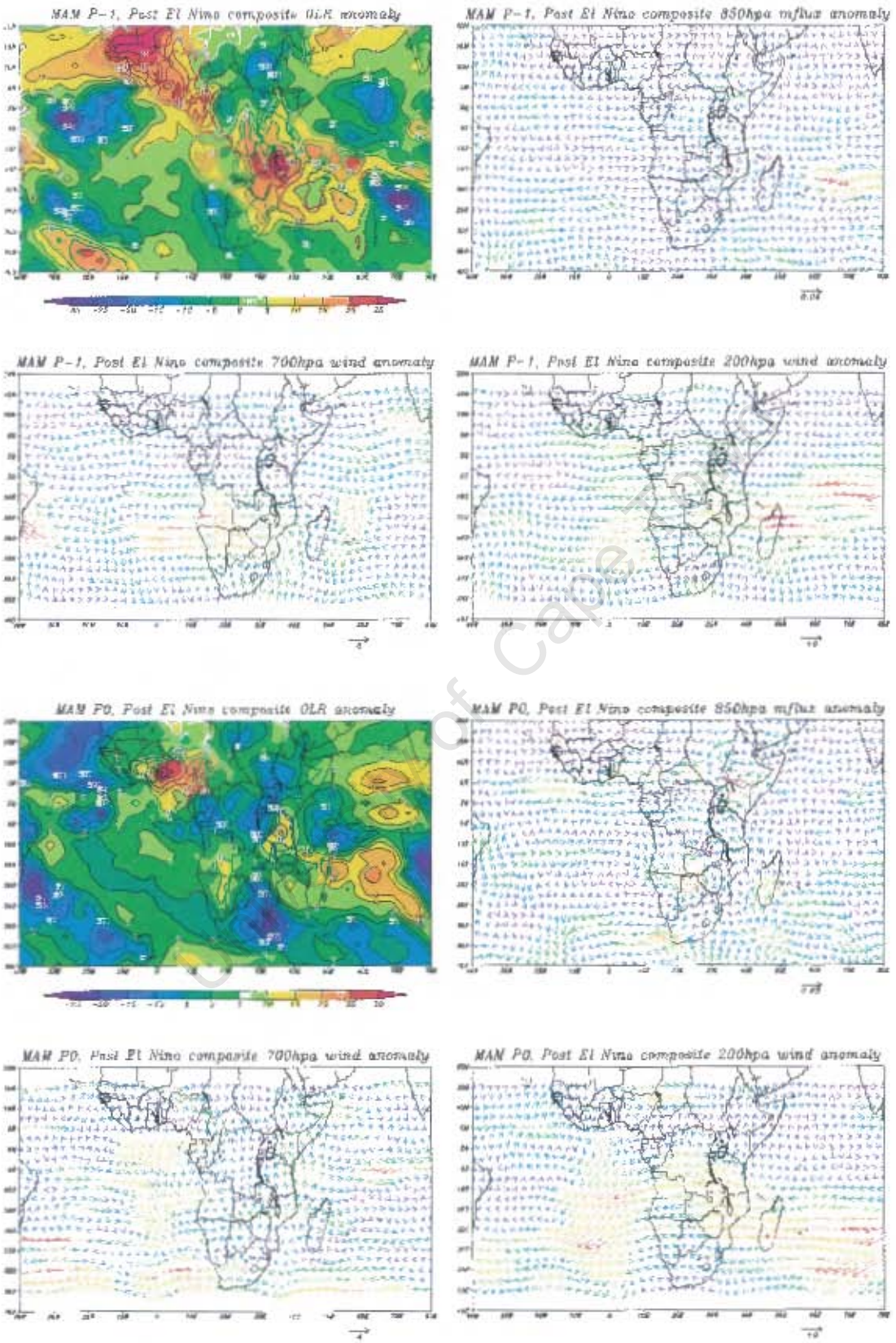

Figure 6.4c: As for figure 6.4a but for El Niño+1 composite during MAM season

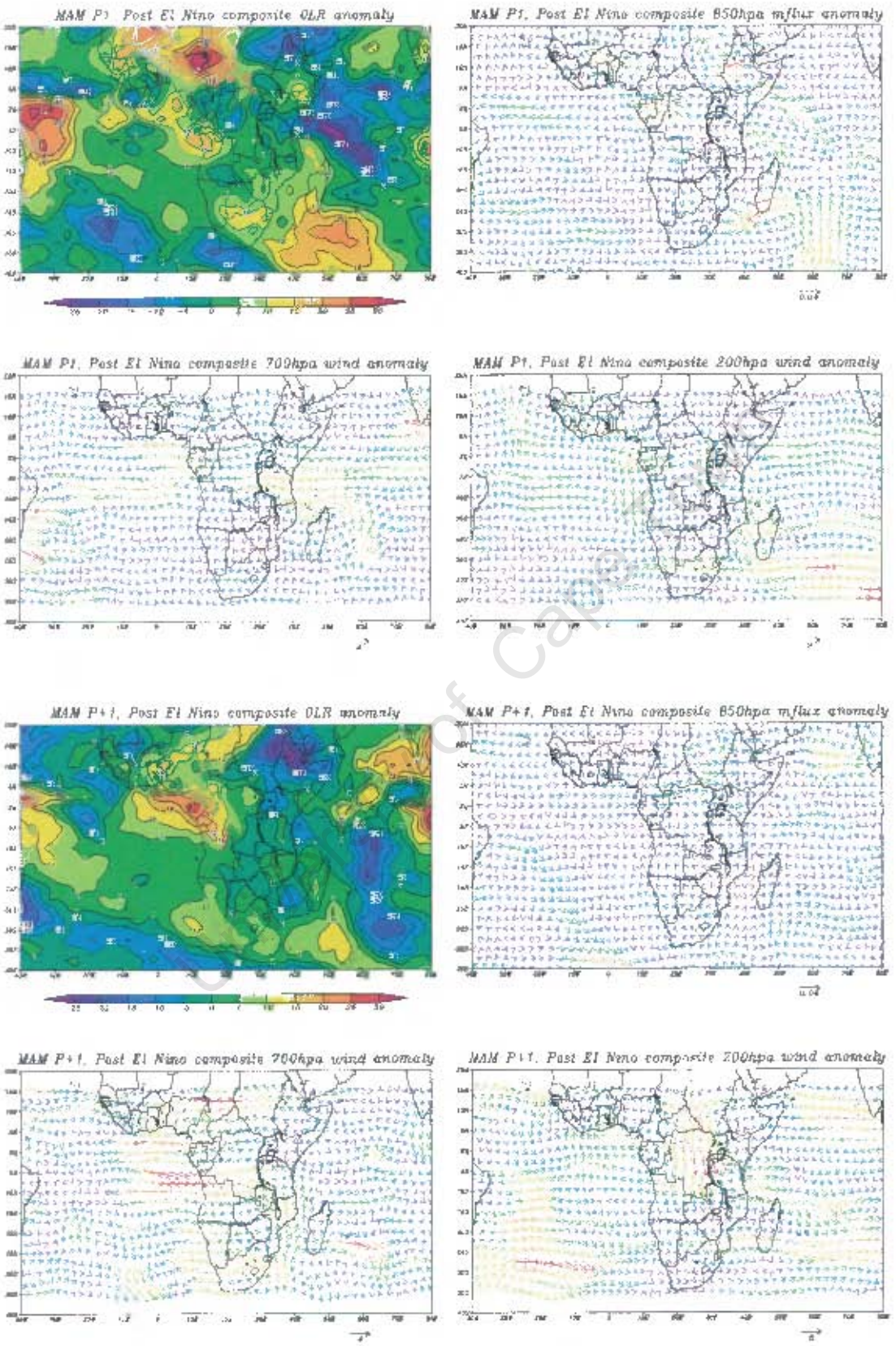

Figure 6.4d: As for figure 6.4a but for (MAM) PI and P+1 for El Niño+1 composites

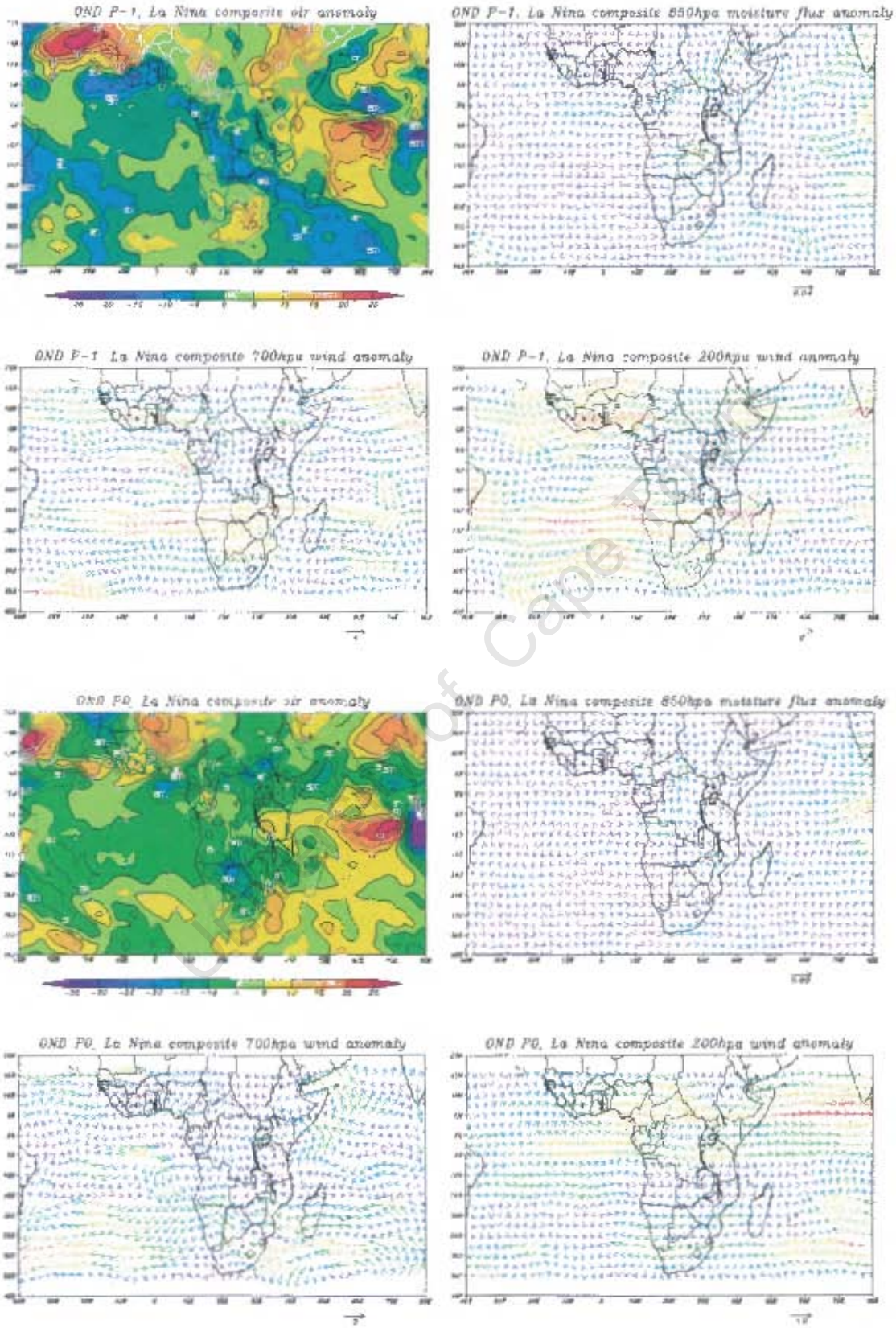

Figure 6.5a: As for figure 6.4a but for La Niña composite

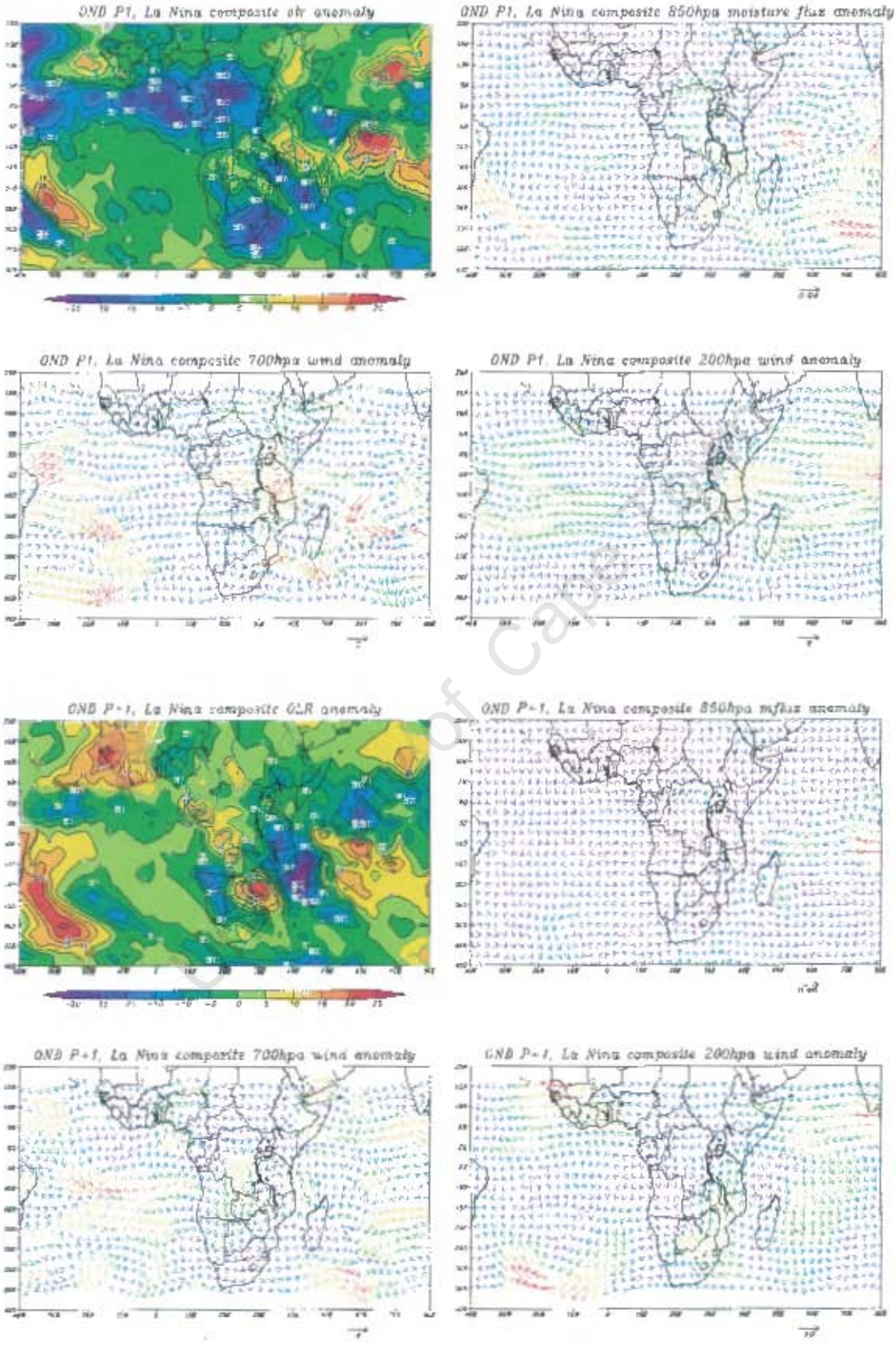

Figure 6.5b: As for figure 6.5a but for P1 and P+1

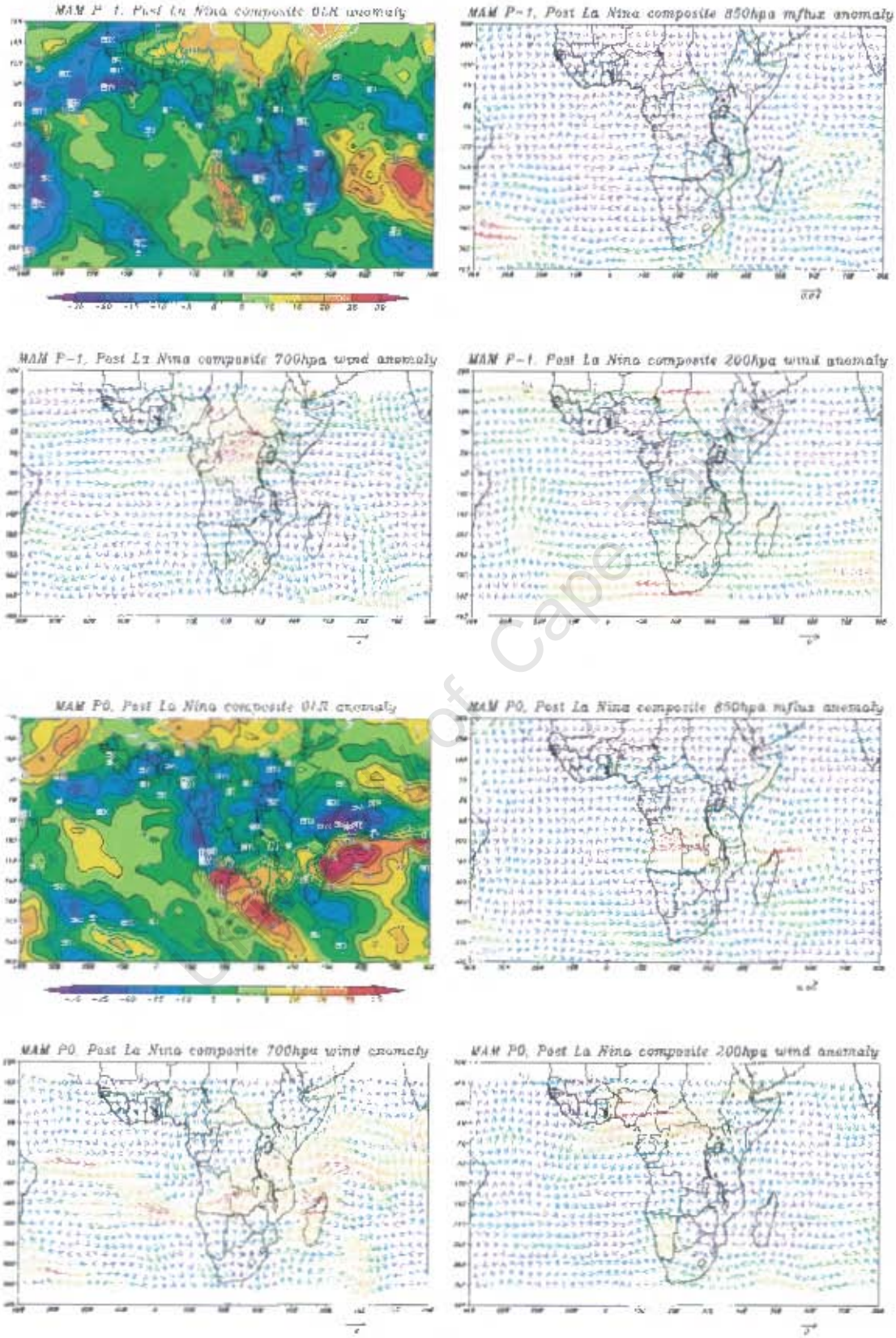

Figure 6.5c: As for figure 6.4a but for La Niña+1 composite during MAM season.

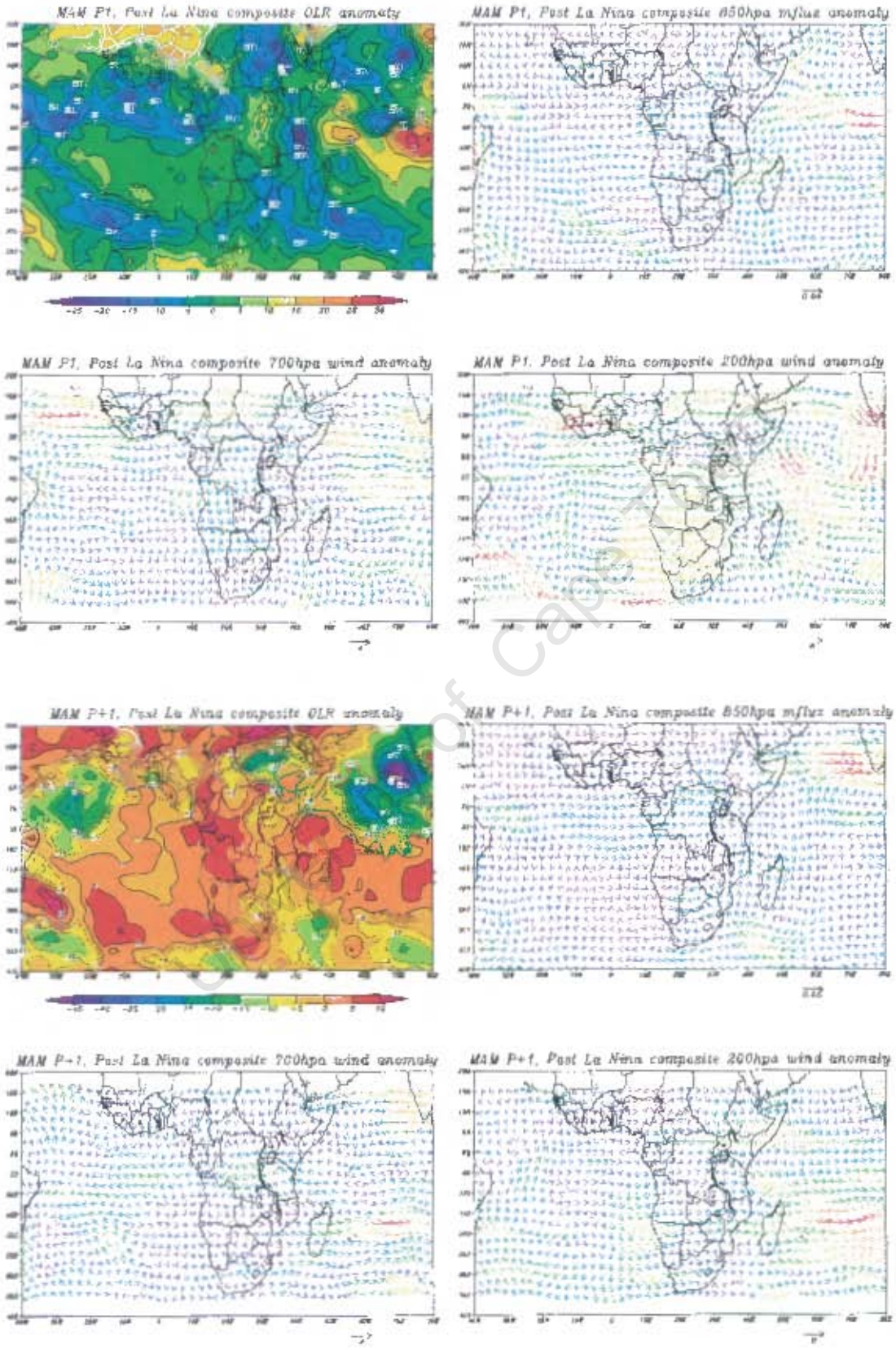

Figure 6.5d: As for figure 6.5c but for P1 and P+1

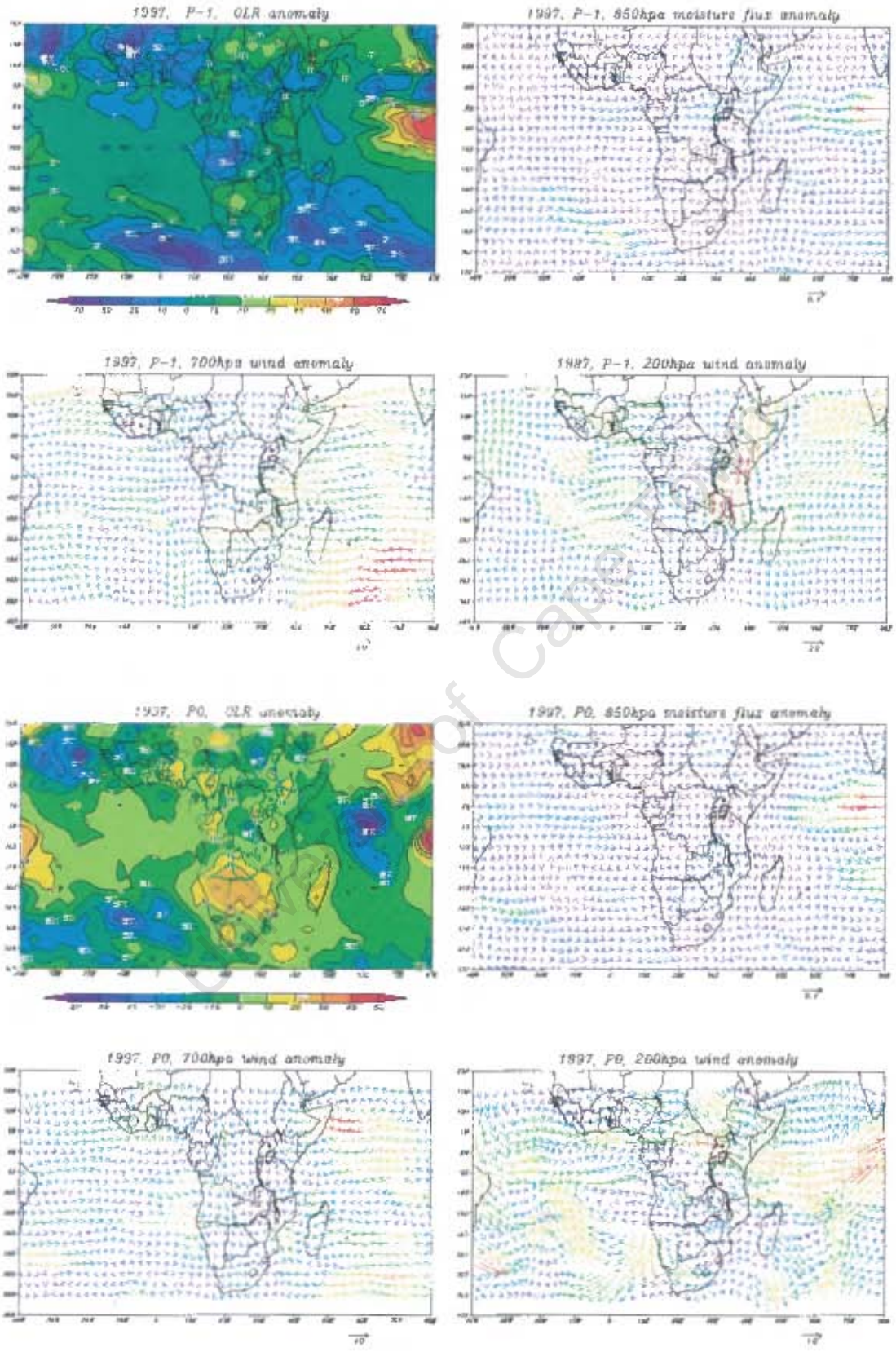

Figure 6.6a: As for figure 6.4a but for 1997

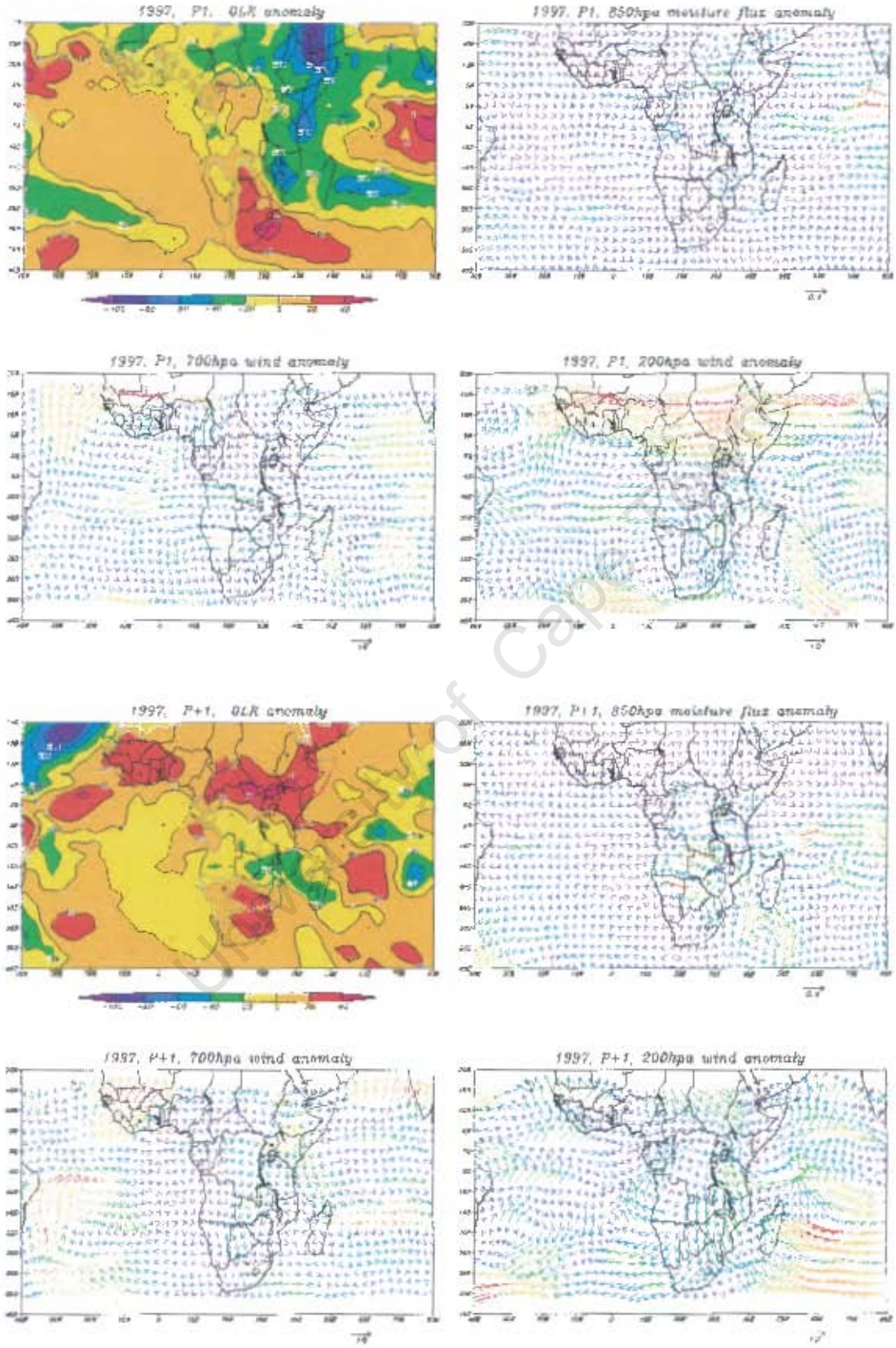

Figure 6.6b: As for figure 6.4a but for P1 and P+1 OND 1997

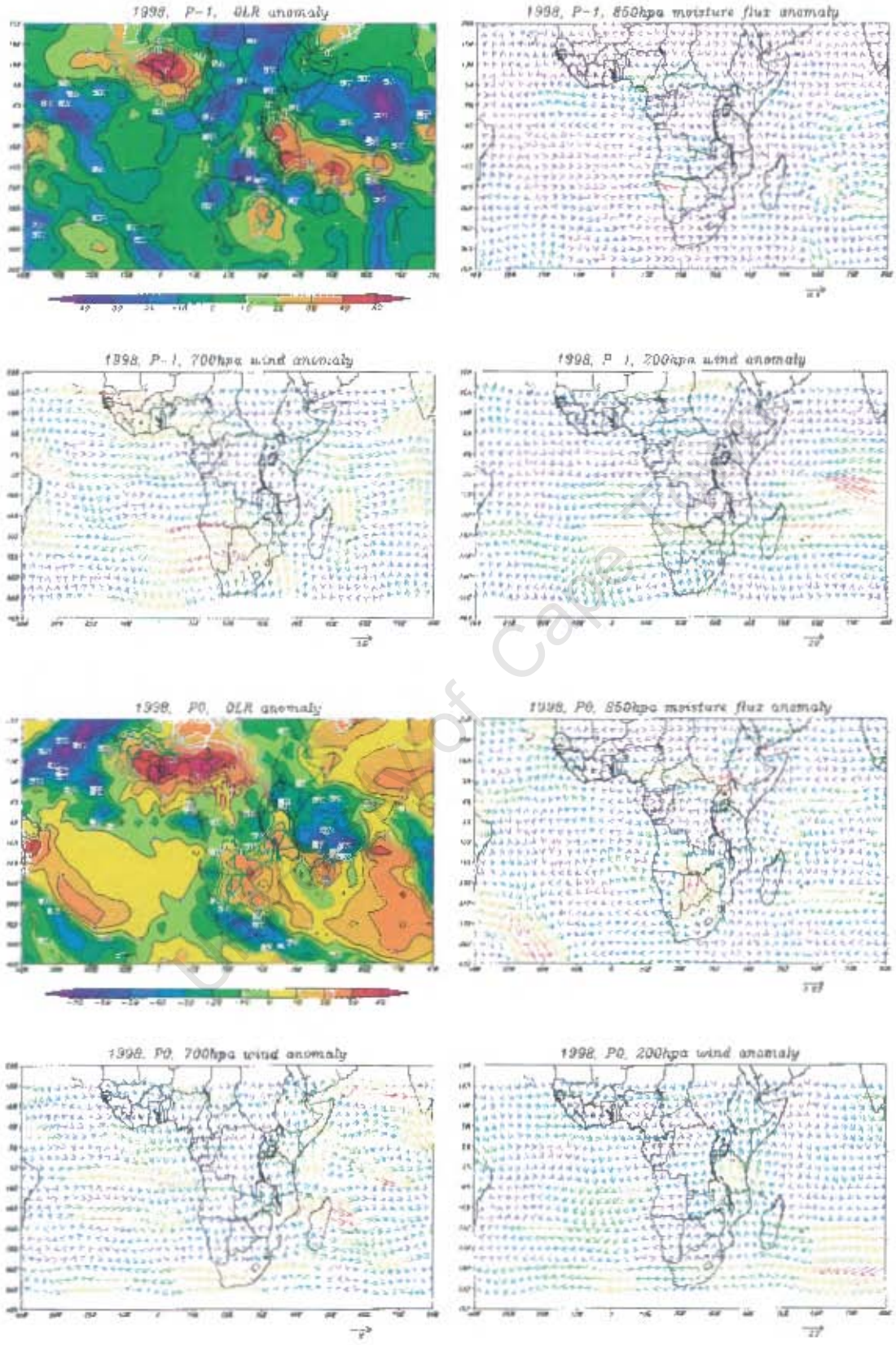

Figure 6.6c: As for figure 6.4a but for MAM 1998

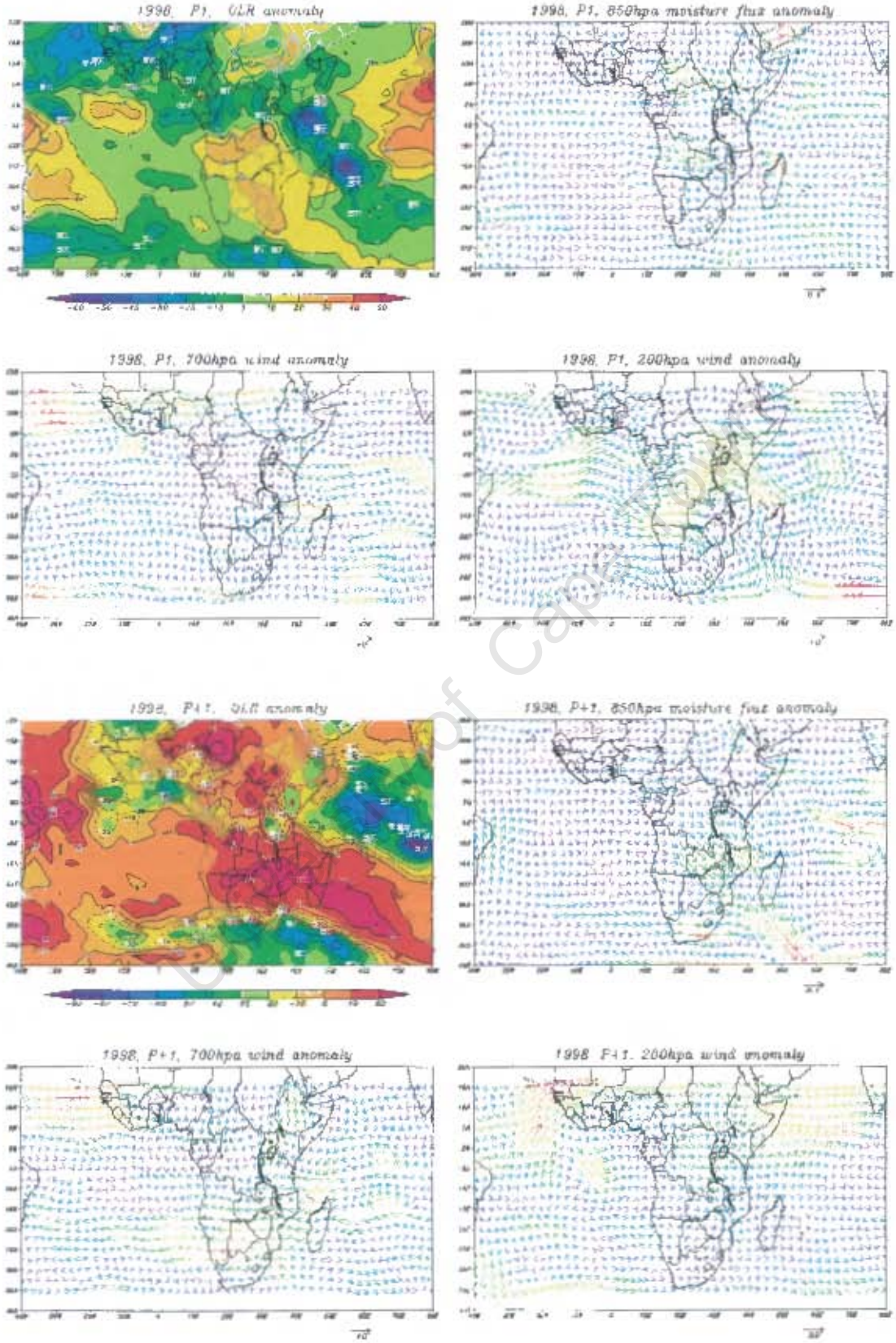

Figure 6.6d: As for figure 6.4a but for 1998 (MAM) P1 and P+1

Chapter 7: Summary and conclusion

The relationship between seasonal rainfall over East Africa with ENSO (El Niño Southern Oscillation), regional SST (Sea Surface Temperature) variability and the QBO (Quasi-Biennial Oscillation) has been documented in earlier studies (e.g. Indeje et al. 2000, Ogallo, 1988 etc). Relatively few investigators have considered the association of ENSO and rainfall over specific sub-regions of East Africa. The main aim of this research was to examine the time space evolution of the ENSO signal in tropical Indian Ocean, and to investigate the observed teleconnections with rainfall over the coastal regions of Tanzania, with the view of extracting main seasonal rainfall precursors during ENSO years. The Atlantic Ocean signal were considered but found to have no significant influence on the Tanzanian coastal rainfall and hence the emphasis was given to the Indian Ocean. This study also considered other patterns of interannual variability (e.g. the Indian Ocean zonal mode) that may influence coastal Tanzania rainfall. It was also aimed at investigating the nature of intraseasonal rainfall variability over coastal Tanzania and how this related to ENSO.

Using data from Tanzanian coastal stations, a rainfall index was formed and used to identify the rainfall characteristics of each ENSO year. Monthly anomalies of selected meteorological fields were analyzed for El Niño/La Niña composites and each event to determine the mechanisms associated with seasonal rainfall over the Tanzanian coast during ENSO years. The analyzed meteorological fields start two months prior to the onset of the rainfall season for potential predictive purposes. Time series plots of rainfall and wind were analyzed at intraseasonal time scale and the rainfall onset dates derived. Time-longitude or Hovmöller plots of bandpass filtered OLR, zonal winds at 850hPa and 200hPa levels, revealed the propagating nature and coupling of local circulations and convection.

The analysis of the monthly climatological fields for both OND and MAM season revealed that the rainfall observed over the Tanzanian coast was mainly

associated with the north-south migration of the ITCZ. Two peaks were evident, one in April when the ITCZ crosses the region on its way to the northern hemisphere. The other peak occurs in November when again the ITCZ crosses the region as it moves to the southern hemisphere. However, significant departures to these mean conditions occur during ENSO years. Scrutiny of the rainfall index for the north coast shows that all El Niño and El Niño+1 years were associated with above normal rainfall while La Niña and La Niña+1 years shows below normal rainfall. Similarly the Indian Ocean positive zonal mode years were observed to have above normal rainfall while Indian Ocean negative zonal mode years reported drier conditions. Signal over the South coast are mixed although most El Niño's led to wet OND there and most La Niña's are dry.

The scrutiny of the anomalies for selected meteorological fields indicates that above average rainfall during El Niño years is associated with the contrasting warm (cool) SST anomaly patterns coupled with the contrasting negative (positive) OLR anomalies in the western (eastern) equatorial Indian Ocean. Easterly wind and moisture flux anomalies occur over the equatorial eastern Indian Ocean with moisture flux convergence over the Tanzanian coast. The most remarkable feature, which enhances convergence over the Tanzanian coast during El Niño years, is the low level wind and moisture flux cyclonic anomaly southeast of Madagascar. The occurrence of the rising limb of the Indian Ocean Walker cell over equatorial western Indian Ocean was also an important feature for increased rainfall over the Tanzanian coast during El Niño years. Note that for the north coast, wet conditions of the OND season of the El Niño years are extended to the usually dry months of January and February of the El Niño+1 years. These conditions reverse during La Niña years and dry conditions persist over the Tanzanian north coast.

During the OND season, the south coast shows ENSO impacts more like the northern coast and the rest of East Africa. Easterly wind and moisture flux anomaly together with moisture flux convergence leads to significant rainfall during El Niño years. For La Niña years, dry conditions persist due to occurrence of moisture flux divergence over the south coast. On the other hand in JFM the south coast indicates a mixed ENSO signal with some wet and dry years occurring during both El Niño and La Niña. It appears that, for JFM, the south coast may be a transition region between the opposite signal impacts of southern Africa and East Africa.

During wet non-ENSO years when there is no zonal mode SST anomaly pattern in the equatorial Indian Ocean, the regional wind circulation patterns are important for determining the nature of the rainfall over the Tanzanian coast. Cyclonic wind and moisture flux anomaly closer to the Tanzanian coast leads to above average rainfall while anticyclonic circulations result in below average rainfall over the Tanzanian coast. Varying surface boundary forcing conditions over the region, including vegetation cover, soil moisture and topography may also be important during these years. However, the lack of high-resolution data, which can identify meso-scale factors, contribute to the difficulties in assessing this contribution and to improving seasonal forecasting.

On the intraseasonal time scale, the OLR and zonal wind Hovmöller plots revealed eastward and westward propagating as well as stationary features over the Indian Ocean. It was observed that the propagating features were absent during strong El Niño years while for strong La Niña years they are present. It is also found that the areas of large negative OLR anomalies (strong convection) couple well with areas of strong westerly anomalies in lower levels with strong easterly anomalies in the upper levels.

The rainfall time series revealed that increased rainfall during El Niño years was associated with an early onset while reduced rainfall during La Niña years was associated with late start of the season. The wind time series indicate that the increased rainfall during El Niño years was associated with low-level easterly anomalies during the onset of the rainfall season weakening towards the peak of the rain season. This situation implies enhanced moisture advection during the onset and moisture convergence during the peak. During La Niña years the reverse is true.

The climatological plots at intraseasonal time scale confirm the association of Tanzanian coast rainfall with the migration of the ITCZ. The peak of the rainfall season is found to occur while the ITCZ is over the region. Similarly, increased rainfall during El Niño years was observed to be associated with enhanced convection and moisture flux convergence over the Tanzanian coast with reverse during La Niña years. The wet conditions of the OND season of the El Niño onset years are extended to the usually dry months of January and February of the post mature phase El Niño year. A good example is 1997/98, which was the strongest event during the period of study.

In conclusion, the association of ENSO with seasonal rainfall over the Tanzanian coast has been clarified in this thesis. However, ENSO explains about 50% of the East African rainfall variance, with other factors explaining the remaining variance (Ogallo, 1988). This thesis focuses on the association of the Tanzanian coast rainfall with ENSO. Future work may look at other factors explaining the remaining 50% variance. Further detailed study could consider the physical and dynamical changes over the Indian Ocean associated with prolonged wet and dry spells over the Tanzanian coast. This will be a step towards finding statistical patterns and predictors for intraseasonal rainfall, which is important for planning of agricultural activities. Another important question to be considered in a future

study involves clarifying the complex ENSO signals over the south coast for the JFM season.

For predictive purposes, SST anomalies, OLR anomalies, wind and moisture flux anomalies over the equatorial Indian Ocean are able to show a distinctive differences between the dry and wet periods.

Some weaknesses of the present study should however, be mentioned. The NCEP re-analyses and CMAP data used in this study are of short duration and hence possible decadal variability has not been significantly identified. The CMAP rainfall data is available from 1979 hence there were no rainfall plot for ENSO years, which occurred before 1979. NCEP re-analyses are at 2.5° resolution and may not necessarily represent the details of SST, topography, soil and vegetation. Also, these re-analyses may not have as many local observations available for assimilation compared to other regions, and this may, potentially reduce the accuracy.

This thesis has contributed to the understanding of the association of ENSO with rainfall over the Tanzanian coast. It is revealed from this study that the ENSO signal for the southern coast of Tanzania is disorganized due to the fact that the region lies in the transition zone between southern Africa and equatorial East Africa, which have contrasting ENSO impacts. Evidence of intra-seasonal variability signals have been examined in this study, which have not been considered in earlier studies work.

A detailed study of the physical and dynamical changes over the Indian Ocean associated with prolonged wet and dry spells over the Tanzanian coast is required. To do so, will require application of atmospheric and ocean models. The knowledge thereby gained will lay facilitation for the formulation of intraseasonal rainfall prediction models.

APPENDIX A

PENTAD	MONTH	DATE	PENTAD	MONTH	DATE
01	JAN	01-05	38	JUL	05-09
02	JAN	06-10	39	JUL	10-14
03	JAN	11-15	40	JUL	15-19
04	JAN	16-20	41	JUL	20-24
05	JAN	21-25	42	JUL	25-29
06	JAN	26-30	43	JUL-AUG	30-03
07	JAN-FEB	31-04	44	AUG	04-08
08	FEB	05-09	45	AUG	09-13
09	FEB	10-14	46	AUG	14-18
10	FEB	15-19	47	AUG	19-23
11	FEB	20-24	48	AUG	24-28
12	FEB-MAR	25-01	49	AUG-SEPT	29-02
13	MAR	02-06	50	SEPT	03-07
14	MAR	07-11	51	SEPT	08-12
15	MAR	12-16	52	SEPT	13-17
16	MAR	17-21	53	SEPT	18-22
17	MAR	22-26	54	SEPT	23-27
18	MAR	27-31	55	SEPT-OCT	28-02
19	APR	01-05	56	OCT	03-07
20	APR	06-10	57	OCT	08-12
21	APR	11-15	58	OCT	13-17
22	APR	16-20	59	OCT	18-22
23	APR	21-25	60	OCT	23-27
24	APR	26-30	61	OCT-NOV	28-01
25	MAY	01-05	62	NOV	02-06
26	MAY	06-10	63	NOV	07-11
27	MAY	11-15	64	NOV	12-16
28	MAY	16-20	65	NOV	17-21
29	MAY	21-25	66	NOV	22-26
30	MAY	26-30	67	NOV-DEC	27-01
31	MAY-JUN	31-04	68	DEC	02-06
32	JUN	05-09	69	DEC	07-11
33	JUN	10-14	70	DEC	12-16
34	JUN	15-19	71	DEC	17-21
35	JUN	20-24	72	DEC	22-26
36	JUN	25-29	73	DEC	27-31
37	JUN-JUL	30-04			

APPENDIX B

Analysis of each ENSO year.

Because of the tendency for composites being biased towards stronger events, a case-by-case examination of ENSO years composited for the OND season is performed here.

Each El Niño year

Scrutiny of each El Niño year reveals that except for 1986 all composited years were also positive Indian Ocean zonal mode years. Those El Niño years occurring within the study period (1970-1999), which were not composited due to insignificant rainfall anomaly values (<1) were non Indian Ocean zonal mode years. This implies that the positive Indian Ocean zonal mode may amplify the El Niño signal over Tanzania. Analysis under this section will attempt to find out why these other El Niño years were not significantly wet. For brevity only the monthly anomaly fields for the rainfall peak in November will be presented. However, the anomaly fields for October 1986, 1990 and 1995 were significantly different from composites and will also be presented.

Monthly anomaly fields for each composited El Niño year during the peak of the OND rainfall season in November are shown in figures A1-A5. Scrutiny of these years indicate that almost all the meteorological fields are more or less similar to the El Niño composites. Warming occurs over the western Indian Ocean with enhanced moisture flux convergence throughout the rainfall season. However in October 1986 (fig D1) the SST and low-level wind anomaly patterns indicate a significant departure from the El Niño composite. Cool SST anomalies extend over much of the equatorial Indian Ocean with low-level westerly wind anomalies between the equator and 5°N. Negative latent heat flux anomalies occur over much of Tanzania with moisture flux divergence over the Tanzanian coast consistent with below average rainfall observed. This year was wet during

November and December resulting into significant rainfall in the seasonal total, and thus this year was included in the composites. It appears that the Indian Ocean signal in 1986 begin later than for other years.

Figures B1-B2 indicates November monthly anomaly fields for 1990 and 1991, which were El Niño years with less than one standard deviation rainfall anomaly and hence not included in the composite. Comparison of these years with El Niño composites indicates that 1990 and 1991 were significantly wet during November only, which resulted in insignificant rainfall anomaly in the seasonal total while El Niño composites indicate wet conditions throughout the rainfall season.

During the onset of the short rainfall season in October both 1990 and1991 experience dry conditions. In October1990 (fig D2), negative SST anomalies were located at about 55°E over the equatorial western Indian Ocean while closer to the Tanzanian coast positive SST anomalies exist. The low level wind and moisture flux anomaly plots show a cyclonic anomaly centered at about 5°S and 65°E. This circulation is associated with moisture flux convergence mainly over the Kenyan coast where above average rainfall was observed. However, the Tanzanian coast experienced dry conditions.

In October 1991 (not shown), warm SST anomalies occurred over much of the equatorial western Indian Ocean. Strong westerly wind anomalies extended over much of the equatorial western Indian Ocean in the lower and middle levels. The 850hPa moisture flux anomaly plot shows a cyclonic moisture flux anomaly northeast of Madagascar with enhanced westerly moisture flux anomalies over the entire East African coast. Southerly moisture flux anomalies advected moisture from the South West Indian Ocean towards the Tanzanian southern coast where significant rainfall occurred. Dry conditions occurred over the Tanzanian northern coast due to the dominance of westerly moisture flux anomalies.

It is evident from the above discussion that each year indicates different SST and wind anomaly patterns that led to dry conditions. It was further observed that wind anomaly patterns are more important for modulating Tanzanian coast rainfall rather than SST alone. Warm SST anomalies closer to the Tanzanian coast coupled with easterly (westerly) wind anomalies leads to wet (dry) conditions. The above average rainfall revealed in the El Niño composite resulted from warm SST anomalies closer to the Tanzanian coast with enhanced easterly wind and moisture flux anomalies over much of the equatorial western Indian Ocean.

At the peak of the short rainfall season in November both 1990 and 1991 observed wet conditions. In November 1990 (fig B1), the SST anomaly plot indicates a significant departure from the El Niño composites. Negative SST anomalies extend over the equatorial western Indian Ocean closer to the Tanzanian coast. However, above average rainfall occurred mainly due to increased evaporation near the coast and easterly wind and moisture flux anomalies over the region.

In November 1991 (fig B2), warm SST anomalies extend over much of the equatorial western Indian Ocean. However, the SST anomalies are weaker compared to the El Niño composites, with a pool of cool SST anomalies closer to the Tanzanian coast. The moisture flux anomaly plot indicates a slight westward shift of the cyclonic moisture flux circulation northeast of Madagascar with enhanced easterly moisture flux anomaly over much of Tanzania and the equatorial western Indian Ocean between the equator and 10°N. Enhanced evaporation occurred offshore for the north coast. These circulations led to above average rainfall observed over the Tanzanian coast.

Again each year indicates its own SST, wind and moisture flux anomaly patterns, which led to above average rainfall. Significant rainfall observed in the El Niño composite resulted from both positive SST anomalies over the equatorial western Indian Ocean and moisture flux convergence over the Tanzanian coast.

Towards the withdrawal of the short rainfall season in December (not shown) both 1990 and 1991 observed cool SST anomalies and moisture flux divergence over the Tanzanian northern coast, which resulted in reduction of rainfall. The significant above average rainfall observed in the El Niño composite resulted from warm SST anomalies over much of the equatorial western Indian Ocean, strong easterly low-level wind anomalies along the equator with enhanced moisture flux convergence over the Tanzanian coast.

In summary, 1990 and 1991 were insignificantly wet since the El Niño signal was not coherent over the Indian Ocean during these years. The other protracted El Niño years of 1992, 1993 have not been considered as they produced below average rainfall over the north coast in OND. During the positive Indian Ocean zonal mode years (e.g. 1994), the El Niño signal over the equatorial western Indian Ocean is amplified with warming over the region throughout the rainfall season. Therefore the El Niño signal which leads to significantly above average rainfall over the Tanzanian coast is the one which manifest itself with significant warming over the equatorial western Indian Ocean and significant easterly anomalies over the central and eastern tropical Indian Ocean.

Each La Niña year

Scrutiny of each La Niña year composited reveals that 1970 and 1998 were negative Indian Ocean zonal mode years; however the rainfall anomalies are similar to other Indian Ocean non-zonal mode La Niña years. This suggests that the negative Indian Ocean zonal mode may have less significant effect on La Niña signal than the positive phase on the El Niño signal. The rainfall anomaly

value for 1995 was less than 1 standard deviation and hence 1995 was not included in the composite. It was shown that October 1995 was a wet month, which led to insignificant dry conditions over the seasonal total. All La Niña years composited were dry throughout the rainfall season and the anomaly fields are more or less similar to the La Niña composites except for 1988 where wet conditions was observed in December mainly over the southern coast. Under this section further analysis of 1995 was carried out to establish the reasons why it was not significantly dry. The meteorological fields will be contrasted with the La Niña composite during the rainfall season.

Figures C1-C5 illustrates November anomaly fields for each composited La Niña year. Scrutiny of these years indicates that almost all the meteorological fields are more or less similar to the La Niña composite. However in December 1988 (not shown), some of the meteorological fields indicate a significant departure from the La Niña composite. Warm SST anomalies occur over much of the equatorial western Indian Ocean with easterly wind anomalies in the lower and middle levels. Positive latent heat flux anomalies and negative OLR anomalies occur over the equatorial western Indian Ocean closer to the Tanzanian coast together with easterly moisture flux anomaly. This situation led to above average rainfall observed over much of the southern coast of Tanzania in December 1988.

Figures D3 and D4 indicate November anomaly fields for 1995, which was a La Niña year with less than one standard deviation rainfall anomaly over the Tanzanian coast and hence not included in the composite. During the onset of the short rainfall season in October 1995 (fig D3), positive SST anomalies cover much of the Indian Ocean and extend to the Tanzanian coast. Easterly moisture flux anomalies exist over the equatorial western Indian Ocean backing to southerly moisture flux anomaly over the Kenyan coast and decelerating towards the Tanzanian coast. Positive latent heat flux anomalies extend over the

Tanzanian coast consistent with above average rainfall observed. However in the La Niña composite the below average rainfall arises from cool SST anomalies over the equatorial western Indian Ocean, negative latent heat flux anomalies over the Tanzanian coast and westerly moisture flux anomalies over much of the equatorial western Indian Ocean.

At the peak of the short rainfall season in November, both 1995 and La Niña composite are characterized by below average rainfall. In November 1995 (fig D4), almost all the meteorological fields indicate similar patterns as the La Niña composite except the pool of warm water closer to the Tanzanian coast. Below average rainfall observed in both 1995 and the La Niña composite resulted from the occurrence of negative SST anomalies with strong westerly wind and moisture flux anomalies over the equatorial western Indian Ocean. The continental negative latent heat flux anomalies with moisture flux divergence over the Tanzanian coast are consistent with dry conditions.

Towards the withdrawal of the short rainfall season in December, again both 1995 and the La Niña composite observe below average rainfall. However the patterns which led to these dry conditions are different in1995 compared to the La Niña composite. In December 1995 (not shown), positive SST anomalies extend over much of the equatorial western Indian Ocean with low-level easterly wind and moisture flux anomalies along the equator. However, below average rainfall was observed over the Tanzanian coast due to suppressed evaporation from the source regions of these easterly anomalies and negative latent heat flux anomalies over much of Tanzania. This was in contrast to the La Niña composite which shows negative SST anomalies over the equatorial western Indian Ocean and low-level westerly wind anomalies along the equator.

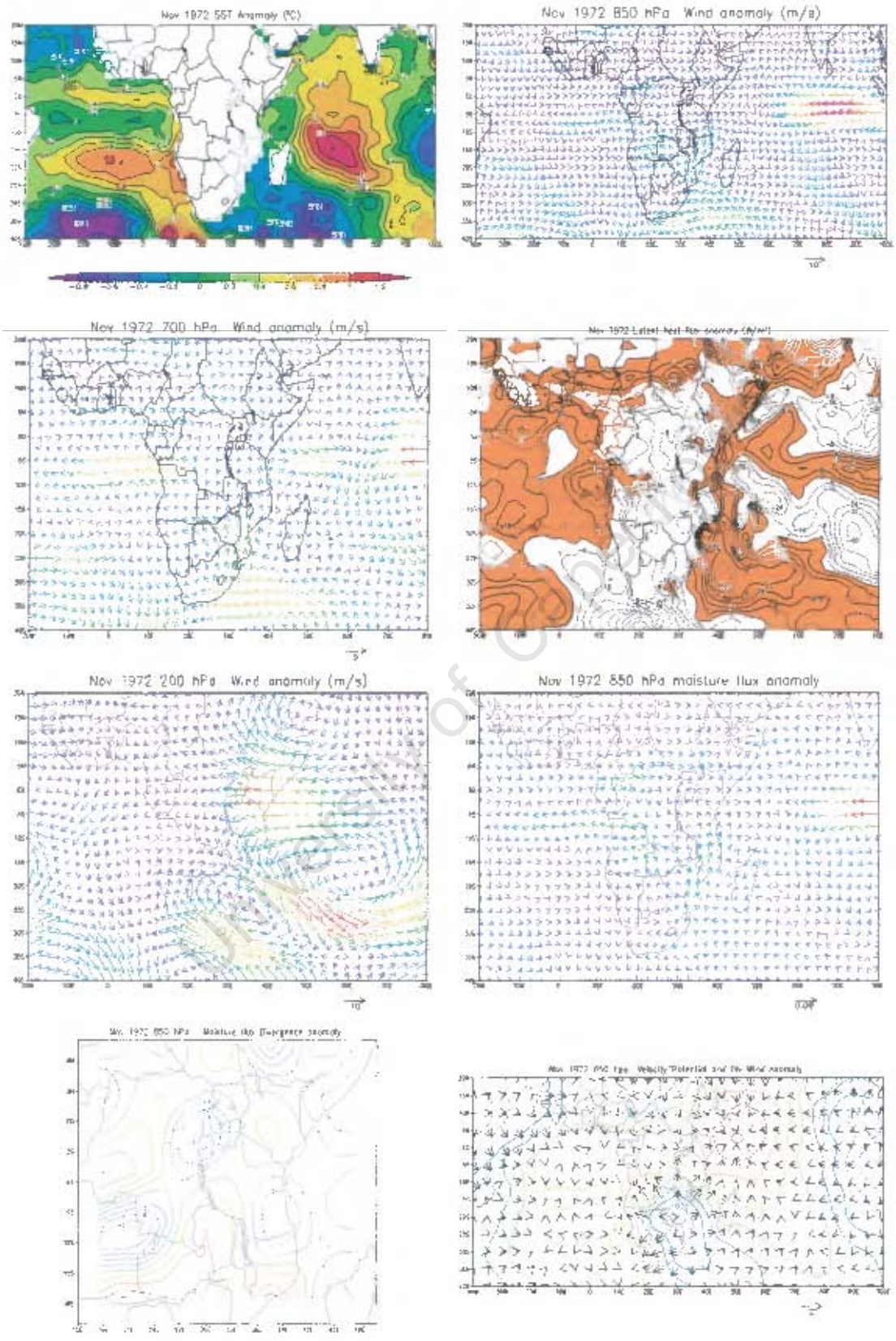

Figure A1: November anomaly fields for El Niño year 1972
Moisture flux in g/kg.m/s, Velocity potential ($m^2\ s^{-1}$)
Divergent wind (s^{-1})

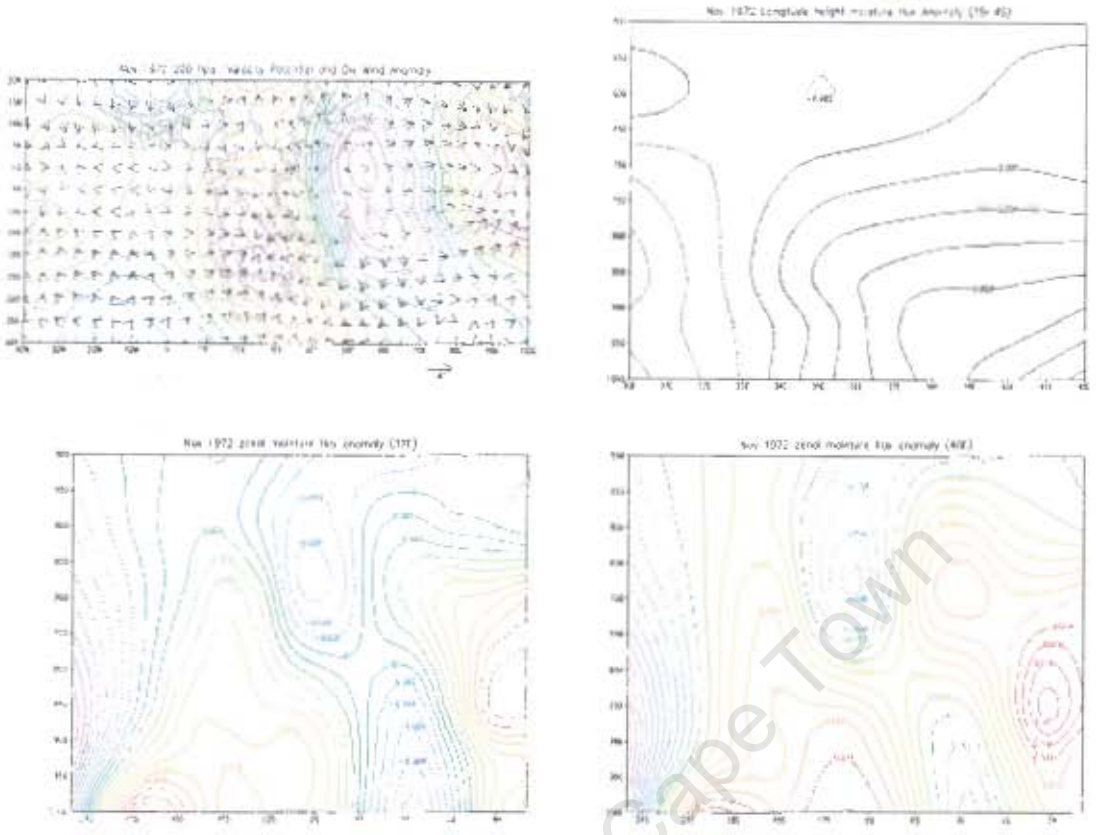

Figure A1 continue

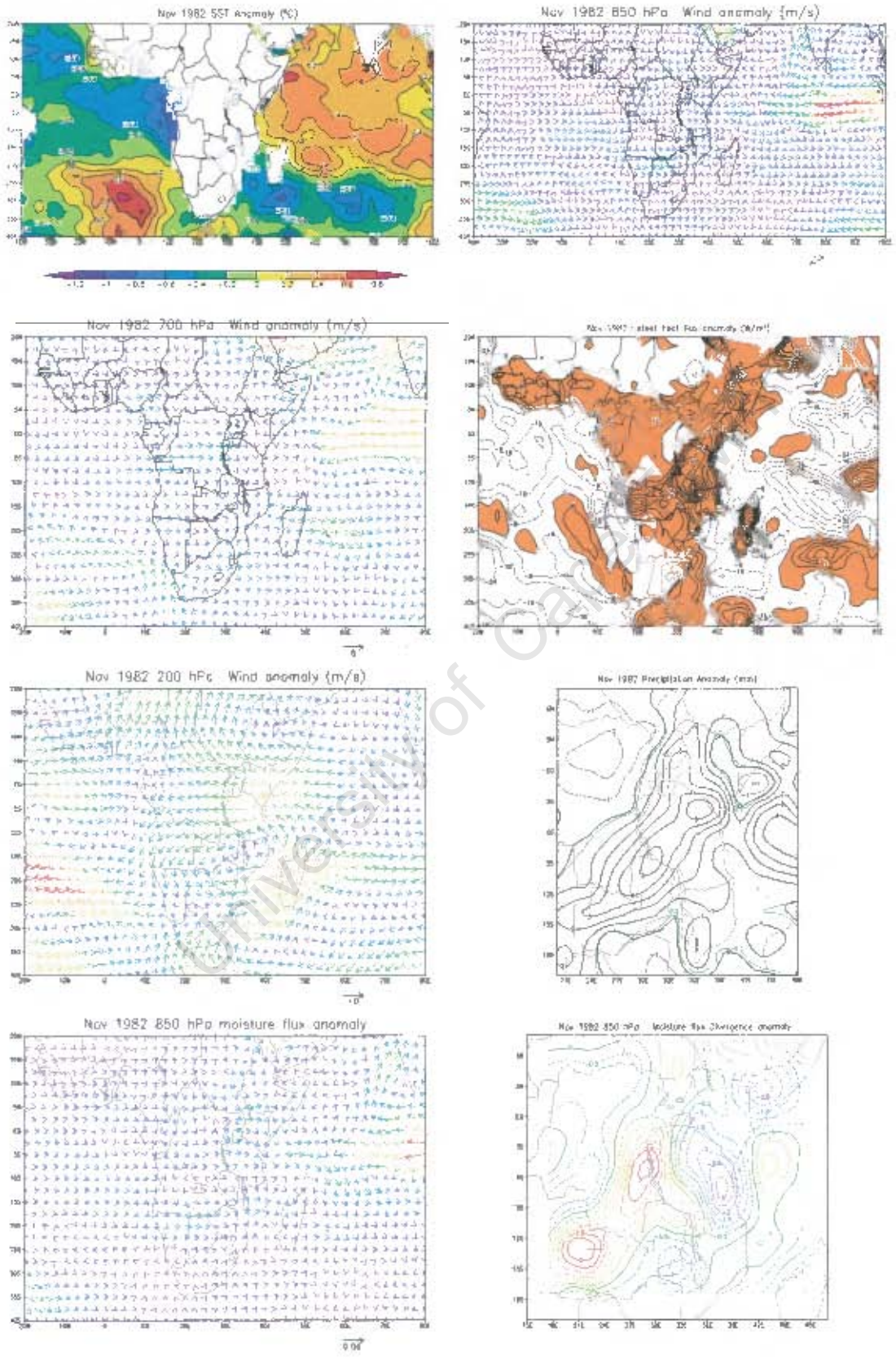

Figure A2: As for fig A1 but for 1982

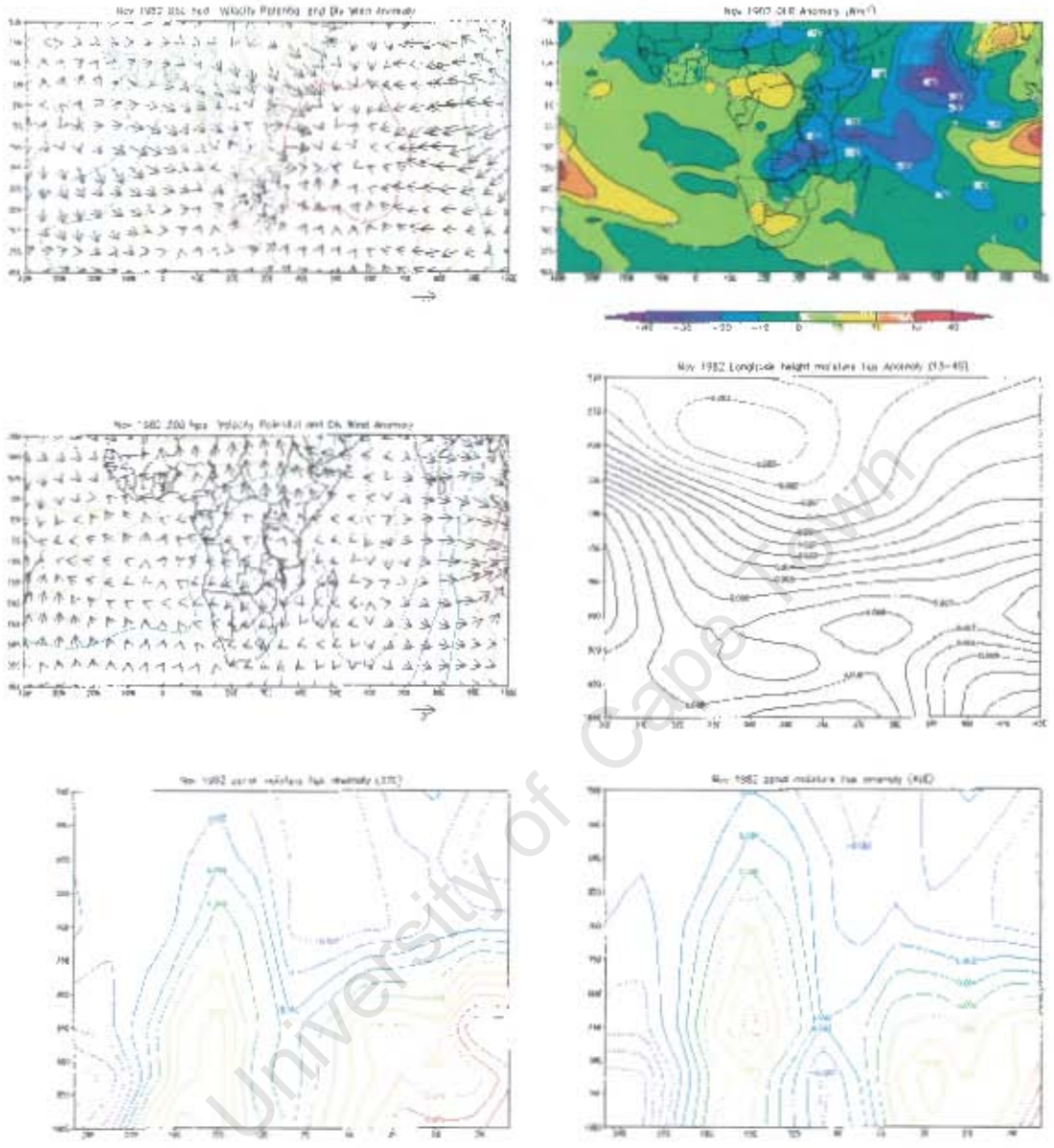

Figure A2 continue

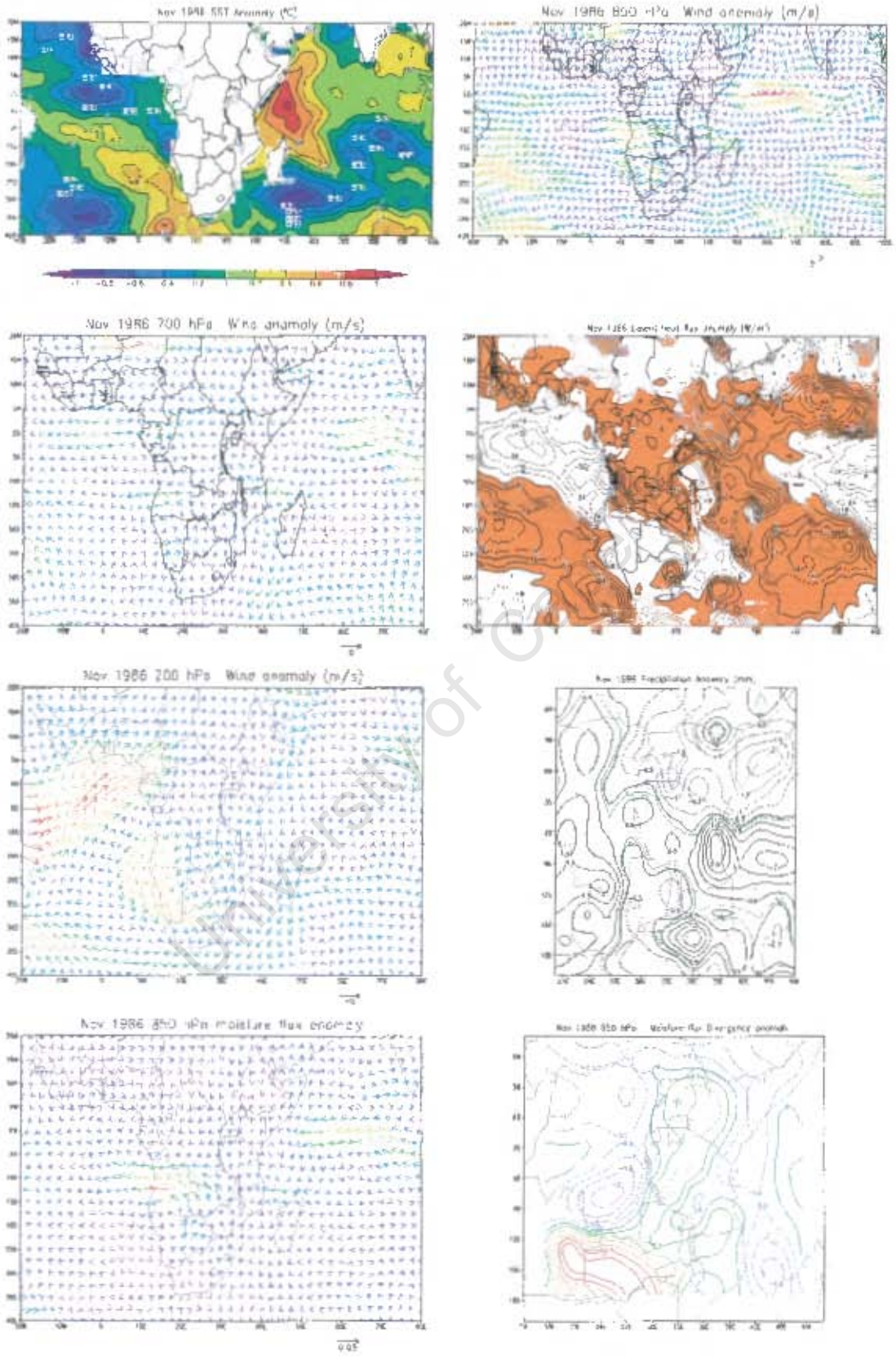

Figure A3: As for figure A1 but for 1986

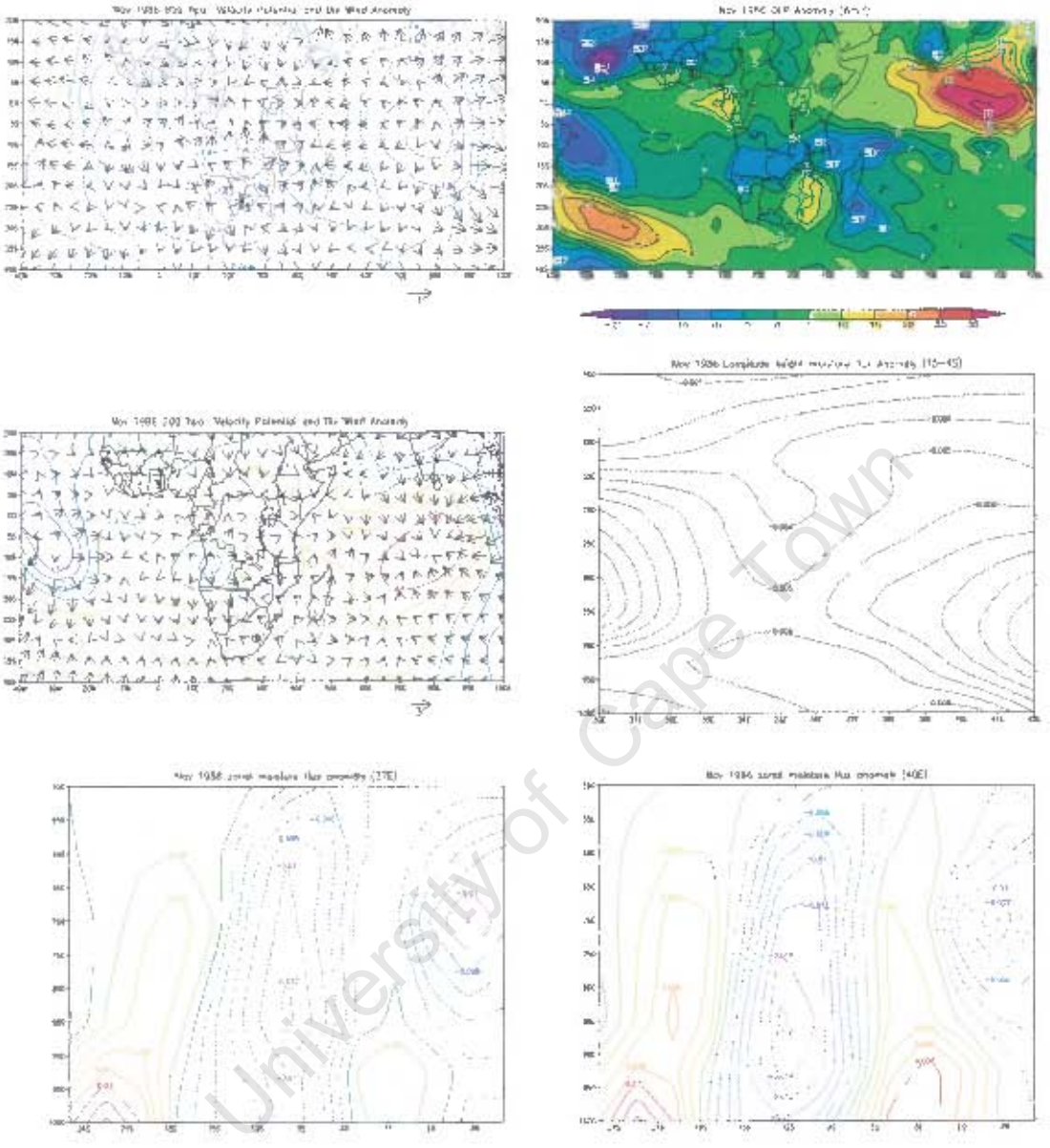

Figure A3 continue

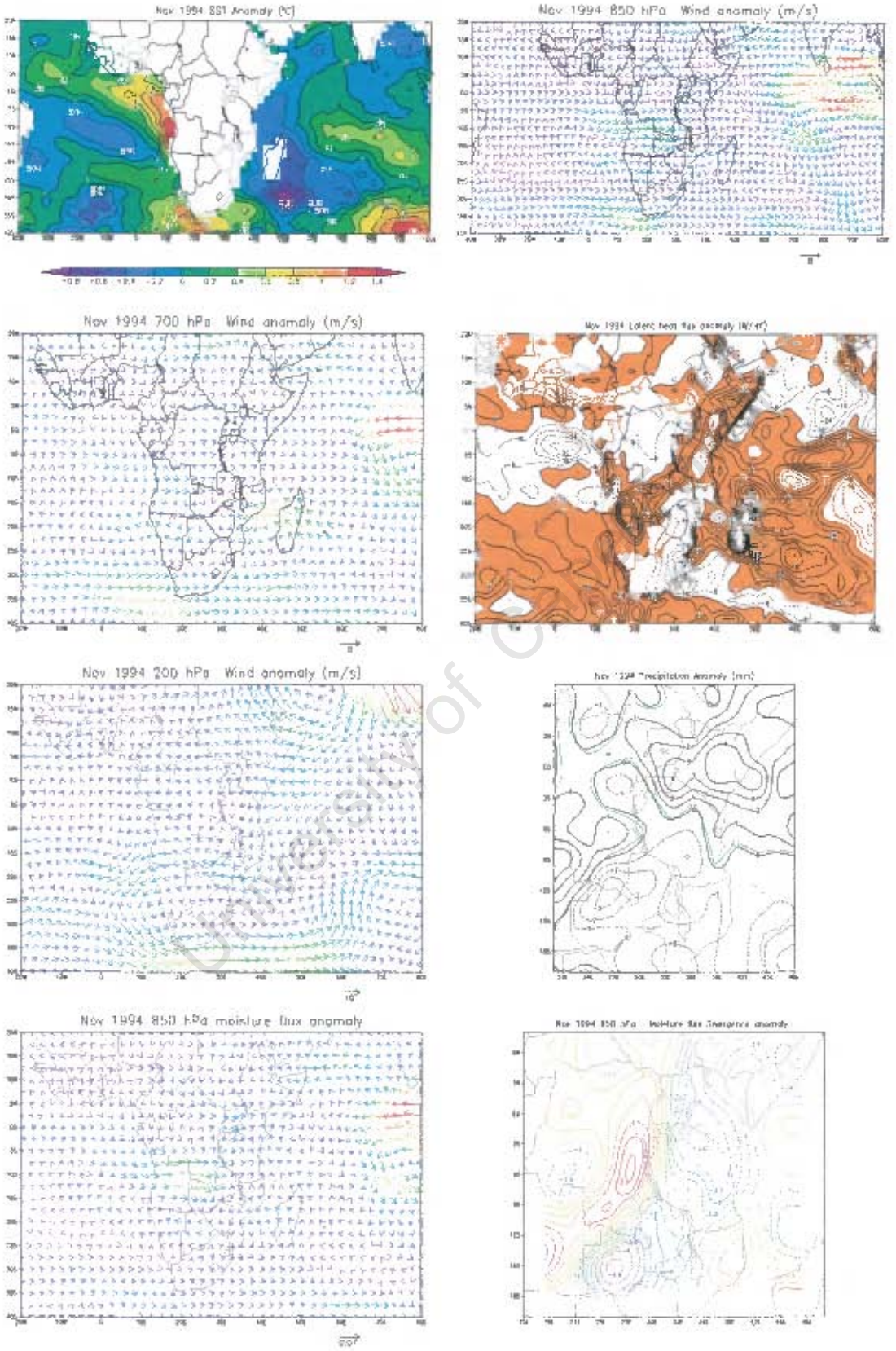

Figure A4: As for figure A1 but for 1994

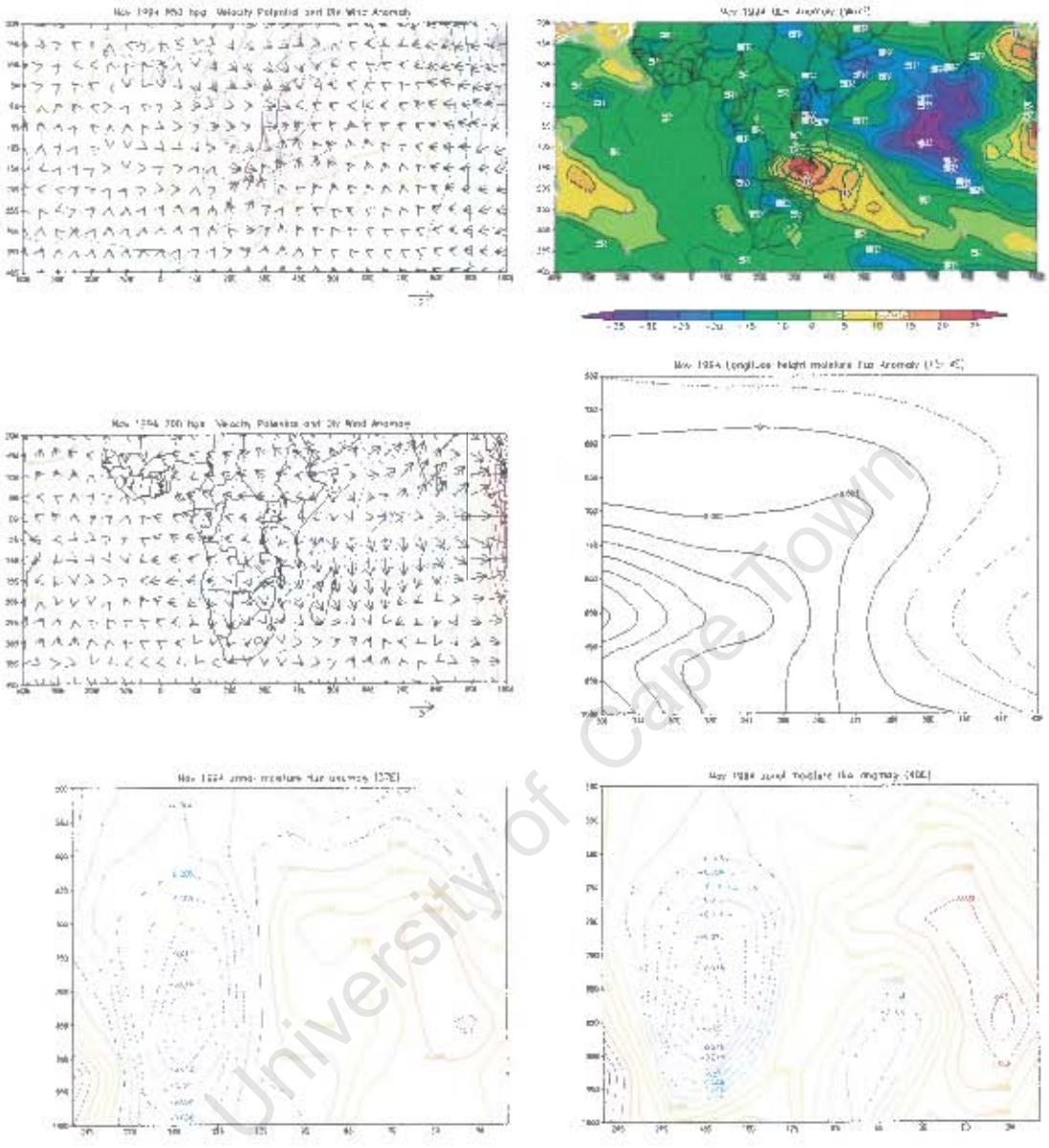

Figure A4continue

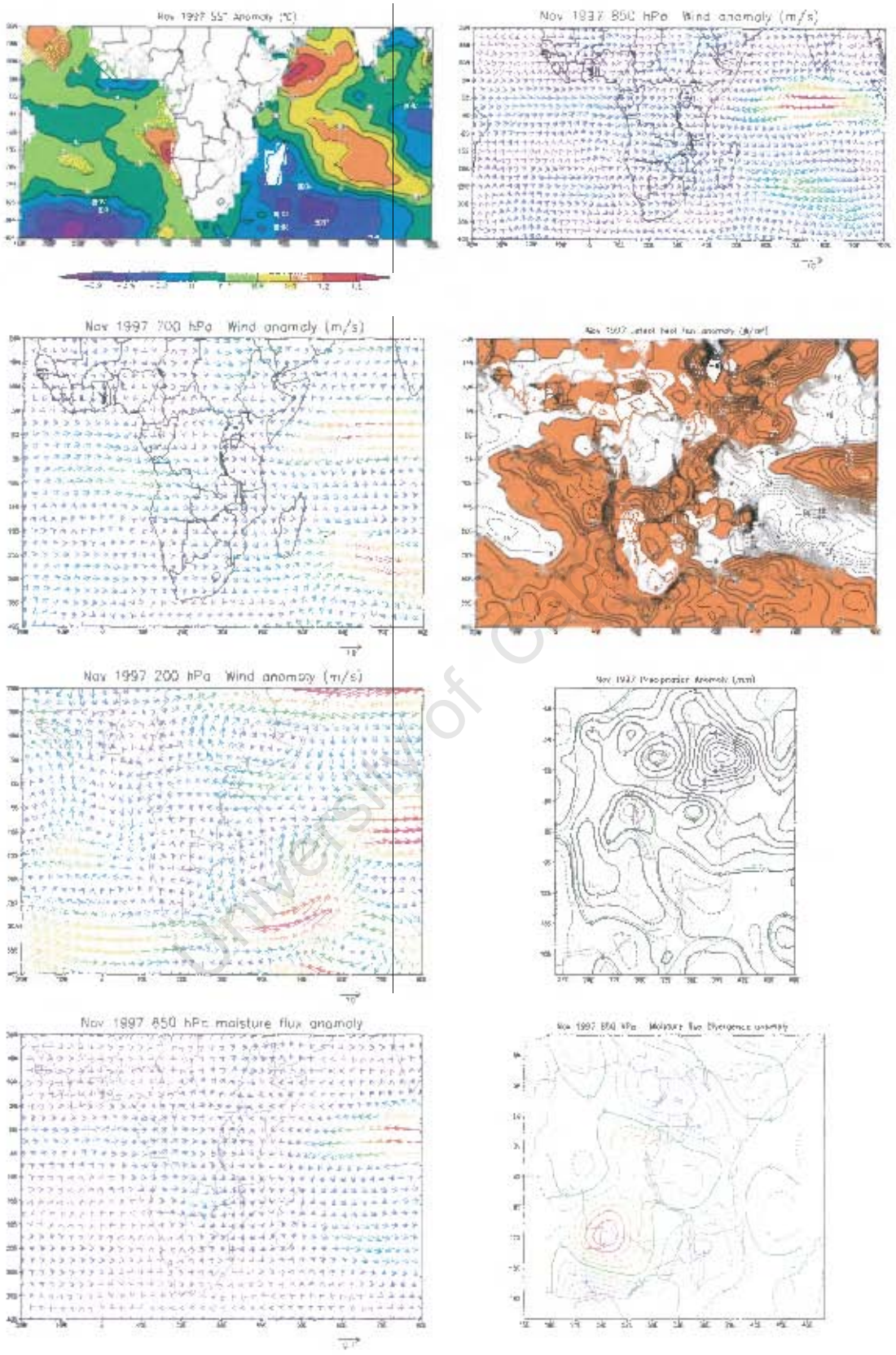

Figure A5: As figure A1 but for 1997

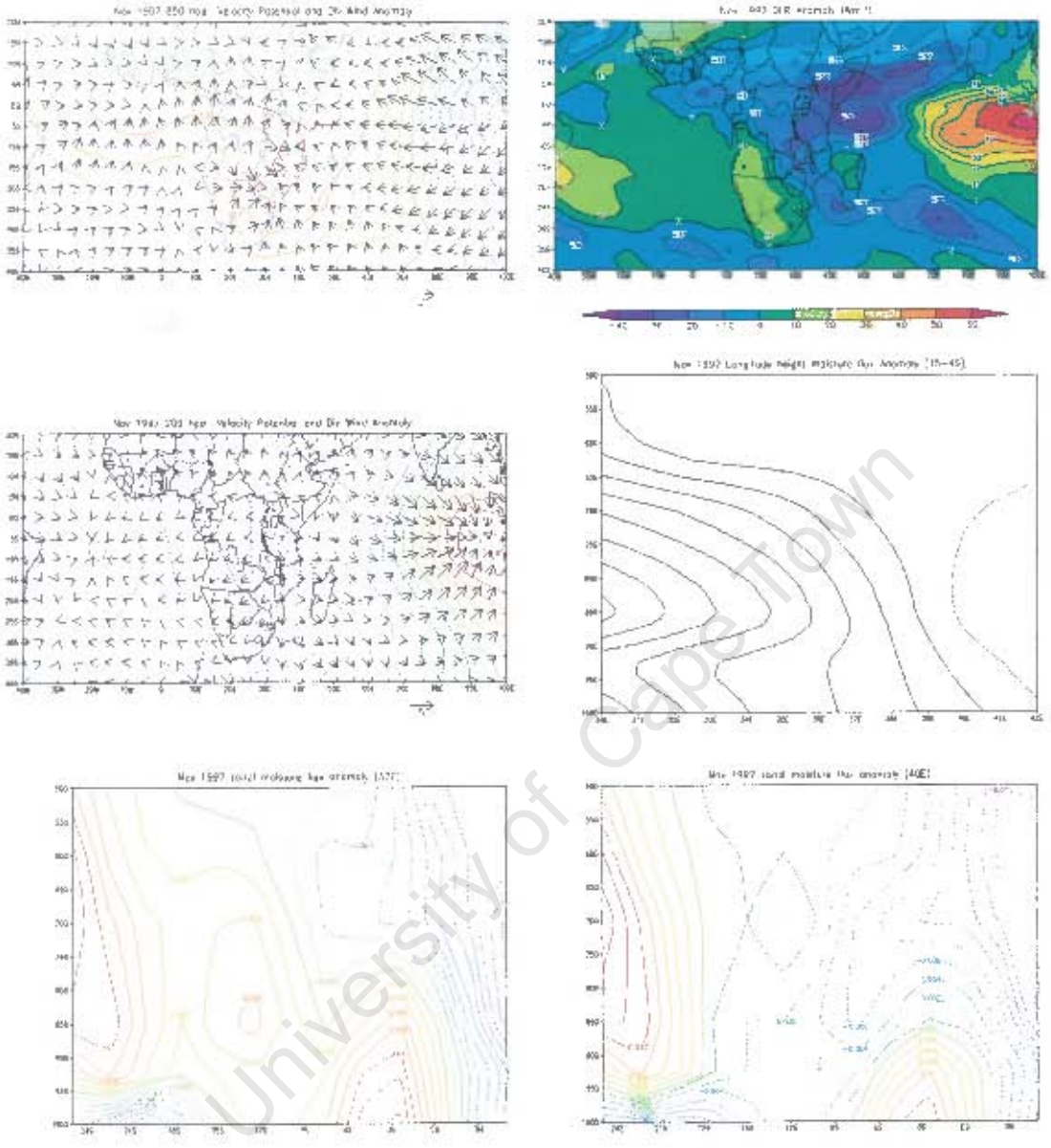

Figure A5 continue

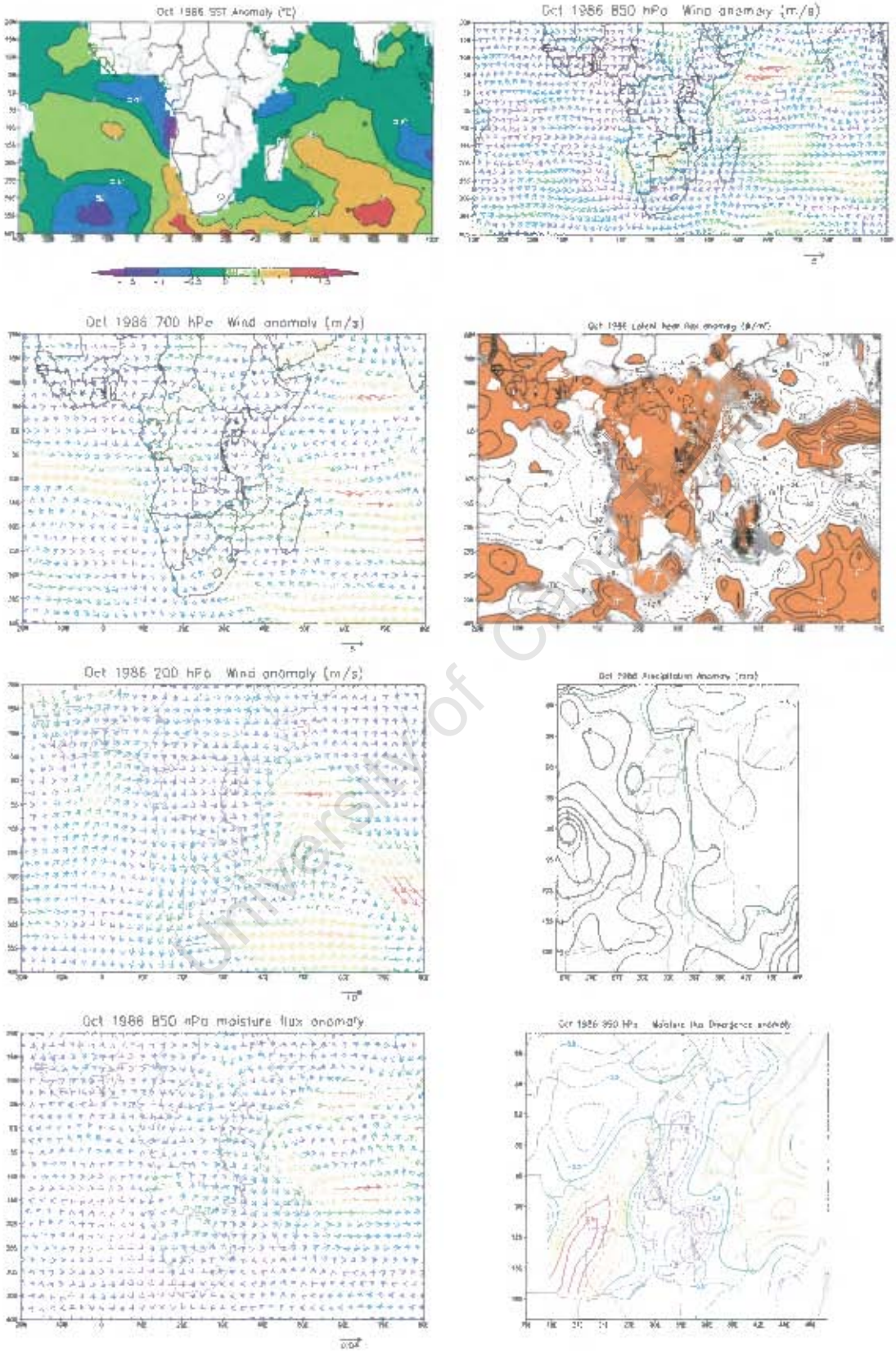

Figure D1: As for figure A1 but for October 1986.

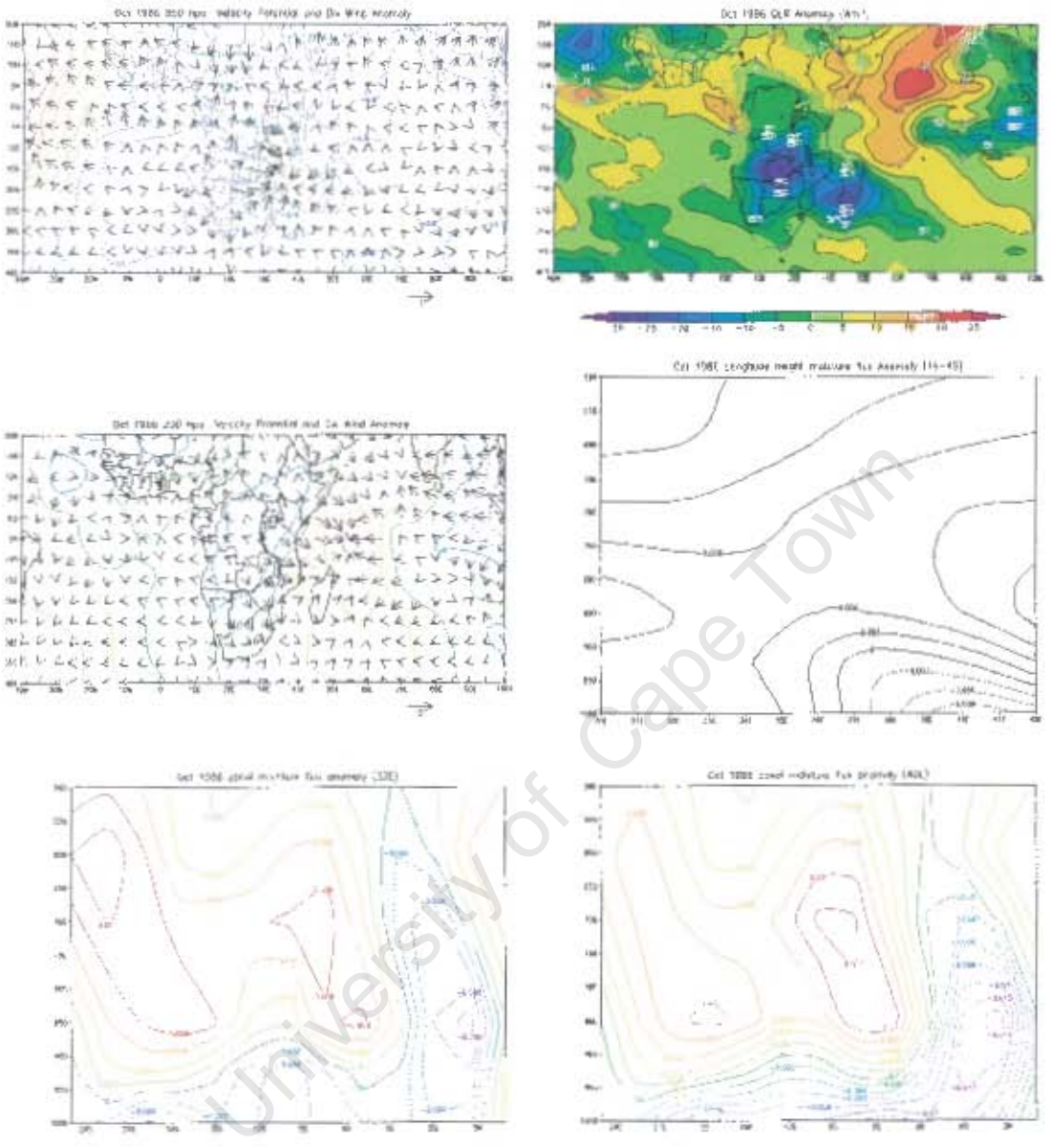

Figure D1 continue

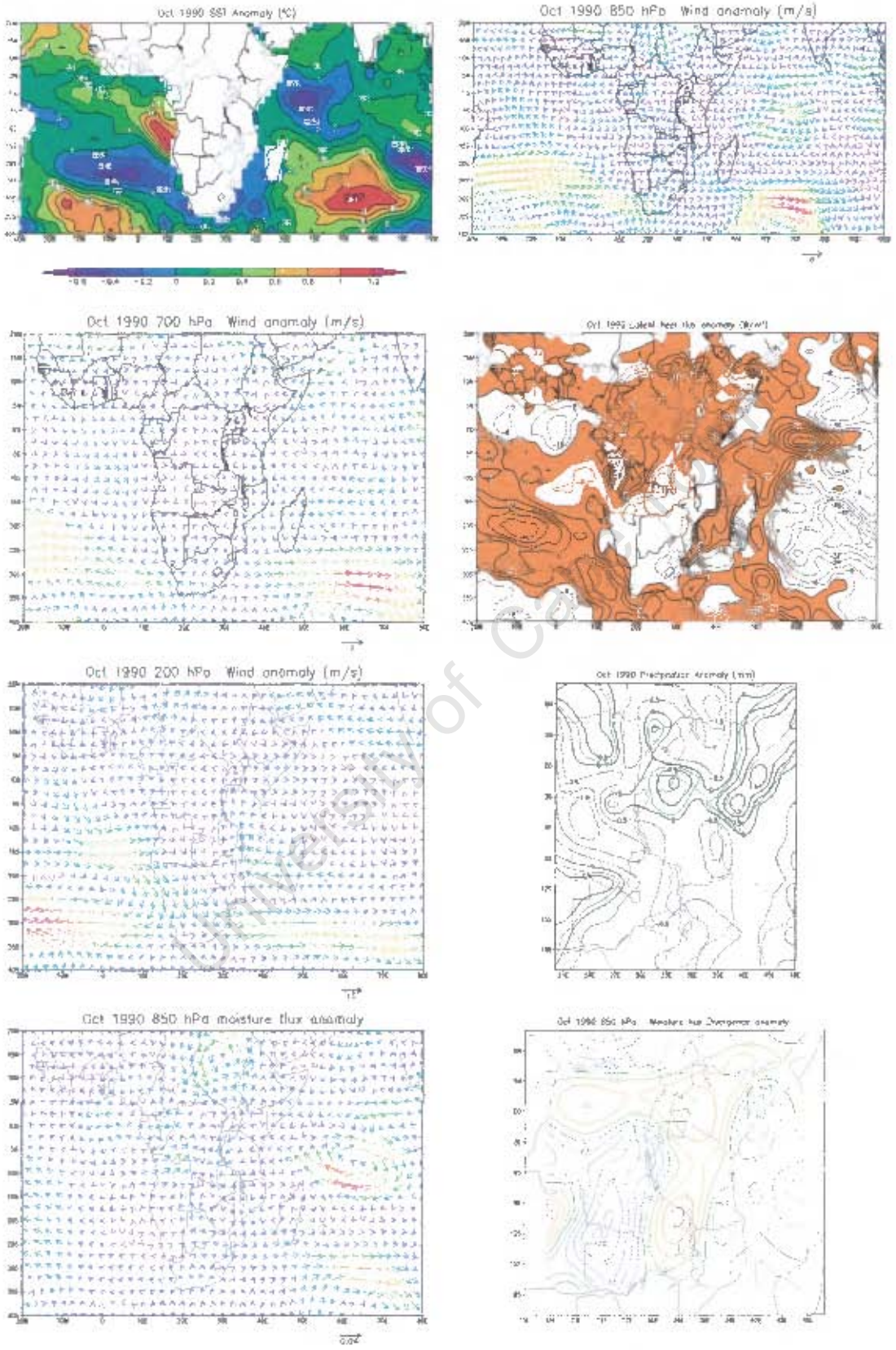

Figure D2: As for figure A1 but for October 1990

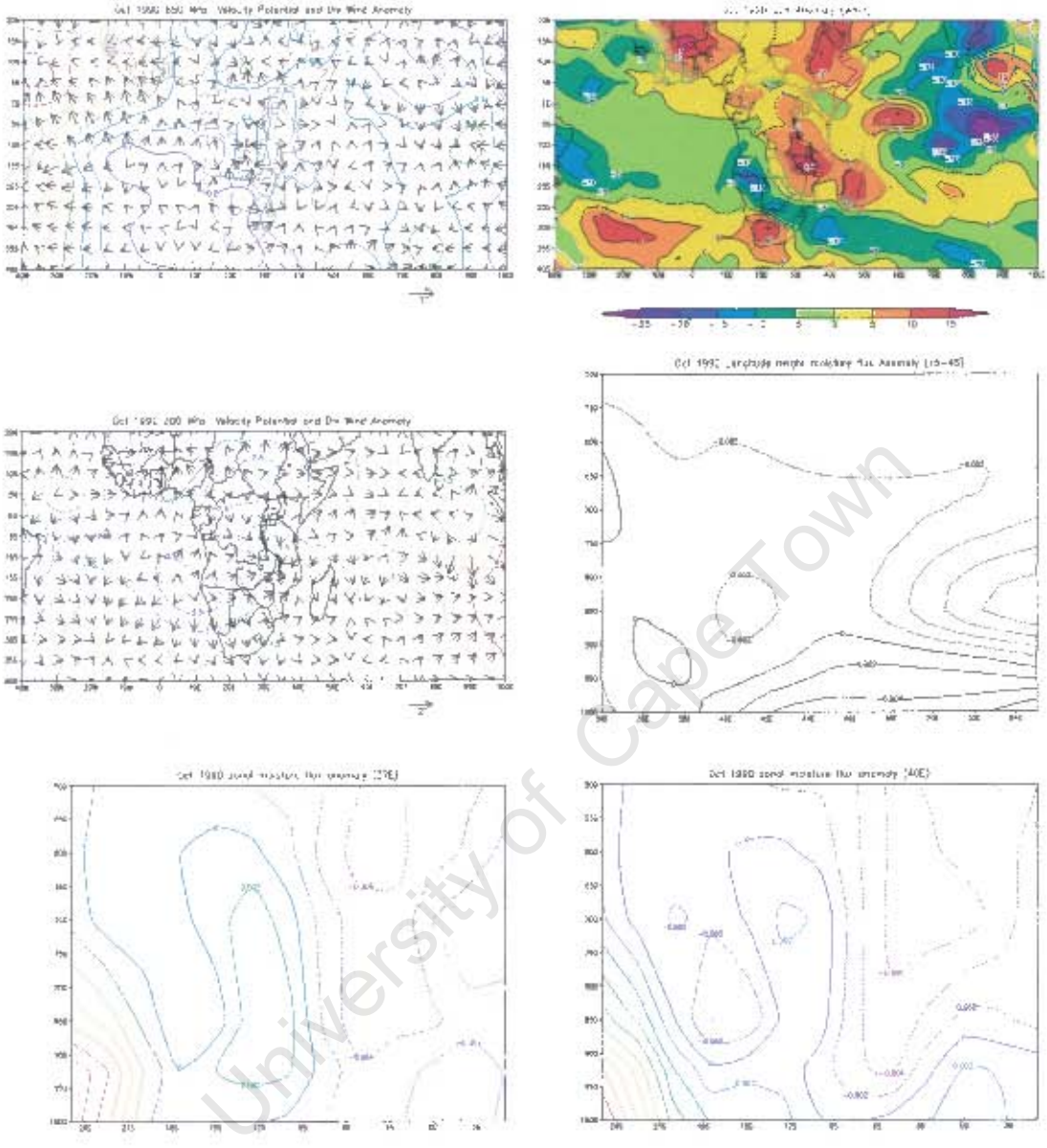

Figure D2 Continue

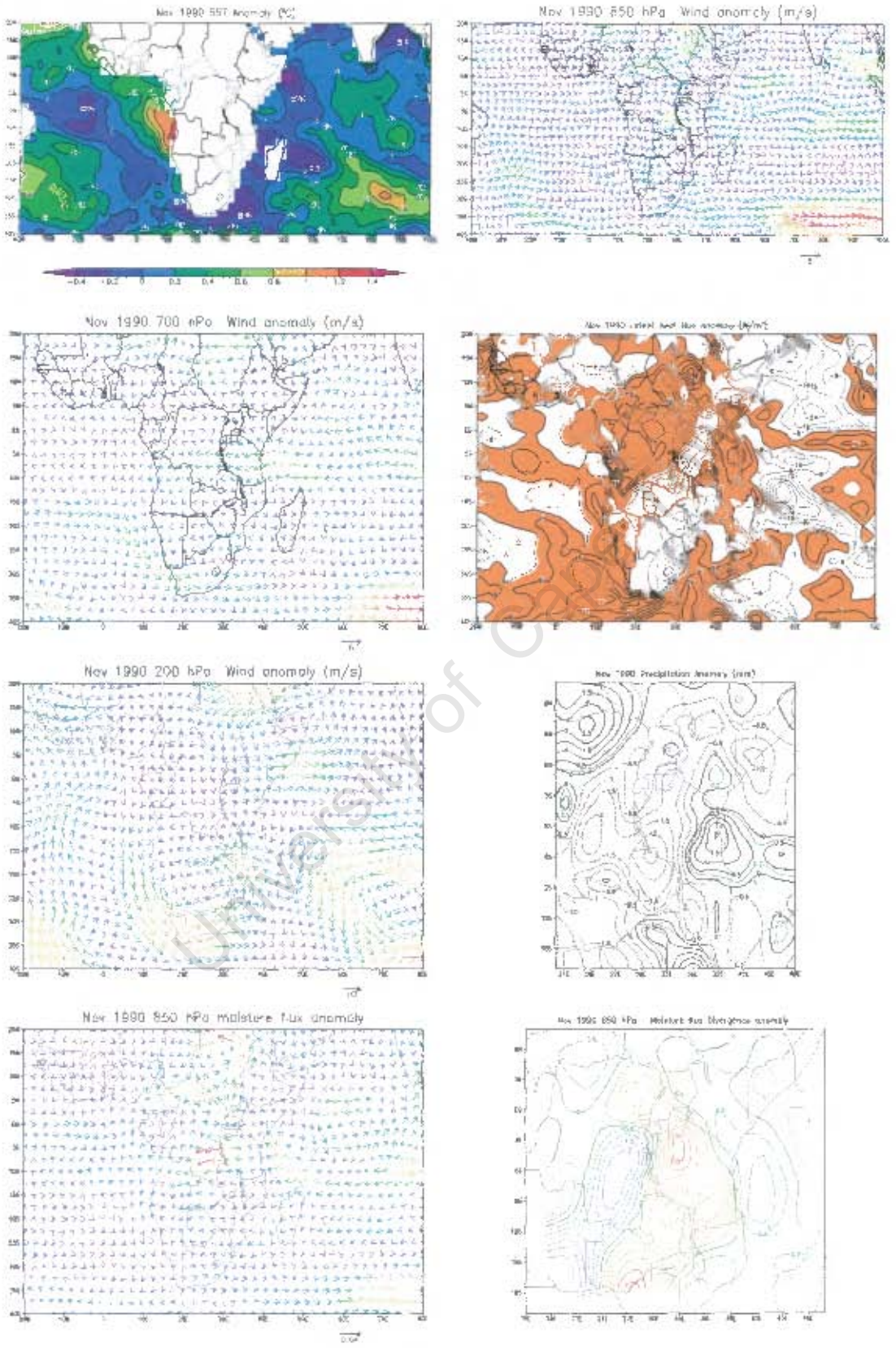

Figure B1: As for A1 but for 1990

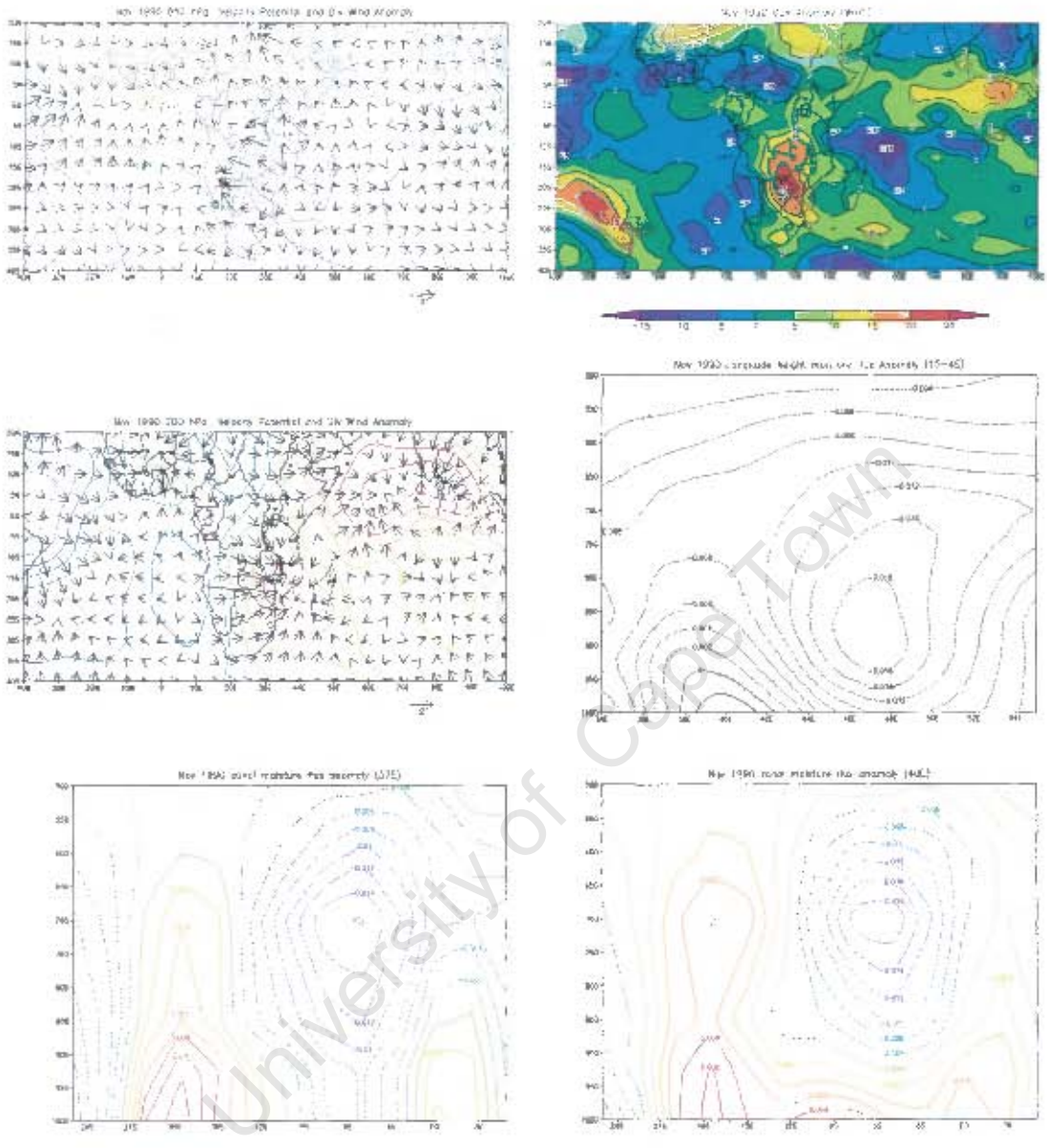

Figure B1 continue

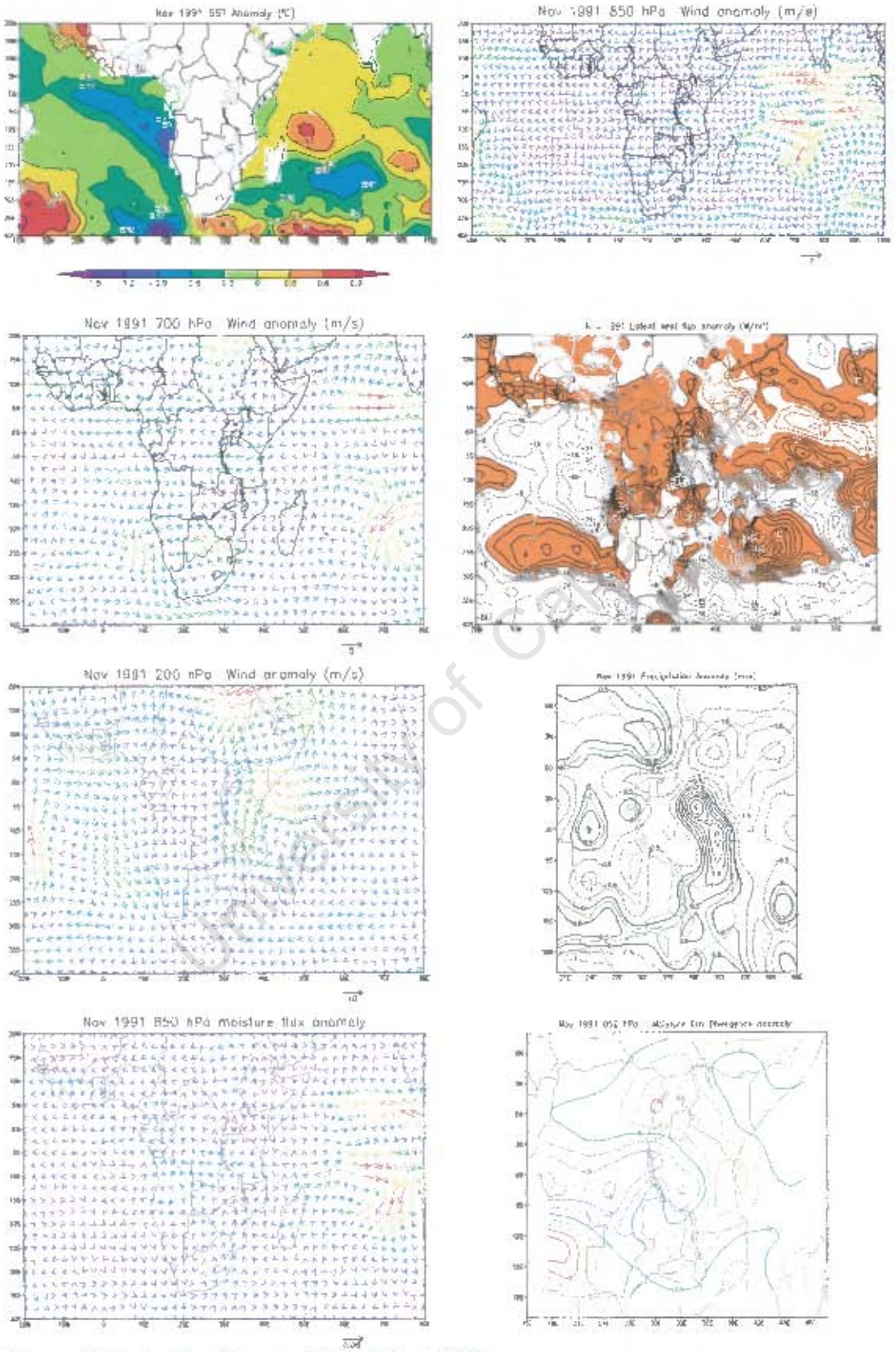

Figure B2: As for figure A1 but for 1991

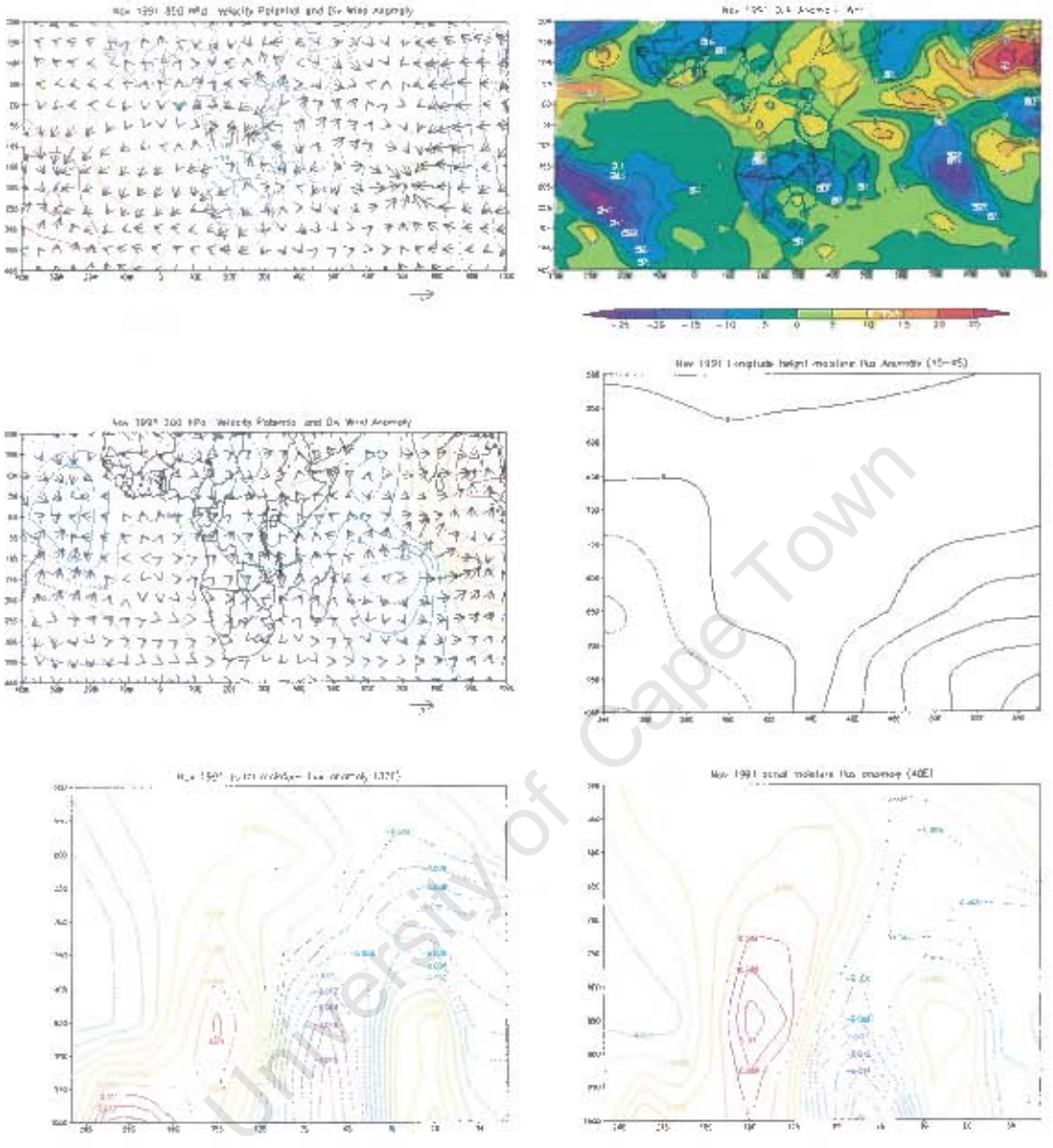

Figure B2 continue

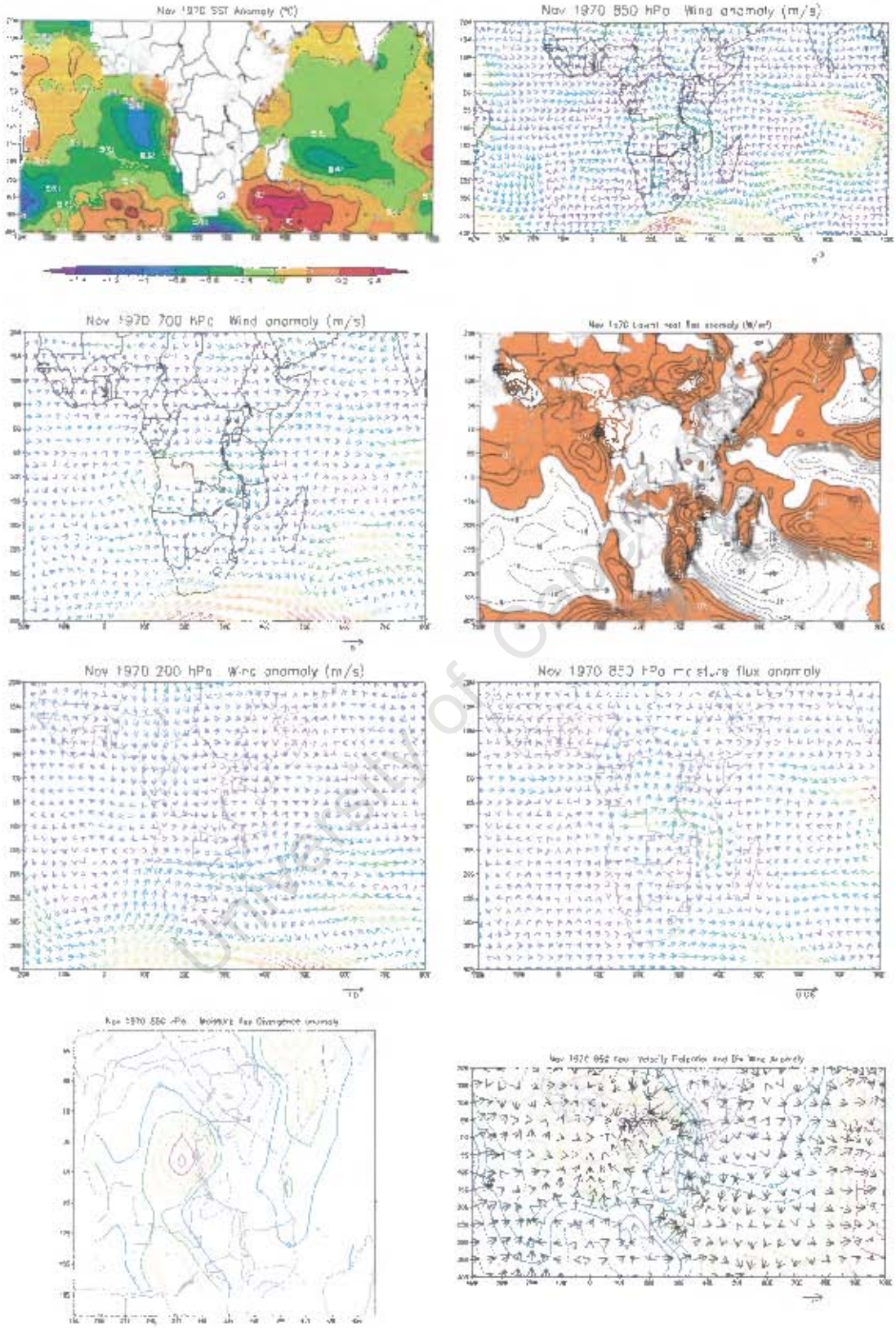

Figure C1: November anomaly fields forLa Niña year 1970
Moisture flux in g/kg.m/s, Velocity potential ($m^2 s^{-1}$)
Divergent wind (s^{-1})

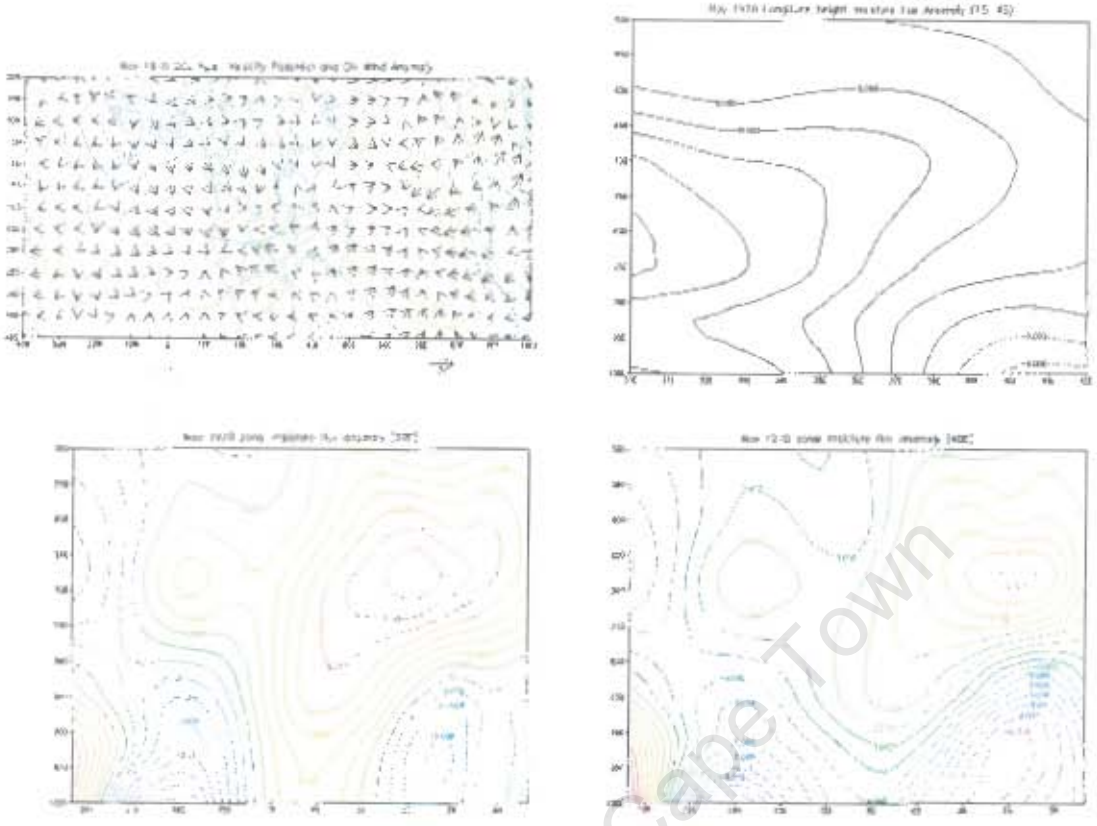

Fig C1 continue

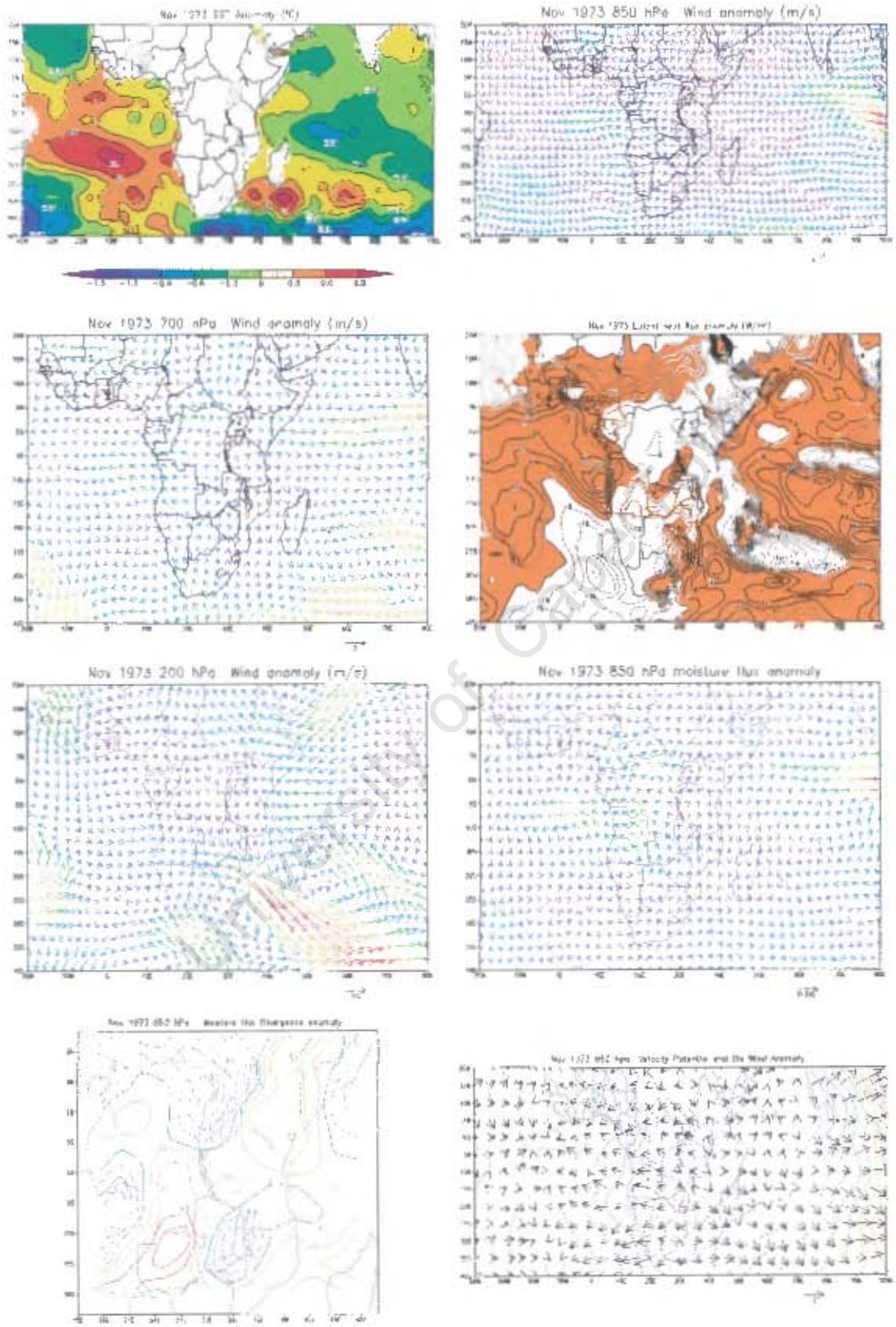

Figure C2: As for figure C1 but for 1973

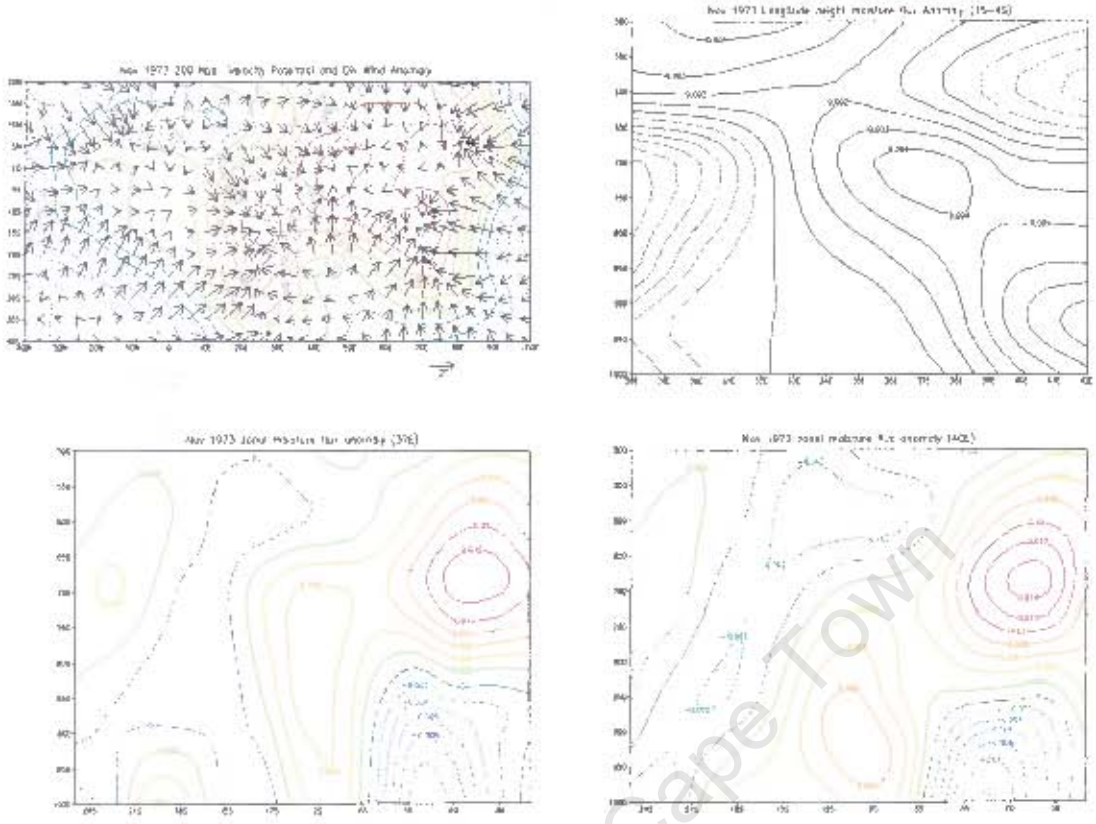

Figure C2 continue

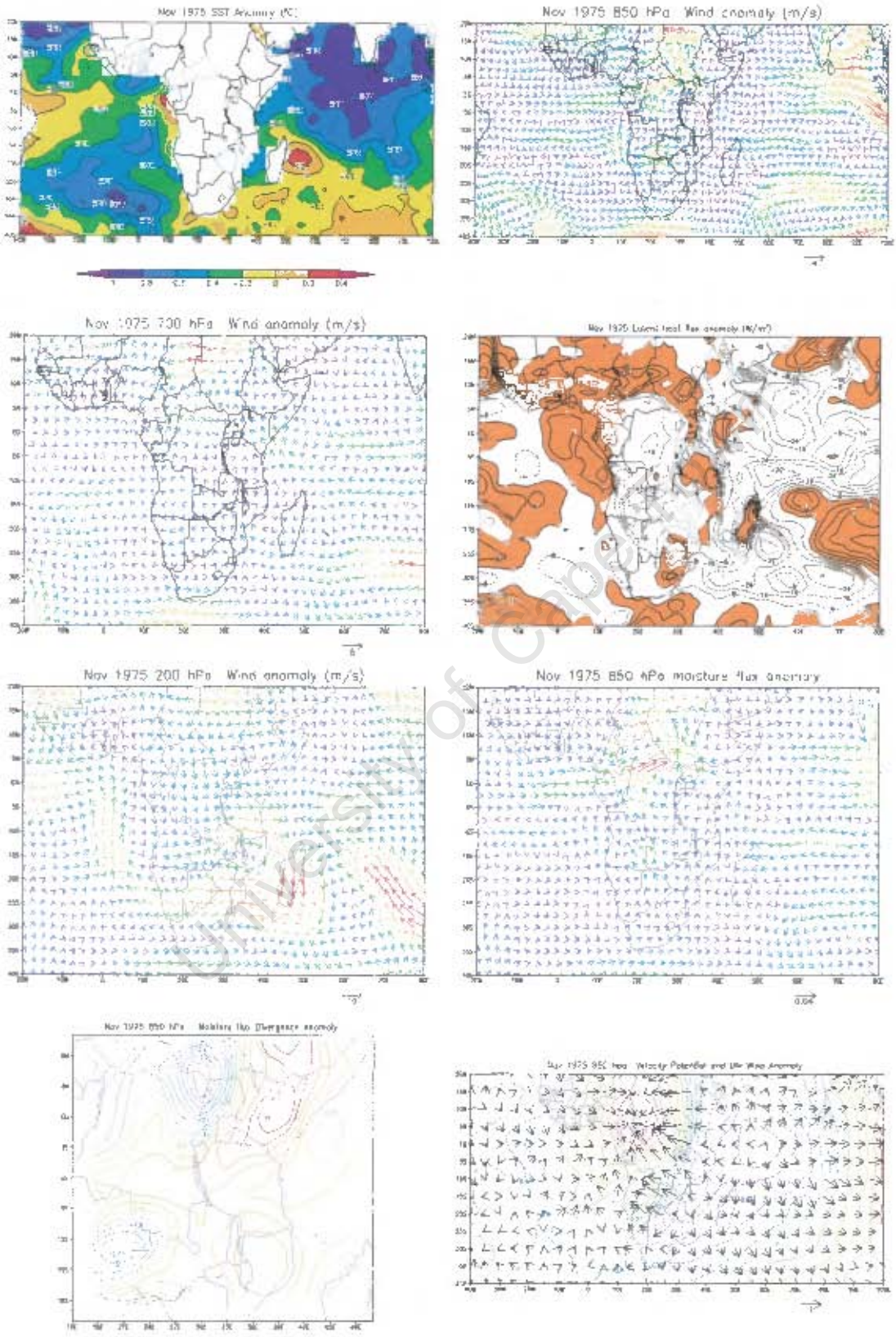

Fig C3: As for C1 but for 1975

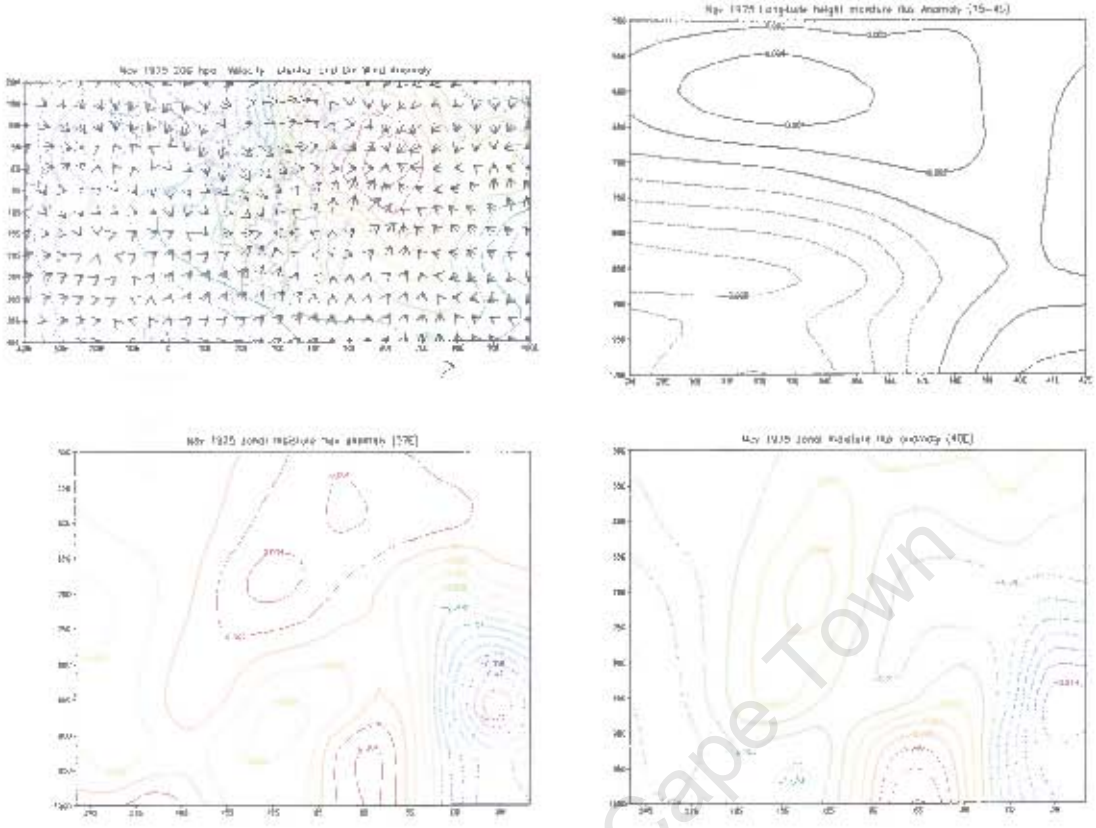

Fig C3 continue

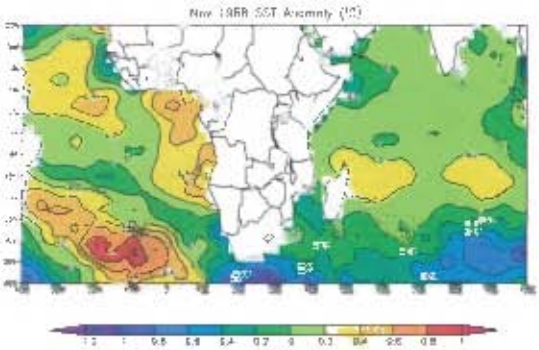

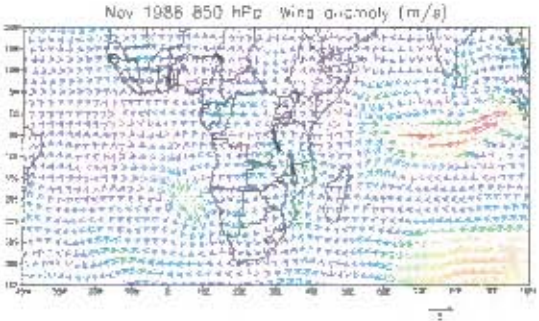

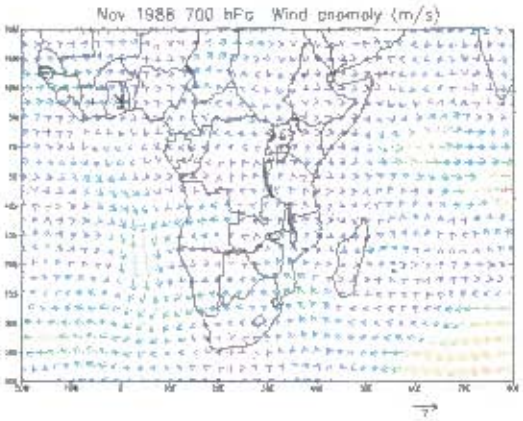

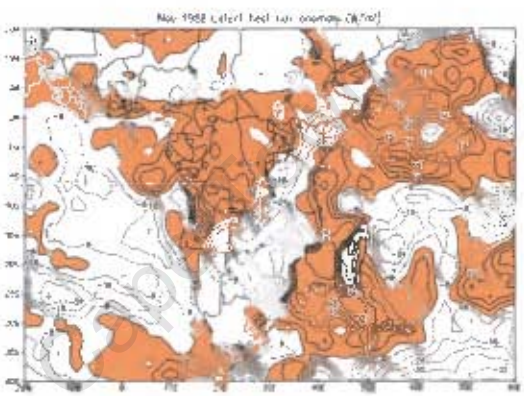

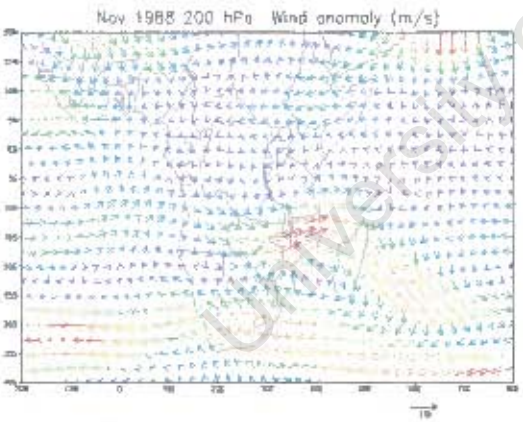

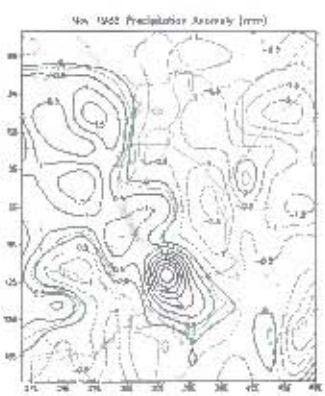

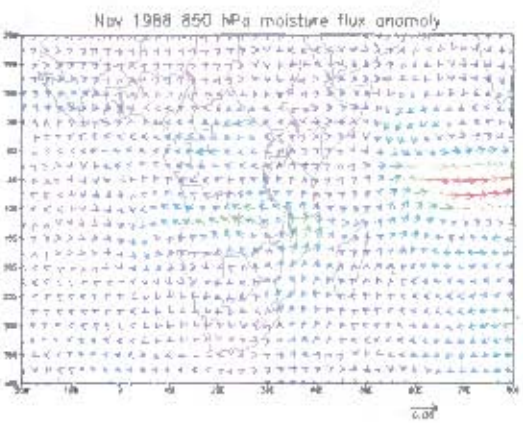

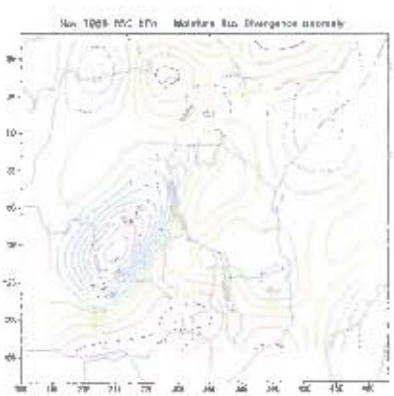

Figure C4 :As for figure C1 but for 1988

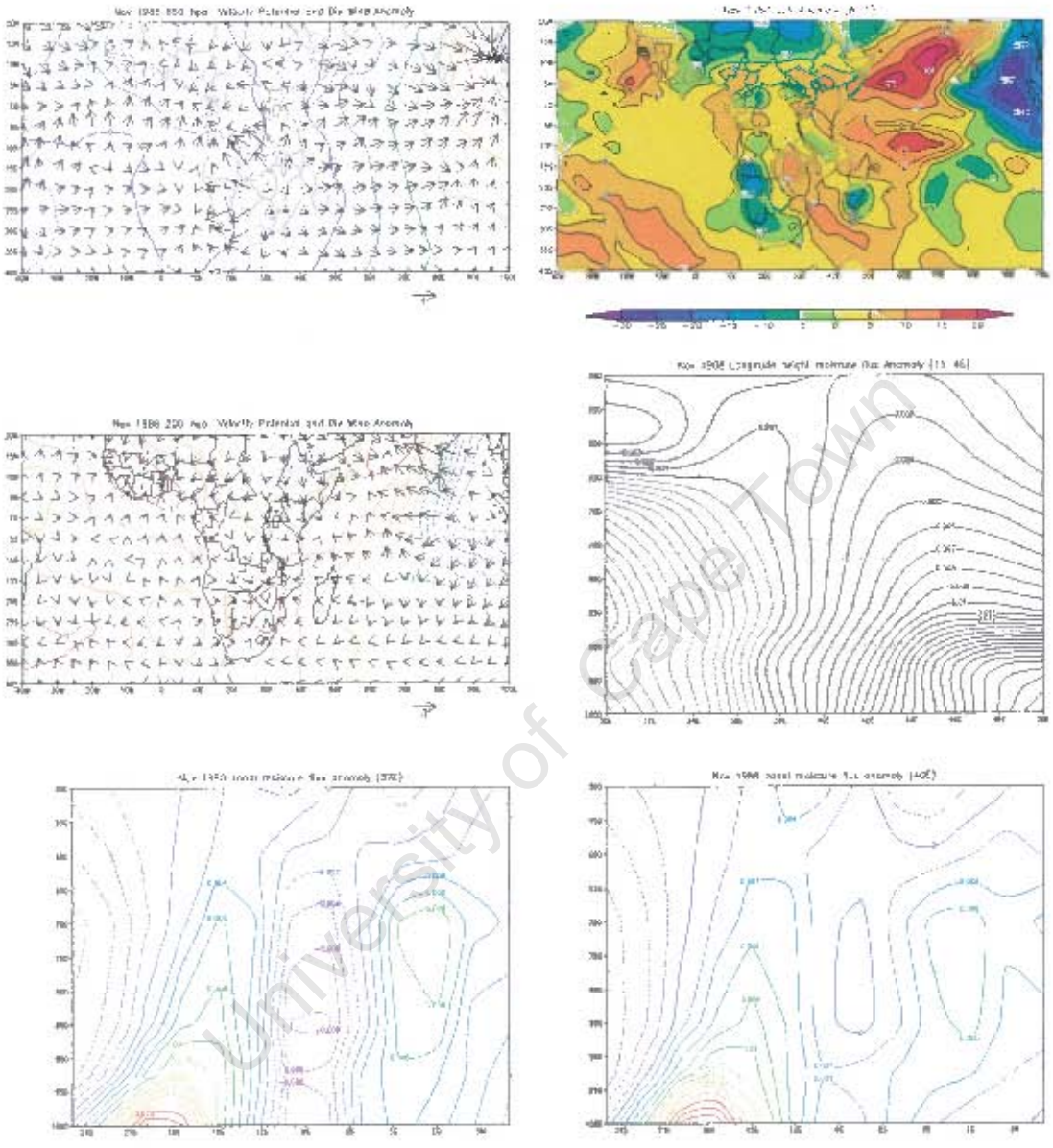

Figure C4 continue

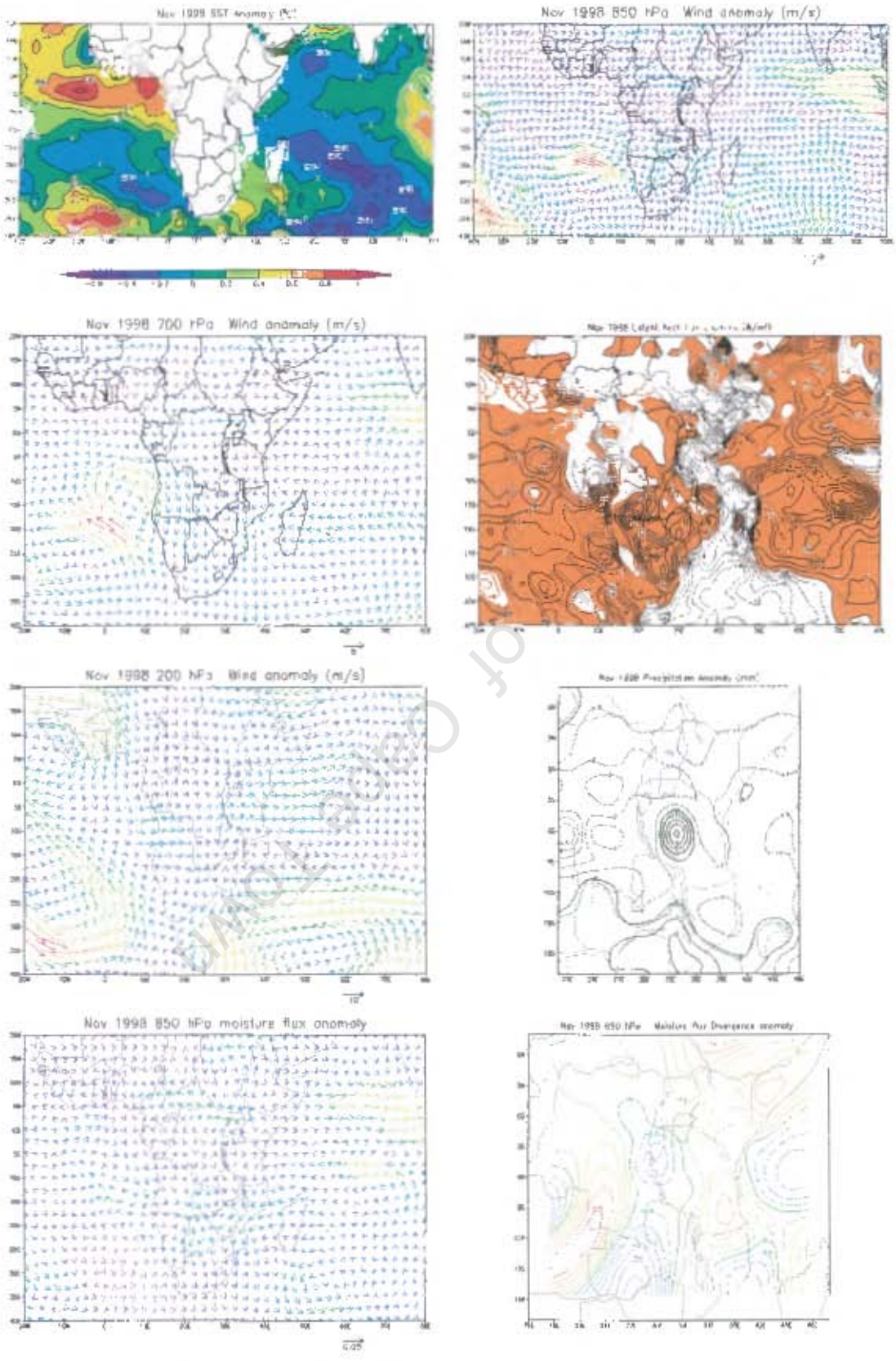

Figure C5: As for C1 but for 1998

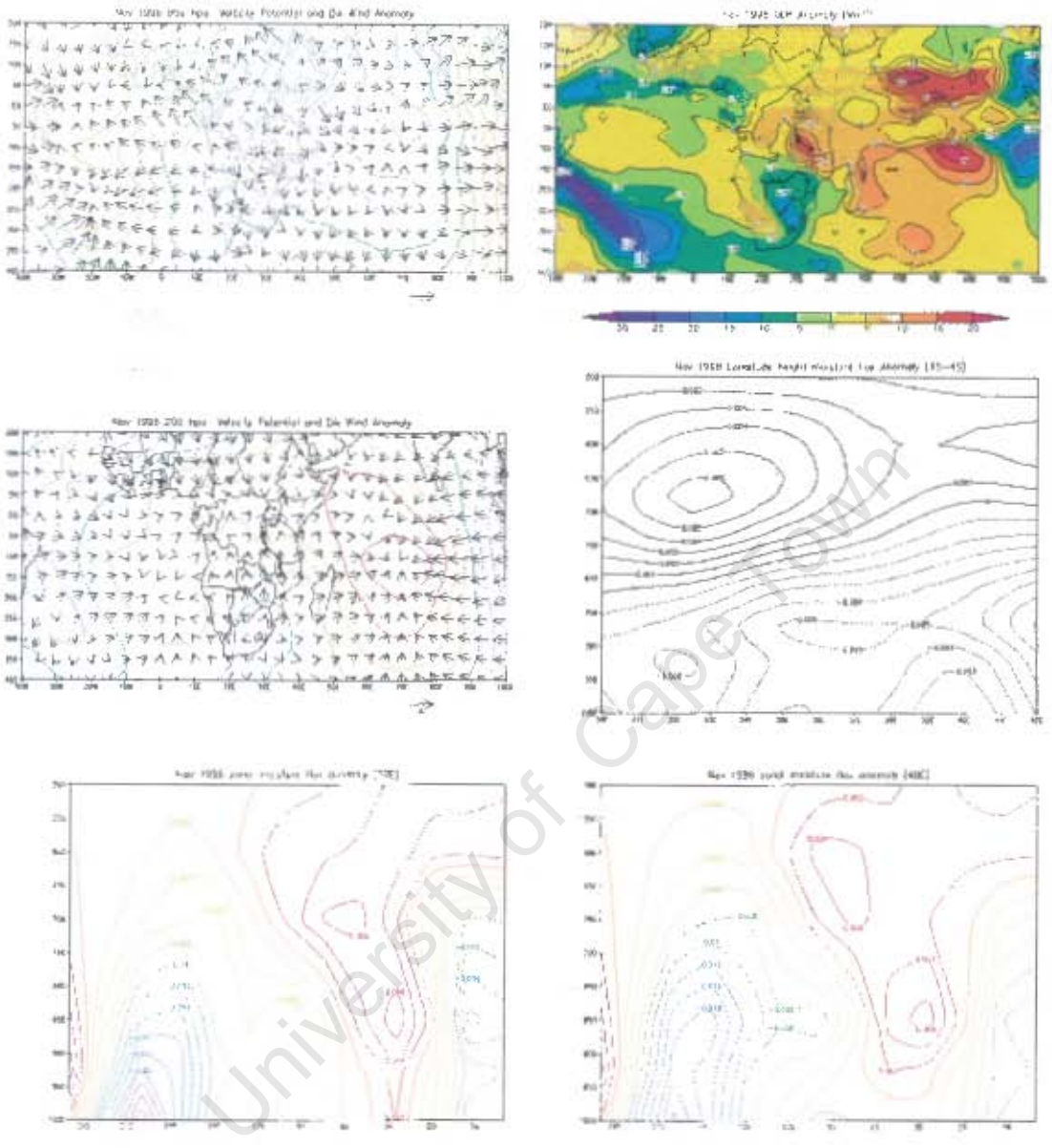

Figure C5 continue

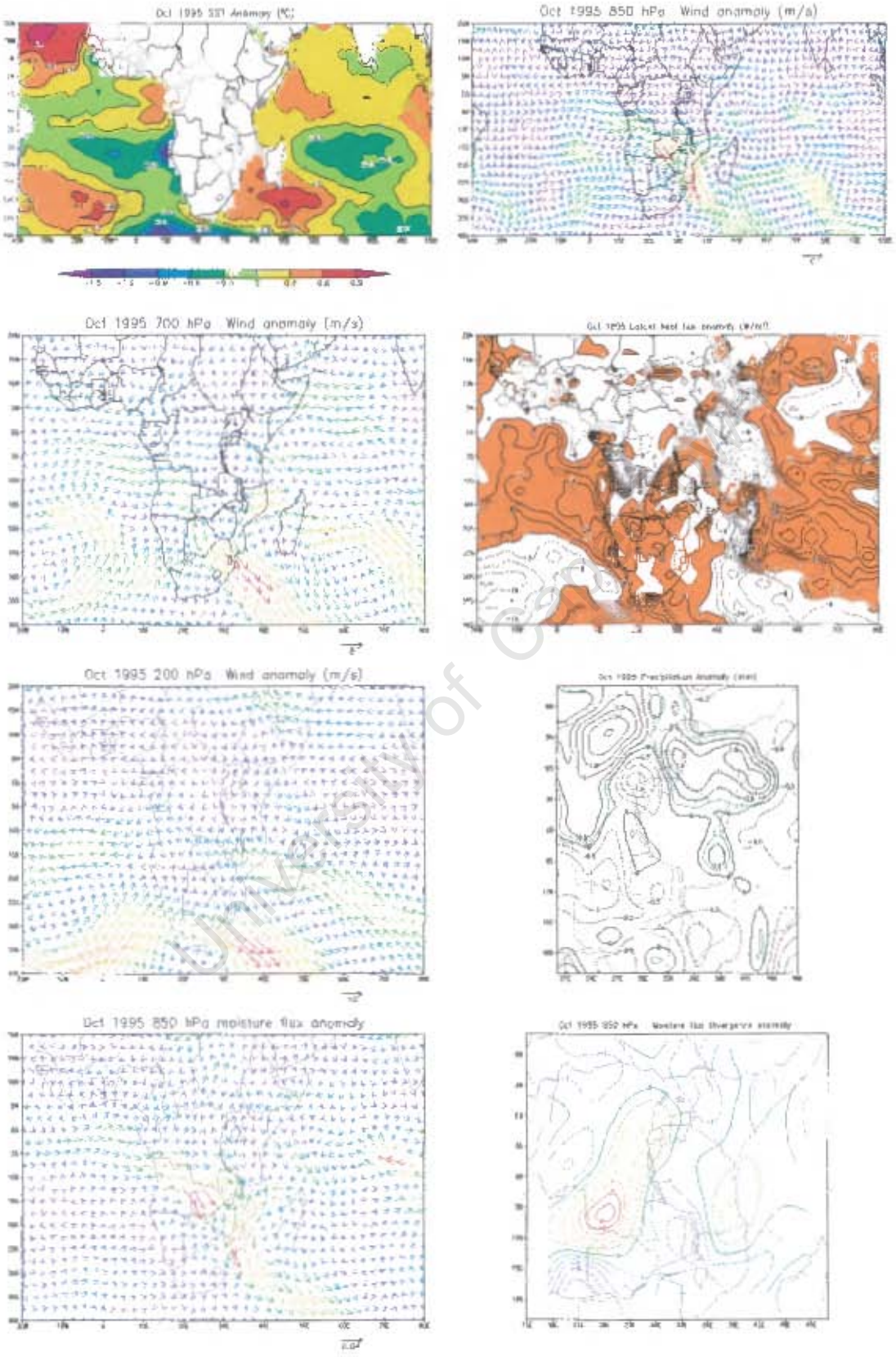

Figure D3: As for figure C1 but for October 1995

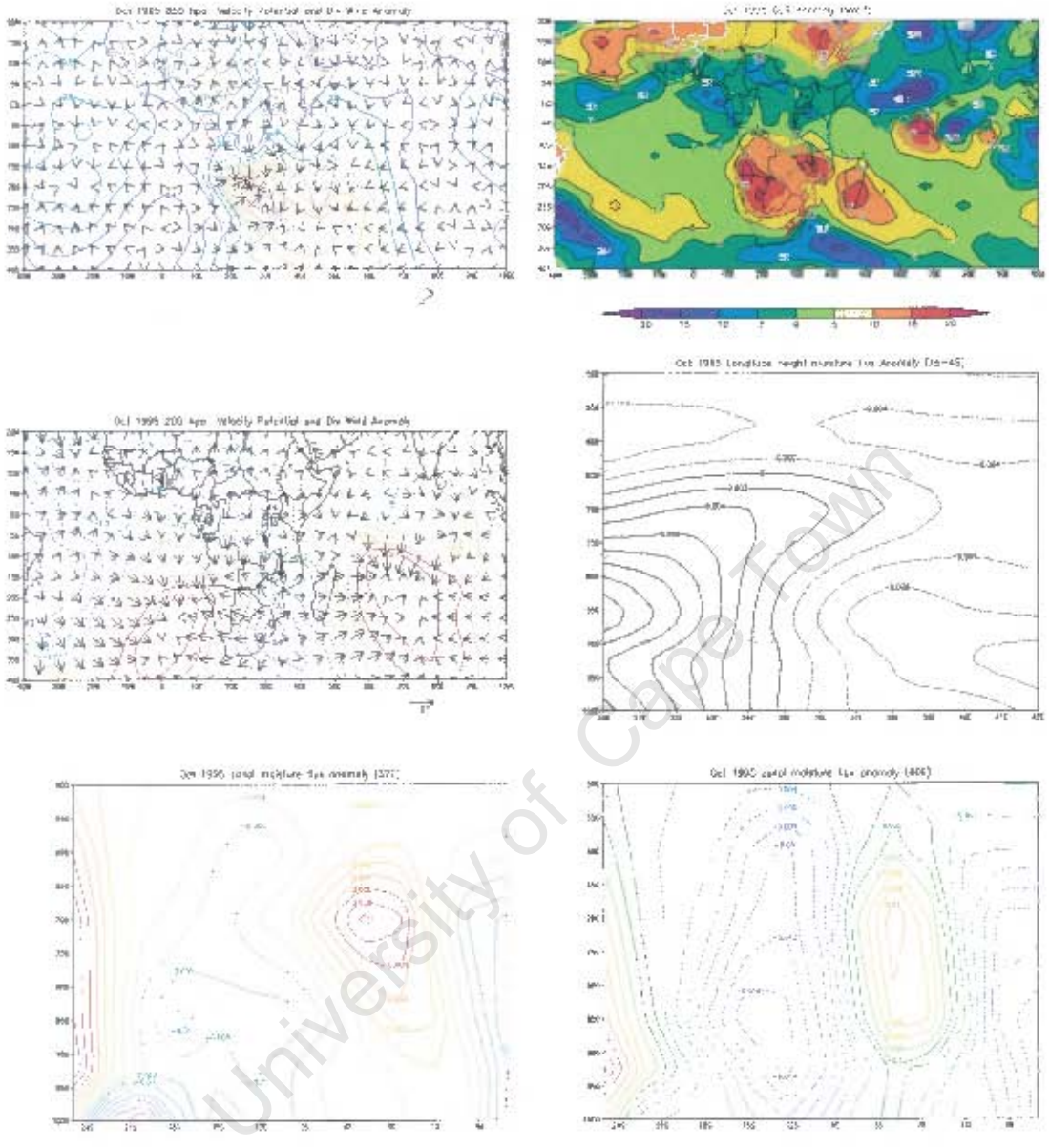

Figure D3 Continue

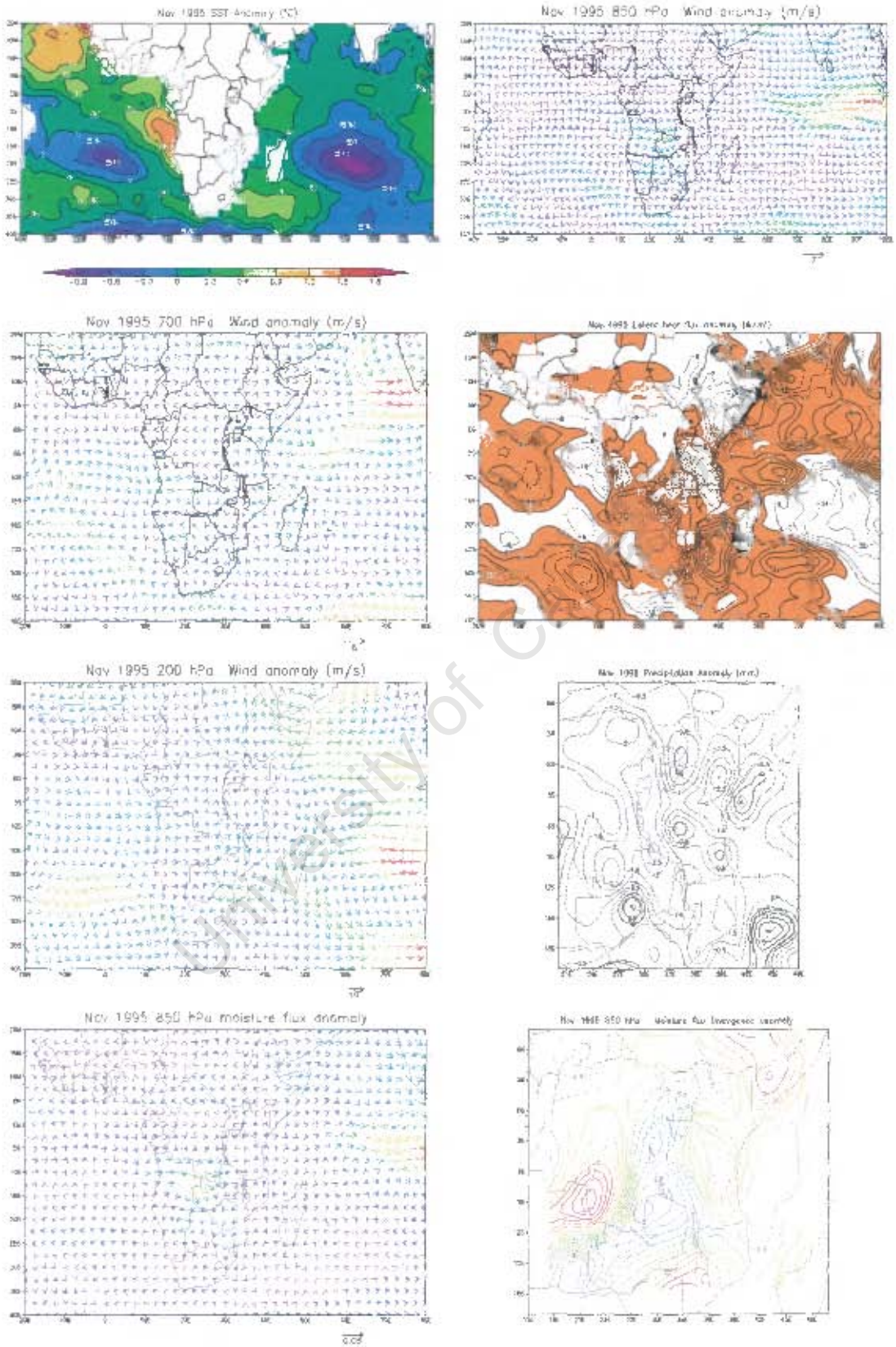

Figure D4: As for C1 but for 1995

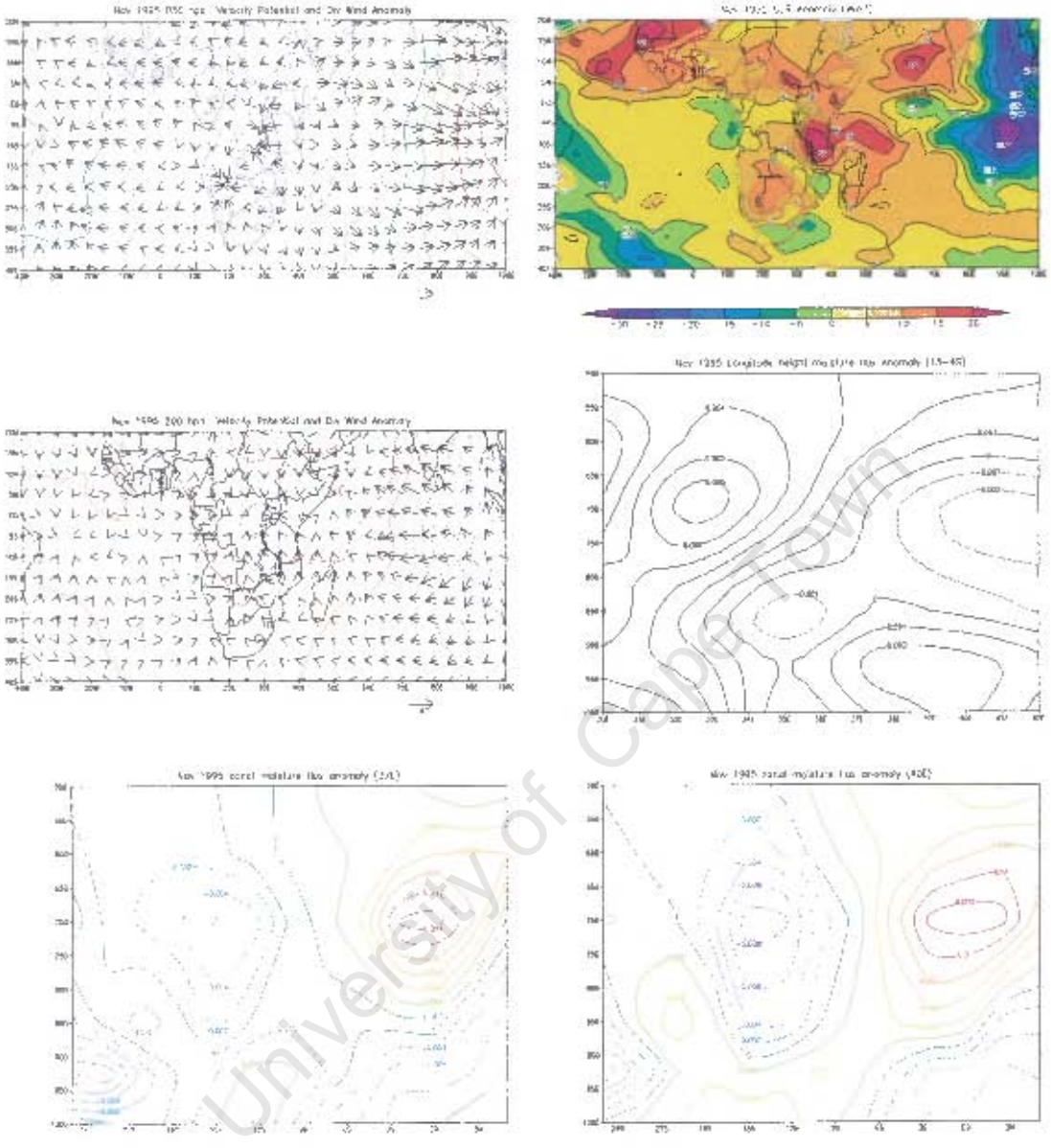

Figure D1: continue

APPENDIX C

Circulations associated with Non ENSO years

The analysis under this section considers monthly anomalies for selected meteorological fields during the OND season of the selected strongest wet/dry non-ENSO years. 1978 was observed to be strongest wet non El Niño year while 1974 was the strongest dry non La Niña year (fig 3.1b). Similarly 1977 and 1996 will be considered in this section to represent pure Indian Ocean positive and negative zonal mode years respectively without an ENSO event also occurring (Yamagata et al 2002).

The main objective of this section is to investigate the circulations associated with non-ENSO years and to contrast the results with ENSO years. Only the meteorological patterns, which significantly differ from composites and significantly influence Tanzanian coast rainfall, will be discussed here. However, the spatial rainfall plot is not shown for the years selected under this section except for 1996 due to the unavailability of CMAP data prior to 1979.

Monthly anomalies for wet non El Niño years.

Figures E1-E6 illustrate monthly anomaly fields for 1978 and 1977, which were particularly wet non El Niño years during the OND season. 1978 was the strongest wet non-ENSO and non Indian Ocean zonal mode year. In October 1978 (fig E1), weak positive SST anomalies existed over the equatorial western Indian Ocean closer to the Somali coast with larger anomalies near Madagascar. The El Niño composites indicate larger positive SST anomalies over this region and cool anomalies confined to the Indian Ocean (fig 5.1e) unlike the broad cooling seen for 1978.

A cyclonic low and middle level wind anomaly occurs over the equatorial western Indian Ocean along the equator centered at about 65°E. This circulation is also reflected in moisture flux anomaly plots with strong westerly and northerly moisture flux anomalies converging over much of Tanzania. Positive latent heat flux anomalies were observed through the path of these wind anomalies implying high moisture content and above average rainfall.

On the other hand, the El Niño composite indicates strong easterly wind and moisture flux anomalies over this region.

During the peak of the rainfall season in November 1978 (fig E2), the SST anomaly plot is more or less opposite to the El Niño composite with negative SST anomalies over the equatorial western Indian Ocean and positive SST anomalies over the subtropical South Indian Ocean. However, above average rainfall occurred due to the existence of easterly wind and moisture flux anomalies over the equatorial western Indian Ocean between 5°S and 5°N with strong moisture flux convergence over the East African coast.

The descending limb of the Indian Ocean Walker cell indicates a westward shift compared to the El Niño composite and is located at about 70°E as revealed by negative (positive) velocity potential with divergent (convergent) wind in lower (upper) levels. The corresponding ascending limb is located over the equatorial western Indian Ocean closer to the Tanzanian coast consistent with above average rainfall observed over the region. In this case, the rainfall is more likely related to regional atmospheric circulation anomalies rather than from any clear influence from warm SST anomalies over the Indian Ocean unlike for El Niño.

Towards the withdrawal of the rainfall season in December 1978 (fig E3), again the SST anomaly patterns are roughly a reverse of the El Niño composite. Negative SST anomalies occur over the equatorial Indian Ocean north of 20°S with positive SST anomalies to the south. A low-level cyclonic wind and moisture flux anomaly centered over Mozambique is apparent with strong easterly wind and moisture flux anomalies over the equatorial western Indian Ocean. This circulation extends to the middle levels with enhanced moisture flux convergence over much of the East African region. Again the observed rainfall occurred as a result of regional wind and moisture flux circulation patterns rather than any obvious SST influence. It is worth noting that regional wind anomaly circulation patterns are important for describing the nature of Tanzanian coast rainfall during the non-ENSO years. However,

the wind and moisture flux anomaly circulations are significantly different for each month implying that combining the three months in the seasonal mean may distort the results.

1977 was a positive Indian Ocean zonal mode year and was a wet year over the Tanzanian coast. In October 1977 (fig E4), the zonal mode SST patterns over the equatorial Indian Ocean was evident with warm SST anomalies over the equatorial western Indian Ocean and cool SST anomalies over the equatorial East Indian Ocean. Both positive and negative SST anomalies indicate slightly lower values compared to the El Niño composite.

The low-level wind patterns indicate a cyclonic anomaly southeast of Madagascar centered at about 65°E. An anticyclonic anomaly exists over the equatorial eastern Indian Ocean with strong northeasterly wind anomalies in the central equatorial Indian Ocean. However, in the El Niño composite the cyclonic circulation over southeast Madagascar is not evident and strong easterly wind anomalies exist over equatorial Indian Ocean along the equator. The middle level wind anomaly patterns indicate significant departures from the El Niño composite with cyclonic anomalies over the equatorial western Indian Ocean and southeasterly wind anomalies over the Tanzanian coast.

The moisture flux anomaly plot reveals westerly anomalies over the central Indian Ocean between equator and 5°N, the region that is occupied by strong easterly moisture flux anomaly in the El Niño composites. The cyclonic moisture flux anomaly is evident over southeast Madagascar with strong moisture flux convergence over much of East Africa. The occurrence of strong easterly moisture flux anomaly over the equatorial western Indian Ocean between 5°S and 10°S with strong moisture flux convergence over the entire East Africa is consistent with above average rainfall over the region during Indian Ocean positive zonal mode years. However, the wind and moisture flux anomaly circulations are significantly different from the El Niño composite despite similar SST anomaly patterns.

In November 1977 (fig E5), the SST zonal mode pattern over the equatorial Indian Ocean weakens. An anticyclonic wind anomaly was evident over the region of cool SST anomalies with strong easterly wind anomalies over the tropical South Indian Ocean with the reverse north of the equator. The 700hPa level wind plot indicates a cyclonic circulation over the equatorial Indian Ocean with strong westerly wind anomalies north of the equator and easterly wind anomalies south of the equator. In the El Niño composite, strong easterly wind anomalies exist along the equator. A cyclonic moisture flux anomaly exists over the equatorial Indian Ocean with strong moisture flux convergence over the Tanzanian coast.

The longitude height moisture flux transects shows easterly moisture flux anomalies over the region at lower levels while the El Niño composite exhibits westerly moisture flux anomaly. The above average rainfall observed in November 1977 appears to be due to the large amount of moisture advected from the Indian Ocean and enhanced convergence of this moisture near the coast. Again the moisture flux and wind anomaly patterns are significantly different from the El Niño composites.

In December 1977 (fig E6), the zonal mode SST pattern over the equatorial Indian Ocean is no longer apparent. Negative SST anomalies east of Madagascar are stronger than the previous month while positive SST anomalies weaken compared to the El Niño composites. A cyclonic wind anomaly occurs northeast of Madagascar with a strong easterly wind anomaly along the equator. Another cyclonic wind anomaly is centered over Botswana with southeasterly anomalies over the Tanzanian coast veering to southerly anomalies over the Kenyan coast. These cyclonic circulations are also reflected in the moisture flux anomalies and middle level wind anomalies and they are associated with moisture flux convergence over the Tanzanian coast. Again, the moisture flux and wind circulation patterns are significantly different from the El Niño composite.

Monthly anomalies for dry non La Niña years.

Figures F1-F6 illustrate monthly anomaly fields for 1974 and 1996, which were particularly dry non La Niña years during the OND season. 1974 was the strongest dry year when there was no La Niña or Indian Ocean zonal mode. In October 1974 (fig F1), the tongue of positive SST anomalies emanating from equatorial eastern Indian Ocean, which was observed in the La Niña composite is not apparent. Cool SST anomalies extend over much of the Indian Ocean with lower SST anomalies compared to the La Niña composite.

The low level winds are more or less similar to the La Niña composite (fig 5.3e) with strong westerly anomalies over the equatorial Indian Ocean. In the middle levels closer to the East African coast, the wind anomaly patterns indicate roughly the reverse of the La Niña composite with northerly wind anomalies backing to westerly anomalies over the Tanzanian coast. The below average rainfall observed resulted from the existence of westerly moisture flux anomalies over the equatorial Indian Ocean, reduced evaporation near the coast and moisture flux divergence over the East African region.

In November 1974 (fig F2), a La Niña like north-south contrast in SST anomalies is evident over the Indian Ocean. Negative SST anomalies occur over the equatorial Indian Ocean north of 20°S and positive SST anomalies south of 20°S. The SST anomalies are larger than the La Niña composite with lowest anomaly value of about –0.9°C closer to the Tanzanian coast. Again, the lower and middle level wind anomalies indicate similar patterns to the La Niña composite. The below average rainfall observed is mainly due to the occurrence of westerly moisture flux anomalies over the equatorial Indian Ocean with moisture flux divergence over the northern coast of Tanzania. The moisture flux convergence over the southern coast suggests wet conditions there as seen in the seasonal total (fig 3.2b).

In December 1974 (fig F3), the western Indian Ocean becomes warmer than average whereas the central and eastern regions continued to show cool anomalies. The wind anomaly patterns indicate a significant departure from the La Niña composite. Easterly wind anomalies exist over the equatorial western Indian Ocean, a region covered by westerly wind anomalies in the La Niña composite. At 700hPa, a cyclonic wind anomaly exists over the Tanzanian coast. This type of circulation implies increased rainfall over the Tanzanian coast consistent with moisture flux convergence. However, October and November 1974 contributed to below average rainfall in the 1974 seasonal total while for La Niña composites, dry conditions persisted throughout the rainfall season.

1996 was a negative Indian Ocean zonal mode year but the 1995/96 La Niña event had decayed by OND 1996. In October 1996 (fig F4), the negative zonal mode in SST anomalies is apparent over the equatorial Indian Ocean. Positive SST anomalies exist over the equatorial eastern Indian Ocean and negative SST anomalies over the equatorial western Indian Ocean. The negative SST anomaly values are larger than the La Niña composite with lowest anomaly value of –1.2°C closer to the Somali coast. The region near the Tanzanian coast that was covered by warm SST anomalies in the La Niña composite indicated cool SST anomalies of the order of –0.6°C in 1996.

The low level wind indicates a region of westerly wind anomalies over the Tanzanian coast, which is also evident at 700hPa. In the La Niña composite, this region showed southerly wind anomalies. Westerly moisture flux anomalies exist over the equatorial western Indian Ocean with moisture flux divergence over the East African coast consistent with below average rainfall observed. Over the region, westerly wind anomalies dominate as reflected in the longitude height moisture flux anomaly plot, while for the La Niña composite easterly wind anomalies occurs over 850hPa and middle levels. The circulation patterns that resulted in below average rainfall over the Tanzanian coast are more or less similar to the La Niña composite.

In November 1996 (fig F5), the zonal mode in SST anomalies weakens over the tropical Indian Ocean. Much of the Indian Ocean shows variable wind anomalies with strong easterly anomalies over the equatorial western Indian Ocean closer to the Somali coast. These easterly wind anomalies also exist at 700hPa with westerly anomalies over the Tanzanian coast. The La Niña composite shows equatorial westerly anomalies at both 850 and 700hPa. At 850hPa anticyclonic moisture flux anomaly is apparent over the Indian Ocean northeast of Madagascar with moisture flux divergence over the Tanzanian coast consistent with below average rainfall observed. The above average rainfall observed over Kenya is consistent with easterly moisture flux anomaly over the region. However, the low-level moisture flux divergence anomalies cover the region indicating the involvement of local factors on the rainfall formation. This above average rainfall over Kenya was also confirmed by negative OLR anomalies over the region. The wind and moisture flux anomaly patterns that resulted in below average rainfall over the Tanzanian coast are slightly different from La Niña composite.

In December 1996 (fig F6), the zonal mode in SST anomaly patterns over the equatorial Indian Ocean weakens further. The positive SST anomalies extend towards the west resulting in the negative SST anomalies being confined nearer to the East African and Somali coast. Strong low level westerly wind anomalies occur over the Tanzanian coast whereas this region shows weak variable anomalies in the La Niña composite. The moisture flux plot indicates significantly different patterns from the La Niña composite. Westerly moisture flux anomalies extend over much of the Indian Ocean including the Tanzanian coast.

Southwestern Tanzania experienced above average rainfall in December 1996 consistent with moisture flux convergence over the region. On the other hand, the Tanzanian coast observes below average rainfall despite the moisture flux convergence over the region. This may be partly due to the long track of westerly moisture flux over the land. However, the negative latent heat flux anomalies and positive OLR anomalies over the region are

consistent with this below average rainfall. Again, note that the regional wind circulation patterns are important for determining the nature of the rainfall over the Tanzanian coast and need to be considered as well as the moisture flux divergence. Thus, the circulation patterns that led to below average rainfall are significantly different from the La Niña composite.

Generally, the wet conditions over the Tanzanian coast during non El Niño years are associated with changes in the regional atmospheric conditions. These changes are partly caused by varying surface boundary conditions, for example vegetation cover, soil moisture and topography. Also the high variability of the monthly circulation patterns leading to wet and dry conditions during non-ENSO years, suggest high contribution from meso-scale factors. The high contribution from such factors other than large scale forcing to the rainfall variability over Tanzania especially during non-ENSO years contribute to the difficulties in forecasting. For example the current resolution of the NCEP data cannot significantly identify meso-scale factors over Tanzania.

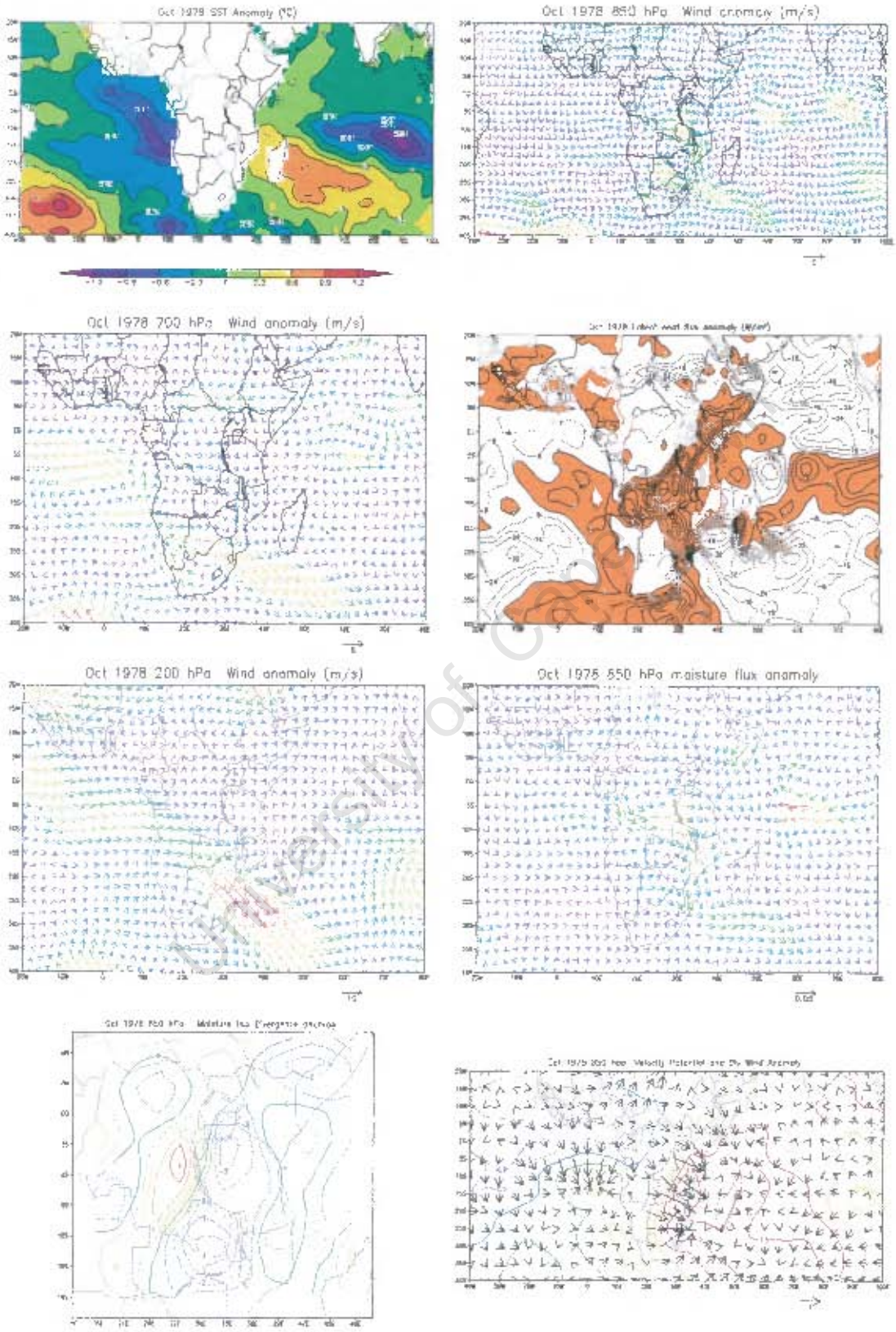

Figure E1: October anomaly fields for wet non El Niño year 1978
Moisture flux in g/kg.m/s, Velocity potential ($m^2 s^{-1}$)
Divergent wind (s^{-1})

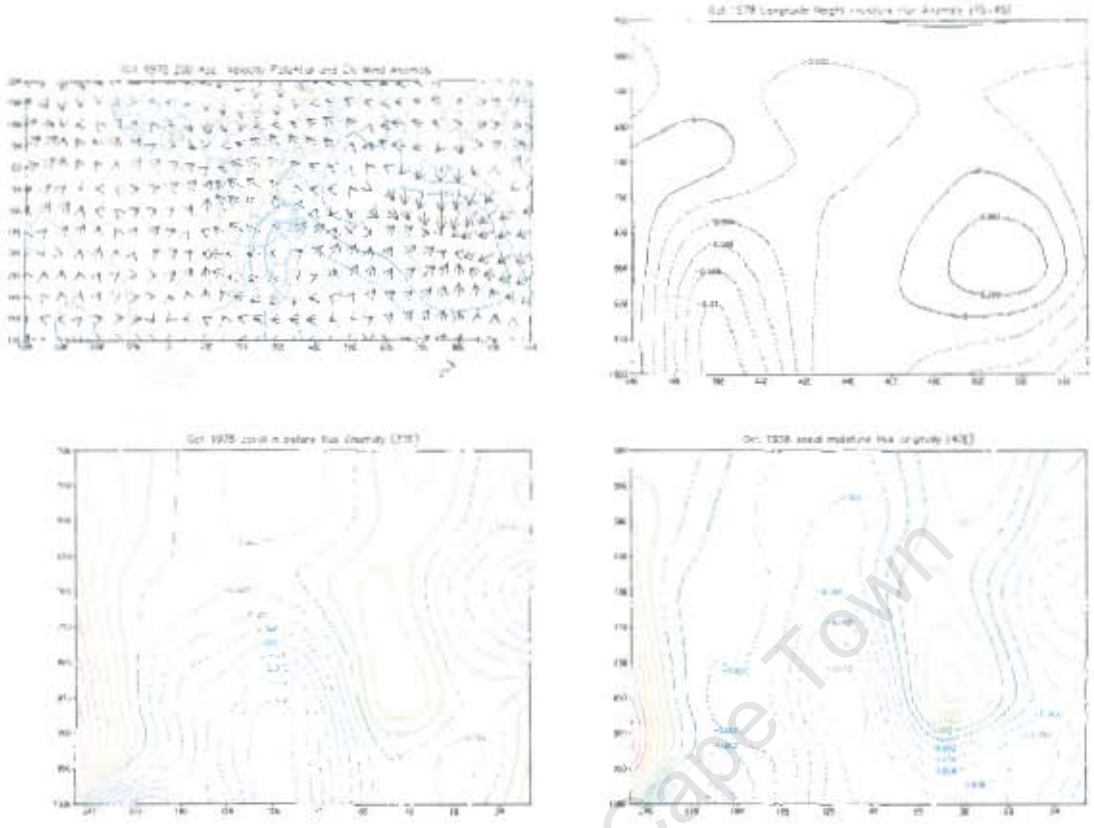

Figure E1 continue

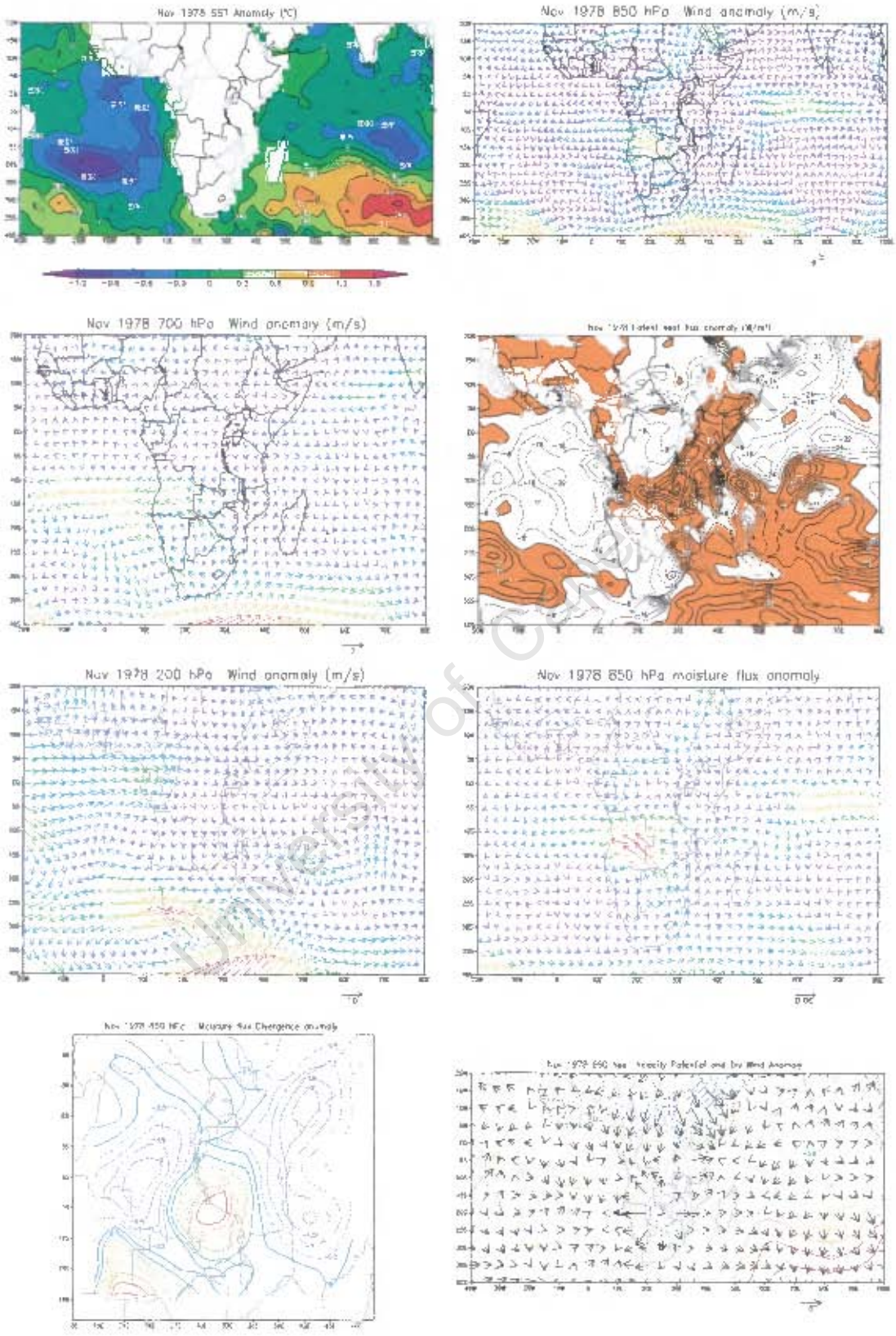

Figure E2: As for figure E1 but for November.

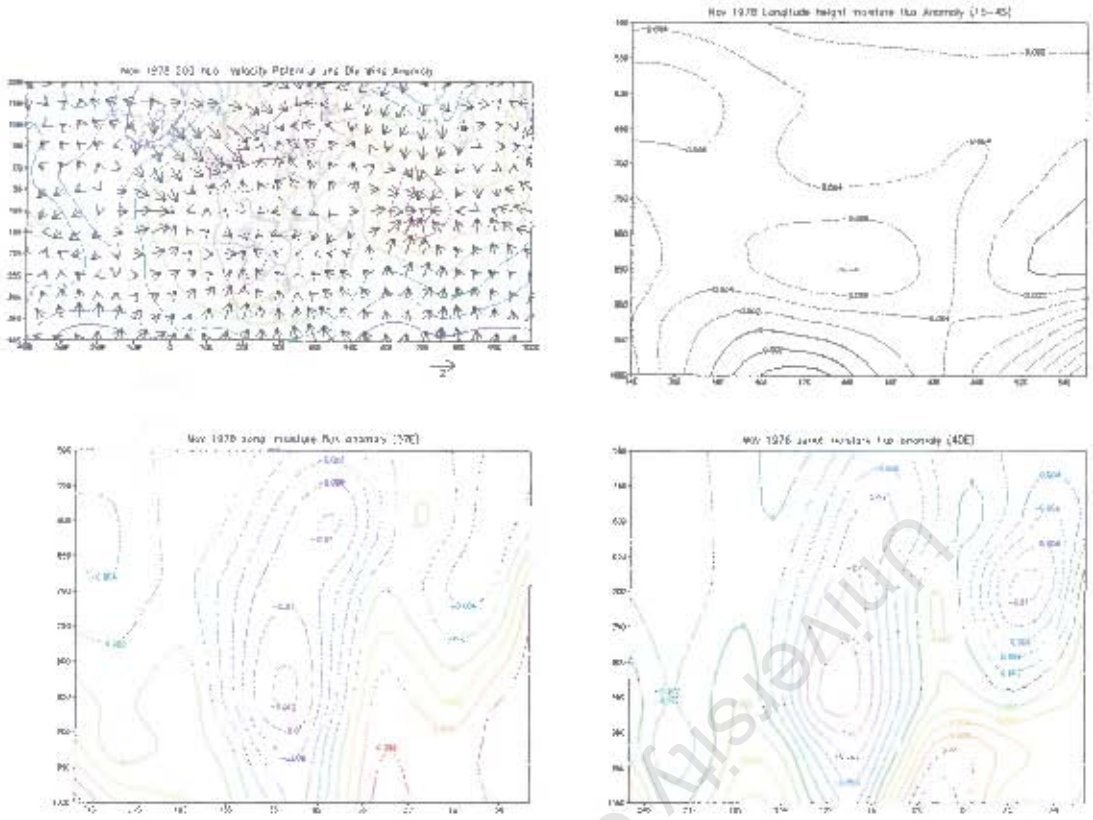

Figure E2 continue

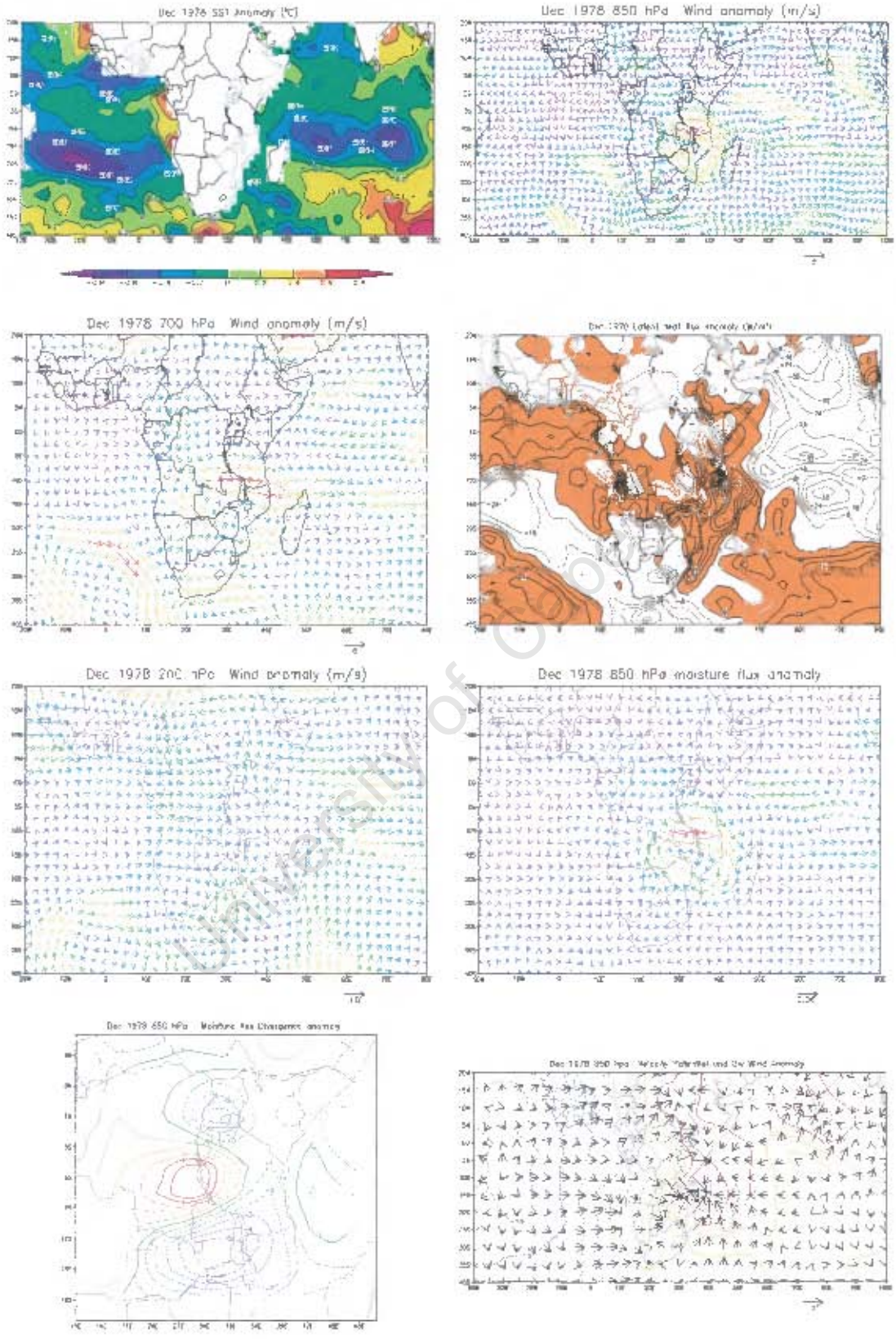

Figure E3: As for figure E1 but for December.

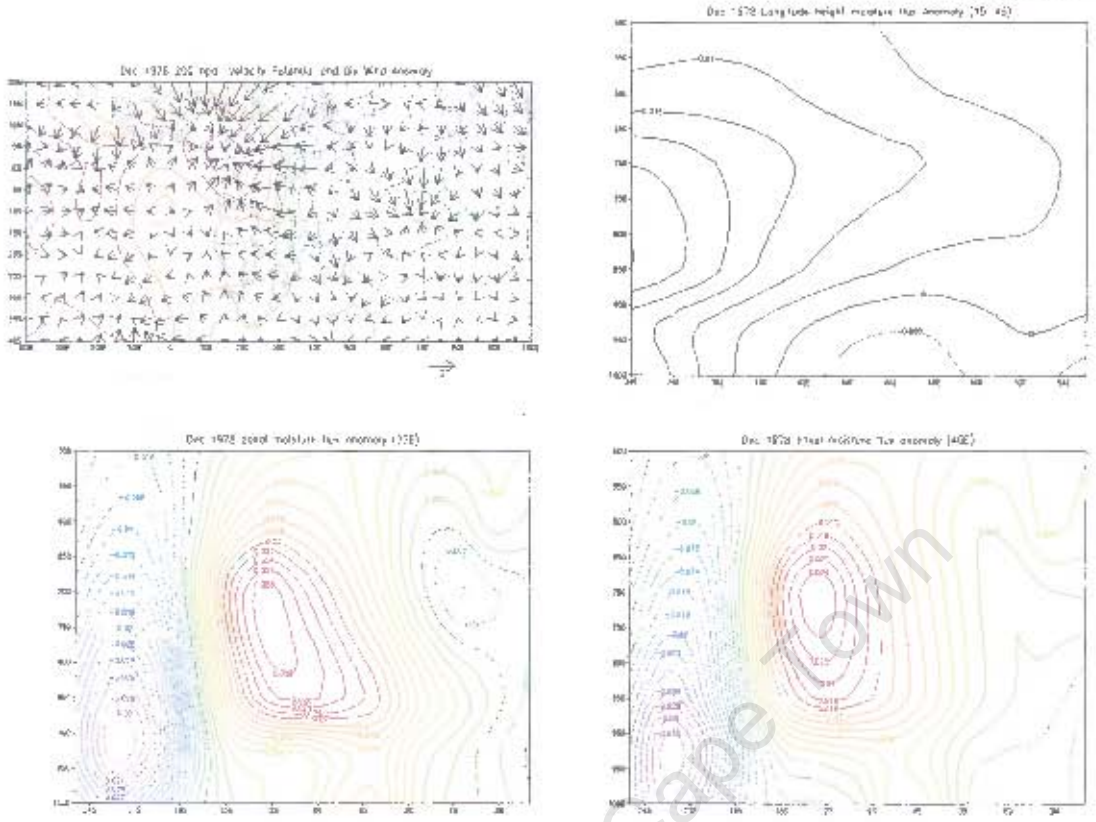

FigureE3 continue

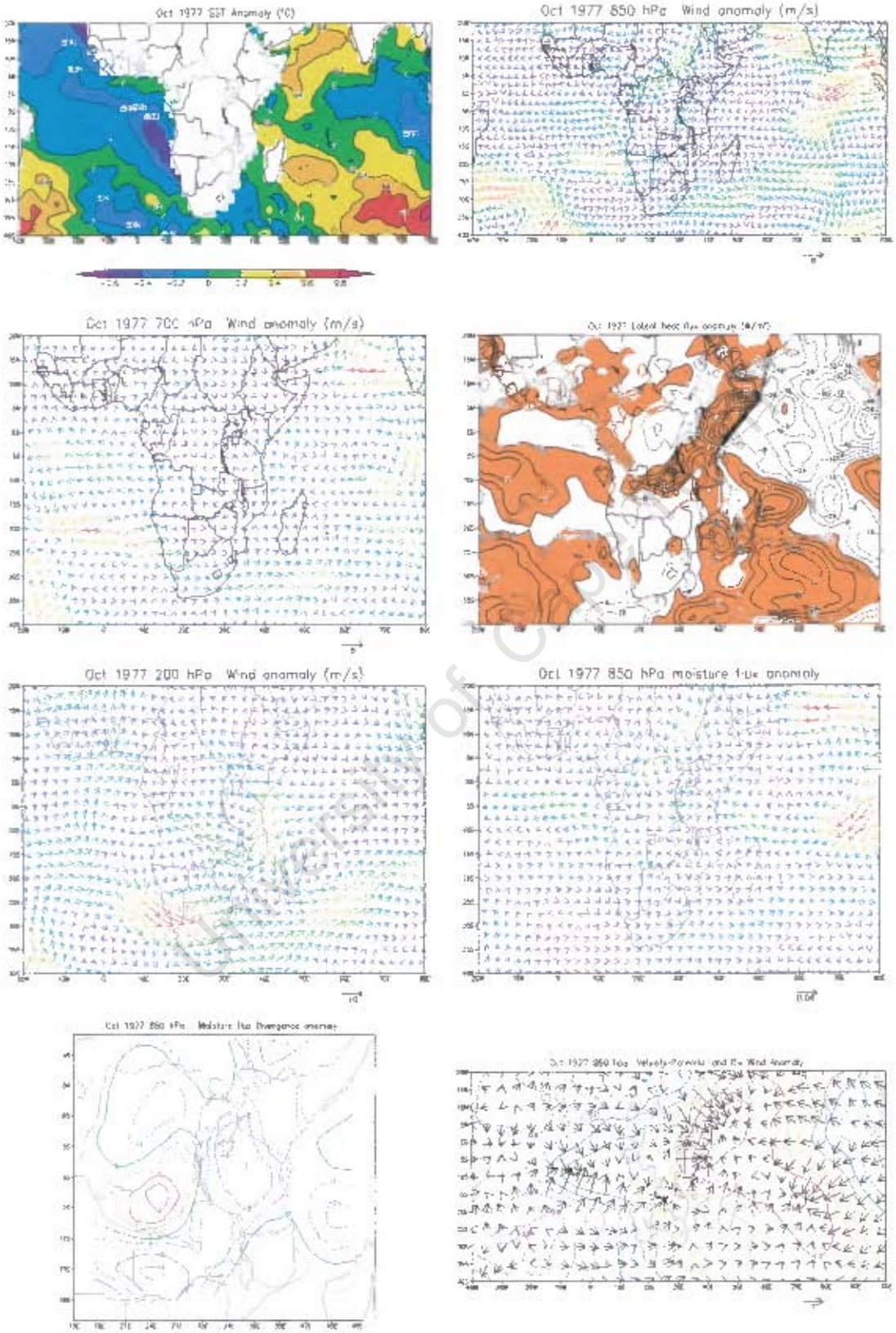

Figure E4: October anomaly fields for wet positive IOZM year 1977 Moisture flux in g/kg.m/s, Velocity potential ($m^2 s^{-1}$) Divergent wind (s^{-1})

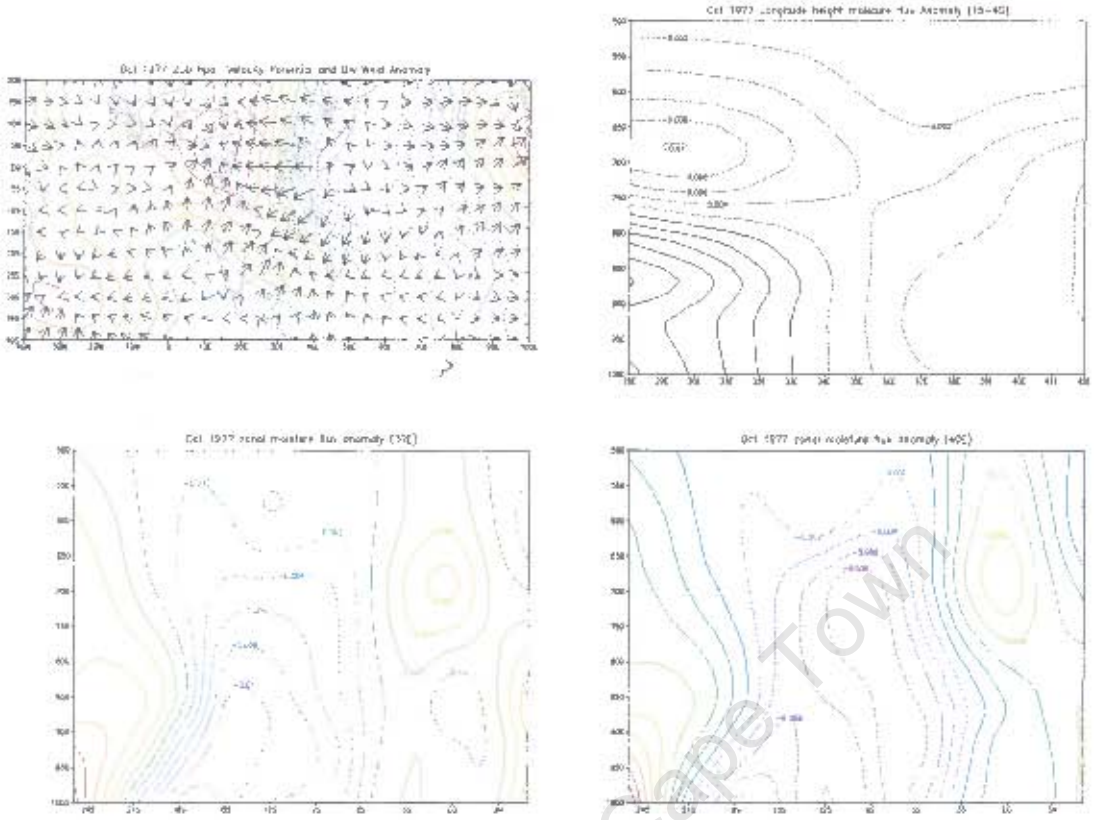

Figure E4 continue

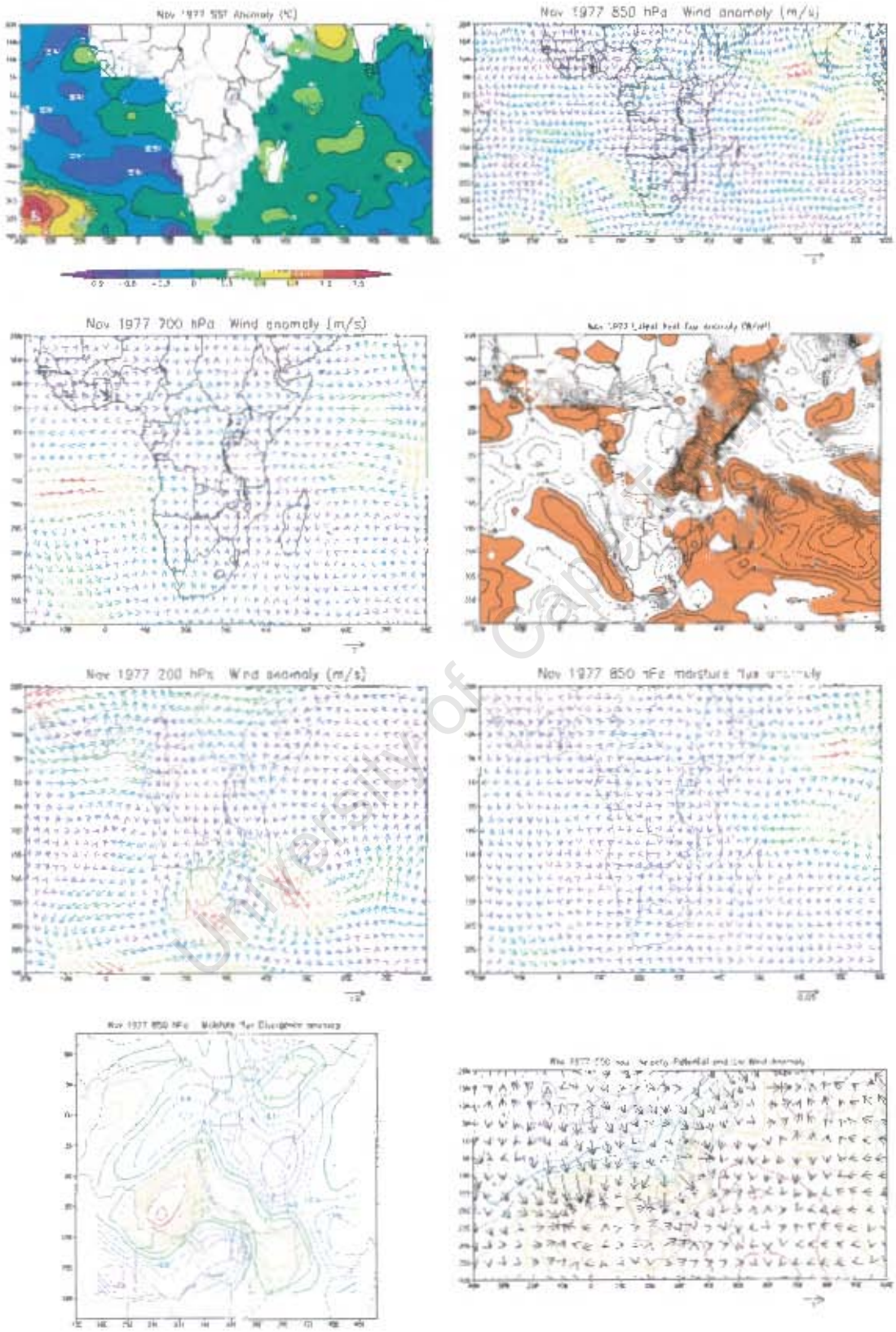

Figure E5: As for figure E4 but for November

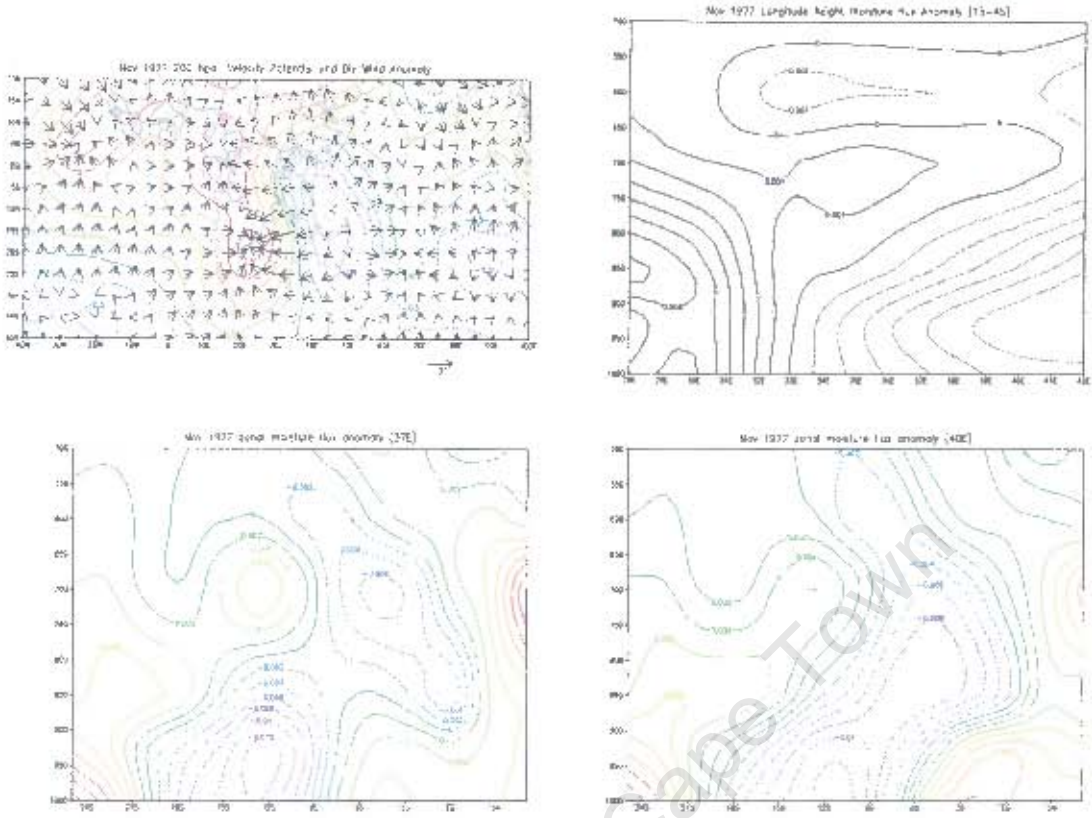

Figure E5 continue

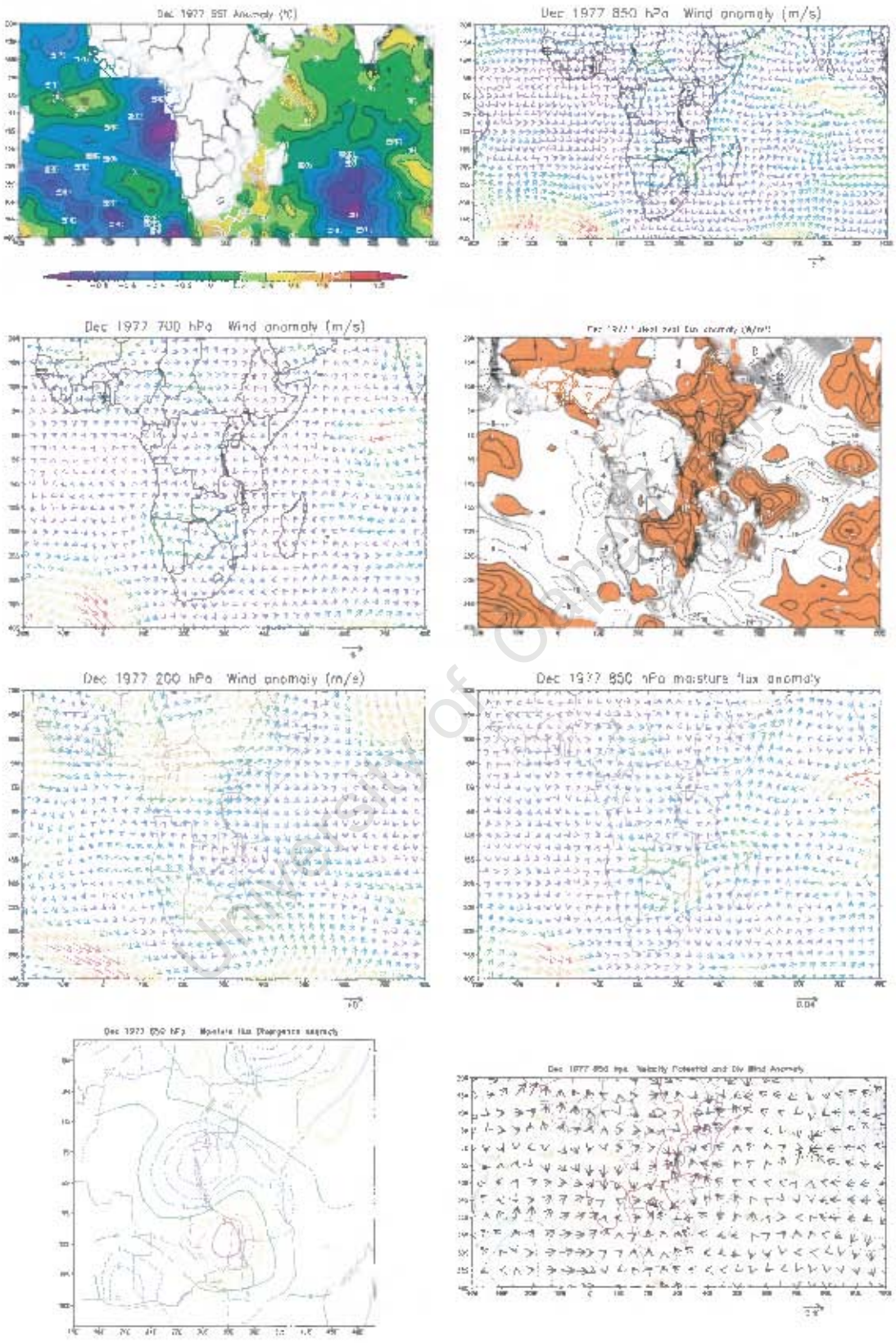

Figure E6: As for figure 5.5d but for December

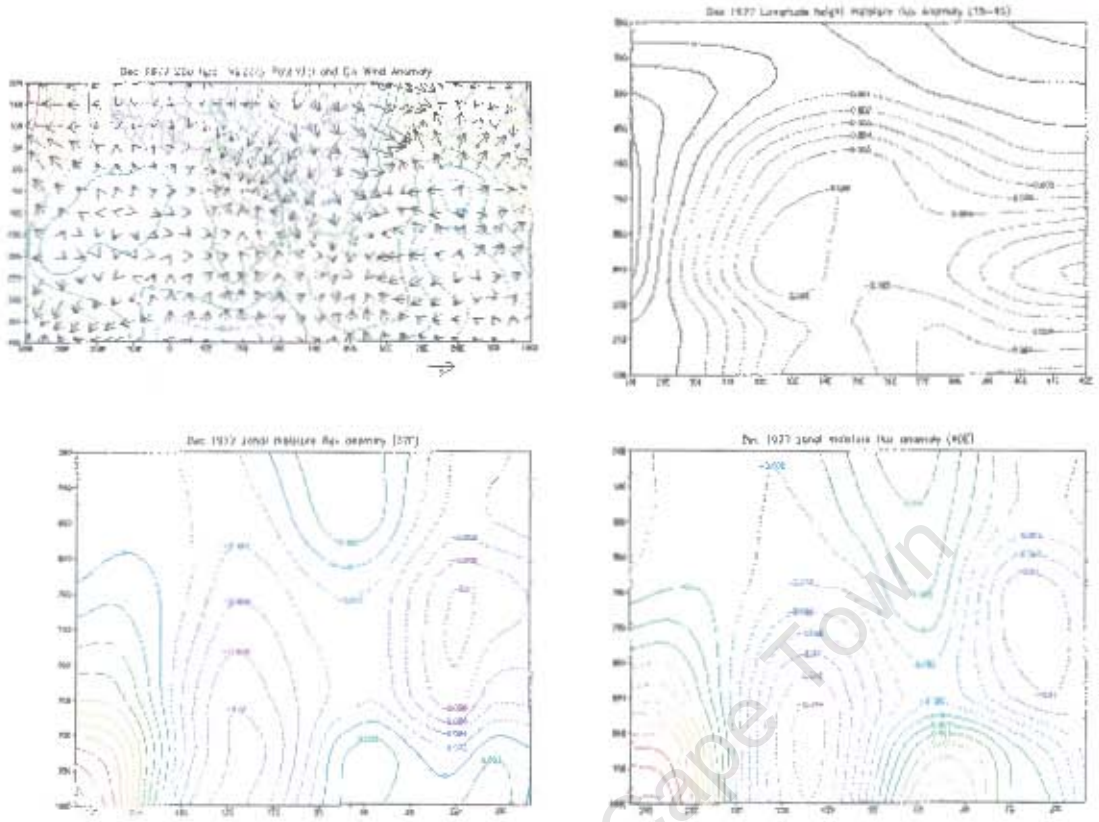

Figure E6 continue

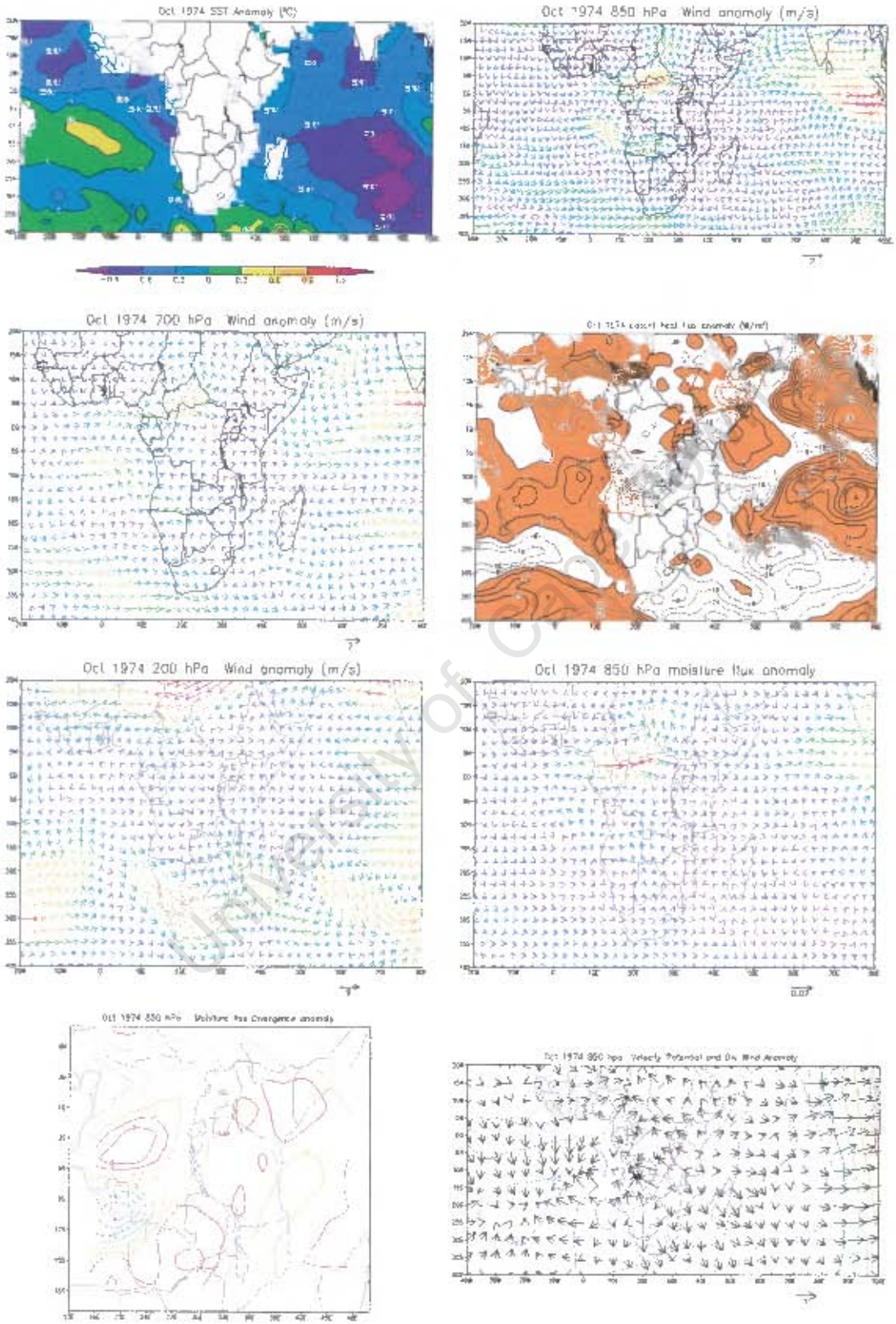

Figure F1: October anomaly fields for dry non El Niño year 1974
Moisture flux in g/kg.m/s, Velocity potential ($m^2 s^{-1}$)
Divergent wind (s^{-1})

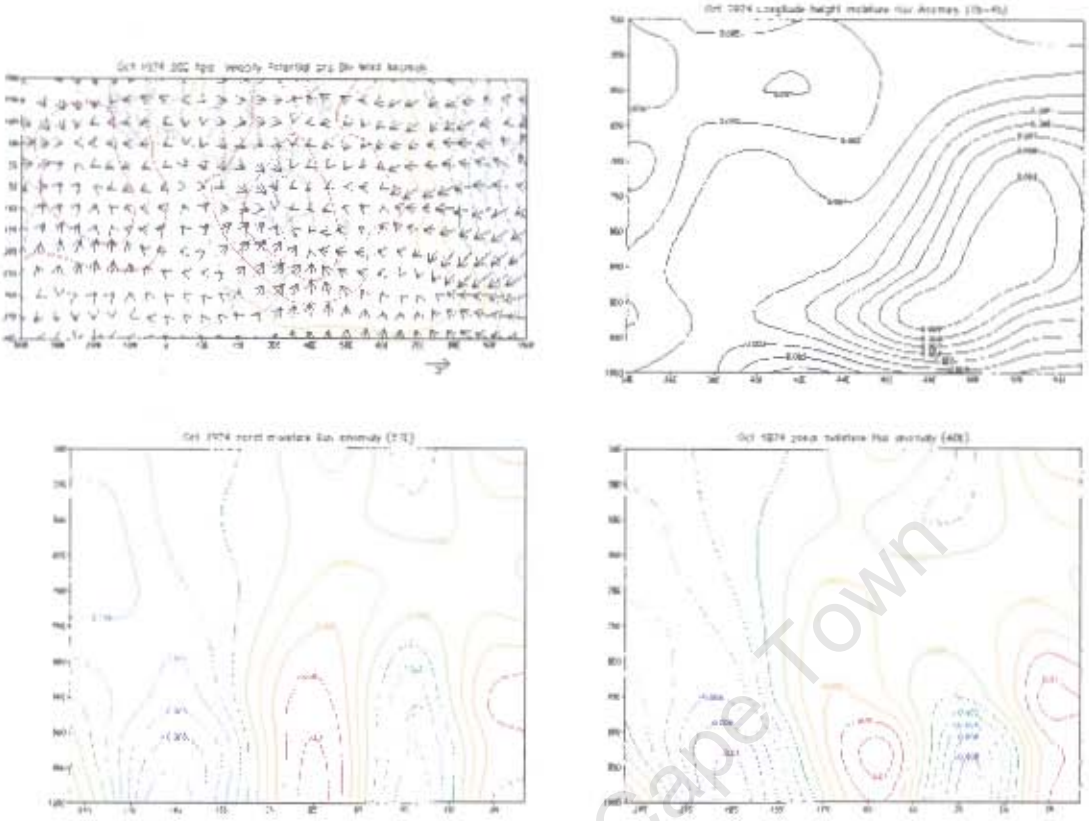

Figure F1 continue

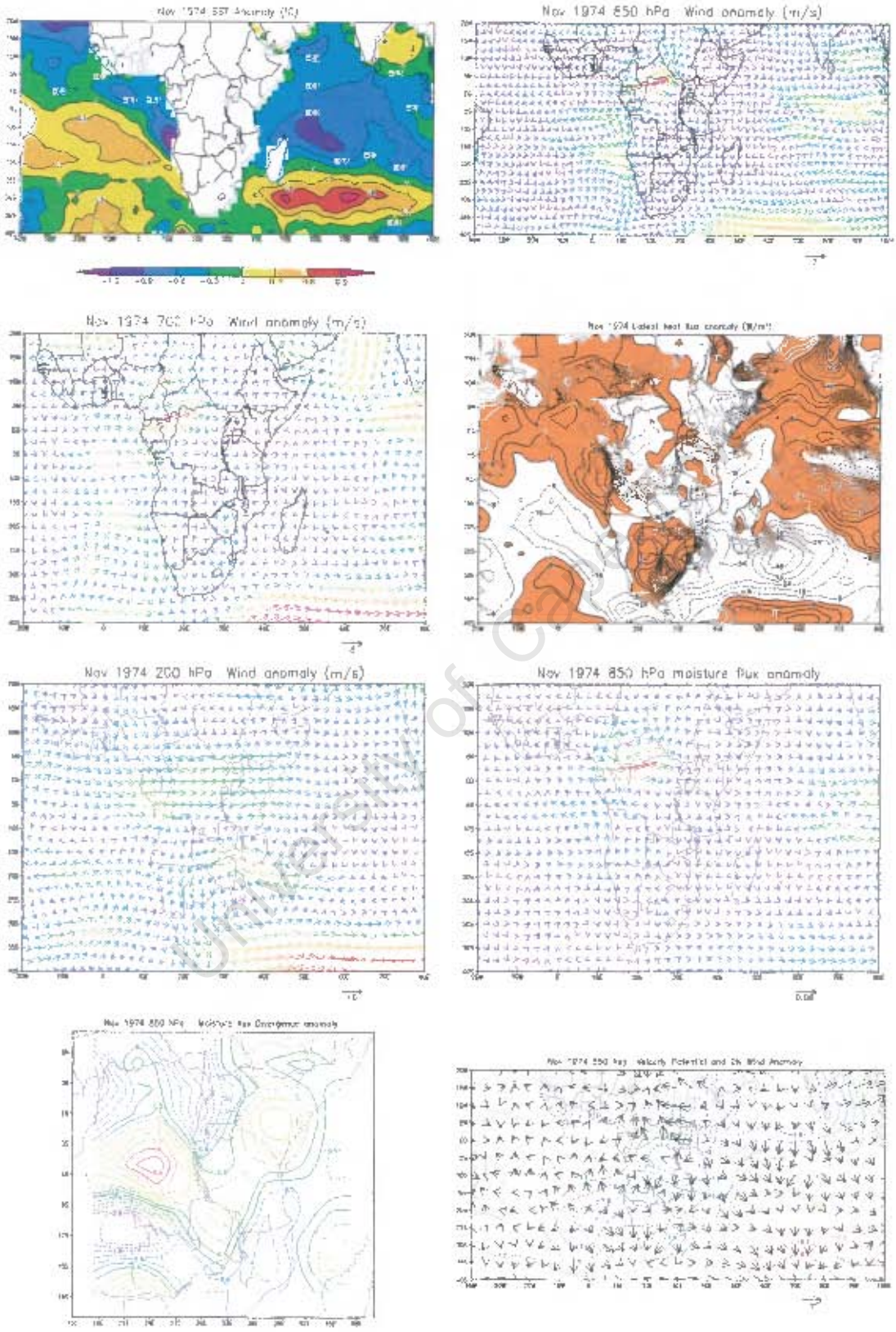

Figure F2: As for figure F1 but for November

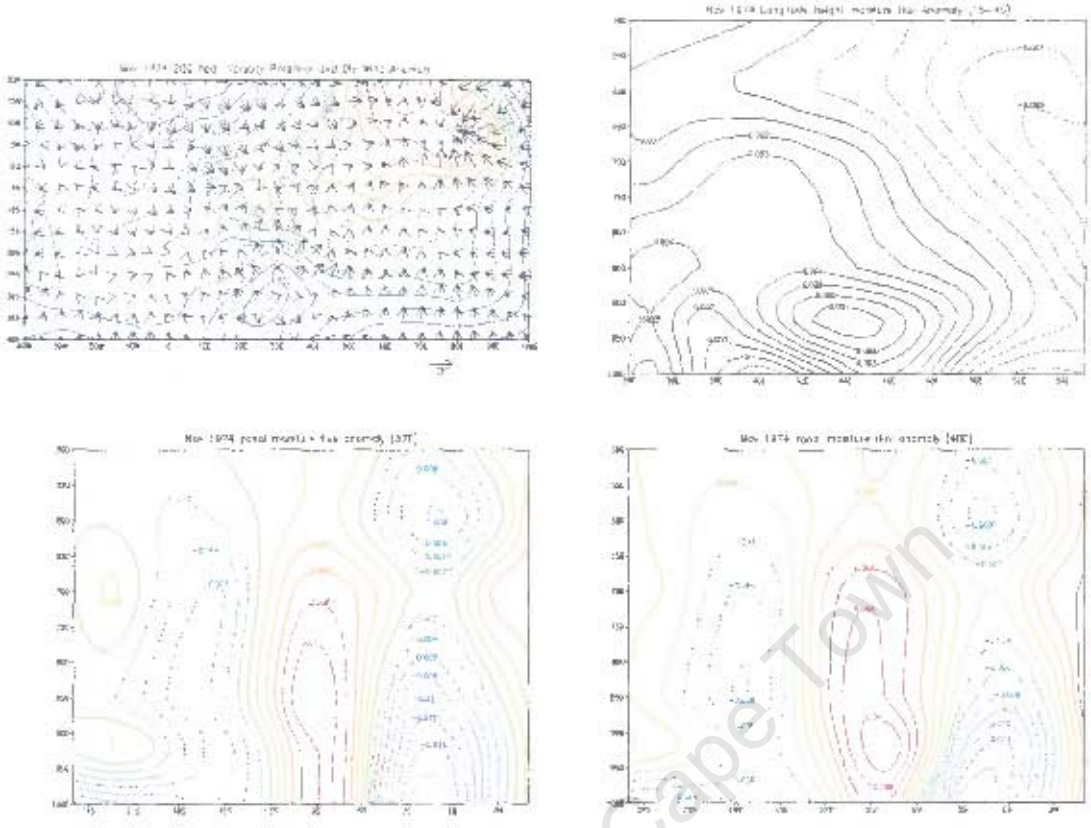

Figure F2 continue

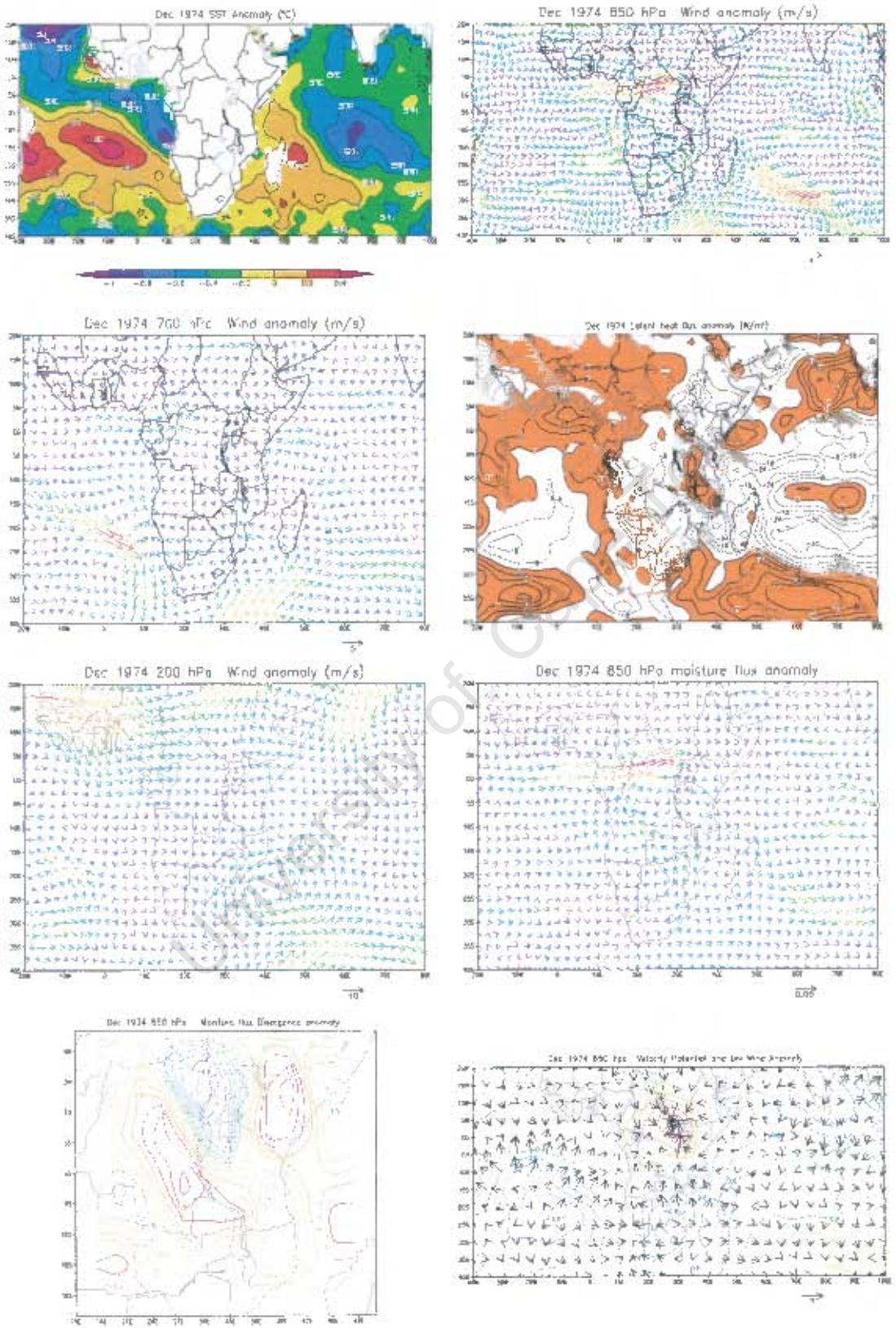

Figure F3: As for figure F1 but for December

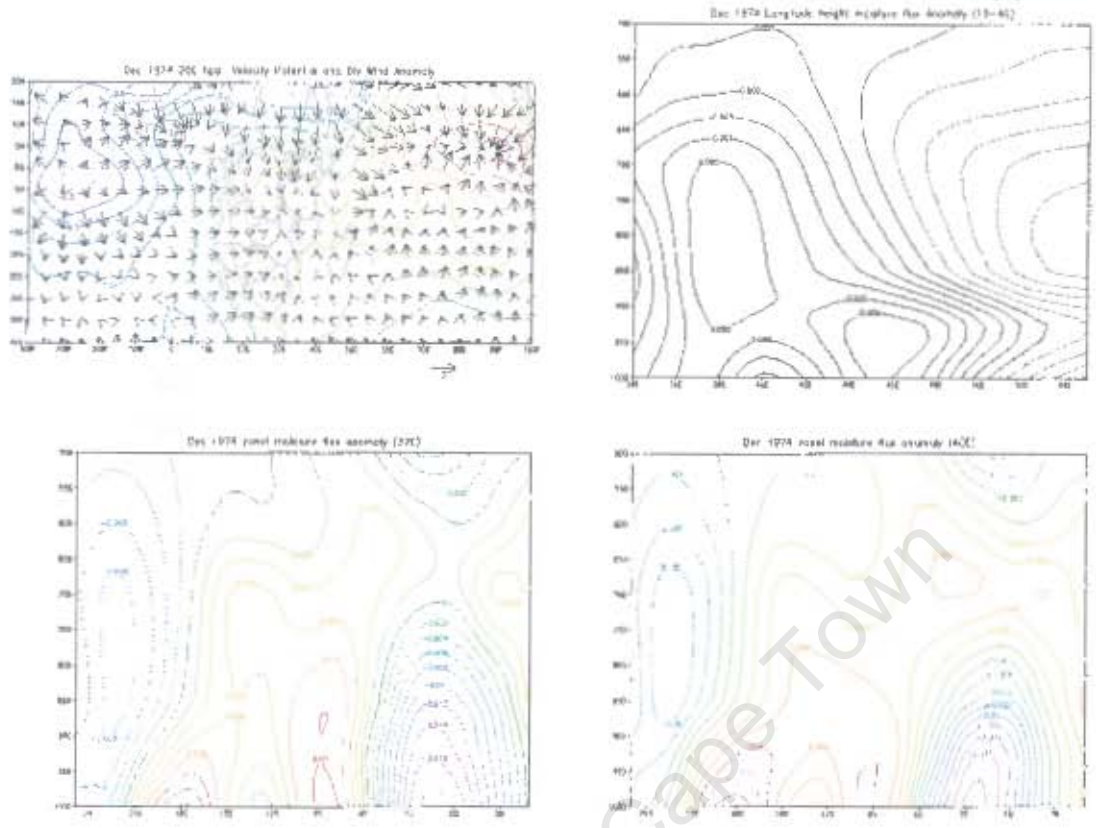

Figure F3 continue

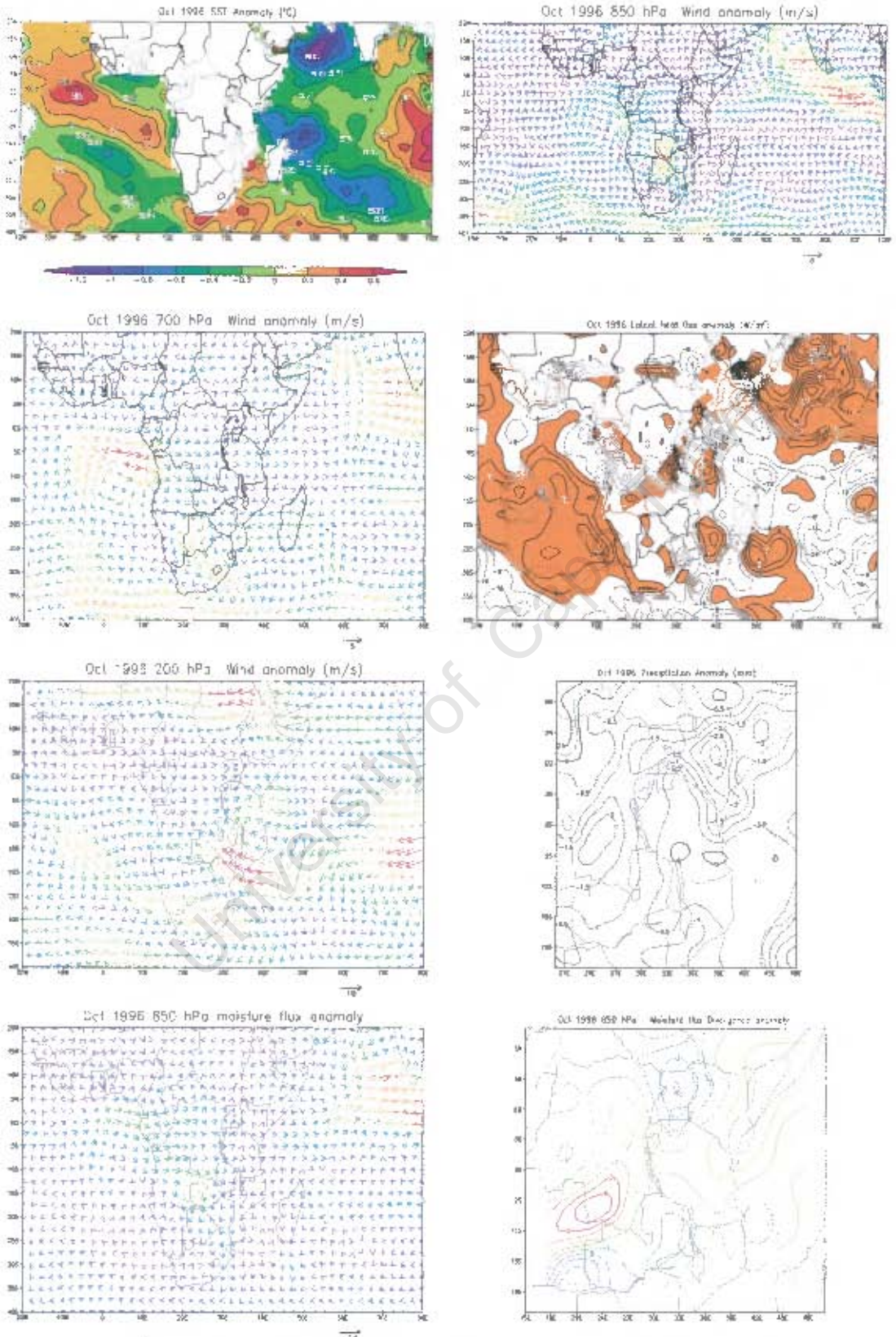

Figure F4: October anomaly fields for dry negative IOZM year 1996
Moisture flux in g/kg.m/s, Velocity potential (m^2 s^{-1})
Divergent wind (s^{-1})

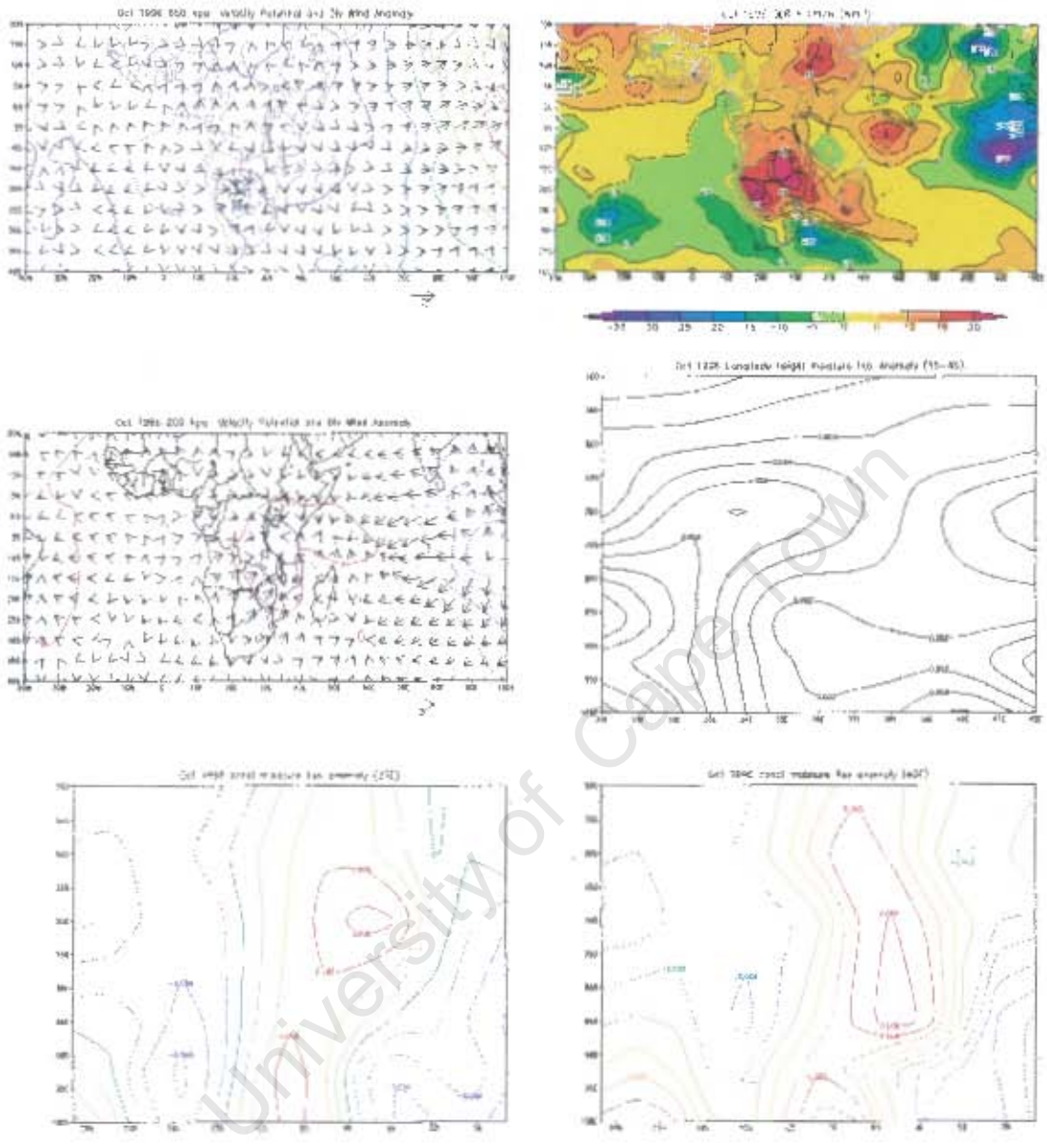

Figure F4 continue

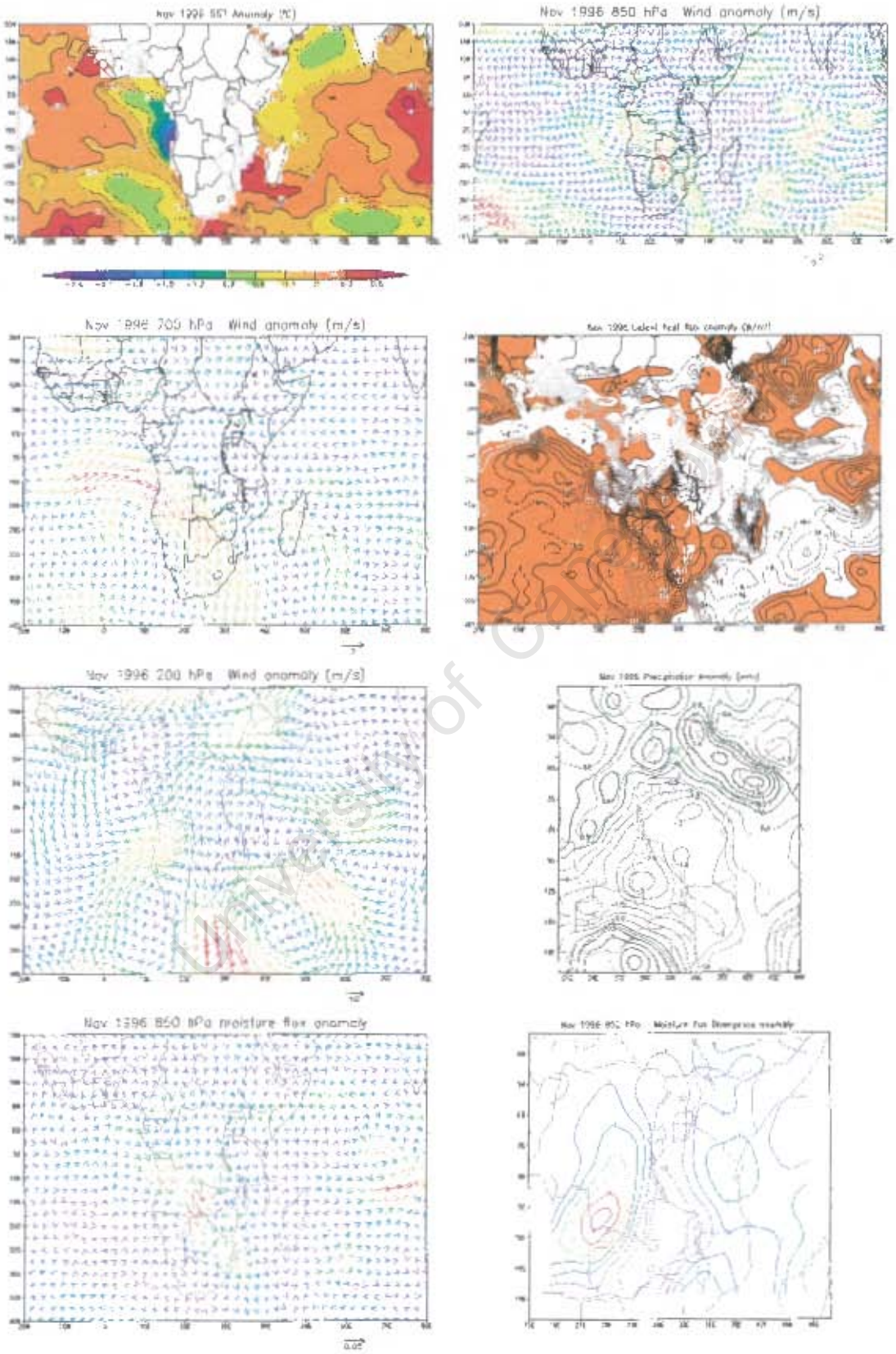

Figure F5: As for figure F4 but for November

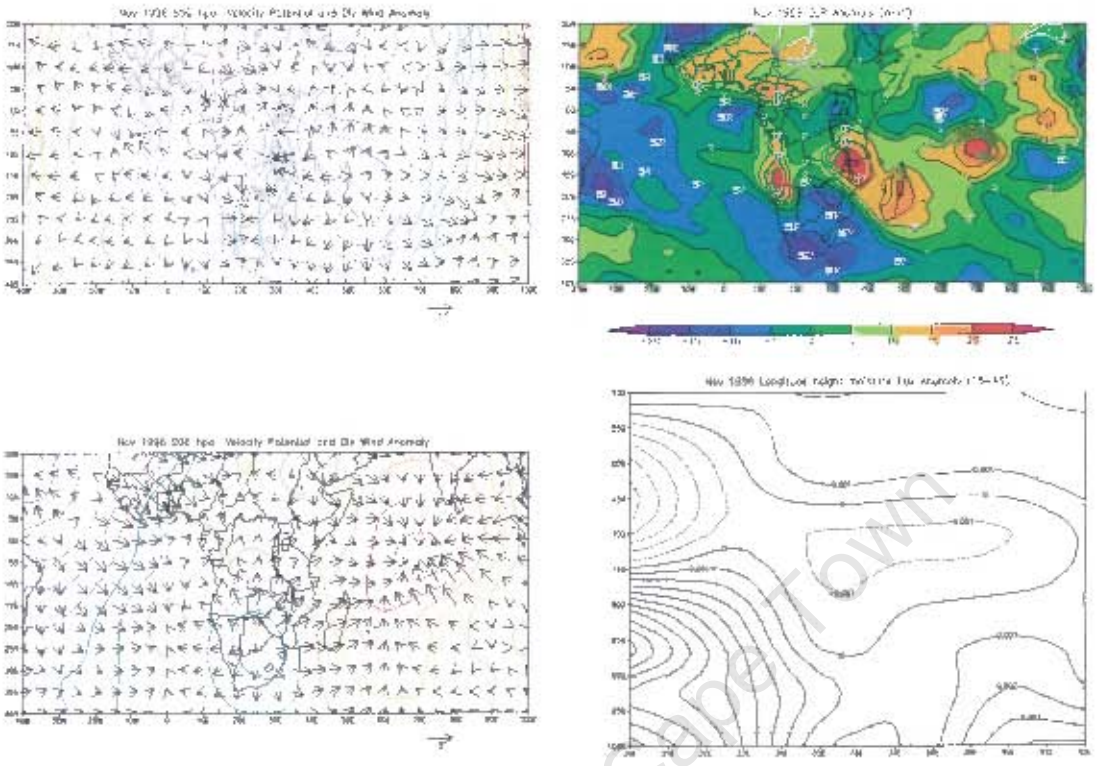

Figure F5 continue

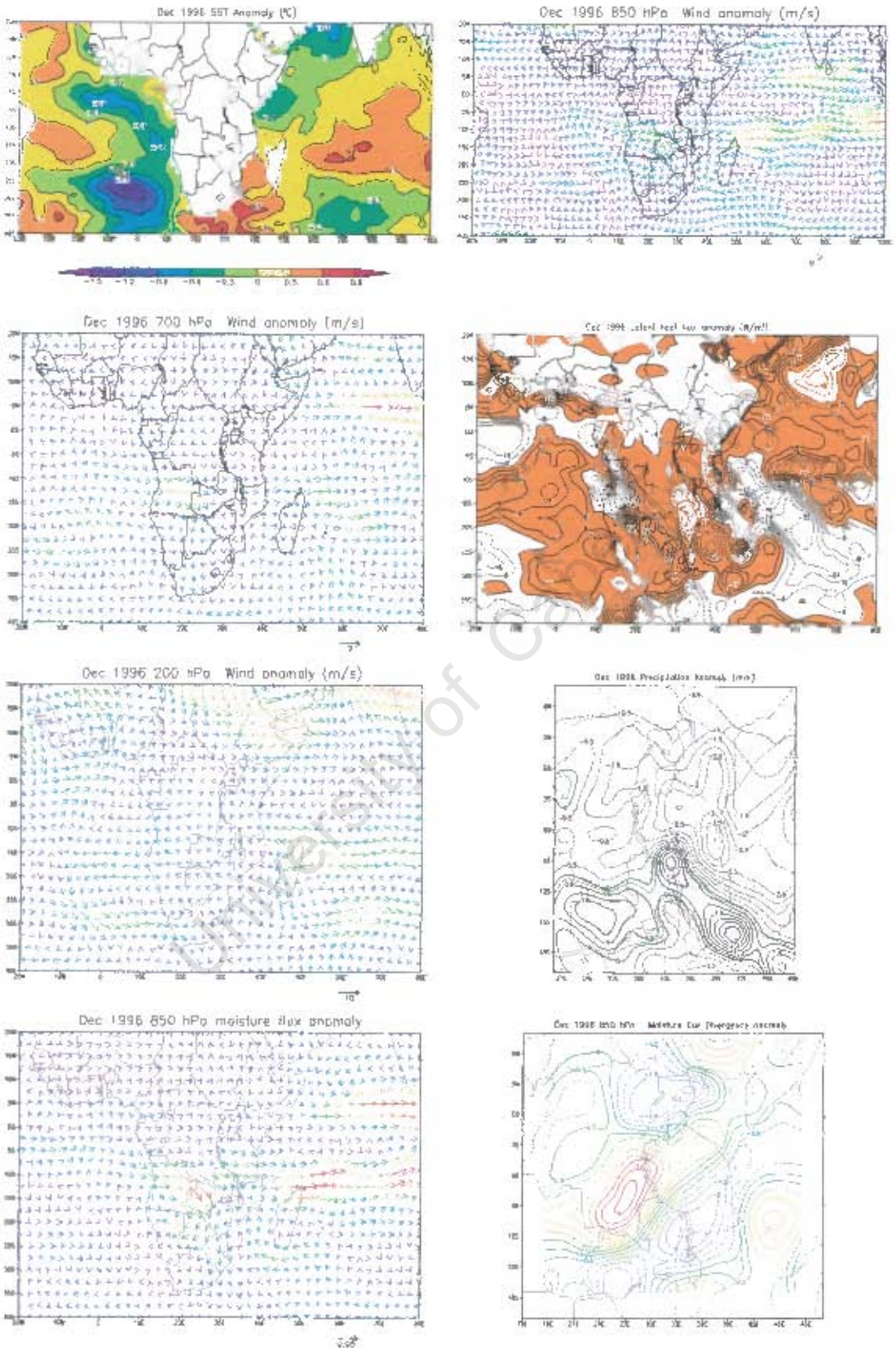

Figure F6: As for figure F4 but for December

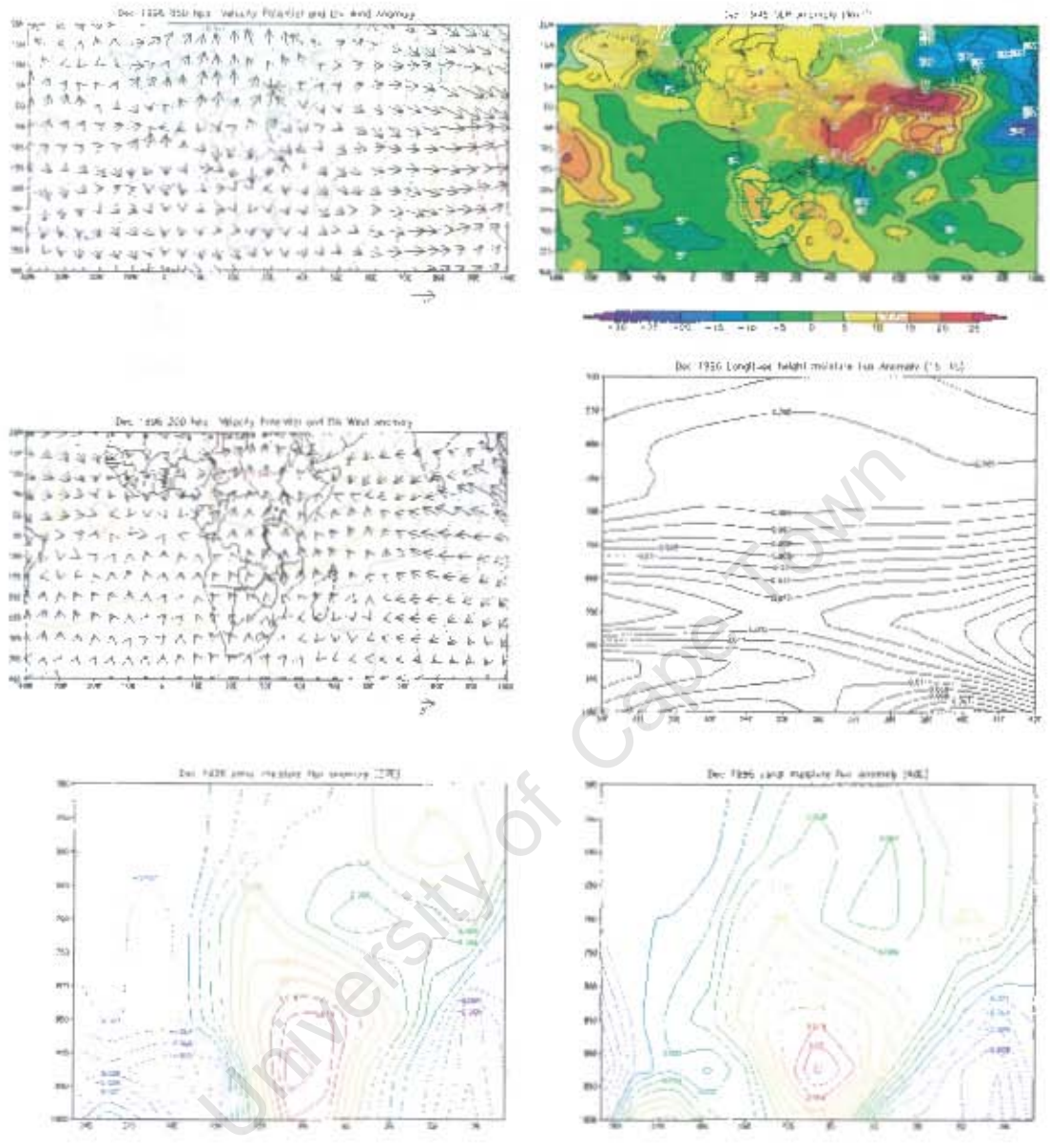

Figure F6 continue

References

Allan RJ, Lindesay JA, Parker DE. 1996. El Niño Southern Oscillation and Climatic variability *CSIRO Publications*, Melbourne,Australia, 405

Allan RJ, Reason CJC, Lindesay JA, Ansell TJ. 2003. Protracted ENSO episodes over the Indian Ocean region. *Deep-Sea Reasearch II*, **50**, 2331-2347.

Arkin PA. 1982. The relationship between interannual variability in the 200mb tropical wind field and the Southern Oscillation. *Mon.Wea. Rev.*, **110**, 1393-1404.

Alusa AL, Gwange PM. 1978. The occurance of dry spells during the East African long rains. *Research report* No. 5/78, E.A Institute for Meteorology, 1-18.

Amissah-Arthur A, Jagtap S, Rosenzweig C. 2002. Spatio-Temporal effects of El Niño events on rainfall and maize yield in Kenya. *Int.J. Climatol.*, **22**, 1849-1860 (2002)

Anyamba EK. 1992. Some properties of a 20-30 day oscillation in tropical convection. *J. Afr. Met.Soc.* **1**, 1-19.

Asnani GC. Tropical meteorology, Vol 1. 80,383 pp

Asnani GC, Kinuthia JH.1979. Diurnal variation of precipitation over East Africa. East African Meteorological Department Research Report No. 8/79.

Barring L. 1988. Regionalization of daily rainfall in Kenya by means of common factor analysis. *Journal of Climatology*, **8**, 371-389

Beltrando G. 1990. Space-time variability of rainfall in April and October-November over East Africa during the period 1932-1983. *Int. J. Climatol.*, **10**,691-702.

Bengtsson L, Shukla J. 1988. Integration of Space and In situ Observations to study Global climate change, *Bulletin of American Meteorological Society*, **69**, 10, 1130-1143.

Bjerknes J. 1969. Atmospheric teleconnections from the equatorial Pacific. *Mon. Wea. Rev.*, **97**, 163-172

Cadet DL, Diehl BC. 1984. Inter annual variability of surface fields over the Indian Ocean during recent decades. *Monthly Weather Review*, **112,** 1921-1935.

Cadet DL, Beltrando B. 1987. Relationship between surface fields over the Indian Ocean and rainfall over East Africa. *Indian Ocean Rep.*, 3rd sess., 6-10, SCOR-TOC/CCCO Indian Clim. Stud. Progr. Vacoas, Mauritius.

Camberlin P.1995. June-September rainfall in north-eastern Africa and atmospheric signals over the tropics: a zonal perspective. *International Journal of Climatology*, **15,** 773-783.

Cane MA, Zebiak SE, Dolan SC. 1986. Experimental forecasts of El Niño. *Nature.* **321**, 827-832.

Charney JG. 1975. Dynamics of deserts and drought in the Sahel. *Quart. J. Roy. Meteor. Soc.*, **101**, 193-202

Charnery JG, Shukla J. 1981. Predictability of monsoos. In: Monsoon Dyanamics, Eds. J. Lighthill and R.P. Pearce, *Cambridge University Press*, 99-109

Conway D, Hulme M. 1993. Recent fluctuations in precipitation and runoff over the Nile sub-basins and their impact on main Nile discharge. *Climatic change*, **25**, 127-151.

Doblas-Reyes FJ, Déqué M. 1998. A flexible Bandpass Filter Design procedure Apllied to midlatitude Intraseasonal variability. *Mon. Wea. Rev.* **126**. 3326-3335

EAMD, 1963. Climatic seasons of East Africa. E.A.Met.Dept. Report No.**8**,4pp

EAMD, 1963. The weather of East Africa. East African Meteorological Department. Pamphlect series No. **7**, 13pp

Flohn H. 1987. East African rains of 1961/62 and the abrupt changec of the White Nile discharge. Paleoecology of Africa **18**, 3-18.

Fransisco J, Doblas –Reyes, Déqué M. 1998. A flexible band pass filter Design procedure applied to mid latitude intraseasonal variability. *Monthly Weather Review*, **126**, 3326- 3335.

Fremming D.1970. *Notes on an easterly disturbances affecting East Africa 5-7 September 1967*, East African Meteorological Department Technical Memo, No. 13.

Glantz M, Katz R, Nicholls N.1991. ENSO *teleconnections linking worldwide climate anomalies: scientific basis and societal impacts.* Cambridge University press, Cambridge,UK, 535pp.

Gill AE. 1977. Coastaly trapped waves in the Atmosphere. *Quart. J. Roy. Meteor. Soc.*,103, 43-440.

Gill AE. 1980. Some simple solutions for heat-induced tropical circulations. *Quart. J. Roy. Meteor. Soc.*, 106, 447-462.

Goddard L, Graham NE. 1999. Importance of the Indian Ocean for simulating rainfall anomalies over eastern and southern Africa. *Journal of Geophysical Research* ,**104**, D16, 19099-19116.

Griffiths JF. 1972. Eastern Africa. In Climates of Africa, World survey of Climatology, Vol. **10**, *Elsevier*, 604.

Hastenrath S., Nicklis A. and Greischar L. 1993. Atmospheric hydrospheric mechanisms of climate anomalies in the western equatorial Indian Ocean. *J Geophys Res **98** (C 11)*, 20219-20235

Hendon HH and Liebmann. 1990. The Intra seasonal (30-50) Oscillation of the Australian Summer Monsoon. *J. Atmos. Sci.*,**47**, 24, 2904-2923.

Hirota I. 1978. Equatorial waves in the upper stratosphere and mesosphere in relation to the semi annual oscillation of the zonal wind, *J. Atmos. Sci.*,**35**,714-722.

Hills R. 1979. The structure of the Inter-Tropical Convergence zone in the Equatorial African rainfall. *Transaction of the Institute of British geographers*. **4**, 329-352

Horel JD, Wallace JM. 1981. planetary scale atmospheric phenomena associated with the Southern Oscillation. *Monthly Weather Review*, **109**, 813-829.

Hoskins BJ, Neale RB, Rodwell M, yang G.-Y. 1999. Aspects of the large-scale tropical atmospheric circulation, *Tellus*, **51A**, 33-44.

Indeje M, Semazzi FHM, Ogallo LJ.2000. ENSO signals in East African Rainfall Seasons *International Journal of Climatology*, **20**, 19-46

Ininda JM. 1987. Spatial and temporal characteristics of drought in Eastern and Southern Africa. *MSc Thesis*, University of Nairobi. Kenya.

Ininda JM. 1994. Numerical simulation of the influence of the sea surface temperature anomalies on the East African seasonal rainfall. *PhD thesis*, University of Nairobi, Kenya.

Janowiak, 1988. An investigation of Inter annual rainfall, *Journal of Climate*, **1**, 240-255.

Johnson DH. 1962. Rain in East Africa. *Quarterly Journal of the Royal Meteorological society,* **88**,1-19

Kabanda TA. 1995. Seasonal and intraseasonal dynamics and precursors of rainfall over northern Tanzania. *Msc thesis University of Cape Town.*

Kabanda TA, Jury MR. 1999. Inter-annual variability of short rains over northern Tanzania, *Climate Research* , Vol.**13**, 231-241

Kalnay E. and Co-authors. 1996. The NCEP/NCAR 40-year Reanalysis Project, *Bulletin of the American Meteorological Society*, **77**, 437-471.

Kiladiz GN and Diaz HF. 1989. Global climatic anomalies associated with extremes in the Southern Oscillation. *Journal of climate*, 2, 1069-1090.

Knutson TR, Welckmann KM. 1987. 30-60 day atmospheric circulations: Composite life circles of convection and circulation anomalies. *Mon.Wea. Rev.,* **115**, 1407-1436.

Krishnamurti TN. 1961. The sub tropical jet stream of winter. *Journal of Meteorology,***18**,172-191.

Krishnamurti TN, Kanamitsu M, Koss WJ, Lee JD.1973. Tropical east-west circulation during the northern winter. *Journal of Atmospheric Science,* **30,** 780-787.

Latif M, Dommenget D, Dima M, Grotzner A.1999. The role of Indian Ocean Sea Surface Temperature in forcing East Africa rainfall anomalies during December-January 1997/98. *Journal of Climate*, **12**, 3497-3504

Leètmaa R, Reynolds R, Jenne and Joseph D. 1996. The NCEP/NCAR 40-year reanalysis project. *Bulletin of the American Meteorological society,* **77**,437-471

Levey KM, 1993. Intra-seasonal oscillations of convection over Southern Africa. *MSc. Thesis*, University of Cape town.

Liebmann B, Hartmann DL. 1982. Interannual variations of outgoing IR associated with tropical circulation changes during 1974-78. *J. Atmos. Sci.,* **39**, 1153-1162.

Loschnigg J, Meehl GA, Webster PJ. Arblaster JM, Compo GP. 2003. The Asian Monsoon, the Tropospheric Biennial Oscillation, and the Indian Ocean Zonal Mode in the NCAR CSM. *Journal of Climate*, **16**, no 11, 1617-1642.

Madden RA, Julian PR. 1971. Detection of a 40-50 day oscillation in the zonal wind in the tropical Pacific. *J. Atmos. Sci.*, **28,**702-708

Makarau A. 1994. Intra-seasonal oscillatory modes of the Southern Africa summer circulations. PhD. Thesis, University of Cape Town.

Matarira CH, Jury MR. 1992. Contrasting Meteorological structure of Intra seasonal wet and dry spells in Zimbabwe. *International Journal of Climatology*, **12,** 165-176

Matsuno T.1966. Quasi-geostrophic motions in the equatorial area. *J. of Meteor. Soc. Japan*, **44**, 25-43

Mhita MS. 1984. The use of water balance models in the optimation of cereal yields in seasonally-arid tropical regions. PhD Thesis. University of Reading. P211

Mhita MS, Nassib IR. 1987. The onset and end of rain in Tanzania. *Proc.1st Tech. Conference*. Meteor. Res. Eastern and Southern Africa, Nairobi , p.101-115.

Mhita MS, Venäläinen A. 1992. The variability of rainfall in Tanzania. FINNIDA/SATCC/WMO-meteorology project Helsinki. Finnish Meteorological Institute.

Mistry VV, Conway D. 2003. Remote forcing of East African Rainfall and relationships with fluctuations in levels of lake Victoria. *Int. J. Climatol.*, **23**, 67-89

Mpeta EJ. 1997. Intra-seasonal convection dynamics over southwest and northeast Tanzania: An observational study. MSc thesis, University of Cape Town.

Mukabana JR, Pielke RA. 1991. Numerical simulation of the effects of monsoon winds on the weather patterns over Kenya: A case study during the 'long rains 'season. *9th Conference on Numerical Weather Prediction.* October 14-18, 1991, American Meteorological Society, Denver, CO.

Mulenga H.M. 1999. Southern Africa Climatic anomaly, Summer rainfall and the Angola low . PhD thesis University of Cape Town 232pp.

Mutai CC, Ward MN, Colman AW. (1998). Towards the prediction of East African short rains based on Sea-Surface Temperature-Atmosphere Coupling. *International journal of climatology* **18,** 975-997

Namias J. 1963. Interaction of circulation and weather between hemispheres. *Mon. Wea. Rev.*, **91**, 482-486.

Newell RE, Kidson JW, Vincent and Boer GJ. 1972. The general circulation of tropical atmosphere and interaction with extra tropical latitudes. Vol 1, MIT press, Cambridge, MA, 256pp

Nicholson SE, Entekhabi D. 1986. The quasi periodic behavior of rainfall variability in Africa and its relationship to the Southern Oscillation. *Archiv für Meteorologie, Geophysik und Bioklimatologie* **A34**, 311-348

Nicholson SE, Nyenzi BS. 1990. Temporal and spatial variability of SSTs in the tropical Atlantic and Indian Oceans. *Meteorol. Atmos. Phys.*, **42**, 1-17.

Nicholson SE. 1996. Areview of climate dyanamics and climate variability in Eastern Africa. In the *Limnology, Climatology and Paleoclimatology of the East African lakes*, Jonhson TC, Odata E (eds). Gordon and Breach Publishers; The Netherlands.

Nicholson SE. 1997. An analysis of the ENSO signal in the Tropical Atlantic and Western Indian Oceans. *International Journal of Climatology*, **17,** 345-375

Nicholson SE, Kim J. 1997. The relationship of the El Nino-Southern Oscillation to African Rainfall. *International Journal of Climatology*, **17,** 117-135

Nicholson SE, Selato JC. 2000. The influence of La Niña on African rainfall. *International journal of climatology*, **20**, 1761-1776

Nicholson SE 2000. The nature of rainfall variability over Africa on time-scales of Decades to Millenia. *Global and Planetary change*, **26**, 137-158.

Njau L., 1987. Seasonal Variability of Kenya rainfall and its teleconnection. Proc. First Technical conference on Met Research in Eastern and Southern Africa. Nairobi Kenya, 6-9 January 1987, 160-165.

Nyenzi BS. 1984. equatorial zonally moving disturbances which contribute to East African long rains March to May 1979, Msc. Thesis, Florida state University 73pp.

Nyenzi BS. 1988. Mechanisms of East African Rainfall variability. PhD. Thesis Florida State University 184pp.

Ogallo LJ. 1980. Regional classification of East African rainfall stations into homogeneous groups using the method of principal component analysis. *Stat. Clim. Devel. Atmos. Sci.*, **13**,255-266.

Ogallo LJ. 1983. Review of current knowledge on climate and drought in Africa. *Expert group meeting on climate and drought over Africa, Geneva.*

Ogallo LJ, Nassib IR. 1984. Drought patterns and famines in East Africa during 1922-1983. The second WMO symposium on meteorological aspects of Tropical droughts. Fu. 1984, 41-44.

Ogallo LJ, Suleiman KA. 1987. rainfall characteristic in East Africa during El Niño year. Proc. First Technical Conference on Met Reaserch in Eastern and Southern Africa. Nairobi, Kenya, 6-9 January 1987, 76-80.

Ogallo LJ. 1988. Relationship between seasonal rainfall in East Africa and Southern Oscillation. *Journal of Climatology*, **8,** 34-43.

Ogallo LJ 1989. The spatial and temporal patterns of the East African seasonal rainfall derived from principal component analysis. *International Journal of Climatology* , **9**, 145-167

Ogallo LJ, Janowiak JE, Halpert MS. 1989. Teleconnection between seasonal rainfall over East Africa and global sea surface temperature anomalies. *J. Meteorol.Soc. Jpn,* **66**,807-821.

Ogallo LJ, Okoola RE, Wanjohi DN. 1994. Characteristics of quasi-biennial oscillation over Kenya and predictability potential for seasonal rainfall. *Mausam*, **45**, 57-62.

Okeyo AE. 1986. The influence of lake Victoria on the convective systems over the Kenya highlands. *Proceedings of an international conference on Short, Medium Range Weather Forecasting.* August 1986. Tokyo Japan.

Rasmusson EM, Carpenter TH. 1982. Variations in tropical sea surface temperature and surface wind fields associated with Southern Oscillation/ El Nino. *Monthly Weather Review* **110**, 354-384

Reason CJC, Allan RJ, Lindesay JA, Ansell TA. 2000. ENSO and Climatic signals across the Indian Ocean basin in the global context. *International Journal of Climatology, 20,* 1285-1327

Reason CJC. 2001. Subtropical Indian Ocean SST dipole events and southern African rainfall. *Geophysical Research* Letters, **28**,11, 2225-2227.

Reason CJC, Rouault M. 2002. ENSO-like decadal patterns and South African rainfall. *Geophys. Res. Lett.*, **29** (13), 16-1 – 16-4.

Reverdin G, Cadet DL, Gutzler D. 1986. Inter annual displacements of convection and surface circulation over the equatorial Indian Ocean. *Quart. J. Roy. Meteor. Soc.*, **112**, 46-67.

Richard Y, Fauchereau N, Poccard I, Rouault M, Trzaska S. 2001. XXth Century Droughts in Southern Africa Spatial and temporal variability, teleconnections with oceanic and atmospheric conditions. *Inter. J. Climatology,* **21**, 873-885

Riehl H. 1979. Climate and Weather in the Tropics. *Academic press, London, 611pp.*

Rodhe H, Virji H,1976: Trends and periodicities in East African rainfall data. *Monthly Weather Review* **104**: 307-315

Ropelewski CF, Halpert MS. 1987.Global and regional scale precipitation patterns associated with the El Nino/Southern Oscillation, *Monthly Weather Review*,**115**,1606-1626.

Rui H, Wang B. 1990. Development characteristics and dynamic structure of tropical intra seasonal convection anomalies. *J. Atmos. Sci.*, **47**, 357-379.

Saji NH, Goswami BN, vinayachandran PN, Yamagata T.1999. A dipole mode in the tropical Indian Ocean. *Nature* **401**: 360-363

Semazzi FH, Indeje M.1999. Inter-seasonal variability of the ENSO rainfall signal over East Africa. *J. African Meteorological society*, **4 (no1)**, 81-89

Stoeckenius T. 1981. Interannual variations of tropical precipitation patterns. *Mon. Weather Rev.*, **109**, 1233-1247.

Tegart WJ, Zillman JW, 1993: Climate science in Australia with particular reference to climate change. *International Journal of Environmental pollution*, **3**, 1-3.

Tourre YM, White WB. 1997. Evolution of ENSO signal over the Indo-Pacific domain. *J.Phys. Oceanogr.*, **27**, 683-696.

Vincent DG, Sperling T, Fink A, Zube S, Speth P. 1991. Intraseasonal Oscillation of Convective Activity in the Tropical southern hemisphere: May,1984-April, 1986. *Journal of Climatology*, **4**, 40-53.

Walker GT.1923. Correlation in seasonal variations of weather, viii. A preliminary study of world weather.

Walker GT. 1924. Correlation in seasonal variatios of weather, ix. A further study of world weather. Memoirs. Indian Meteor.Dept.,24, 275-332.

Walker GT. 1928. World weather iii. Memoirs .Roy.Meteor.Soc.,2,97-106

Walker GT, Bliss EW. 1932. World weather V.*mem.Roy.Met.Soc.*, **4**, 53-84.

Walker GT, Bliss EW. 1937. World weather V1.*mem.Roy.Met.Soc.*, **4**, 119-139.

Wallace J.M., Rassmusson E.M, Mitchell TP, Kousky VE, Sarachick ES,Von Storch H.1998. On the structure and evolution of ENSO-related climate variability in the tropical Pacific: lessons from TOGA. *Journal of Geophysical Research,* **103**,14,241-14,260.

Wang B, Rui H. 1990. Synoptic Climatology of transient Tropical Intra seasonal convection Anomalies: 1975-1985, Meteorology and Atmospheric physics, **44**, 43-61

Wang B, Xie X. 1997. A model for the Boreal Summer Intra seasonal Oscillation. *J. Atmos. Sci.*, **54**, 1,72-86

Weickmann KM, Lussky GR, Kutzbach JE. 1985. Intrasasonal (30-60 day) fluctuations of outgoing longwave radiation and 250mb stream function during northern winter. *Monthly Weather Review*, **113**,941-961

Webster PJ. 1983. The large-scale structure of the tropical atmosphere. In: Hoskins and Pearce (eds) *General Circulation of the Atmosphere,* pp. 235-275. London: Academic Press.

Webster PJ., Moore AM., Loschnigg JP., Lebden RR. 1999. Coupled ocean-atmosphere dynamics in the Indian Ocean during 1997-98. *Nature* 401: 356-360

Xie P., Arkin PA. 1997. Global Precipitation: A 17-year monthly analysis based on gauge observations, satellite estimates and numerical model outputs. *Bulletin of American Meteorological Society*, **78**, 2539-2558.

Zhu B., Wang B. 1993. The 30-60 day convective seesaw between the tropical Indian and western Pacific Oceans. *J. Atmos. Sci.*, **50**, 184-199.